Investigating the role of tetraspanin proteins in *Salmonella* infection

By

Fawwaz Fadhil Ali

A thesis submitted in partial fulfilment of the requirements for the degree of
Doctor of Philosophy

The University of Sheffield
Faculty of Science
Department of Molecular Biology and Biotechnology

July 2016

Acknowledgments

Firstly, I would like to offer my sincerest gratitude to my supervisors Dr Lynda Partridge and Dr Peter Monk for guidance and continuous support throughout my PhD study, for their patience, inspiration, and immense knowledge. Their guidance helped me throughout my research and writing this thesis.

Besides my supervisors, I would like to thank my advisors Prof Mike Williamson and Prof Robert Poole, for their insightful advice and encouragement.

My sincere thanks also goes to Dr Paul Heath, Mrs Catherine Gelsthorpe and Dr Nadhim Bayatti (Sheffield Institute for Translational Neuroscience) for helping me in microarray work and Dr Darren Robinson (Light Microscope Facility, University of Sheffield) for microscopy imaging support and Susan, Kay and Julie (Flow Cytometry Unit, Medical School, University of Sheffield) for flow cytometry support.

A great thanks also goes to the friendly and cheerful lab members both past and present, for all the great help and support, my grateful thanks to Atiga, John, Ibrahim, Ahmmed, Shaymaa, Rachel, Jehan, Marzieh, Daniel, Dr Andrew, Muslim and Jenny for all help, support and friendship.

It is an honour for me to express my deep sense of thankful to the Higher Committee for Education Development in Iraq (HCED) for giving me the chance to undertake this study.

Last but not the least, I would like to thank my family, my great brothers and sisters for supporting me spiritually throughout my PhD, this work could not have been completed without their help and support. Special and grateful thanks to my wife Dr Israa Al-Hamid and my two beautiful and lovely children Anas and Ibrahim for their love, patience, endurance and continuous support that kept me highly motivated throughout my PhD.

This thesis is dedicated to the memory of my mother Sabeeha M. Jameel and my father Fadhil A. Hussain, they would have been delighted to see me reaching this stage.

Abstract

Tetraspanin proteins are a family of transmembrane proteins that are broadly expressed on different tissues and in multi-cellular organisms. Their main characteristic is the ability to organize multi-molecular complexes through their association with different proteins and lipids to form tetraspanin enriched microdomains or TEMs. These microdomains have important roles in many cell functions, cancer malignancy and infectious diseases. However relatively few studies have investigated tetraspanin proteins in bacterial infection. Recently, tetraspanins have been shown to be involved in bacterial adhesion and invasion of human epithelial cell lines and human primary monocyte derived macrophages (MDMs). Specific monoclonal antibodies (mAb) and soluble recombinant versions of the large extracellular domains (EC2s) of tetraspanins were shown to inhibit adhesion of various bacterial species to human cells, possibly by disrupting TEM (Green et al., 2011). Therefore, treatments that target tetraspanins could offer a potential therapeutic alternative to antibiotics, in infections where resistance is an increasing problem.

In this study, we further investigate the role of tetraspanin proteins in *Salmonella enterica* serovar Typhimurium NCTC12023 and LT2 strains using mouse and human phagocytic and human epithelial cell line models. As macrophage models, the well-characterised mouse cell lines J774, RAW247 were used, along with macrophage cell lines established from CD9 KO and wild type mice. In addition, macrophages derived from THP-1 cells were used as a human cell line model. The human epithelial cell line HEC-1- B and HeLa were similarly investigated. Assays were developed to assess infection by flow cytometry (FACS) analysis in addition to conventional microscopy. Additionally, the role of syntenin, a CD63 tetraspanin partner protein, on *Salmonella* infection of HeLa cells was investigated.

Different patterns of tetraspanin expression were observed on the cell lines by flow cytometry, with CD9 and CD81 generally highly expressed. Interestingly, tetraspanin CD63 showed high expression in human THP-1 derived macrophages, but was present at very low levels on mouse macrophage cell lines. *Salmonella* expressing green and red

fluorescent protein were also successfully generated to facilitate the investigation of infection.

Pre-treatment of mouse macrophage cells with anti-CD9, anti-CD81 monoclonal antibody (mAb) significantly decreased *Salmonella* infection. Comparable results were obtained using both immunofluorescence microscopy and FACS analysis. Anti-CD63 mAbs had no effect, which is likely to relate to the low expression of the tetraspanin by these cells. By contrast, anti-CD63 mAb inhibited infection of human THP1 derived macrophages, whereas anti-CD9 mAb had no effect, which is similar to previously reported findings for human MDM (Hassuna, PhD thesis, University of Sheffield, 2010). In this study, no significant effect on *Salmonella* infection of epithelial cell lines HEC-1-B and HeLa cells was observed on pre-treatment with individual tetraspanin-specific mAbs. This suggests less involvement of tetraspanins in *Salmonella* infection of non-phagocytic cells. Pre-treatment of J774 cells with soluble recombinant versions of human or mouse CD9- EC2 showed no effect on *Salmonella* association. This difference in activity between mAb and EC2s may indicate that *Salmonella* binding to J774 cells is not reliant on TEMs and the antibodies have a different mechanism of action here.

Differences in the infectivity of the CD9KO and wild type mouse macrophage cell lines were noted, although this varied depending on the virulence of the *Salmonella* strain. CD9 KO cells also showed some differences in expression of other tetraspanins at protein, but not mRNA level as determined by microarray analysis. HeLa cells stably knocked down for syntenin expression were more susceptible to *Salmonella* infection than control cells; however, no changes were observed in early stages of *Salmonella* binding. The effects of syntenin KD could relate to alternative syntenin partner proteins such as syndecan.

This study suggests a prominent role for tetraspanin CD9 and other tetraspanins in *Salmonella* infection of mouse macrophages and confirms a role for tetraspanins in infection of human macrophages. The different effects observed between cell lines when targeting tetraspanins could be related to differences in bacterial types, strains and mode of uptake, as well as differences in tetraspanin expression.

Table of Contents

List of Tables

List of Figures

Chapter 1

Chapter 2

Chapter 3

Chapter 4

Chapter 5

Chapter 6

Chapter 7

Table of abbreviations

Abbreviation	Meaning
A	
a.a.	**a**mino **a**cid
ADAM	**A** **d**isintegrin **a**nd **m**etalloprotease
AF®	**A**lexa **f**luor
AIDS	**A**cquired **i**mmune **d**eficiency **s**yndrome
ALCAM	**A**ctivated **l**eukocytes **c**ell **a**dhesion **m**olecules
ANOVA	**An**alysis **o**f **va**riance
AP	**A**daptor **p**rotein
APS	**A**mmonium **p**er**s**ulfate
Arg-tag	Poly-**arg**inine-**tag**
B	
B/B/N	**B**SS/**B**SA/**N**aN_3
B. thailandensis	***B**urkholderia **thailandensis***
BMDM	**B**one **m**arrow **d**erived **m**acrophages
bp	**B**ase **p**airs
BSA	**B**ovine **s**erum **a**lbumin
BSS	**B**alanced **s**alt **s**olution
β ME	**B**eta **m**ercapto**e**thanol
C	
CD	**C**luster of **d**ifferentiation
Cas9	**C**RISPR **as**sociated protein **9**
Cdc42	**C**ell **d**ivision **c**ycle **42**
cDNA	**C**omplementary **DNA**
CDV	**C**anine **d**istemper **v**irus
CFU	**C**olony **f**orming **u**nit
CRISPR	**C**lustered **R**egularly **I**nterspaced **S**hort **P**alindromic **R**epeat
CXCL12	**C**-**X**-**C** Chemokine **l**igand **12**
CXCR4	**C**-**X**-**C** Chemokine **r**eceptor type **4**
D	
DAPI	4-6-**d**i**a**midino-2-**p**heny**l**indole
DAVID	**D**atabase for **A**nnotation, **V**isualisation and **I**ntegrated **D**iscovery
DCs	**D**endritic **c**ell**s**
ddH_2O	**d**istilled **d**eionised water (**H_2O**)
dH_2O	**d**istilled water (**H_2O**)
DLG	**D**iscs **l**ar**g**e tumour suppressor protein

DMEM	**D**ulbecco's **M**odified **E**agles **M**edium
DMSO	**D**i**m**ethyl **s**ulph**o**xide
DNA	**D**eoxyribo**n**ucleic **a**cid
dNTPs	**d**eoxyribo**n**ucleotide **t**ri**p**hosphate**s**
DSb	**D**i**s**ulfide **b**ond
DsRed	***D****iscosoma* **s**p. **Red** fluorescent protein

E

E.coli	***E****scherichia* ***c****oli*
EC	**E**xtra**c**ellular
EC1	**E**xtra**c**ellular domain **1**
EC2	**E**xtra**c**ellular domain **2**
EDTA	**E**thylene**d**iamine**t**etra-**a**cetic acid
EEA-1	**E**arly **e**ndosome **a**ntigen-**1**
EGFR	**E**pidermal **g**rowth **f**actor **r**eceptor
EMEM	**E**agle's **M**inimum **E**ssential **M**edium
ER	**E**ndoplasmic **r**eticulum

F

FACS	**F**luorescence **A**ctivated **C**ell **S**orter
Fc	**F**ragment **c**rystalline
FCS	**F**oetal **c**alf **s**erum
FimH	Type-1 fimbriae adhesion
FimI	Type-1 fimbriae subunit
FITC	**F**luorescein **i**so**t**hio**c**yanate
FSC	**F**orward **sc**atter

G

GDP	**G**uanosine **d**i**p**hosphate
GFP	**G**reen **f**luorescent **p**rotein
GST	**G**lutathione **S**-**t**ransferase
GTPase	**G**uanosine **t**ri**p**hosphat**ase**

H

HBSS	**H**ank's **b**alanced **s**alts **s**olution
hCD9	**H**uman **CD9**
HCV	**H**epatitis **C** **v**irus
HCV-E2	**HCV e**nvelope glycoprotein-**2**
HEK	**H**uman **e**mbryonic **k**idney
HI	**H**eat **i**nactivated
HIV-1	**H**uman **i**mmunodeficiency **v**irus-**1**
H-K-ATPase	Hydrogen (**H**) Potassium (**K**) **a**denosine**t**ri**p**hosphat**ase**
HPV	**H**uman **p**apilloma **v**irus

HRP	**H**orse **r**adish **p**eroxidase
HTLV-1	**H**uman **T**-cell **l**eukemia **v**irus type-**1**
HTLV-1 Env	**HIV-1 Env**elope protein

I

ICAM	**I**ntercellular **a**dhesion **m**olecules
Ig	**I**mmuno**g**lobulin
IL-2	**I**nter**l**eukin **2**
IPTG	**I**so**p**ropyl-β-D- **t**hio**g**alactopyranoside

K

Kb	**K**ilo**b**ase
KDa	**K**ilo**da**lton
KD	**K**nock **d**own
KO	**K**nock **o**ut
kv	**k**ilo **v**olt

L

LAMP	**L**ysosomal **a**ssociated **m**embrane **p**rotein
LB	Lysogeny **b**roth
LEL	**L**arge **e**xtracellular **l**oop
LFA-1	**L**ymphocyte **f**unction-associated **a**ntigen-**1**
LIMP	**L**ysosomal **i**ntegral membrane **p**rotein
LPS	**L**ipo**p**oly**s**accharides
LR11	**l**ow density lipoprotein **r**eceptor
LT2	*Salmonella enterica* serovar Typhimurium LT2

M

mAb	**m**onoclonal **a**nti**b**ody
mCD9	**M**ouse **CD9**
MDMs	**M**onocytes **d**erived **m**acrophage**s**
MFI	**M**edian **f**luorescence **i**ntensity
µF	microfarad
µg	microgram
µl	microlitre
µm	micrometre
µM	micromolar
MHC	**M**ajor **h**istocompatibility **c**omplex
MisL	**M**embrane **i**nsertion and **s**ecretion protein
MMP	**M**atrix **m**etallo**p**roteinases
MOI	**M**ultiplicity **o**f **i**nfection
mRNA	**m**essenger **RNA**
MVBs	**M**ulti**v**esicular **b**odie**s**

N-O

N. meningitidis	***N**eisseria **meningitidis***
NAG2	**N**ovel **a**nti**g**en **2**
NCTC12023	*Salmonella enterica* serovar Typhimurium **NCTC12023**
NO	**N**itric **o**xide
NTS	**N**on-**t**yphoid ***S**almonella*
Nus-tag	**N-u**tilization **s**ubstance-**tag**
O.D.	**O**ptical **d**ensity

P-Q

PagN	**P**hoP-**a**ctivated **g**ene **N**
PAMPs	**P**athogen **a**ssociated **m**olecular **p**atterns
PBS	**P**hosphate **b**uffered **s**aline
PCA	**P**rincipal **c**omponent **a**nalysis
PCR	**P**olymerase **c**hain **r**eaction
PDZ	**P**SD-95, **D**LG and **Z**O-1
Pef	**P**lasmid-**e**ncoded **f**imbria
PFA	**P**ara**f**orm**a**ldehyde
PKA	**P**rotein **k**inase **A**
PIP_2	**P**hosphatidy**l**inositol 4,5-bis**p**hosphate
PMA	**P**horbol **m**yristate **a**cetate
PrgH	**P**hoP-**r**epressed **g**ene **H**
PSD-95	**P**ost-**s**ynaptic **d**ensity
Poly (I:C)	**Poly-i**nosinic-**poly-c**ytidylic acid
qPCR	**q**uantitative **PCR**

R

Rab	**Ra**s-related protein
RAC1	**Ra**s-related **C**3 botulinum toxin substrate **1**
RAS	**Ra**t **s**arcoma
RDS	**R**etinal **d**egeneration **s**low
RFP	**R**ed **f**luorescent **p**rotein
Rho	**R**as **ho**mology gene family
RNA	**R**ibo**n**ucleic **a**cid
ROM-1	**R**etinal **o**uter segment **m**embrane protein-**1**
rpm	**r**evolutions **p**er **m**inute
RPMI	**R**oswell **P**ark **M**emorial **I**nstitute
Rs	**R**eceptor**s**
RT	**R**oom **t**emperature

S

S. aureus	***S**taphylococcus **aureus***

S. cerevisiae	***S****accharomyces* ***cerevisiae***
S. Typhimurium	***S****almonella enterica* serovar **Typhimurium**
SBP	**S**treptavidin-**b**inding **p**eptide
SCV	***S****almonella* **c**ontaining **v**acuole
SDS-PAGE	**S**odium **d**odecyl **s**ulphate- **p**oly**a**crylamide **g**el **e**lectrophoresis
SEL	**S**mall **e**xtracellular **l**oop
shRNA	**S**mall **h**airpin **RNA**
Sif	***S****almonella* **i**nduced **f**ilament
Sip	***S****almonella* **i**nvasion **p**rotein
siRNA	**S**mall **i**nterference **RNA**
SOC	**S**uper **o**ptimal broth for **c**atabolite repression
Sop	***S****almonella* **o**uter **p**rotein
SPI	***S****almonella* **p**athogenicity **i**sland
SSC	**S**ide **sc**atter

T

T3SS	**T**ype **3** **s**ecretion **s**ystem
TAE	**T**ris **a**cetate **E**DTA
TBS	**T**ris **–b**uffer **s**aline
TEM	**T**etraspanin **e**nriched **m**icro domain
TEMED	**Te**tra**m**ethyl**e**thylene**d**iamine
TM	**T**rans**m**embrane
TM4SF	**T**rans**m**embrane **4** **s**uper **f**amily
TNF	**T**umour **n**ecrosis **f**actor
TRAF	**T**NF **r**eceptor **a**ssociated **f**actor
Tris	2-Amino-2-(hydroxymethyl)-1,3-propanediol
Tween-20	Polyoxyethylene sorbitol monolaurate

U-Z

UP	**U**ro**p**lakin
UV	**U**ltra **V**iolet
VCAM	**V**ascular **c**ell **a**dhesion **m**olecule
WT	**W**ild **t**ype
ZO-1	**Z**onula **o**ccludens **1** protein

Chapter 1: General introduction

1.1 Tetraspanin proteins

Tetraspanins are a large family of transmembrane proteins; this family consists of thirty three members in mammals, which can be subdivided into four subfamilies: the CD family, the CD63 family, the Uroplakin family and the RDS family (Table 1.1) (Kashef, Diana et al. 2012, DeSalle, Sun et al. 2013). These transmembrane proteins have four hydrophobic regions and two extracellular loops. The tetraspanins were discovered first on human leukocyte surfaces, but it was quickly found that they had a broad expression on tissues and organisms including on human melanoma (CD63) and *Schistosoma* (Sm 23). The specific functions of many tetraspanins are unknown, but data from biochemical studies or knockout mice suggest an important role in membrane structure. Their unique characteristic is their ability to form a complicated multimolecular net, the "tetraspanin web ", which includes proteins such as integrins (Fan and Brindley 1998, Boucheix and Rubinstein 2001, Pols and Klumperman 2009). It has also been suggested that their ability to interact with proteins and lipids leads to the formation of a specialized type of microdomain; tetraspanin enriched microdomains or TEM (Hemler, 2003). The significant variety in the dynamics and composition of tetraspanin complexes lends the proteins a great deal of flexibility to contribute to various biological roles (Yunta and Lazo 2003), for instance cellular motility, activation, adhesion, invasion of cancer (Tarrant, Robb et al. 2003) and apoptosis (Lapalombella, Yeh et al. 2012). The emerging genetics and studies on tetraspanin function and biochemistry powerfully supports the importance of tetraspanins (Hemler 2001, Stipp, Kolesnikova et al. 2003, Hemler 2005, Wang, Li et al. 2011, Hemler 2014).

Some tetraspanin protein that have been identified in mammals show particular functions and limited expression, but the distribution of many is very wide with many cells expressing multiple tetraspanins on the surface or interior membranes (Monk and Partridge 2012). In addition, analysis of the evolution of all known tetraspanins has shown that they include 20 members in the genome of *Caenorhabditis elegans* (nematode); also 37 members of the group are present in the genome of the fruit fly *Drosophila melanogaster* (Shi, Ke et al. 2010), in a certain set of eighteen contiguous genes of the genome (Todres, Nardi et al. 2000) and there are at least 47 members in zebrafish (Garcia-España, Mares et al. 2009). Tetraspanins are also found in plants (Wang, Vandepoele et al. 2012), sponge (Garcia-España, Mares et al. 2009) and fungi (Lambou, Tharreau et al. 2008).

Table 1.1: The identified human tetraspanins members with their alternative names.

HGM-2005 Tetraspanin name	Tetraspanin	Family	Protein (Gen Pept)	DNA (Gen Bank)	Alternative Name(s)
1	TSPAN-1	CD	NP_005718	NM_005727	TM4-C, 9030418M05Rik, RP11-322N21.1, NET1
2	TSPAN-2	CD	NP_005716	NM_005725	FLJ12082, RP4-666F24.2, 6330415F13Rik
3	TSPAN-3 -isoform 2	CD63	NP_005715 NP_944492	NM_198902 NM_005724	TM4SF8.1, TM4-A, TM4SF8.2
4	TSPAN-4	CD	NP_003262	NM_003271	TM4SF7, NAG-2
5	TSPAN-5	RDS	NP_005714	NM_005723	2810455A09Rik, 4930505M03Rik, TM4SF9, NET-4
6	TSPAN-6	CD63	NP_003261	NM_003270	TM4SF6, T425, TM4-D, A15 homologue
7	CD231	CD63	NP_004606	NM_004615	A15, MXS1, CCG-B7, TALLA-1, TM4SF2b, DXS1692E, MRX58
8	CO-029	CD	NP_004607	NM_004616	D6.1, TM4SF3
9	NET5	CD	NP_006666	NM_006675	PP1057
10	Oculospanin	RDS	NP_114151	NM_031945	FLJ39607
11	TSPAN11	RDS	NP_001073978	NM_001080509	UNQ1971, VSSW1971
12	NET2	Uroplakin	NP_036470	NM_012338	TM4SF12
13	NET6	CD63	NP_055214	NM_014399	TM4SF13, FLJ22934
14	DC-TM4F2	RDS	NP_112189	NM_030927	BC002920, NEW2, TMSF14
15	NET7	RDS	NP_036471	NM_012339	2700063A19Rik, TMSF15
16	TM4B	CD	NP_036598	NM_012466	TM-8, TMSF16
17	CAD35489	RDS	NP_569732	NM_130465	F-Box23, SB134, BC067105, NEW3, TMSF17
18	BAB55318	CD	NP_570139	NM_130783	AK027715.1, UP1 homologue
19	Tetraspanin 19	CD	NP_001094387	NM_001100917	FLJ44351
20	Uroplakin Ib	Uroplakin	NP_008883	NM_006952	UPIB, UPK1
21	Uroplakin Ia	Uroplakin	NP_008931	NM_007000	UPIA, UP1A, UPKA
22	Peripherin	RDS	NP_000313	NM_000322	RDS, RP7, AVMD, PRPH, AOFMD, PRPH2, RD2
23	Rom1	RDS	NP_000318	NM_000327	ROSP1
24	CD151 - UTR variant	CD	NP_004348 NP_620599	NM_004357 NM_139030	PETA3, SFA1, gp27, RAPH, MER2
25	CD53	CD	NP_000551	NM_000560	MOX44
26	CD37	CD	NP_001765	NM_001774	GP52-40
27	CD82	CD	NP_002222	NM_002231	Kangai1, R2, 4F9, C33, IA4, ST6, GR15, KAI1, SAR2
28	CD81	CD	NP_004347	NM_004356	TAPA-1, S5.7
29	CD9	CD	NP_001760	NM_004356	BA2, p24, GIG2, MIC3, MRP-1, BTCC-1, DRAP-27, 5H9
30	CD63	CD63	NP_001771	NM_001769	MEL1, ME491, granulophysin, LAMP3, OMA81H, MLA1, neuroglandular Ag (Hara-Kaonga and Pistole), LIMP
31	SAS	CD63	NP_005972	NM_005981	
32	TSSC6	Uroplakin	NP_620591	NM_139022	PHEMX, ART1, FLJ17158, FLJ97586
33	MGC50844	CD	NP_848657	NM_178562	PEN

This table was kindly provided by P.N. Monk, Department of Infection and Immunity, University of Sheffield, and modified according to (DeSalle, Sun et al. 2013).

1.1.1 Tetraspanin structure

The four transmembrane domains are the main characteristic of tetraspanins and the proteins consist of 204 (SAS) - 355 (oculospanin) amino acids. The proteins have two different sized extracellular loops, the small one (EC1) composed of 20-28 amino acids, and the other extracellular loop (EC2) composed of 76-131 amino acids (Boucheix and Rubinstein 2001).These unequal loops separate the four transmembrane regions (TM1-TM2 and TM3-TM4) with a small intracellular domain lying between TM2 and TM3 (Figure 1.1). The EC2 shows the greatest variability in sequence but also has highly conserved residues that include a CCG motif. This motif and two other cysteine residues are the only signature residues. Disulphide bonding between 2 of these cysteines creates a subdomain in the EC2 (Figure 1.1).

There is variability in the number of cysteine residues in the EC2 sequence with tetraspanins showing either 4, 6 or 8. This variety of cysteine number in the EC2 is a feature that has been used to divide tetraspanins into three groups: group1 have four cysteines and consequently have two disulfides. Group 2 have six cysteines and may form three disulphide bonds. Group 3 consists of a small number of tetraspanins that have an extra two cysteine residues in the EC2 which are close relative to one another and they may form a fourth disulfide bond (Seigneuret, Delaguillaumie et al. 2001).

The X-ray structure of tetraspanin CD81 EC2, which acts as co-receptor for hepatitis C virus (HCV), was solved and shown to consist of an umbrella-shaped structure organized from 5 alpha-helices placed in "stalk" and "head" sub-domains. The stalk sub-domain was suggested to gather on the cell membrane into homodimers and/or heterodimers via a preserved hydrophobic region, whereas the head sub-domain may be responsible for interacting with other ligand proteins such as HCV E2 (Kitadokoro, Bordo et al. 2001). In studies on CD81and its interaction with HCV, it was found that the EC1 is important to the expression of EC2 in mediating translocation of entire CD81 to the surface of the cells (Masciopinto, Campagnoli et al. 2001). However, recently the CD81 EC2 structural characterization by NMR has been reported. The HCV-E2 glycoprotein interaction with tetraspanin CD81 is mediated through a dynamic loop on the helical region that appears to have a different structure from that which was shown in the crystal structure. A membrane binding site is also postulated adjacent to the interaction area of HCV in the extracellular loop of tetraspanin CD81 (Figure1.2) (Rajesh, Sridhar et al. 2012).

From modelling studies, the transmembrane domains are predicted to form four left handed coiled coil strands that connect directly to the two EC2 helices. The small extracellular domain EC1 has a mostly hydrophobic small beta- strand, which may interact with an EC2 conserved hydrophobic groove. The hypervariable subdomain of EC2 and the cytoplasmic

regions are the sites in which the variability in construction generally occurs (Seigneuret 2006). Generally, the EC2s homology between family members varies by 5 - 40%.
There are high homologies of tetraspanin transmembrane domains between human and zebra fish orthologues (83%), and this similarity indicates essential functional roles. The 1, 3 and 4 transmembrane domains show 70-90% conservation of extremely polar residues (asparagine, glutamine and glutamate) between all tetraspanins and the conservation is 100% between four human and zebrafish tetraspanin orthologues. The molecular pattern of polar residues of TM 1, 2 and 3 of CD82 are suspected to rest at internal TM-TM connections instead of outer TM lipid connections. It has been suggested that these residues might participate in strong hydrogen bonds within TMs or with other molecules (Stipp, Kolesnikova et al. 2003). More recent studies indicate that the polar residues are important in interactions between the TM regions and maintaining conformational stability of the tetraspanins (Bari, Zhang et al. 2009).

Tetraspanins are commonly palmitoylated at inner juxta-membrane cysteines and this helps form and/or stabilize tetraspanins interactions (Charrin, Manie et al. 2002). Almost all tetraspanins have preserved residues of cys at least at some similar sites. The intracellular N and C tails and the small intracellular domain altogether have 72-78% similarity between mammalian and zebrafish tetraspanins.

Many attempts have been made to relate the structural features of tetraspanins to specific functions. As mentioned above, the EC2 domain has a variable sub-region, which moderates interactions particularly with different polypeptides and in addition has a more conserved area thought to be involved in homodimerisation. The four transmembrane domains are involved in intra- and inter-molecular interactions which are essential throughout synthesis and interactions of tetraspanin proteins to form what it is known as the "tetraspanin-web" (Charrin, Le Naour et al. 2001). The intracellular juxta-membrane palmitoylation sites are also involved in tetraspanin-web regulation (Charrin, Manie et al. 2002).

Whilst most specific tetraspanin protein functions are linked to the extracellular domains, the cytoplasmic regions are important for some functions. For example the intracellular C-tail region might act as a cytoskeleton and protein signaling bridge in some tetraspanins, as seems to be the case for CD82 in activated T cells (Stipp, Kolesnikova et al. 2003) and discussed further below. Also, mutations induced in the CD9-C- terminus led to a change of CD9 function in cell adhesion and spreading (Wang, Kolesnikova et al. 2011). In addition, recently an association between tetraspanin CD9 and metalloprotease CD10 was identified and the involvement of TM4 and the C terminal of CD9 in this interaction was determined (Mazurov, Barbashova et al. 2013). In another study, the CD9 C-tail has been shown to have a role in RAC1 activation and actin remodeling as a response to CXCL12 (Arnaud, Vallee et al. 2015). The Gly-Try-Glu-Val-Met sequence in the cytoplasmic C-tail of CD63 is essential for targeting to intracellular compartments (Stipp, Kolesnikova et al. 2003) and the role of this lysosomal targeting motif is discussed further below. Furthermore, the tetraspanin C-terminus is shown to play an important role in tetraspanin - associated cytoplasmic protein interactions; deletion of the last two amino acids from the CD63 C-tail eliminated the entire CD63-Syntenin-1 interaction (Latysheva, Muratov et al. 2006).

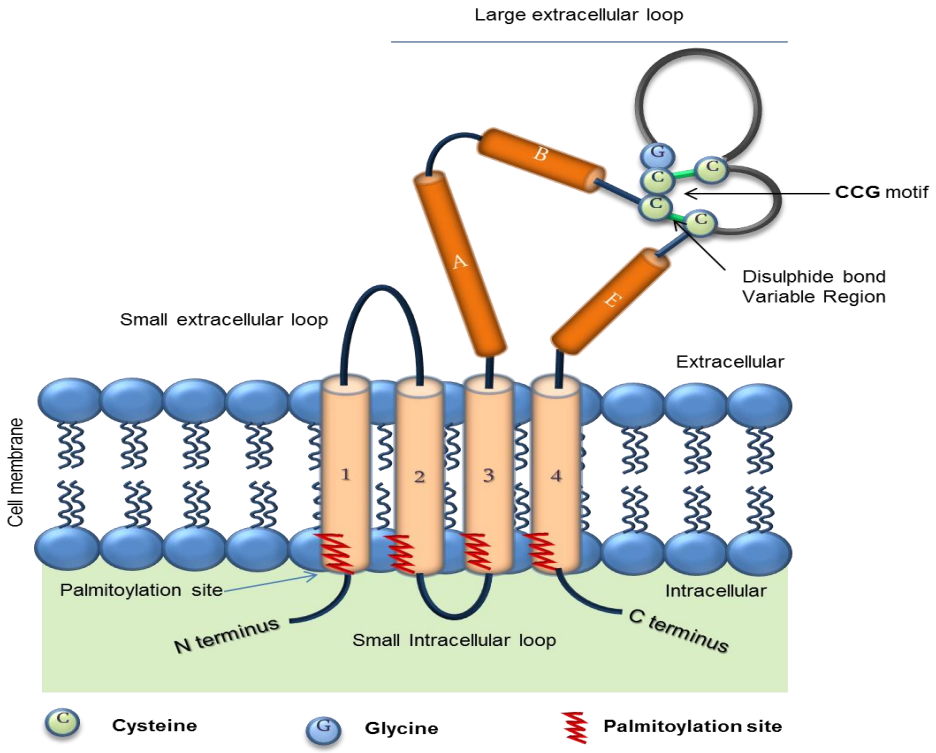

Figure 1.1. The structure of tetraspanins: The diagram shows a tetraspanin protein which is composed of four transmembrane protein (TM) residues (1-4), a large extracellular loop (LEL or EC2), and cysteines that form a di-sulfide bond to create a subdomain in the large extracellular loop, a small extracellular loop (SEL or EC1), a short intracellular loop and two intracellular termini (N and C). The EC2 is composed of two regions, a variable region with a conserved CCG motif and a constant region that contains A, B and E α helices.

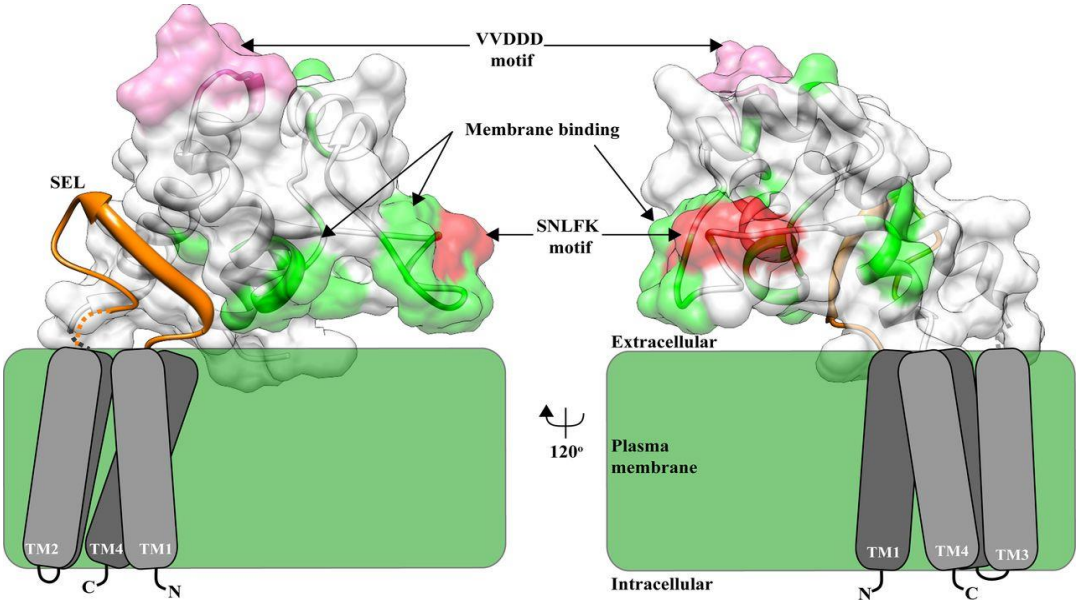

Figure 1.2: A model of the large extracellular domain (LEL) of CD81 monomer showing the binding of ligand residues. (Left) monomer of CD81 acquired by using crystal structure of CD81-EC2 with the small extracellular loop EC1 shaped from the full length CD81model. The red color shows the Hepatitis C protein E2 binding SNLFK motif, while the green color shows the dodecylphosphocholine (DPC) binding interface and the pink color shows the *Plasmodium* sporozoites interacting site (VVDDD). (Right): 120º rotation around vertical axis of the left image focusing of HCV-E2 and membrane binding border, adapted from (Rajesh, Sridhar et al. 2012).

1.1.2 Tetraspanin enriched microdomains (TEMs) and the tetraspanin web

The general effect of anti-tetraspanin antibodies on cell behaviour reflects their importance in cell functions. However, results that were obtained from knockout mice did not meet the predictions found using antibodies. This could be because the antibodies that were used are not only targeted a particular tetraspanin, but also disrupt their associated proteins, in contrast to knocking-out a specific tetraspanin which tends to keep other components integrated (Hemler 2005). This revealed the importance of tetraspanin proteins in organizing cell membranes by engaging associated proteins into specialized tetraspanin enriched microdomains (TEMs) that regulate many cellular events (Bailey, Herbert et al. 2011, Charrin, Jouannet et al. 2014). Looking at proteins that co-immunoprecipited with tetraspanins in different types of detergents gave rise to the ideas of primary, secondary and tertiary tetraspanin interactions (reviewed in Hemler 2003, Yanez-Mo et al 2009, Charrin et al 2014).

Chemical cross-linking studies indicate that tetraspanin homodimers or higher multitimers may form the basic units inside TEMs. The tetraspanins may interact with other tetraspanins members homogeneously or heterogeneously to form tetraspanin-tetraspanin complexes and the EC2 is suggested to play a vital role in homodimerization (Hemler 2005). In addition, direct interactions between tetraspanins and non-tetraspanin proteins occur (Boucheix and Rubinstein 2001, Martin, Roth et al. 2005, Charrin, Jouannet et al. 2014) such as CD151 with integrins, CD9 and CD81 with EWI proteins (members of the immunoglobulin superfamily), uroplakins UP1a with UPll and other hetero-interactions. These direct interactions have been classed as ***primary interactions*** (Hemler, 2003; Hemler, 2005). This protein assembling may serve as a basis for other tetraspanin interactions, for instance those linking to CD151, CD9, CD81 and their associates. These interactions are classed as ***secondary interactions*** and the propensity of tetraspanins to link heterophilically is important for this. Various associated proteins can then be engaged by tetraspanins into functionally essential compositions through indirect interactions, preserved only in mild detergents, termed ***tertiary interactions***. There are various possible tetraspanins partners such as immunoglobulin (Ig) supergene family proteins, integrins, proteoglycans, complement regulatory proteins, proteases, cadherin, membrane proteases, signaling enzymes and others. Tetraspanins can thus construct an interacting net or so called "tetraspan-web" on the cell surface (Figure 1.3) (Charrin, le Naour et al. 2009).

Furthermore, the importance of tetraspanins association has been shown in many studies; in an early study of tetraspanin CD63 association in melanoma cell lines, CD9 and CD81 were shown to be associated with CD63, in addition, CD9 and CD63 associated with integrins. This tetraspanin- tetraspanin and tetraspanin- tetraspanin partner protein linkage gives the ability to form proteins interactions clusters (Radford, Thorne et al. 1996). The association of CD9 and CD81 with α3β1 and α6β1integrins was also observed (Berditchevski, Zutter et al. 1996). In addition to cluster formation, TEMs may have an important roles in signaling; for example in *C. elegans*, a recent study showed that TEMs are involved in bone morphogenetic protein signaling (Liu, Shi et al. 2015). TEMs have also been shown to be exploited by some pathogens and have important roles in different stages of viral infections. A recent study, for example, showed that proteases present in TEM facilitate Corona virus infection and targeting CD9 disturbed the viral receptor binding and protease cleavage needed prior to virus:cell membrane fusion (Earnest, Hantak et al. 2015). Overall, tetraspanin proteins appear to play a central role in organizing their associated proteins in the cell membrane (Hemler 2005), explaining why these proteins are involved in so many activities including cell differentiation, adhesion, cell activation, cancer invasion (Pols and Klumperman 2009), angiogenesis (Takeda, Kazarov et al. 2007), development of the embryo (Kashef, Diana et al. 2012), cell migration (Powner, Kopp et al. 2011) and infections (Silvie, Franetich et al. 2007, Artavanis-Tsakonas, Kasperkovitz et al. 2011, Gui, Wang et al. 2012).

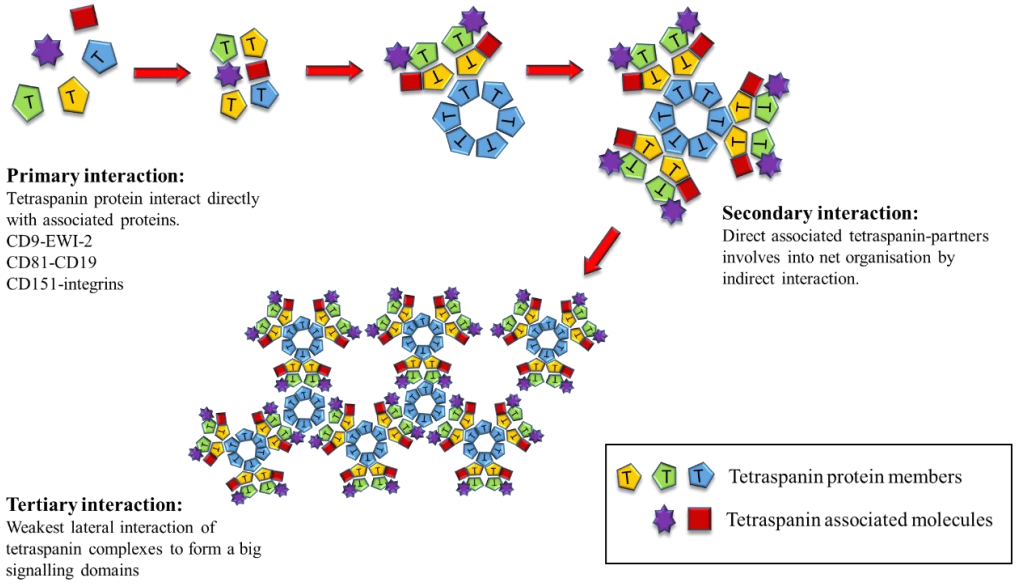

Figure 1.3. The potential structure of the tetraspanin web. The main connections of TEMs are through primary connections that involve the interaction of TEM proteins directly. The various connections between different tetraspanins is included in secondary connections which are less strong and enhances interaction indirectly of primary tetraspanins protein complexes. Tertiary connections are the weakest complexes and are considered to represent significant coalescence of the advanced organized connections into big signaling domains, figure modified from (Martin, Roth et al. 2005).

High resolution microscopy has been used to add more understanding to tetraspanins pattern of association and tetraspanin web construction. Earlier fluorescence microscopy studies of single molecules of tetraspanin dynamics within TEMs revealed that the tetraspanin web was distinct from lipid raft microdomains and that palmitoylation of CD9 and plasma membrane cholesterol have a role in tetraspanin CD9 movement and segregation in the membrane (Espenel, Margeat et al. 2008). Recently, a high resolution microscopy technique called dual color stimulated emission (STED) was used to observe 4 tetraspanins and their partner proteins distribution in the plasma membrane. CD53 appeared to be arranged in clusters of approximately 10 molecules, and only slight overlap was shown between CD53 and CD37 clusters with CD81or CD82 containing complexes. CD81 and CD53 were shown to closest to their MHC II and CD19 partner proteins, rather than other tetraspanins. This was taken to indicate that rather than containing multiple tetraspanins, as widely thought, the basic unit of TEM is made up of clusters of individual tetraspanins and their partner proteins. These may then form dynamic secondary interactions with other tetraspanin clusters or partners in the plasma membrane (Zuidscherwoude, Gottfert et al. 2015).

1.1.3 Palmitoylation

Palmitoylation is responsible for tetraspanin function and web or TEMs organization and has been shown to have an impact on cell phenotype and signaling (Stipp, Kolesnikova et al. 2003, Montpellier, Tews et al. 2011). Palmitoylation of tetraspanin proteins occurs in the Golgi apparatus or post Golgi compartment (Yang, Claas et al. 2002). Tetraspanin CD82 subcellular distribution and interaction with other family members is organized by palmitoylation (Zhou, Liu et al. 2004). This precise function is also important for stabilizing the CD9/CD21/CD81 complex raft function (Cherukuri, Carter et al. 2004) and palmitoylation of CD9 was shown to be essential in the CD9-CD81 interaction (Charrin, Manie et al. 2002). Palmitoylation has an impact on protein-protein interaction as mutation of cysteines involved in palmitoylation changed the contact between CD81 and other proteins (Delandre, Penabaz et al. 2009). Palmitoylation of CD9 and CD151 also encouraged the physical relationship between CD9 and CD151 and between α3 integrin and other proteins. It is also important in protein interaction with cholesterol-rich domains (Zhu, Luo et al. 2012). Palmitoylation also protects CD151 and CD9 from enzyme digestion in lysosomes and enhances cell-cell contact (Sharma, Yang et al. 2008). Studying the role of palmitoylation of CD9 and CD63 confirmed the need for palmitoylation for tetraspanins interaction with other tetraspanin or with integrins in platelets (Israels and McMillan-Ward 2010). Also, β4 integrin

palmitoylation enhanced CD151-α6β4 integration into secondary tetraspanin interactions with CD9, CD81, CD63 (Yang, Kovalenko et al. 2004).

1.1.4 Glycosylation

In eukaryotic cells, the most common post-translation modification of proteins is glycosylation (Zhao, Takahashi et al. 2008). Glycosylation occurs in most tetraspanins (Levy and Shoham 2005) and CD63 is shown to be highly N-glycosylated (Tominaga, Hagiwara et al. 2014), with three N-linked glycosylation sites. In contrast to other tetraspanins, however, tetraspanin CD81 is non-glycosylated (Levy 2014). The glycosylation occurs mainly in the large extracellular domain (EC2) on putative N-glycosylation sites. Nevertheless, glycosylation could also occur in the small extracellular loop (EC1) of CD9 (Boucheix and Rubinstein 2001). In glycosylated tetraspanins, the glycosylation may be needed to obtain correct protein folding and successful tetraspanin passing from the endoplasmic reticulum (ER) (Scholz, Sauer et al. 2009). Furthermore, it could be essential for tetraspanin function and association with partner proteins: disruption of N-linked -glycosylation sites of CD82 affected cell motility and association with α5 integrin (Ono, Handa et al. 2000). On the other hand, α3β1 integrin glycosylation was shown to be vital in tetraspanin CD151 action (Baldwin, Novitskaya et al. 2008) and has an impact on its association with tetraspanin CD151 and cell motility (Ranjan, Bane et al. 2014). The importance of CD63 glycosylation was indicated in lateral association; CD63-CXCR4 receptor interaction was decreased as a consequence of CD63 glycosylation interruption and consequently led to reduced cell surface level of CXCR4 (Yoshida, Ebina et al. 2009).

1.1.5 Tetraspanin trafficking

The production of tetraspanin proteins, as for many proteins, occurs in the endoplasmic reticulum (ER) (Tsai and Weissman 2010); the transmembrane regions plays a part in the exit of the tetraspanins from the ER. Any alterations in the transmembrane regions of CD9, CD82, CD151and uroplakins (lb) leads to ER retention and prevents the tetraspanin protein reaching cytoplasmic membranes or the plasma membrane (Toyo-oka, Yashiro-Ohtani et al. 1999, Berditchevski, Gilbert et al. 2001, Cannon and Cresswell 2001, Zhou, Liu et al. 2004, Tu, Kong et al. 2006). In some cases, the interaction of tetraspanins with partner proteins in the ER plays a role in their trafficking to the plasma membrane (Berditchevski and Odintsova 2007).

The tetraspanins were first recognized as cell surface markers, but now it is obvious that several tetraspanins are related to the endosomal pathway, for example early and late endosomes, multi-vesicular bodies (MVBs) and lysosomes and also with many type of

secretory vesicles. (Berditchevski and Odintsova 2007, Andreu and Yanez-Mo 2014). The internalization of tetraspanins may occur by endocytosis and transfer into intracellular vesicles. On the other hand, the fusion of these secretory tetraspanin containing vesicles with the cytoplasmic membrane can occur. In the same manner, the fusion of late endosomes and multi-vesicular bodies with the cell membrane may also occur and release tetraspanin protein-enriched exosomes (Andreu and Yanez-Mo 2014).

Tetraspanin internalisation could occur through a tyrosine-based motif YXXØ (where Y indicates tyrosine, X indicates any amino acid and Ø indicates a hydrophobic amino acid) that is found in the CD63 C-tail domain. This motif interacts with adaptor protein (AP) complexes that are involved in CD63 internalisation (Rana and Zoller 2011). However, not all tetraspanins have this motif (e.g. CD9). In addition to CD63, this motif is found in another 12 tetraspanins members. Nevertheless, in about half of these tetraspanins, this motif may be located too close to the plasma membrane spanning regions, which may inhibit the interaction with the AP complex. Other potential sorting motifs are present in some tetraspanins (e.g. di-leucine motifs in tetraspanin RDS, oculospanin and CD231), as reviewed in (Berditchevski and Odintsova 2007). Removing the signal of the supposed tyrosine-based sorting in some tetraspanins did not inhibit their internalisation, however, so the trafficking of these tetraspanins could be independent of the AP pathway or involve the non-cytoplasmic region, for example TM domains, to associate them into appropriate cargo for AP adaptors (Berditchevski and Odintsova 2007). Moreover, it has been hypothesised that the tetraspanins without a tyrosine-based motif or those that cannot mediate tyrosine-based motif/AP complex interactions could rely on their associated partners that have functional YXXØ motif to obtain internalisation (reviewed in (Rana and Zoller 2011).

Tetraspanin CD63 synthesis has been well studied and the role of tetraspanin CD63 in endocytosis was identified early (Marks, Ohno et al. 1997, Bonifacino and Traub 2003). Due to the presence of the GYEM lysosomal targeting/internalisation motif, the C-terminal intracellular domain interacts with various subunits of adaptor proteins (µ2, µ3A, µ3B and µ4). In consequence, CD63 trafficking is linked with the clathrin dependent route and alteration of tyrosine to alanine in this tetraspanin in a rat fibroblast cell line completely abolished CD63 trafficking to lysosomes (Rous, Reaves et al. 2002). Furthermore, syntenin-1, that is associated with CD63, can prevent the AP-2 dependent internalization pathway; moreover, syntenin-1 was shown to interact directly with CD63, and this interaction is driven by the cytoplasmic CD63 C-tail. Increased expression of syntenin-1 lowered constitutive tetraspanin internalization and expressing syntenin-1 mutants in cells completely abolished CD63 internalization (Latysheva, Muratov et al. 2006). More details on this will covered in

the Introduction section of chapter 7. The tetraspanin CD63 is present and transferred between many cellular compartments such as lysosomes, late endosomes, secretory vesicles and the plasma membrane. A number of studies have indicated that CD63-mediated internalization of associated partner proteins may regulate their cell surface expression and activity. For example, it associates with the H-K-ATPase proton pump found in gastric parietal cells and enhances its internalization (Duffield, Kamsteeg et al. 2003). Other tetraspanins may also control expression of their partner proteins by inducing their internalization, as noticed in CD151 and integrins, CD82 and EGFR, reviewed in (Berditchevski and Odintsova 2007).

1.1.6 Tetraspanin function

TEMs have been associated with various cell events including primarily adhesion, motility, cell:cell fusion, intracellular signaling and cell: cell interactions (Figure 1.4) (Yanez-Mo, Barreiro et al. 2009) as well as invasion of cancer (Tarrant, Robb et al. 2003) and apoptosis (Lapalombella, Yeh et al. 2012). Furthermore, tetraspanin proteins are found to be involved in infectious disease pathology (Martin, Roth et al. 2005, Hassuna, Monk et al. 2009, van Spriel and Figdor 2010, Monk and Partridge 2012), for instance viral diseases (Pileri, Uematsu et al. 1998, Shanmukhappa, Kim et al. 2007, Thali 2011, Gui, Wang et al. 2012), prion infection (Griffiths, Heesom et al. 2007), fungal diseases (Rittenour and Harris 2008), parasitic diseases (Yalaoui, Huby et al. 2008, Dang, Yagi et al. 2012, Piratae, Tesana et al. 2012) and bacterial diseases (Tham, Gouin et al. 2010, Green, Monk et al. 2011). In this section, the main implications of tetraspanin proteins involvement in different biological cell functions will be highlighted in more detail.

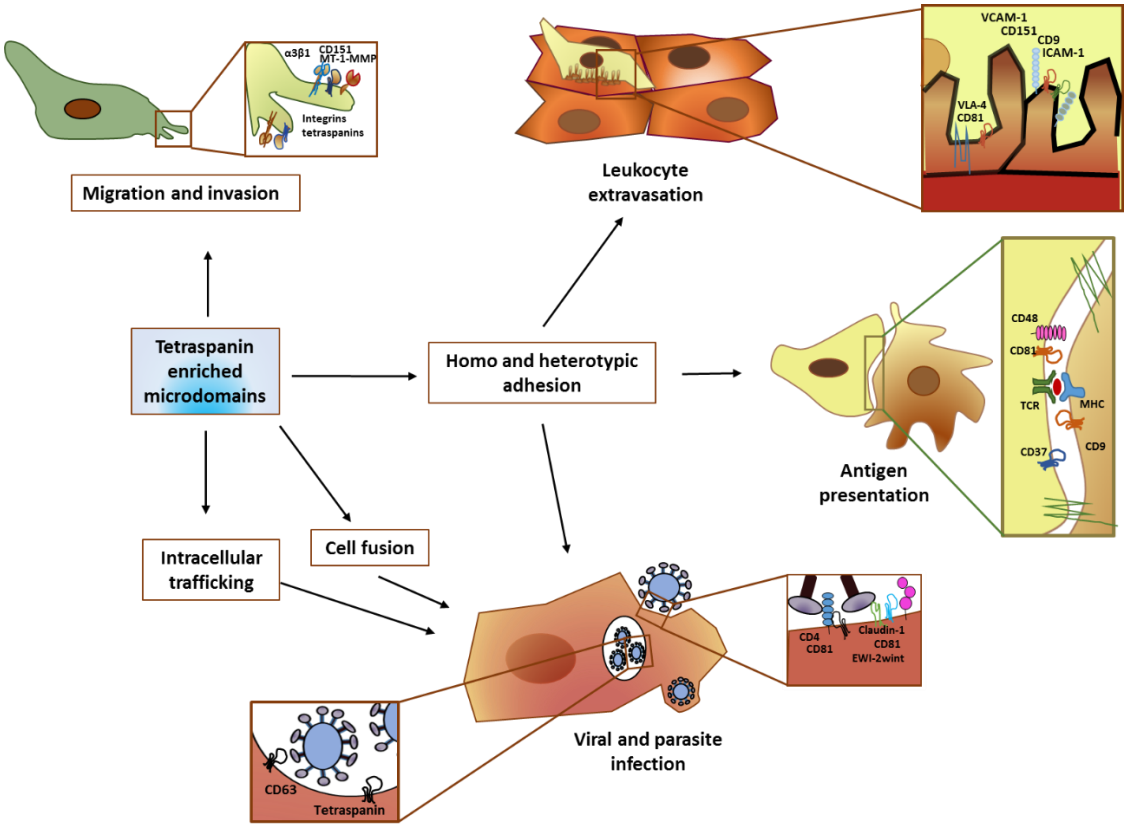

Figure 1.4: Functions of tetraspanin-enriched microdomains (TEMs). TEMs promote adhesion receptor clustering or segregation to mediate different cellular events such as invasion and cell migration, related cell membrane fusion function, intracellular trafficking events. This figure is reproduced with permission from Trends in Cell Biology (Yanez-Mo, Barreiro et al. 2009).

1.1.6.1 Cell adhesion and motility

Tetraspanin microdomains are associated with many of the cellular events related to intercellular adhesion and migration (Mazzocca, Carloni et al. 2002, Barreiro, Yanez-Mo et al. 2005, Yanez-Mo, Sanchez-Madrid et al. 2011). The tetraspanins such as CD9, CD63, CD53, CD82, CD81, CD151 and Tspan-4 (NAG2) engage in primary and secondary interactions with laminin binding integrins including α7β1, α3β1, α6β1, α6β4 and α4 integrins. There is no indication, however, that tetraspanins change the conformation of integrins or their affinity for ligand and the tetraspanins commonly show no effect on stationary cell adhesion, whereas they have significant impact on integrin dependent migration, spreading and cell morphology (Hemler 2003). The best characterized interaction is that of CD151 with α3β1 integrin; this is a direct, primary interaction and it has been studied via site-directed mutagenesis (Berditchevski, Gilbert et al. 2001, Kazarov, Yang et al. 2002). CD151 is also reported to associate with α6 integrin (Kazarov, Yang et al. 2002). Mutations in EC2-CD151 altered primary integrin interactions with α3 and α6 integrins; this did not affect integrin dependent cell adhesion but altered cell spreading and cellular morphology.

Deletion of palmitoylation sites had less impact on primary interaction with α6β3 integrin, but the secondary interactions with other tetraspanins were reduced.

The tetraspanin-web also provides a means for engaging phosphatases, kinases and other signaling molecules which are linked with tetraspanins that might regulate integrin dependent activities. Thus, a variety of tetraspanins were shown to interact with phosphatidylinositol 4-kinase (PI(4)K) and protein kinase C (PKC) isoform, that can enhance aggregation of signaling compounds via binding these enzymes with integrin hetero-dimers (Berditchevski 2001).

Some membrane proteases have been confirmed to reside in TEMs and their location is essential for their co-recruitment with integrins and proteolysis of the extracellular matrix during cell migration (Yanez-Mo, Barreiro et al. 2009). A disintegrin and metalloprotease (ADAM) are another TEMs associated group of proteins which have important roles in cell adhesion and shedding of a rising number of common substrates including adhesion proteins, cytokines, receptors and growth factors, and thus impact on many different types of cell activities (Yanez-Mo, Sanchez-Madrid et al. 2011).

The action of tetraspanins members as adhesion regulators with other associated proteins has been studied. CD9 plays an important role in cell adhesion and is directly associated with ALCAM (a member of the immunoglobulin superfamily of cell adhesion molecules (Ig-CAMs)) on the surface of leukocytes. CD9 was shown to enhance ALCAM function by facilitating clustering of the protein and up-regulating its surface expression (Gilsanz, Sanchez-Martin et al. 2012). Furthermore, it was found that tetraspanin CD151 engages Ras, Ras1, and Cdc42 to the plasma membrane area promoting production of α3β1/ α6β1 integrin-CD151-GTPase complexes that enhance adhesion (Hong, Jeoung et al. 2012). In another study, a role for CD151 in epithelial cell-cell adhesion as a regulator of PKC and Cdc42-dependent actin cytoskeletal reorganization was described (Shigeta, Sanzen et al. 2003). In addition, tetraspanins CD9 and CD151 associate with and have a critical role in the appropriate adhesion function of ICAM-1 and VCAM-1 during trans-endothelial migration and adhesion of white blood cells (WBCs) (Barreiro, Yanez-Mo et al. 2005). Tetraspanin CD63 is also associated with two other proteins MMP-3 and Cdc42 involved in cell adhesion and migration processes (Lee, Hadi et al. 2005).

1.1.6.2 Tetraspanins and the cytoskeleton

The tetraspanin-enriched microdomains can be linked with the cytoskeleton and are associated especially with microvilli and cell to cell contact structures (Yanez-Mo, Barreiro et al. 2009). Binding between tetraspanin CD81 C- terminal domain and the actin linker ezrin-radoxin-moesin (ERM) has been proved and this direct connection works as a linker to connect the actin cytoskeleton with tetraspanin microdomains to regulate cell mobility and division (Sala-Valdes, Ursa et al. 2006). Furthermore, there is evidence for a role for tetraspanins in organizing the formation of large tubular structures in the cell membrane. Tetraspanins and their related proteins localize at tubular structures (adhesion zipper, microvilli, penetration peg and foot processes). It has been suggested that tetraspanins may act as constructional and/or developmental regulators of tubular structures such as microvilli or nanovilli, cell-matrix and cell-cell interfaces membranes tubules and intracellular membrane compartment tubules (Zhang and Huang 2012). Furthermore, CD9 has been found in egg membrane microvilli, which is important in sperm-egg fusion and targeting CD9 leads to changes in the density, length and thickness of microvilli, that lead to sperm losing fusion ability (Runge, Evans et al. 2007). Tetraspanins CD63 and CD9 have been found in "filopodia" of platelets activated by thrombin (Israels and McMillan-Ward 2007). Tetraspanin CD81 is also found in microvilli of the interior side of retinal pigment epithelium cells (Pan, Brown et al. 2007).

Signaling through CD82 in T-cells produces long-term adhesion and membrane extension development and there is an inducible association between CD82 and the cytoskeleton matrix (Lagaudriere-Gesbert, Lebel-Binay et al. 1998). CD82 was shown to regulate the association of lipid rafts with the actin cytoskeleton in T cells which is important for T-cell co-stimulation (Delaguillaumie, Harriague et al. 2004). Finally, in a model of aortic smooth muscle, knocking down CD9 led to cells that were smaller, rounder and less contractile than controls as a result of changes in actin fiber arrangement. This appeared to be related to a role for CD9 in RhoA activation, since levels of GTP-bound (active) Rho were also lowered in the CD9 KD cells. (Herr, Mabry et al. 2014).

1.1.6.3 Fusion

There are essential biological events underlying cell membrane fusion such as sperm-egg fusion, myofibril formation, cell invasion by viruses, formation of multinucleated giant cells and osteoclasts from macrophages and trafficking of intracellular proteins (Le Naour, Rubinstein et al. 2000, Horsley and Pavlath 2004, Fanaei, Monk et al. 2011). Many

researchers have considered the importance of tetraspanins in cell:cell fusion. CD9-/- female mice show an extreme decline in fertility, because sperm lack the ability to integrate with the ovulated eggs in CD9-/- females (Le Naour, Rubinstein et al. 2000). Also, sperm-oocyte fusion is entirely blocked by targeting CD9 with monoclonal anti-CD9 antibody (Miller, Georges-Labouesse et al. 2000). It has also been suggested that the capability of the zona pellucida to merge with sperm could be controlled by production of CD9 by the oocyte (Komorowski, Baranowska et al. 2006). The EC2 region of CD9 is suggested to have a crucial role in male and female gametocytes binding and fertilization (Longhurst, Jacobs et al. 2002, Zhu, Miller et al. 2002, Higginbottom, Takahashi et al. 2003). Several proteins known to associate with tetraspanins may play a role in sperm-oocyte adhesion and fertilization. It was found that the sperm ADAMs and oocyte β1 integrin-associated proteins are involved in sperm-oocyte adhesion and fertilization, and it has been suggested the female gametocyte tetraspanin-web enhances fertilization and promotes connections between ADAMs and integrin (Evans 2001, Takahashi, Bigler et al. 2001, Wong, Zhu et al. 2001). It has also been proposed that the role of CD9 might be to regulate the redistribution of several proteins on the cell membrane in clusters with α6/β1-integrin (Ziyyat, Rubinstein et al. 2006). Other studies have shown a complementary effect of CD9 and CD81 in fertilization events (Sutovsky 2009). In mice, by deleting the CD81 gene, the female fertility was reduced, because of loss of the oocyte ability to bind with sperm, whereas knock out of both CD9 and CD81 lead to complete female sterility (Rubinstein, Ziyyat et al. 2006, Tanigawa, Miyamoto et al. 2008, Sutovsky 2009).

The formation of multinucleated muscle fibers from myoblast fusion is essential for muscle development (Taylor 2000). The tetraspanins CD9 and CD81were shown to be essential to support myotube fusion and maintenance in vitro (Tachibana and Hemler 1999). Furthermore, CD9 and CD81 appear to be involved in controlling muscle cell fusion during muscular regeneration (Charrin, Latil et al. 2013).

Tetraspanins have also been implicated in the fusion of mononuclear phagocytes to form osteoclasts (involved in bone homeostasis) and multinucleated giant cells associated with chronic inflammation or infection, reviewed in (Fanaei, Monk et al. 2011). By targeting CD9 and CD81via mAbs, the giant cell formation induced by Con A stimulation of human monocytes was enhanced (Takeda, Tachibana et al 2003; Parthasarathy, Martin et al 2009). Recombinant CD63 and CD9 EC2 proteins were also shown to prevent giant cells formation, while there was no effect of CD81 EC2 (Parthasarathy, Martin et al. 2009). Knock-out CD9 and CD81 mice spontaneously formed giant cells in alveolar tissue and osteoclasts in the

osseous tissue, suggesting that CD9 and CD81 work cooperatively to inhibit multinuclear cells formation (Takeda, Tachibana et al. 2003). Recent studies from our group using recombinant CD9/CD81 EC2 chimeras, identified a distinct region of CD9 that appears to be involved in regulation human monocyte fusion (Hulme, Higginbottom et al. 2014).

Tetraspanin microdomains may also be important in cell fusion involved in the development of tumor metastasis, whereby cancer cells acquire metastatic properties. Tetraspanins CD81/CD9 along with GTP-binding protein, ADAM10, radixin, α13, RhoA and myosin regulatory light chain where shown to be involved in colon tumor cell fusion regulation (Carloni, Mazzocca et al. 2012).

Fusion can also occur in enveloped viral infections such as HIV-1 virus; the viral envelope protein (Env) attaches to the target cell surface structure and enhances penetration into the cell (Larsson, Bjerregaard et al. 2008). A role for tetraspanins CD81 and CD9 in HIV-1Env-cell membrane fusion was indicated by the finding that when the CD9 and CD81expression is knocked down, the formation of syncytia and viral entrance are increased (Gordón-Alonso, Yañez-Mó et al. 2006). Recent overexpression and microscopy studies indicate that CD9 and CD63 negatively regulates HIV-induced fusion by inhibiting a particular stage of the fusion process (Symeonides, Lambele et al. 2014). Also, the Env viral protein is able to induce formation of multinuclear syncytia resulting from the fusion between infected cells and non-infected cells, yet the syncytia forming mechanism is still poorly understood (Fanaei, Monk et al. 2011). In canine distemper virus (CDV) infected cells, studies using anti-CD9 antibodies indicate CD9 acts as a cell-cell fusion regulator by restricting access of the viral fusion machinery at cell: cell contact regions (Singethan, Muller et al. 2008). More recent work showed that tetraspanins appear to regulate fusion induced by *Burkholderia* bacteria (Elgawidi, 2016, PhD thesis, University of Sheffield).

1.1.6.4 The role of tetraspanins in cancer

Various studies of human tumors and cancer cell lines have shown a role for tetraspanin proteins in promoting or suppressing tumor adhesion, invasion, migration, angiogenesis and metastasis, and targeting particular tetraspanins could have value in terms of cancer treatment or prognosis. Their involvement in cancer appears in many cases to be related to their interaction with proteins involved in cell adhesion and migration (integrins, membrane proteases) and signaling molecules. Some tetraspanins, for instance CD151, appear to promote cancer development and metastasis and their expression is associated with poor prognosis, whereas others (e.g. CD82) are described as metastasis suppressors. A full analysis

of the role of tetraspanins in cancers is outside the scope of this introduction but is covered in recent reviews (Wang, Li et al. 2011, Sala-Valdes, Ailane et al. 2012, Hemler 2014).

1.1.6.5 Tetraspanins and infections

The tetraspanins have important roles in infectious disease pathology (Martin, Roth et al. 2005, Hassuna, Monk et al. 2009, van Spriel and Figdor 2010, Monk and Partridge 2012). Their involvement in viral diseases has long been recognized e.g. HCV, HIV, influenza virus, white spot syndrome virus (WSSV), and porcine reproductive and respiratory syndrome virus (PRRS) (Pileri, Uematsu et al. 1998, Shanmukhappa, Kim et al. 2007, Thali 2011, Gui, Wang et al. 2012). However they may also be involved in prion infection (Griffiths, Heesom et al. 2007) and roles in bacterial diseases such as *Neisseria meningitidis*, *Listeria monocytogenes* (Tham, Gouin et al. 2010, Green, Monk et al. 2011, Martinez del Hoyo, Ramirez-Huesca et al. 2015) have been reported. They are also linked to fungal diseases such as *Aspergillus* and *Candida* infection (Artavanis-Tsakonas, Kasperkovitz et al. 2011) and parasitic diseases such as malaria, human liver fluke and *Echinococcosis* (Yalaoui, Huby et al. 2008, Dang, Yagi et al. 2012, Piratae, Tesana et al. 2012) (Figure 1.5).

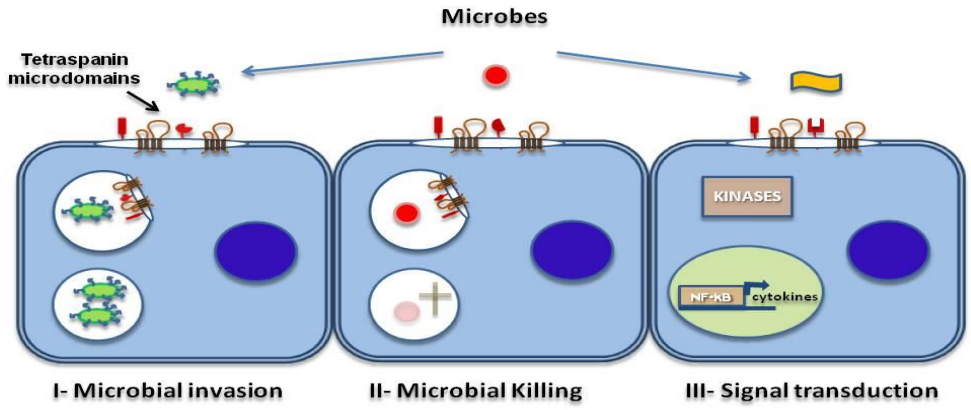

Figure 1.5: The role of tetraspanins in microbial infections explaining the possible mechanisms. I- Using TEMs by microbe to invade the host cell. II- The cooperative role of tetraspanins and receptors to kill the microbes. III- Tetraspanins modulate signaling pathway and interfere with production of cytokines. Figure modified with permission from Microbes and Infection (van Spriel and Figdor, 2010).

1.1.6.5.1 Tetraspanins and viral diseases

The tetraspanins are involved in many stages of viral infections including attachment, development of syncytia and exit of the virus (Martin, Roth et al. 2005, Martin, Roth et al. 2005, Meuleman, Hesselgesser et al. 2008, van Spriel and Figdor 2010, Monk and Partridge 2012). As will be described below, I am going to consider the best characterized examples for viral infection such as HCV and HIV infection.

1.1.6.5.1.1 Hepatitis C Virus (HCV)

The hepatitis C virus is the main cause of viral hepatitis and this infection occurs in 3% of the global population. Chronic HCV infection is the primary cause of hepatic disease, which includes cirrhosis, fibrosis and hepatocellular carcinoma (Bartosch and Dubuisson 2010, Feneant, Levy et al. 2014). In addition, it is related to B lymphocyte proliferative disorder and cryoglobulinemia (Pileri, Uematsu et al. 1998). The hepatocytes are the main target of this RNA enveloped virus. A complex sequence of steps occurs to initiate and develop HCV infection in which tetraspanin CD81 takes a part (reviewed in (Feneant, Levy et al. 2014)). The envelope protein of HCV (E2) attaches to CD81, which acts as a virus co- receptor for human cells and is expressed on hepatocytes and lymphocytes (Pileri, Uematsu et al. 1998). Prevention of attachment between CD81 and HCV E2 is one key point to prevent virus entry and the basis for production of drugs for HCV disease treatment (Ziegler, Kronenberger et al. 2009). By targeting the HCV E2 and their receptors in the cell (CD81 and low density lipoprotein receptor (LDLR)) via siRNAs, the number of HCV particles in infected cells is decreased significantly (Jahan, Khaliq et al. 2011, Jahan, Samreen et al. 2011, Davis, Harris et al. 2012). CD81 de-palmitoylation also reduces the sensitivity of target cells to HCV (Zhu, Luo et al. 2012).The interaction of HCV E2 with CD81 has also been implicated in the down-regulation of IL-2 secretion by T-cells, by targeting the translocation of protein kinase C beta (which is required for IL-2 secretion) to lipid rafts. This may provide a new mechanism for HCV to avoid the immune response (Petrovic, Stamataki et al. 2011). The formation of claudin-CD81 complexes plays a role in virus trafficking and enhances virus entry (Harris, Davis et al. 2010, Farquhar, Harris et al. 2011, Farquhar, Hu et al. 2012). An essential role for CD81 residues T149, T153 and E152 in the association of claudin-1 and infection with HCV was found (Davis, Harris et al. 2012).

1.1.6.5.1.2 Human immunodeficiency virus (HIV)

HIV-1 is a venereal viral disease; in the early stages, it infects lymphatic tissue to set up a persistent infection and this tissue acts as producer and reservoir of the virus in an active

process which gradually exhausts the immune systems CD4+ T cells and macrophages to set the stage for AIDS (Haase 1999, Li, Dziuba et al. 2011). In macrophages, the tetraspanin CD63 seems to have an important role in production of HIV-1, either in early post invasion or during the reverse transcription phase (Li, Dziuba et al. 2011). Knocking-down CD63 in macrophages reduced infection by laboratory strains of HIV and in CD4+ve T cells led to a significant decrease of virus production in these cells (Li, Endsley et al. 2014). In contrast, other research has found that tetraspanin CD63 expression is not essential "at least in tissue culture" for HIV-1 infection or replication (Ruiz-Mateos, Pelchen-Matthews et al. 2008). The exit of HIV-1 from T lymphocytes is reported to involve TEMs. The tetraspanins CD81, CD63 and to a smaller extent CD9 are inducted into the virological synapse, thus, targeting those tetraspanins decreases viral spread (Jolly and Sattentau 2007). Other data using antibodies and specific knock-down have shown TEMs in T lymphocytes, in particular CD81, are important in release of HIV-1 and of HIV replication (Grigorov, Attuil-Audenis et al. 2009). As mentioned previously (1.1.6.3) CD81 and CD9 may also play a part in negatively regulating membrane fusion induced by the HIV-1 envelope protein Env (Gordon-Alonso, Yanez-Mo et al. 2006). Tetraspanin over-expression also down-regulated syncytium formation and this also required viral Gag, which is required for the engagement of Env to TEMs (Weng, Krementsov et al. 2009). In dendritic cells, HIV-1 was shown to be internalized into a non-lysosomal and non-conventional endocytic compartment containing tetraspanins. It may selectively overturn elements of the intracellular trafficking system that are needed for development of the dendritic cell immunological synapse to enhance its own transference and distribution between cells (Garcia, Pion et al. 2005). Generally, tetraspanins expression, in particular CD81, was shown to be decreased in cells infected with HIV-1, and it has been reported that the HIV-1 viral accessory protein (Vpu) is responsible for CD81 down-regulation in HIV-1 infected T cells and increased HIV-1 virus infectivity (Lambele, Koppensteiner et al. 2015).

1.1.6.5.1.3 Influenza virus

Infection by influenza virus is a major world health worry causing high illness and death rates and economic disadvantage (Perwitasari, Yan et al. 2013). The incorporation of tetraspanins CD9 and CD82 into the viral envelope has been identified; β1 integrin that is associated with tetraspanin was also discovered. A role for the tetraspanin CD81 in influenza A virus uncoating and virus budding has been implicated, since CD81 depletion affected both of these processes; influenza trafficking was also shown to occur in CD63 positive late endosomes (He,Sun et al 2013). A recent study found that TEMs were involved in infection by Corona

viruses and low pathogenic type A influenza virus; cleavage of viral glycoproteins (priming) prior to virus: membrane fusion occurred in TEMs which contained virus receptors and priming proteases (Earnest, Hantak et al. 2015).

1.1.5.5.1.4 Other viral infections

There are many studies investigating the importance of tetraspanins in viral diseases apart from all those mentioned previously in this review. An association of tetraspanin CD9 in adeno-associated virus (AAV) infection that causes breast cancer was investigated (Kurzeder, Koppold et al. 2007). The relation of tetraspanin CD82 with adhesion of human T cell lymphotrophic virus, type1(HTLV-1) and the importance of intracellular tetraspanin domains of CD81 and CD82 in mediation of this virus Gag protein with TEMs is suggested (Pique, Lagaudriere-Gesbert et al. 2000, Mazurov, Heidecker et al. 2006, Mazurov, Heidecker et al. 2007). Furthermore, CD151 is reported to be associated with different stages of human papilloma virus (HPV) infection (reviewed in (Scheffer, Berditchevski et al. 2014). The tetraspanin CD151 is also suggested to participate in infection by porcine reproductive and respiratory syndrome virus (PRRSV) in cell culture (Shanmukhappa, Kim et al. 2007).

1.1.6.5.2 Tetraspanin and prion diseases

The term prion related protein (PrP) is used to define active infectious proteins which cause a spongiform encephalopathy in humans and animals (Lantos 1992, Caughey and Chesebro 1997, Edskes and Wickner 2004). TEMs have been implicated in PrP (s) trafficking and internalization (Griffiths, Heesom et al. 2007). In addition an interaction between tetraspanin-7 (CD231) and cellular prion protein has been suggested with PrP(C) binding with CD231 through the region in bovine PrP (154-182) containing α-helix 1(Guo, Huang et al. 2008). The up-regulation of tetraspanin protein CD9, usually expressed in nervous system cells, may play a part in glial cells degeneration of mice with transmissible spongiform encephalopathy (Doh-Ura, Mekada et al. 2000).

1.1.6.5.3 Tetraspanin and fungal diseases

Frequently opportunistic diseases are caused by fungi, which live in normal individuals commensally. Yet, these may be able to induce infections if the host immune status is changed (Bar, Gladiator et al. 2012). Various studies have shown interactions of fungal pattern-recognition receptor (F-PRRs) and tetraspanins in a variety of antigen presenting cells such as B cell, monocytes, neutrophils and macrophages (Figdor and van Spriel 2010). Dectin-1

molecules play an essential role in starting the immune responses against fungi and tetraspanins CD63 and CD37 are suggested to interact with human Dectin-1 (van Spriel and Figdor 2010). Another study reports that CD37-deficient mice have obviously improved protection against *Candida albicans* infection compared with wild type mice (van Spriel, Sofi et al. 2009). Another lethal disease in immune deficient patients is the *Cryptococcus neoformans* fungal infection (de, Fontes et al. 2016). The tetraspanin CD63 was shown to be recruited to phagosomes containing *C. neoformans* independently of MHC class II and LAMP-1 (Artavanis-Tsakonas, Love et al. 2006). Furthermore, CD82 was also shown to be recruited to *Cryptococcus neoformans*-containing phagosomes before it fuses with lysosomes (Artavanis-Tsakonas, Kasperkovitz et al. 2011).

1.1.6.5.4 Tetraspanin and protozoal infection

Protozoal diseases are one of the most fatal types of infections, in particular malaria, a disease that is caused by the genus *Plasmodium*. This protozoa causes millions of deaths annually (Craft 2008). The liver cells are the main initial targets from this parasite, which forms a parasite oophorous vesicle and is then transmitted into red blood cells as an invasive merozoite leading to the appearance of malarial clinical signs (Silvie, Rubinstein et al. 2003). The tetraspanin CD81 is essential for invasion and infection of the liver cells via sporozoites (Silvie, Rubinstein et al. 2003, Monk and Partridge 2012). Another study found that the infection with malarial parasites depends on the type of infected cells; for some cells the *Plasmodium berghei* infection does not rely on tetraspanin CD81 or membrane cholesterol of host cells, whilst in other cells they play an important role for this parasite infection (Silvie, Franetich et al. 2007). The interaction between tetraspanin CD81 and one of its partner proteins EWI-F in hepatocytes was found to negatively affect the function of this tetraspanin in *P. yoelii* infection (Charrin, Yalaoui et al. 2009). Recently, increasing levels of immunoglobulin E autoantibodies to the brain 14-3-3 epsilon protein was recognized in *Plasmodium falciparum* subclinical malaria. This protein is able to bind to tetraspanin CD81 and IgE antibodies to it may interfere with CD81-dependent entry of the parasite at the liver stage of disease (Duarte, Herbert et al. 2012).

1.1.6.5.5 Tetraspanin and Bacterial infection

One of the first described examples of tetraspanins being involved in bacterial infections was the role of uroplakin tetraspanins in infection by uropathogenic *E.coli*. The four various uroplakins (Ia, Ib, II and III with Ia and Ib being tetraspanin members) are integral membrane proteins found in membrane plaques that cover the apical urinary epithelium surface of

mammals. The assembly of UPs into the plaques have a special barrier activity for water and toxic substances in urine (Lee 2011). Uropathogenic *Escherichia coli* accounts for 90 percent of total urinary tract infections in humans. The infection is initiated by bacterial adhesion to urothelial cells via lectin type 1-fimbria (FimH) (Katnik-Prastowska, Lis et al. 2014). Many uropathogenic *E. coli* (UPECs) showed the ability to express type 1 and P fimbriae that bind urothelium cell surface receptors. The recognition of two main glycoproteins of urothelial-apical plaques (uroplakins Ia and Ib) was shown in type 1-fimbrinated UPECSs (Wu, Sun et al. 1996, Min, Stolz et al. 2002, Wang, Min et al. 2009, Lee 2011). The specific binding of FimH to mannose-rich glycans connected to Asn 169 of 1a uroplakin was demonstrated. The binding of the uroplakin embedded membrane and a bacterial envelope has been indicated by EM studies. The shedding of necrotic and/or damaged epithelial cells follows the binding of positive FimH Pilli bacteria and the epithelial cells of urinary bladder. This appears as a part of innate immune response against the infection. Survival of the bacteria may occur through invasion of deep layers, however, in which the bacteria are able to replicate leading to latent or persistent infections and antibiotic avoidance (reviewed in Monk and Partridge 2012).

The interaction of TEMs in the plasma membrane may include bacterial adhesion receptors. The essential role of tetraspanin proteins in bacteria adhesion to epithelial cells has been suggested by studying the role of tetraspanins CD9 and CD63 in the adhesion of *Neisseria meningitidis* and other species of bacteria such as *Neisseria lactamica*, *Streptococcus pneumonia*, *Escherichia coli*, and *Staphylococcus aureus*. It was found that the tetraspanins are needed for optimal bacterial adhesion (Green, Monk et al. 2011). Furthermore, other research using siRNA has shown the role of tetraspanin CD81 in *Listeria monocytogenes* invasion into host cells, possibly through its recruitment of Type II phosphoinositol kinases 4 (PI4KIIβ) to entry sites (Tham, Gouin et al. 2010). Association of CD81 with Rac was also shown to regulate both non-specific and acquired immune responses against bacterial infections. Generalized Listeriosis was decreased in CD81-KO compared with WT infected mice; this result was shown to be correlated with high number of splenic monocytes and dendritic cells in CD81-KO mice. In addition, the CD81 suppresses Rac activation resulting in decreased expression of both TNF-α and NO in dendritic inflammatory cells (Martinez del Hoyo, Ramirez-Huesca et al. 2015).

Chlamydia is an obligate intracellular pathogen which causes a venereal diseases, atypical pneumonia and eye infections This pathogen grows only in a vacuole called an inclusion body; and within this vacuole the bacteria acquires important survival resources from the host cell (Valdivia 2008). An association between Chlamydia inclusion body and selective

delivery of CD63 from MVBs was reported and suggested to be involved the supply of lipids needed for bacterial survival and infection, since treatment with anti-CD63 antibodies reduced Chlamydia production (Beatty 2006, Valdivia 2008). However later studies by the same group failed to find a direct link with CD63 (Beatty 2008).

1.2 *Salmonella* infection

Salmonella is one of the Gram negative bacilli linked with human and animal diseases (Sánchez-Vargas, Abu-El-Haija et al. 2011) and this bacteria can grow and survive in various environments (Spector and Kenyon 2012). The early discovery of genus *Salmonella* dates back to 1885 when both Daniel E. Salmon and Theobald Smith (American Veterinary pathologist and his assistant respectively) had been searching for the causative agent of hog cholera that led them to discover what it so called *Salmonella cholerae-suis* (Fabrega and Vila 2013). Infection with *Salmonella* species is widespread (Santhi, Sunkoji et al. 2012) throughout Eastern and Western countries with a high death rate in poorest countries. The bacteria are characterized by the ability to invade phagocytic and non-phagocytic cells such as intestinal epithelial cells. After host cell invasion by *Salmonella*, these bacteria localize inside a membrane vesicle called the *Salmonella*-containing vacuole (SCVs) (Finlay, Ruschkowski et al. 1991, Lajarin, Rubio et al. 1996, Martinez-Lorenzo, Meresse et al. 2001, Sánchez-Vargas, Abu-El-Haija et al. 2011).

1.2.1 *Salmonella* classification

Classification and update of *Salmonella* bacteria is defined by the Collaborating Center of World Health Organization (WHO) for *Salmonella* Reference and Research that present in Pasteur Institute, France, Paris, according to Kauffmann-White scheme (Issenhuth-Jeanjean, Roggentin et al. 2014). Despite the complexity of *Salmonella* classification (Brenner, Villar et al. 2000), according to Kauffmann-White scheme, the *Salmonella* genus is classified into two species *S. bongori*, and *S. enterica* then sub-classified into 6 subspecies: *S. enterica subsp. enterica, S. enterica subsp. salamae, S. enterica subsp. arizonae, S. enterica subsp. diarizonae, S. enterica subsp. houtenae and S. enterica subsp. indica*. The *S. enterica subsp*. enterica group contains most *Salmonella* bacteria related to human and domestic animal diseases, while other *S. enterica* subspecies with *S. bongori* were found in the environment and in cold-blooded animals (Fabrega and Vila 2013). Otherwise, the flagellar H and O lipopolysaccharide (LPS) antigens are also used to classify *Salmonella enterica* bacteria into 2,637 serotypes including both typhoid (human specific pathogen) and non-typhoid related serotypes (Issenhuth-Jeanjean, Roggentin et al. 2014, LaRock, Chaudhary et al. 2015). This

includes 1586 serotypes belonging to *S. enterica* subsp. *enterica*, while 22 serotypes belong to *S. bongori* species (Issenhuth-Jeanjean, Roggentin et al. 2014).

1.2.2 *Salmonella* pathogenesis

According to the World Health Organization (WHO), tens of millions of foodborne infections are caused by non-typhoid *Salmonella* (NTS) resulting in hundreds of thousand deaths each year (http://www.who.int/mediacentre/factsheets/fs139/en/). Different *Salmonella enterica* serovar exhibit different species specificity; *Salmonella enterica* serovar Typhi and *Salmonella enterica* serovar Paratyphi (A and B) affect only humans and cause a systemic disease called typhoid fever, that is associated with increased body temperature, headache, temporary diarrhea or constipation and abdominal pain (Ohl and Miller 2001); this infection could lead to lethal damage in the liver, spleen, pulmonary and/or nervous organs. The case fatality rate in non treated patients could reach 10-20% and drop to 1% in properly treated patients (Fabrega and Vila 2013). The non-typhoid serotypes (NTS) such as *S. enterica* subsp. *enterica* serotype Enteritidis and *S. enterica* subsp. *enterica* serotype Typhimurium have a wide range of specificity and cause infection in both human and animals, causing gastroenteritis in humans and domestic animals (LaRock, Chaudhary et al. 2015). In mice, *S.* serovar Typhimurium causes a typhoid-like systemic disease (Coburn, Grassl et al. 2007). However, they could also cause bacteremia and generalized infection in immunocompromised patients (Feasey, Dougan et al. , Gordon 2008, Dhanoa and Fatt 2009, Dadwal, Tegtmeier et al. 2011), in particular, in very young and older populations and rarely in adults individuals and animals in good health (LaRock, Chaudhary et al. 2015). *Salmonella* infections cause a various range of illness such as fever, diarrhea (with or without blood as a consequence of lower intestine inflammation), abdominal pain and, usually, nausea and vomiting, thus, it is difficult to distinguish, depending on these clinical signs, between gastroenteritis that is caused by enteric *Salmonella* from other enteric bacterial pathogens (Coburn, Grassl et al. 2007).

Salmonella infection usually occurs by oral ingesting of contaminated food or water and resisting the gastric acidic environment to pass to invade epithelial cells of the intestine. Here, NTS strains provoke inflammatory changes in these cells, including neutrophil and fluid infiltration into the lumen of intestine (LaRock, Chaudhary et al. 2015). Relatively high numbers of bacteria, about 50,000 ingested bacteria for 6-72 hours incubaton time are needed to intiate *Salmonella* infection depending on inoculum and host susceptibility (Fabrega and Vila 2013). The systemic infection is generated initially by *Salmonella* invasion of intestinal epithelial cells, particularly in the distal ileum and probably the cecum at the sites covering

Peyer's patches (PPs) (Carter and Collins 1974). This invasion process occurs effectively through luminal microfold cells (M-cells) (Jones, Ghori et al. 1994, Rescigno, Urbano et al. 2001), and bacteria reach the mesantric lymph node through PPs by mesantric vessels that allows the initiation of systemic infection. *Salmonella* can be phagocytosed by different cells including dendritic cells (DCs), neutrophils and macrophages differentiated from inflammatory monocytes; the last two types of cells are aquired from blood as a response to inflammatary signals (Cheminay, Chakravortty et al. 2004, Johansson, Ingman et al. 2006, Fabrega and Vila 2013). However, DCs can directly take up *Salmonella* from the intestinal lumen by a different mechanisum, which invovles opening epithelial cell tight junctions and presenting its dendrites outside the epithelium to directly contact and phagocytose bacteria (Rescigno, Urbano et al. 2001). Once *Salmonella* has invaded the intestinal epithelium, and is contained in salmonella-containing vesicles (SCVs); some of these then trans-cytose to the epithelial basolateral membranse and cross these cells to be engulfed by phagocytes. Migration of these phagocytic cells through the blood stream enhances systemic infection (Figure 1.6) (Muller, Kaiser et al. 2012).

Bacteraemia develops in approximately 5% of individuals with gastroenteritis caused by NTS, a severe and potentially lethal problem that occurs particularly in immunocompromised pationts: old and young patients, HIV infected patients and those with chronic illness. Such patients are more at risk of developing focal infections as well (Hohmann 2001), such as septic artheritis, meningitis, osteomylitis, pericarditis and endocarditis, penumonia and cholangitis (Lee, Puthucheary et al. 1999, Zaidi, Bachur et al. 1999, Hohmann 2001, Gulan, Jotanovic et al. 2010, Lakew, Girma et al. 2013, Uygur, Reddy et al. 2013, Ortiz, Siegal et al. 2014, Khan, Kumar et al. 2015). Furthermore, development of endarteritis particularly that associated with the abdominal aorta in adults is a serious complication of *Salmonella* bacteraemia (Hohmann 2001, Fabrega and Vila 2013). By contrast, the fatality rate due to NTS infection is about 24% in 3rd world countries, where infections by *Salmonella* contribute to diarrhea morbidity and mortality and are a common cause of hospital admissions among children, and a frequent cause of bacteremia. Symptoms in children are often severe, for instance increased inflammation, bloody diarrhea, with longer infection times and a higher risk of complications arising (Mandomando, Macete et al. 2009, Mtove, Amos et al. 2010, Ansari, Sherchand et al. 2012).

Also clinically important is the existence of a carrier state for NTS infection, which is evident in NTS in human and farm animals (Monack 2012, Fabrega and Vila 2013). This is often associated with production of biofilms and asymptomatic carriers can act as a

reservoirs of infection and spreading the disease (Fabrega and Vila 2013). The carrier form of the disease has been investigated using serovar Typhimurium to establish a long-term chronic infection in a mouse model. Using a mouse strain that does not succumb to acute infection, *Salmonella* can be recovered up to 12 months after infection from systemic sites in symptom-free mice. Surviving bacteria, many of which may be in a non-replicative or latent state, were segregated inside tissue macrophages. Bacterial survival in macrophages may therefore enhance persistent infection (Monack 2012).

1.2.3 SPIs and *Salmonella* infection

Salmonella are characterized by the ability to invade phagocytic and non-phagocytic cells such as intestinal epithelial cells. After the host cell invasion by *Salmonella*, these bacteria localize inside a membrane vesicle called the *Salmonella*-containing vacuole (SCV), where they can survive and replicate (Finlay, Ruschkowski et al. 1991, Martinez-Lorenzo, Meresse et al. 2001, Sánchez-Vargas, Abu-El-Haija et al. 2011).

Following interaction between the bacterium and the host cell, entry into non-phagocytic cells involves cytoskeletal rearrangement, membrane ruffling and uptake. Early evidence of *Salmonella* virulence factors described a 35-40 kb area in *Salmonella's* DNA located at centisome 63 that contained the main loci coding for a type 3 secretion system (T3SS, also called contact dependent secretion system) (Shea, Hensel et al. 1996). This region, which corresponded to a pathogenicity island, encoded *Salmonella* virulence factors required for entry into non-phagocytic cells. Another *Salmonella* pathogenicity island (SPI-2), also encoding a T3SS, was shown to be required for intracellular bacterial survival (Ochman, Soncini et al. 1996, Hansen-Wester and Hensel 2001). The T3SS consists of a supra-molecular structure or needle complex that spans the inner and outer membranes of *S.* Typhimurium and directs effector proteins into host cells (Kubori, Matsushima et al. 1998).

The contribution of five *Salmonella* SPIs to the interaction with the host cell have now been discovered (Marcus, Brumell et al. 2000). These, together with other chromosomal and non-chromosomal factors (such as pSLT plasmid, adhesion, flagella and biofilm formation essential proteins) are involved in *Salmonella* virulence and pathogenicity (Fig 1.6) (Fabrega and Vila 2013).

Genes encoded by SPI-1 encode the complex and sophisticated machinery involved in *Salmonella* entrance into non-phagocytic host cells, but also other activities in the infection process, such as multiplication, host responses (including induction of intestinal

inflammation) and biofilm formation (Que, Wu et al. 2013). These effector proteins activate the invasion of host cells mediating the rearrangement of the actin cytoskeleton and enhancing internalization of bacteria. These effectors are translocated into the host cell through the action of the T3SS, called T3SS-1 (Fabrega and Vila 2013). SPI-1 is also associated with the development of SCV, the niche in which *Salmonella* undergo multiplication within the host (Que, Wu et al. 2013).

Genes encoded by SPI-2 are generally more involved in intracellular survival. The SPI-2 T3SS has a vital significance for intracellular *Salmonella* behavior and *Salmonella* pathogenicity in animal models of systemic infection (Liss and Hensel 2015). Internalized *Salmonella* use this system to translocate more than 30 proteins over the membrane of the SCV, which cooperatively enhance the viability and multiplication of *Salmonella* inside this organelle (Figueira and Holden 2012, Liss and Hensel 2015). SPI-2 contains two segments, small and large, and the large segment of SPI-2 encodes genes important in providing *Salmonella* with a suitable environment inside the SCV within epithelial and macrophage host cells (Fabrega and Vila 2013). It is also responsible for modulating infected host cells signaling pathways and altering infected cells behavior (Agbor and McCormick 2011). Less is known about the small segment, but the genes may confer a growth advantage over the host microbiota (Hensel, Nikolaus et al. 1999, Marcus, Brumell et al. 2000, Winter, Thiennimitr et al. 2010).

Less research has been carried out on SPIs other than SPI-1 and SPI-2. SPI-3 has only four ORFs encoding proteins with no clear functional association between them, but it seems to be involved in the initial attachment, long term persistence and bacterial survival during systemic infection. SPI-4 also plays a role in initial contact with intestinal epithelium and has a probable role in long term persistent infection. SPI-5 is implicated in numerous pathogenic processes throughout infection (Fabrega and Vila 2013).

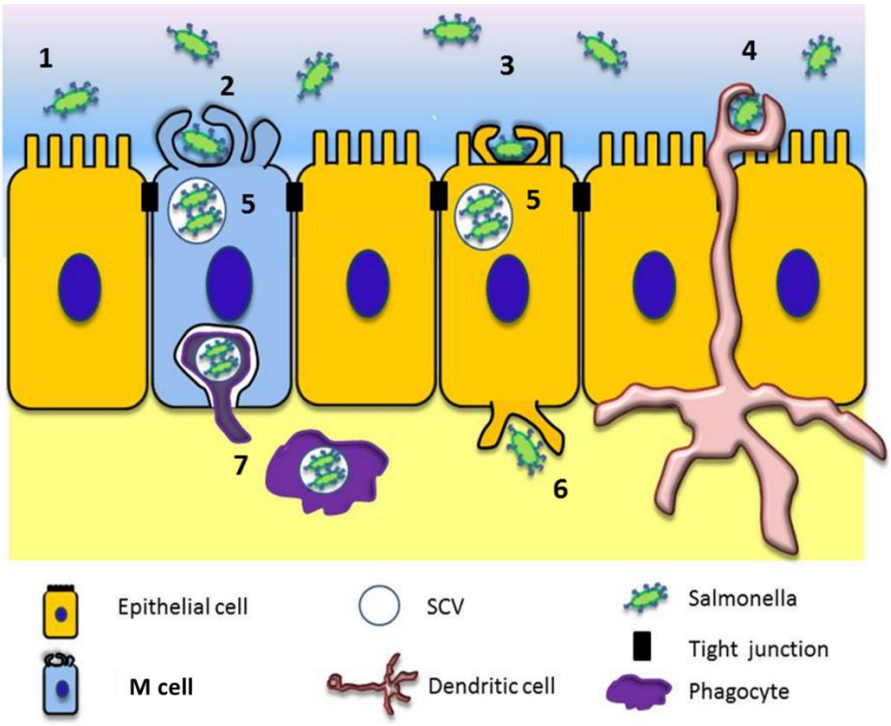

Figure 1.6: *Salmonella enterica* serotype Typhimurium pathogenicity model. 1. Attachment of *Salmonella* to epithelial cells mediated by SPI-3 and SPI-4 encoded proteins**. 2 and 3** *Salmonella* invasion and uptake mediated by SPI-1 and SPI-5 T3SS effectors. **4:** direct uptake of *Salmonella* by dendritic cells. **5:** intracellular *Salmonella* present within SCV, factors encoded by SPI-2 and the pSLT plasmid enhance *Salmonella* survival and replication within SCV. **6:** Release *Salmonella* after transcytosis of SCVs to host cell basolateral membrane. 7: *Salmonella* are uptaken by phagocytes and present inside SCV, pSLT plasmid, SPI-2 and SPI-3 play a role in this process. Modified from (Fabrega and Vila 2013)

1.2.4 Adhesion and uptake

Salmonella bacteria have the ability to infect non phagocytic cells by a sequence of steps starting from adhesion of bacteria to host cells and activation of *Salmonella* T3SS-1, spreading a wave of effector proteins into the cell and triggering the rearrangement of the host cells actin-cytoskeleton, which is has a vital role in bacterial invasion (Misselwitz, Kreibich et al. 2011). Different virulence elements are involved in establishing close *Salmonella* attachment to host cells. Although the Salmonella Typhimurium genome contains a number of different fimbrial operons, little is known about the targets of most of these on host cells (reviewed in Fabrega and Vila 2013). Type-1 fimbriae are encoded by the *fim* genes and the major subunit FimA, adhesions FimI and FimH, and adaptor FimF are the main structural units vital to type-1 fimbriae assembly in serovar Typhimurium (Zeiner, Dwyer et al. 2012). These mediate attachment to the extracellular matrix through binding to oligomannose side chains of the laminin network, with poor adhesion to host fibronectin, type-1, type-3, type-4 or type-5 collagen (Kukkonen, Raunio et al. 1993). However, curli fimbriae (aka SEF-17) appear to be involved in the binding of *S.* Enteritidis to eukaryotic extracellular matrix protein fibronectin (Collinson, Doig et al. 1993). *Pef* fimbriae, encoded

by the *pef* genes on *S.* Typhimurium virulence plasmid, showed to bind to the trisaccharide Lewis X blood group antigen, which is expressed on intestinal crypt epithelial cells (Chessa, Dorsey et al. 2008).

The *Salmonella* autotransporter protein *MisL* is an example of a *Salmonella* protein encoded by SPI-3 that may contribute to the bacterial adhesion process through binding with eukaryotic extracellular matrix fibronectin. This binding was found to enhance colonisation of intestine epithelial cells (Dorsey, Laarakker et al. 2005). The outer membrane protein PagN has also been shown to involve in *S.* Typhimurium uptake, probably through adhesion to heparan sulphate proteoglycans on host cells (Lambert and Smith, 2009).

The host cell protein PECAM/CD31, which has a high level of mannose sugars, has been shown to be involved with *S.* serovar Typhimurium binding and also has a role in extra-intestinal transmission of *Salmonella* infection to deeper tissues and controlling production of inflammatory cytokines by macrophages infected by *Salmonella*. PECAM-1 knockout mice were less infected with *S.* serovar Typhimurium with lower hepatic, splenic and mesenteric *Salmonella*, and this correlated with decreased levels of tumor necrosis factor (TNF), interleukin-6 (IL-6 and monocyte chemoattractant protein (MCP). The production of IL-6 and TNF was also reduced in macrophages from PECAM-1 KO mice and stimulated with whole *Salmonella*, Toll-like receptor 4 (TLR-4) ligand or poly (I:C) (TLR-3 ligand) in vitro (Lovelace, Yap et al. 2013).

As described before, effector proteins released by T3SS are translocated into the host cells to promote bacterial adhesion and internalization (Hansen-Wester and Hensel 2001, LaRock, Chaudhary et al. 2015). Membrane ruffling and actin cytoskeleton rearrangement are mediated by *Salmonella* to enhance its invasion to non-phagocytes by macropinocytosis. This process is dependent on SPI-1 T3SS that also reverses this action after invasion. In phagocytic cells such as macrophages, *Salmonella* uptake could be either dependent or not dependent on the SPI-1 system (LaRock, Chaudhary et al. 2015). Pattern recognition receptors (PRRs) including scavenger receptors such as CD36, the mannose receptor and members of the Toll-like family may be involved in recognition and uptake of *Salmonella* by the SPI-1 independent pathway. Opsonic receptors (e.g. complement receptors, Fc receptors) facilitate macrophage uptake of bacteria opsonised with complement fragments or antibodies (Drecktrah, Knodler et al. 2006).

Cytoskeletal reorganization leading to bacterial uptake is mediated mainly by translocated effector proteins SopB/SigD, SopE and SopE2 (Wood, Rosqvist et al. 1996, Norris, Wilson et al. 1998, Bakshi, Singh et al. 2000). SopB/SigD is an inositol phosphatase that as well as promoting actin rearrangement manipulates different cellular phospatidylinositol signaling pathways; for example it has an anti-apoptotic activity in epithelial cells (Knodler, Finlay et al. 2005) and protects SCV from cellular lysozome activity (Bakowski, Braun et al. 2010). Structural studies of this effector protein showed that it also interacts with the host cell Rho GTPase Cdc42 that plays a role in actin cytoskeleton dynamics (Burkinshaw, Prehna et al. 2012). SopE and SopE2 also activate the Rho GTPases RAC1 and Cdc42 by stimulating GDP/GTP nucleotide exchange (Friebel, Ilchmann et al. 2001). These bacterial effectors, together with bacterial actin binding proteins SipA and SipC, promote localised actin polymerization and uptake of the bacteria into vacuoles (Schlumberger and Hardt 2006, LaRock, Chaudhary et al. 2015).

1.2.5 Intracellular *Salmonella* survival

After that, the biogenesis and maintenance of this vacuole occurs to avoid entrance of host antimicrobial factors by alteration of cytoskeleton arrangement of the host cells and reduced vascular transport, which plays a role in *Salmonella* replication inside its vacuole. This process is controlled basically by the transporting action of T3SS-2 and its translocation machinery. Effectors encoded inside and outside SPI-2 are translocated to cooperate with the cytoskeleton of the host cells and to encourage achievement of a proper intracellular environment for survival and replication (Fabrega and Vila 2013).

Bacterial uptake occurs quickly after the attachment process and the bacteria are contained in spacious phagosomes that develop into SCV (Oh, Alpuche-Aranda et al. 1996). At this stage, the SPI-2 T3SS effectors are involved in developing and maintaining the SCV and avoiding the entrance of host antimicrobial factors (Steele-Mortimer 2008). This involves changes to the host cell vesicular transport system (for example preventing fusion of lysosomes with the SCV) and cytoskeleton arrangement. Its protein and lipid components are modified and its morphology changed, with association of polymerized actin with the cytosolic membrane, which maintains and stabilizes the SCV, and vascular membrane endosomal tubules, which may allow movement of the SCV within the cell (Martinez-Lorenzo, Meresse et al. 2001, LaRock, Chaudhary et al. 2015).

In the early steps of SCV biogenesis, many endosomal markers are acquired such as early endosomal markers Rab5 and EEA1 and then late endosomal markers such as Rab7, and the

lysosomal glycoproteins LAMP1, LAMP2 and LAMP3 (CD63) as well as the vacuolar ATPase. The involvement of these early and late endosomal markers shows the possible modulation of the endocytic network of the host. *Salmonella* may also exclude other markers from interacting with SCVs, such as mannose-6-phosphate receptor (M6PR). Some SPI-2-T3SS effectors may remove host proteins form the SCV by post-translational modifications such as ubiquitination (LaRock, Chaudhary et al. 2015). Virulent *Salmonella* Typhimurium need to replicate within the SCVs and this requires T3SS-2 effectors, which localise to the SCV and some show enzymatic activities; for example SseJ modifies cholesterol and phospholipids in the membrane. This allows recruitment of SifA which can connect the SCV to microtubular network, allowing trafficking of the SCV in the cell (LaRock, Chaudhary et al. 2015). Host cells infected with *Salmonella* are characterized by the presence of *Salmonella* induced filaments (SIFs), membrane tubular structures enriched in late endosomal marker and formed by alteration and extension of endosomal membranes by effector proteins including SifA. Another pathway has also been shown in which the *Salmonella* causes formation of membrane tubules positive for trans-Golgi-network-derived Scamp3 and it is suggested that the host secretory pathway may also interact with SCV. Endosomal tubules may allow acquisition of components and nutrients needed for bacterial survival. After uptake and migration to the perinuclear area, most SCVs are surrounded by Golgi network membranes in epithelial cells, where replication occurs. The *Salmonella* T3SS2 effectors such as SseG, which localizes to the trans-Golgi is important in this process, reviewed in (da Silva, Cruz et al. 2012).

Recognition of bacterial PAMPs (Pathogen-associated molecular patterns) by Toll-like receptors in macrophages causes acidification in phagosomes which activates SPI-2 genes and effector translocation (Arpaia, Godec et al. 2011, Buckner and Finlay 2011).

1.3 Aims

Previous studies in the laboratory investigated the role of tetraspanins in the uptake of *Salmonella enterica* serovar Typhimurium by human monocyte derived macrophages (MDMs). Specific monoclonal antibodies (mAbs) for various tetraspanins showed different effects, enhancing or inhibiting *Salmonella* binding to cells. The inhibition of *Salmonella* binding to MDMs was shown by using mAb to tetraspanin CD63 and recombinant proteins corresponding to CD63-EC2 and CD9-EC2. In addition, the siRNA-mediated knockdown of CD63 also inhibited *Salmonella* Typhimurium adhesion. Immunofluorescence microscopy used in this study showed that CD63 co-localized with

Salmonella containing vacuoles (SCVs) at different time periods after infection. In this study an important role for tetraspanin CD63 in initial binding of *Salmonella* Typhimurium to macrophage was suggested (Hassuna, 2010).

The aim of the present project was to further investigate the mechanism whereby tetraspanins are involved in *Salmonella* infection of macrophages and non-phagocytic cell lines.

1. Development of a cell line model. One of the drawbacks of the previous work in the laboratory was that it relied on primary human derived macrophages (MDM). These are subject to donor variation and it is difficult to generate these in large amounts. This could be overcome by the use of macrophage cell lines such as J774.2 cells and RAW 247 cells. One problem is that these cell lines are murine and relatively few antibodies to native murine tetraspanins are available. It was therefore also of interest to try to develop a human macrophage cell line model of infection using e.g. THP-1 cells.
2. Investigation of additional tetraspanins. Preliminary work indicated that tetraspanins CD9, and to some extent CD151 and CD37, also affected uptake of *Salmonella* by macrophages, but their mechanisms of action appear different to that of CD63. It was hoped to investigate the roles of these tetraspanins further.
3. Co-localization of tetraspanins and *Salmonella*. Preliminary experiments using confocal microscopy suggested some co-localization of CD63 and *Salmonella* entering macrophages. It was hoped to extend these studies, also for other tetraspanins. Cell lines can more easily be transfected with constructs coding for GFP-tagged tetraspanins for immunofluorescence studies.
4. Attempts were made to develop flow cytometry assays for investigating infections, which would be more objective and permit analysis of large numbers of cells than the conventional microscopy assay previously used.
5. It was also of interest to determine if tetraspanins were involved in adhesion/uptake of *Salmonella* to epithelial cell lines, especially since they have been shown to play a role in adhesion of *N. meningitidis* and other bacteria, including *E. coli* and *S. aureus*, to such cells (Green et al. 2011).

Chapter 2: Materials and methods

2.1 Materials

2.1.1 General materials

Unless stated otherwise, chemical and general reagents were supplied from SLS, Bio-Rad, Sigma and Fisher Scientific, and were analytical grade or equivalent.

2.1.2 Water

All the water used to prepare solutions and buffers was ultrapure deionized sterile water filtered from a Neptune (Purite) System.

2.1.3 Buffers and Solutions

Table 2.1: **Buffers and solutions used.**

Type of buffer	Preparation	Store temperature
1% agarose gel	1g of agarose (MetaPhor agarose, Lonza) in 100ml 1x TAE buffer, dissolved by heating in a microwave.	
10x blotting buffer	144g glycine plus 20.23g Tris, dissolved up to 1L with dH_2O.	RT
1x blotting buffer	100ml 10x blotting buffer, 200ml methanol and 700ml dH_20	RT
5% blocking buffer	5g of skimmed milk powder dissolved in 100ml 1x TBST	4-8 °C
Cell dissociation solution	Cell dissociation solution (SDS) was provided from Sigma (C5914) as 1x solution, 5ml was used for a T75 Flask.	-20 °C for long term 4-8 °C for short term
Cell lysis buffer	0.5% triton x-100 (Sigma) and 0.5% Brij 98 (Acros Organic) in PBS with protease inhibitor Cocktail (Thermo Scientific, 78429).	4-8 °C
Coomassie de-staining solution	400ml methanol, 100ml acetic acid, 500ml dH_2O	RT
Coomassie staining solution	2.5g Brilliant Blue R (Sigma), 500ml absolute methanol, 100ml acetic acid, prepared up to 1L with dH_2O	RT
DAPI staining solution	0.1 % triton x-100, 0.02 % sodium dodecyl sulphate and 0.5 µg /ml of 4, 6-diamidino2-phenyl-indole hydrochloride (DAPI) in PBS.	4-8 °C

FACS buffer (B/B/N)	0.1% sodium azide and 0.2% bovine serum albumin (BSA) in HBSS.	4-8 °C
FIX and PERM®	Fixation and permeabilisation of mammalian cells, ADG, GAS-002 or Invitrogen, GAS004	RT
25mM glutathione elution buffer	30.8mg reduced glutathione, 60.6mg Tris, volume brought up to 10ml with dH_2O and pH adjusted to pH 8.0	4-8 °C
60% glycerol	12ml 100% glycerol, 8ml dH_20. Sterilized by filtration.	RT
60% v/v glycerol stock solution	60ml of 100% glycerol was mixed with 40ml dH_2O and sterilized by autoclaving.	RT
Halt™ Protease inhibitor	Protease inhibitor (to prevent protein degradation) Thermo Scientific, OJ 190691A	4-8 °C
Hanks buffered saline solution (HBSS)	HBSS with/without Ca^{2+} and Mg^{2+} was from Lonza.	RT
2x Laemmle sample buffer (reducing buffer)	50 µl β-ME added to 950 µl sample buffer (BioRad, 161-0737).	RT
Mild stripping buffer for nitrocellulose membranes	15g glycine, 1g SDS, 10ml Tween20 pH adjusted to 2.2 with HCl prepared up to 1L with dH_2O	RT
4X non-reducing protein loading buffer	5ml 0.5M of Tris (pH adjusted to 6.8), 2ml 20% SDS, 4ml glycerol, 1ml 2mg/ml bromophenol	RT
1x PBS	100ml 10x PBS, 900ml dH_20	RT
4% paraformaldehyde solution	4g of paraformaldehyde was dissolved in 50 ml H_2O by adding 1ml of 1M solution NaOH and heating in a water bath for 60 minutes at 60ºC. After cooling, 10 ml of 10x PBS was added, the pH was adjusted to 7.4 and dH_2O added to 100 ml. After mixing, the solution was filtered and stored.	-20 °C for long term 4-8 °C for short term
Permeabilising buffer for confocal microscopy	0.1% saponin, 2% goat serum and 2% bovine serum albumin (BSA) in PBS	4°C
Phosphate buffered saline (PBS), 10x pH 7.2	NaCl 80g, KCl 2g, $Na_2HPO_4$14.4g, KH_2PO_4 /litredH_2O	RT
Propidium iodide stain	1:1000 dilution of propodium iodide (1mg/ml, Sigma, P4864) in PBS	RT
20x SDS-PAGE running buffer	EZ-Run™ running buffer (Fisher Scientific) BP7700-500	RT

4x stacking gel buffer	6.06g Tris, 4ml 10% SDS, pH adjusted to 6.8 with HCl, made up to 100ml with dH_2O	4-8 °C
SDS-PAGE stacking gel	1ml H_2O, 300µl 30% acrylamide, 444 µl 4x stacking buffer, 28µl 10% ammonium persulphate, 5µl TEMED	RT
10x TBS (Tris buffer saline)	24.2g Tris, 87.66g NaCl pH adjusted to 7.6 with HCl prepared up to 1L with dH_2O	RT
1x TBST (TBS with Tween 20)	100ml 10x TBS, 900ml dH_2O and 250µl Tween20	RT
1x trypsin-EDTA solution	This solution was prepared from 10x solution provided from Sigma (59418C) and was diluted 1:10 with HBSS (without phenol red, Mg and Ca).	4-8°C
50X TAE (tri-acetate-EDTA) buffer	242g Tris base, 100ml 0.5M EDTA, 57.1 ml glacial acetic acid, volume adjusted to 1L.	RT
Vectashield Mountiing Medium	To reduce bleaching of fluorescence. Vector Laboratories Inc. H 1000	4-8°C

2.1.4 Bacterial growth media

Table 2.2: Bacterial growth media used.

Media and reagents	Preparation
Lysogeny Broth (LB broth)	10 g of tryptone (Oxoid, LP0042) + 5g of yeast extract (Oxoid, LP0021) + 10g NaCl /1L dH_2O
LB Agar	15g of bacteriological agar (Oxoid, LP0011) / 1L LB broth
Super optimal broth for catabolite repression (SOC) media	The media was from Novagen, (Cat. No. 69319)

2.1.5 Antibiotics

Table 2.3: Anti-microbial reagents used.

Antibiotic	Preparation of stock solution
Ampicillin	Stock solution of 100mg ml^{-1} ampicillin in H_2O, sterilized by filtration.
Carbenicillin	Stock solution of 100mg ml^{-1} of carbenicillin in H_2O, sterilized by filtration.
Chloramphenicol	Stock solution of 34 mg ml^{-1} chloramphenicol in ethyl alcohol, sterilized by filtration.
G418	250mg ml^{-1} stock solution in H_2O was from Gibco (Cat. No. 11811-064).

Kanamycin	Stock solution of 100mg ml^{-1} of Kanamycin in H_2O, sterilized by filtration.
Puromycin	10mg ml^{-1} stock solution in 20 mM HEPES buffer (pH 7.2-7.5) was from Gibco, (Cat. No. A1113803).

2.1.6 Commercial kits used

Table 2.4: Commercial kits used.

Kit name	Purpose	Origen, catalogue number
EZNA plasmid DNA Mini Kit	Small scale extraction of plasmid DNA.	OMEGA, D6942-01
HiSpeed Plasmid Midi Kit	Large scale plasmid DNA purification	Qiagen, 12643
QIAquick®, gel extraction Kit	Extraction and purification of PCR products from agarose gels	Qiagen, 28704
QIAquick®, PCR purification Kit	Purification of PCR product	Qiagen, 28104
Qprep® Spin, Miniprep Kit	Small scale plasmid DNA extraction	Qiagen, 27104
RNeasy® Mini Kit	To extract total RNA from mammalian cells	Qiagen, 74104

2.1.7 Immunological reagents used

2.1.7.1 Primary and secondary Antibodies:

All primary monoclonal antibodies and secondary polyclonal antibodies used are described in Tables 2.5 (A and B) and 2.6 respectively.

Table 2.5 A: Primary antibodies.

Target	Host species, isotype	Working concentration (µg/ml)	Source	Catalogue Number or reference
Human CD9	Mouse IgG1	10	Prof. Peter Andrews, University of Sheffield	*Clone 602.29 (Andrews, Knowles et al. 1981)
Human CD37	Mouse IgG1	10	Prof. Martin Glennie, University of Southampton	WR-17 (Moore, Cooper et al. 1987)
Human CD53	Mouse IgG1	10	AbD serotic	MCA723GT

Human CD63	Mouse IgG1	10	Developmental Studies Hybridoma Bank In House	*Clone H5C6 (Azorsa, Hyman et al. 1991)
Human CD81	Mouse IgG1	10	AbD Serotec	MCA1847
Human CD81	Mouse IgG1	10	Ancell	302-820 (preservative free)
Human CD81	Mouse IgG1	10	BioLegend	349502
Human CD82	Rabbit polyclonal	10	AbD Serotec	AHP1709
Human CD82	Mouse IgG1	10	BioRad	MCA1311
Human CD82	Mouse IgG1	10	B & D system	MAB4616
Human CD82	Rabbit polyclonal	1-10	BioRad	AHP1709
Human CD82	Mouse IgG1	10	BioLegend	342102
Human CD151	Mouse IgG1	10	Prof. Leonie Ashman, University of Newcastle, Australia.	*Clone 14A2 (Fitter, Tetaz et al. 1995)
Human syntenin	Rabbit polyclonal	1-10	Abcam	Ab19903
Mouse CD9	Rat IgG2b	10	AbD Serotec	MCA2749
Mouse CD63	Rat IgG2a	10	Biolegend	143904
Mouse CD81	Hamster, IgG1	10	AbD Serotec	MCA1846
Isotype control	Hamster IgG1	10	BioRad	MCA2356
Isotype control	Mouse IgG1	10	In House	*Clone JC1 (Muranova, Ruzheinikov et al. 2004)
Isotype control	Rat IgG2a	10	Biolegend	400501
Isotype control	Rat IgG2b	10	Biolegend	400601
Salmonella	Rabbit polyclonal	1:80	AbD Seroteic	8209-4006
Salmonella groups A, B, D, E1, E2, E3, E4, L	Rabbit polyclonal	1:20	Difco™	225341

*****Purified from hybridoma supernatants by Bioserv UK Ltd.

Table 2.5 B: Primary conjugated antibodies.

Target	Host species, isotype	Dilution µg/ml	Label	Source	Catalogue Number
GST	Rabbit polyclonal	1:5000	HRP	Sigma	A7340
Human LAMP-1 (CD107a)	Mouse IgG1	1:100	AF® 647	BioLegend	328611
Isotype control	Hamster IgG	10	AF® 647	AbD serotec	MCA2356A647
Isotype control	Rat IgG2a	10	AF® 647	BioLegend	400526
Isotype control	Rat IgG2b	10	AF® 647	AbD serotec	MCA1125A647
Mouse CD9	Rat IgG2a	10	AF® 647	BioLegend	124810
Mouse CD81	Hamster IgG	10	AF® 647	AbD serotec	MCA1846A647
Salmonella enteriditis, S. typhimurium, S. heidelburg	Rabbit IgG	1:1000	FITC	Online.com antibodies	ABIN464723

Table 2.6: Secondary antibodies.

Target	Host species	Dilution	Label	Source	Catalogue Number
Mouse IgG	Goat	1:250	FITC	Sigma	F1010
Mouse polyclonal IgG fraction	Rabbit	1:5000	HRP	Sigma	A9044
Rabbit IgG	Goat	1:320	FITC	Sigma	F9887
Rabbit IgG (H and L)	Goat	1:1000	AF® 647	Abcam	Ab150083
Rabbit IgG	Goat	1:2000	HRP	Sigma	A6154
Rat IgG	Rabbit	1:320	FITC	Sigma	F9387
Rat IgG (H and L)	Goat	1:250	AF® 546	Life technologies	A11081
Rat IgG	Goat	1:5000	HRP	Abcam	Ab97057
Syrian hamster IgG	Goat	1:100	FITC	Abcam	ab6888

2.1.8 Cell line culture and media used

2.1.8.1 Media for tissue culture

Dulbecco's Modified Eagle's Medium (DMEM) media was from Gibco or Lonza. For the RAW cell line DMEM with Glutamax^{TM} was used. For J774, HeLa syntenin KD and control, CD9 KO, CD81 KO and corresponding WT mouse macrophages controls, DMEM with high glucose (4.5 g/litre) was used. For HEC-1B and HeLa cell lines, Eagle's Minimum Essential (EMEM) media (Lonza) was used. For THP-1 cells, RPMI media (Gibco) was used. All media were purchased as 1x solutions and heat inactivated (HI) FCS (Biowest) was added to a final concentration of 10%.

2.1.8.2 Cell line types

2.1.8.2.1 Semi-adherent phagocyte cell lines

RAW 247 cell line: This macrophage cell line was obtained from American Type Culture Collection (ATCC). The cell line was originally established from a Balb/c mouse by Abelson leukemia virus transformation (Ralph and Nakoinz 1977).

J774.2 cell line: This cell line is a mouse BALB/c monocyte/macrophage cell line re-cloned from an original ascites and solid tumor mass J774.1. (Ralph and Nakoinz 1975). This cell line was obtained from the European Collection of Authenticated Cell Cultures (ECACC).

CD9-KO mouse macrophages and corresponding wild type control: The CD9 -/- macrophage cell line and corresponding wild type CD9 +/+ macrophage cell lines were kind gifts from Gabriela Dveksler (Dept. Pathology, Uniformed Services University of the Health Sciences, Bethesda, Maryland, USA) (Ha, Waterhouse et al. 2005).

CD82-KO mouse macrophages and corresponding wild type control: The CD82 -/- macrophage cell line and corresponding wild type CD82 +/+ macrophage cell lines were kindly provided by Professor Jatin Vyas, Harvard Medical School, Boston, USA (Risinger, Custer et al. 2014).

THP-1 cell line: This is an human monocyte cell line derived from a patient with acute monocytic leukemia (Tsuchiya, Yamabe et al. 1980). Current stocks were from ECACC.

2.1.8.2.2 Non phagocytic cell lines

HEC-1B cell line: This is an adherent human endometrial carcinoma epithelial cell line. This sub-strain of HEC-1A that was isolated in 1968 by H. Kuramoto was obtained from ATCC (Kuramoto, Tamura et al. 1972).

HeLa cell line: This is a human epithelial cell line derived from cervix adenocarcinoma (Gey, Coffman et al. 1952, Scherer, Syverton et al. 1953). Current stocks were from ECACC.

HeLa syntenin knockdown (KD) and HeLa wild type (WT) cell lines: These cell lines were kind gifts from Professor Fedor Berditchevski (Institute for Cancer Studies, the University of Birmingham, Birmingham, United Kingdom). Stable knockdown of syntenin expression was achieved using a plasmid expressing shRNA specific for the syntenin gene, whereas control cells were transfected with empty vector (Fedor Berditchevski, personal communication).

2.1.9 *Salmonella* strains used

The bacterial strains used in the experiments were *Salmonella* Typhimurium NCTC 12023 (Le Minor, Veron et al. 1982) (obtained from Professor Rob Read, Department of Infection and Immunity, University of Sheffield), *S.* Typhimurium LT2 (McClelland, Sanderson et al. 2001) (obtained from Professor Jeffery Green, Department of Molecular Biology and Biotechnology). *Salmonella* Typhimurium SL1344 (Hoiseth and Stocker 1981) transformed with pNB57-mCherry was obtained from Prof Dirk Bumann/ Biozentrum/ University of Basel, Switzerland.

2.1.10 Common laboratory instruments and equipment used

All instruments and equipment used are mentioned in table 2.7.

Table 2.7: Common laboratory instruments and equipment used.

Instruments or equipments	Provider
Bench type cooling lab. centrifuge	Sigma
Class II microbiological cabinet	BioMAT^2
Electroporater (Gene Pulsar II), Capacitance Extender Plus and Pulse Controller Plus	BioRad
Flow cytometry	LSR II flow cytometer, Becton Dickinson. FACsAria (cells sorter), Becton Dickinson.
Gel and western blot documentation	ChemiDoc™ MP System, BioRad GelDoc-lt™ imaging system, UVP
Incubators	Scientific laboratory supplies
Liquid Nitrogen dowers (35 HC)	Statebourne BIO 36
Magnetic stirrer with Hot plate	Stuart

Microcentrifuge (L 13)	Sigma
Microscopes	Nikon A1 Confocal inverted system with EM-CCD Camera. Nikon Eclipse 400UV light, Digital camera DXM1200 Nikon inverted light microscope. Olympus inverted microscope. Widefield imaging system (Nikon dual cam system) inverted Ti eclipse with Oka-lab environmental control chamber (for live imaging).
NanoDrop® Spectrophotometer ND-1000	Labtech international
Ori-Block® 08-1 (Heat block)	Techne
Spectrophotometer	WPI
Ultraviolet transilluminator	Comlab
Water deionizer and sterilizer	Neptune PURITE

2.1.11 Common glassware and plasticware

Most of the glassware and plasticware used are described in Table 2.6.

Table 2.8: Glassware and plasticware used.

Type of glassware and plasticware	Provider
Cryovial (1ml)	Nalgene
FluoroDish™	World Precision Instruments, Inc.20110401
Lab-Tek II chamber slide (8 wells)	Nalgene Nunc international
Microscope slides and coverslips	Thermo scientific, SLS and VWR
Pipette tips (20 µl, 200 µl and 1000 µl)	Starlab
Plastic cell scraper	Sarstedt
Round bottom FACS tubes (12x75mm)	Elkay
Small FACS tubes (Titertube® Micro Test Tube)	BioRad, 223-9390
SnakeSkin® Dialysis Tubing, 3.5 MWCO, 16 mm dry I.D.	life technologies, 88242
Tissue Culture Dish 10cm diameter	FALCON®, 353003
Tissue Culture Dish 14.5 cm diameter	Greiner CELL STAR, 639160
Tissue Culture flasks	Greiner

2.1.12 Plasmids

All vectors used are described in Table 2.9.

Table 2.9: Plasmids used.

Plasmid symbol	Gene insert/ tag	Antibiotic resistance marker (bacteria)	Antibiotic resistance marker (mammalian cells)	Source
pVA49/pIN29	DsRed	Chloramphenicol	N/A	Dr Mark Thomas (Department of infection and immunity/ University of Sheffield) (Vergunst, Meijer et al. 2010)
pDS-Red Expression vector II (Clontech)	DsRed	Ampicillin	N/A	Prof Jeffery Green (Department of Molecular Biology and Biotechnology/ University of Sheffield
pBHR-1	GFP	Kanamycin	N/A	Dr Mark Thomas, Department of infection and immunity, University of Sheffield) (Stevens, Ulrich et al. 2005)
pNB57	mCherry	Ampicillin	N/A	* Prof Dirk Bumann (Biozentrum/ University of Basel/ Switzerland)
pGEX-KG-mCD9-EC2-GST	mCD9-EC2-GST	Ampicillin	G418	This work
pCMV6-AV-mCD9-GFP	mCD9-GFP	Ampicillin	G418	ORIGENE (MG226288)
pGEX-KG	Sj-GST	Ampicillin	G418	(Guan and Dixon 1991)

* This plasmid is carrying the promoter for gene STM0474 is described in (Rollenhagen and Bumann 2006) and the GFP_ova was replaced with mCherry in this plasmid to obtain pNB57-mCherry.

2.1.13 Online tools and software

Table 2.10: Software and online tools used.

Imaging software:		
Software name	**Purpose**	**Online link**
Fiji	Image analysis	http://fiji.sc/Fiji
Lucia image processing	DXM 1200 digital camera image capture software	N/A
Nikon elements software	Nikon A1 confocal running and analyzing software Nikon dual cam system running and analyzing software	N/A
NIS-Elements Viewer 4.20	Microscope image viewer	http://www.nikoninstruments.com/en_GB/Products/Software/NIS-Elements-Advanced-Research/NIS-Elements-Viewer
FACS analysis software:		
Software name	**Purpose**	**Online link**

BD FACSDiva 7.0	LSR II flow cytometer acquisition and analysis of data	N/A
BD FACSDiva™	FACsAria acquisition and analysis software.	N/A
CellQuest Pro	FACS Calibur acquisition and analysis of data	N/A
FlowJo	FACS data analysis	http://www.flowjo.com/download-flowjo/
RNA Microarray analysis:		
Software name	**Purpose**	**Online link**
Qlucore Omics Explorer	Microarray analysis software	http://www.qlucore.com/
Transcriptome Analysis Console (TAC) 3.0, 64bit	Microarray analysis software from Affymetrix	http://www.affymetrix.com/estore/catalog/prod760001/AFFY/Transcriptome+Analysis+Console+%28TAC%29+Software;jsessionid=6A6246FDE91D0BB2983675B812CCA9FC.prd01com#1_1
Data and graph analysis:		
Software name	**Purpose**	**Online link**
Graph pad 6 Prism	Data and graphs analysis	http://www.graphpad.com/scientific-software/prism/
Microsoft Office Excel 2010	Data analysis	
DNA and Protein analysis:		
Tools name	**Purpose**	**Online link**
EMBL-EBI Readseq	To read and convert nucleotide sequences	http://www.ebi.ac.uk/Tools/sfc/readseq/
ExPASy	To translate nucleotide sequence to protein sequence	http://web.expasy.org/translate/
ExPASy Boxshade	To shade multisequence alignment	http://www.ch.embnet.org/software/BOX_form.html
MultAline	To align and cluster multiple sequences	http://multalin.toulouse.inra.fr/multalin/multalin.html
PDB	For molecular protein structure	http://www.rcsb.org/pdb/home/home.do
Phyre2	For protein structure prediction	http://www.sbg.bio.ic.ac.uk/phyre2/html/page.cgi?id=index
PyMOL	To visualize and align protein structure in 3D view	https://www.pymol.org/

2.1.14 Materials used for Cloning

2.1.14.1 Strains of bacteria used for cloning and protein expression

Table 2.11: Bacterial strains used in cloning and protein expression.

***E. coli* strains**	**Using purpose**	**Genotype characteristic**
DH5α (Invitrogen, 18263-012)	Sub-cloning	F- Φ80*lac*ZΔM15Δ(*lac*ZYA-*arg*F) U169 *rec*A1 *end*A1 *hsd*R17(r_{K^-},m_{K^+}) *pho*A*sup*E44 *thi*-1 *gyr*A96 *rel*A1 λ-
Rosetta-gami B (Novagen, 71137).	Tetraspanin EC2 expression	F^- *ompT hsdS*$_B$ (r_B^- m_B^-) *gal dcm lacY1 ahpC* (DE3) *gor522*::Tn*10 trxB*pLysSRARE (Cam^R, Kan^R, Tet^R)

2.1.14.2 Data base sequences of cDNA and protein

Table 2.12: Database sequences of cDNA and protein.

Gene	**RefSeq mRNA accession number**	**Uniport protein accession number**	**Expression Vector**	**Bioinformatics website**
GST (Schistosoma japonicum)	-	P08515	pGEX-KG	http://www.uniprot.org/uniprot/P08515
mCD9	NM_007657.3	P40240-1	pGEX-GST-mCD9 EC2	http://www.uniprot.org/uniprot/P40240

2.1.14.3 Primers

Table 2.13: Forward and reverse primers used in subcloning and DNA sequencing. The specific targeting sequences for tetraspanins are shown in bold.

Primer symbol	**Sequence**
mCD9 EC2 for	5'ATTATTGAATTCTA**ACCCACAAGGATGAGGTGA 3'**
mCD9 EC2 rev	5'ATTATTAAGCTTTCA**GATGTGGAACTTGTTGTTGAAG 3'**
*pGEX-F2	5' GAGCTGTTGACAATTAATCATCGG 3'
*pGEX-R1	5' CCGGGAGCTGCATGTGTCAGAGG 3'

* Primers were designed by previous lab member Mr. Ralph Hyde and generated by Genosys. Other primers were generated by Eurofins Genomics.

2.1.14.4 Restriction Enzymes

The restriction enzymes used were *Eco RI-HI* from (New England Biolabs) and *Hind III* from Promega.

2.2 Methods

2.2.1 Mammalian cell culture methods

2.2.1.1 Cell counting

Cell counting was performed using an improved Neubauer hemocytometer.

2.2.1.2 Cell freezing

Freezing was carried out when the cells reached medium log phase. The cells were harvested as described below, centrifuged at 200g for 5 minutes and re-suspended at between 3-10 $x10^6$ /ml in 1ml of freezing solution (10% DMSO and 90% FCS). Then, the mixture was transferred to cryovials. (All manipulations were performed on ice to avoid the toxic effects of DMSO). The vials were placed in a freezing plug (Jencons) for 90 minutes to allow gradual freezing of the cells in the nitrogen vapor in a liquid nitrogen dewar, then transferred to liquid nitrogen.

2.2.1.3 Cell thawing

After removing the cells from liquid nitrogen, they were directly transferred in to warm water until thawed. Then the vial was placed in ice after wiping with 70% ethanol. The vial contents were transferred into a sterile universal tube on ice and 9ml of medium without FCS was added. The cell suspension was centrifuged at 200g for 5 minutes and the cell pellet re-suspended in fresh medium with 10% HI-FCS and transferred to a screw capped flask. Then the flask was incubated at 37ºC.

2.2.1.4 Growth conditions

All cell lines were cultured in flasks at 37º C in a humid environment. RAW247, J774.2 and Hela syntenin KD and Hela WT control were cultured in an atmosphere of 8% CO_2, while HEC-1-B, HeLa, THP-1, CD9 KO and CD82 KO were incubated in 5% CO_2.

2.2.1.5 Cell harvesting and subculture

Cells were harvested and subcultured depending on cell type.

2.2.1.5.1 Adherent cell lines

For cells growing in T75 flasks, the media was removed and the cells were washed once with 10ml HBSS solution (without Ca and Mg). Then, the cells were treated with 3ml trypsin-EDTA or with 5ml Cell Dissociation Solution for 5 to 20 minutes respectively at 37°C until the all cells detached from the flask surface. The trypsin was then deactivated by adding media with 10% HI-FCS.

2.2.1.5.2 Semi-adherent cell lines

The cells were harvested once confluent by using a cell scraper to detach them from the surface then diluted 1:3 or 1:10 into either the same flask or into a new tissue culture flask with fresh media.

2.2.1.5.3 Non-adherent cell lines

Cells were sub-cultured by removing and replacing half of the media and cells in the flask with fresh media (usually the cells were sub-cultured every day to avoid cells overgrowth).

2.2.1.6 Stimulation of THP-1 cells

A stock solution of phorbol myristate acetate (PMA) was prepared in acetone at a concentration of 100µg ml^{-1} (160µM) and stored in aliquots at -20°C. The cells were counted and re-suspended at concentration of 3 x 10^5 ml^{-1} with RPMI media contain 10% HI-FCS and 20ng ml^{-1} PMA. Then the cells were cultured at 37°C for 3 days to induce differentiation to macrophages. After 3days, the PMA containing media was removed and cells were washed with HBSS and harvested as described in 2.2.1.5.1.

2.2.2 Bacterial methods

2.2.2.1 *Salmonella* transformation:

Salmonella enteriditis serovar Typhimurium NCTC12023 and LT2 strains were transformed with fluorescent protein expressing vectors to generate self-fluorescent bacteria.

2.2.2.1.1 Preparation of S. Typhimurium competent cells (for electroporation)

To prepare the electro-competent cells, *Salmonella* strains NCTC12023 and LT2 were cultured in 5 ml LB media overnight then diluted 1:50 into 100 ml LB broth and cultured at 37°C with shaking (250 rpm). Once the culture reached OD_{600} of 0.2, it was separated into two 50 ml pre-cooled Falcon tubes, then centrifuged at 5500g at 4°C for 10 minutes. The supernatant was removed by vacuum pump suction and the pellets were washed three times in 25 ml of pre-cooled 10% glycerol in dH_2O. After the last wash, the pellets were re-suspended in 1ml of pre-cooled 10% glycerol. The competent cells were aliquoted in 50µl volumes in pre-cooled 1.5 ml Eppendorf tubes and stored at -80°C.

2.2.2.1.2 Transformation of Salmonella by Electroporation

The BioRad gene pulser® II electroporation system with Pulse controller was used for Salmonella transformation. As recommended by the manufacturer, 40µl of competent cells were used per electroporation with 1 µl of DNA plasmid. The cell and plasmid mixture was kept on ice in a 1.5 ml Eppendorf tube and then transferred to a pre-cooled electroporation

cuvette (gap 0.2 cm) and placed in the electroporation chamber. The voltage used was 2.4 kv/cm, the capacitance used was 25 µF and the resistance used was 400Ω (pulse controller) for 1.2 msec. 200µl of LB media (without selective antibiotics) was added immediately after electroporation and the cuvette contents were transferred into a 1.5 ml tube and incubated for 2 hours at 37°C with shaking (150rpm). After incubation, 50µl of the cell suspension was plated on LB agar contain selective antibiotics and incubated at 37°C overnight. On the next day, one transformed colony was re-cultured in LB agar for 24 hours for use in further experiments.

2.2.2.1.3 Detecting the fluorescent protein expressing Salmonella by flow cytometry

One single colony of transformed Salmonella was grown in 5ml LB media with selective reagents overnight at 37°C (without shaking). 200µl of the overnight growth was then cultured in 10 ml LB media with selective reagents until the OD_{600} reached 0.4 – 0.5. Then, the bacteria were cooled on ice, centrifuged at 5400g for 5 minutes, washed twice with cold PBS and fixed by adding 500µl of 4% PFA at RT for 15 minutes. The fixed bacteria were analyzed by flow cytometry using an LSR II FACS machine to determine the percentage of fluorescent cells and the intensity of the fluorescence compared with WT control.

2.2.2.1.4 Detecting the fluorescent protein expressing Salmonella by fluorescence microscopy

The transformed *Salmonella* and WT control were prepared as described above. Bacteria were transferred to a glass slide using a full bacteriological loop and left to dry before adding one small drop of Vectashield mountant with DAPI (Table 2.4). A glass coverslip was added then sealed with nail varnish and allowed to dry in the dark before inspection using a Nikon Eclipse 400UV light microscope with the appropriate filter.

2.2.3 Flow cytometry methods

Flow cytometry analysis was carried out using FACS machines (Table 2.7) at the Flow Cytometry Facility at the Medical School, Sheffield University. Mammalian cell populations were gated depending on their forward scatter (FSC) and side scatter (SSC) characteristics.

2.2.3.1 Indirect immunofluorescence in tubes

This assay was performed using living cells under cold conditions to avoid capping, internalization and shedding of antigen. The cells were harvested and washed twice with cold washing buffer (B/B/N), then re-suspended to 0.5 x 10^6 in B/B/N and dispensed in 1ml aliquots in FACS tubes. The tubes were centrifuged at 200g for 5 minutes and the supernatant removed using a Pasteur pipette attached to a suction pump. The pellet was re-suspended with

50 µl of primary mAbs (at 10µg ml^{-1} or manufacturer's recommendation in B/B/N) mixed by vortexing and incubated for 60 minutes on ice. Next, the cells were re-suspended and washed twice by adding 1ml of B/B/N and centrifuging at 200g for 5 minutes. The cell pellet was re-suspended with 50µl of the secondary fluorescently labeled antibody and incubated for 45 minutes on ice in the dark. Then, the cells were washed two times as described before. The cell pellet was re-suspended in 300µl of washing buffer on ice (if analyzed on the same day) or the cells were fixed by adding 300µl of 2% paraformaldehyde (if analyzed the next day).

2.2.3.2 Direct immunofluorescence in tubes

The method was essentially as described above except that directly labelled primary antibodies (50µl) were used in the first incubation.

2.2.3.3 Indirect immunofluorescence in 96 microtiter plates

This was carried out using V-bottomed 96 wells plates. The cells were harvested and washed as described previously and re-suspended to 2 x 10^6/ml. 100µl/well of cell suspension was aliquoted into the microtiter plate, which was then centrifuged at 400g for 3 minutes. The supernatant then was removed and the plate was placed on ice. 25µl of primary antibody was added (at 10µg ml^{-1} or manufacturer's recommendation in B/B/N) and mixed by placing the plate on a vortex mixer set at low speed. The plate was incubated for 45 minutes on ice, then the cells were washed by adding 75µl B/B/N to the wells, and centrifuging at 400g for 3 minutes twice. The supernatant was removed as previously and the cells were washed once more with 100µl B/B/N. 25µl of FITC-labelled secondary antibody was added, and mixed as previously and the plate was incubated on ice for 45minutes in the dark. The cells were then washed twice as described above and re-suspended with 200µl washing buffer (if the samples were analyzed the same day) or 200µl PFA 2% (if analyzed in the next 24- 48 hours).

2.2.3.4 Direct immunofluorescence staining in 96 microtiter plates

For direct labeling, the method was carried out as above but using 25µl of the primary labelled antibody only.

2.2.3.5 Indirect immunofluorescence staining of permeabilised cells in tube

The commercial Fix and Perm Kit™ was used (Table 2.1) to permeabilise the cells which allowed the antibodies to access cells by making "pores" in the cell membranes. Cells were harvested as described in 2.2.1.5, (0.5 – 1 x 10^6 cells per tube were used in this experiment). The cell pellet was re-suspended with 30µl solution A (fixation reagent) and incubated for 15 minutes at room temperature (RT) then washed with 1ml PBS, in the second washing, the cells suspension was divided equally in to two tubes (one for permeabilisation and the other

not for none permeabilisation) and centrifuged 200g for 5 minutes. The supernatant was aspirated and the cell pellet was re-suspended by vortexing. 25µl of 20µg ml^{-1} of primary antibody was added together with either solution B (permeabilisation reagent) or 25 µl of B/B/N (for fixed only cells) and mixed by briefly vortexing. The suspension was incubated for 30 minutes at RT. The cells then were washed twice with PBS as above then the pellet was re-suspended with 25µl of secondary labelled antibody and the cells were incubated in the dark at RT. After washing the cells were re-suspended with 300µl of 1% PFA solution and stored at 4 °C in dark until FACS analysis.

2.2.3.6 Indirect immunofluorescence staining of permeabilised cells in microtiter plates

Cells were harvested as described previously and re-suspended at 2 x 10^6 ml^{-1} in B/B/N. 100µl aliquots were dispensed into each well of a "V" bottomed 96 well microtiter plate. 20µl of solution A was added to each well and incubated for 15 minutes RT for cell fixation. The fixed cells were washed by adding 100µl PBS per well, centrifuging at 400g for 3 minutes, the supernatant was removed, and the pellet were re-suspended by briefly vortexing. The washing step was repeated but with 150µl PBS.

The cell pellet was re-suspended with 20µl of 20µg ml^{-1} of primary antibody, and either 20µl of reagent B (permeabilisation reagent) or 20µl of B/B/N (for fixed cells only). The cells were incubated for 30 minutes at RT the washed twice with PBS as described before. 25µl of secondary-labelled antibody was added to the cell pellet, mixed and incubated for 15 minutes in dark at RT. The cells were washed twice as previously and the pellet was re-suspended in 200µl 1% PFA solution and the samples were transferred in to Micro Test tubes (Table 2.8) and were stored at 4°C in the dark (up to 48 hours) until they were analyzed by FACS.

2.2.4 Immunofluorescence microscopy for analysis of antigen expression

2.2.4.1 Immunofluorescence of cells grown on chamber slides

This experiment was performed using Lab-Tek II™ chamber slides (8 chambers). The cells were harvested and re-suspended in culture medium at a density of 7x10^4 ml^{-1}. Then, 0.5 ml of the cell suspension was aliquoted into each chamber and cultured overnight. The slides were examined to check cell density and the cells were washed by adding and removing 0.5 ml BSS or PBS. Next, the cells were fixed and permeabilised by adding 0.5 ml acetone to each chamber and incubating for 5 min. The acetone was removed and quickly washed with PBS by immersing the slides into PBS, flicking to remove the PBS, and then placing the slide in a tank containing fresh PBS and washing for 10 min. with stirring. After that, the PBS was

removed from the chambers and replaced with 100 µl of an appropriate dilution of primary mAbs (to cover the well surface). Then, the slide was incubated at room temperature in a dark and humid place for 30 min. After that, the chamber was washed twice by rinsing in PBS, then a third time by immersing the slide in a tank containing PBS with stirring for 15 min. The PBS was removed and replaced with 100µl of an appropriate dilution of FITC- labeled secondary antibody and incubated for 30min in a dark and humid place. The chambers were washed as before and 100µl of 1-10 µg /ml of propidium iodide was added to each chamber and incubated for 3min (to stain the nucleus). The slides were washed as previously then flicked to remove PBS. The plastic chamber was removed according to the manufacturer's instructions and any remaining PBS was removed using a Pasteur pipette before adding a small drop of mountant to each slide section. Then, to seal the slide, a large coverslip and nail varnish was used. The slide was then stored at 4ºC in a dark place until examined by fluorescence microscopy.

2.2.4.2 Immunofluorescence on cells grown on coverslips

The cells were harvested and re-suspended in culture medium at a density of 1.5 $x10^5$ ml^{-1}. Then, 1 ml of the cell suspension was aliquoted into the wells of a 24 well plate containing sterile glass coverslips (12mm no: 1.5) and the plate was incubated overnight. After checking cell density the cells were washed by adding and removing 1ml PBS. Next, the cells were fixed and permeabilised by adding 1 ml acetone to each well and incubating for 5 min. The acetone was removed and the coverslip quickly washed three times with PBS by adding PBS by plastic Pasteur pipette into the wells and removing it by suction using a vacuum pump. Then, 150 µl of an appropriate dilution of primary mAbs (to cover the coverslips) was added and the plate was incubated at room temperature in a dark and humid place for 30 min. After that, the plate was washed three times with PBS (as described above) and 150µl of an appropriate dilution of FITC- labeled secondary antibody was added and incubated for 30min in a dark and humid place. The plate was washed as before and 200 µl of 1µg ml^{-1} of propidium iodide was added to each well and incubated for 3min. The wells were washed again as previously and the coverslips were extracted using thin curved ended forceps onto slides that were prepared by adding one drop of Vectashield mountant (Table 2.4) for each coverslip. The coverslips were placed upside down (the cells facing the mountant) onto the slides. Then, the coverslips were sealed by nail varnish and the slides were stored in slide folder at 4ºC in a dark place until examined using a Nikon Eclipse 400UV light microscope (Table 2.7).

2.2.5 Infection assay

2.2.5.1 Immunofluorescence microscopy for analysis of *Salmonella* infection

2.2.5.1.1 Cell preparation

HEC-1-B and HeLa cell preparation: HEC-1-B and HeLa cells (2.1.7.2.2) were harvested using trypsin-EDTA and counted as described in 2.2.1.5 and re-suspended in fresh culture medium. $1.5x10^5$ cells were seeded in 24 well plates containing 12mm diameter sterile glass coverslips and cultured for 24 hours before use in the experiment.

RAW, J774, CD9 KO and CD9 WT macrophage cell lines: Cells were harvested using a plastic scraper (section 2.2.1.5.2), centrifuged and re-suspended in fresh culture medium. 2 $x10^5$ cells were seeded in 24 well culture plate onto 12mm diameter sterile glass coverslips and were then cultured for 24 hours before use in the experiment.

THP-1 derived macrophages: The human monocyte cell line (2.1.8.2.2) normally grows in suspension and was harvested by centrifugation and re-suspended in fresh culture medium containing PMA 20ng ml^{-1} to differentiate them into macrophages. 2 x 10^5 cells were placed in wells in 24 wells plate containing 12mm sterile glass coverslips and cultured incubated for 3 days before infection.

2.2.5.1.2 Bacteria preparation

Salmonella Typhimurium used in the experiment were prepared as follows: An inoculum obtained from glycerol stock was plated on LB agar media overnight at 37ºC. The next day, 2-3 colonies were picked up and inoculated in 20ml LB broth media at 37ºC overnight without shaking. 400 µl from the stationary phase from this growth was inoculated in 20ml LB broth media the next morning and incubated at 37ºC in a shaker at 250rpm to reach the mid log phase after 2-2.5 hours (OD_{600} ~ 0.4-0.5). Then, the culture was immediately centrifuged at 5400g for 5 minutes. In order to wash the bacteria, the pellet was re-suspended with PBS and centrifuged again as mentioned above. The supernatant was discarded and the pellet re-suspended again with PBS and centrifuged same as before. Then, the pellet was re-suspended in an appropriate amount of cell culture media supplemented with 10% HI-FCS depending on the cells used in the experiment and checked again for accurate cell density (both OD_{600} and viable account were obtained) and then to produce the required multiplicity of infection (MOI).

2.2.5.1.3 Infection of cultured cells

Different MOIs and times of infection were used to optimise conditions. MOIs of 50, 100 and 150 were used for 30, 60 and 90 minutes infection time. The mammalian cells were prepared before infection by removing the existent media from the wells using a Pasteur pipette, followed by1x washing of the cells with PBS. Cells were treated with 1ml of 5% bovine serum albumin (BSA) for 30 minutes to reduce non-specific attachment of bacteria to the cell surface (before treatment with antibodies). The BSA was removed and the wells were washed 2x with PBS. Then, cells were incubated with 150µl of medium or medium containing the appropriate antibody (20µg ml^{-1}) for 60 minutes before washing 2x with PBS. 1ml/well of cell media containing a suitable MOI of bacteria was added for the estimated time of infection. After the time course, unattached bacteria were removed and the cells washed 2x before fixing the infected cells with 4% paraformaldehyde.

2.2.5.1.4 Staining procedure of infected cells

The paraformaldehyde was removed and cells were washed 2x with PBS using a Pasteur pipette to prepare the cells for staining. 200 µl per well of anti-*Salmonella* poly A antibody was used at a concentration of 50µg ml^{-1} (diluted in PBS) for 12 minutes at room temperature as a primary Abs to differentiate between internal and external bacteria. Unattached Abs were then removed and the cells were washed twice with PBS. 200 µl/well of the secondary FITC-conjugated anti-rabbit IgG Ab (diluted 1:320 in PBS with 0.5% goat serum) was added for 12 minutes at room temperature. The cells were kept in the dark through the staining to eliminate bleaching of the fluorescence. Then, unbound Ab was removed and the cells were washed twice with PBS. For DNA staining in both infected cells and bacteria (internal and external bacteria), 400 µl/well of DAPI solution (Table 2.1) was added for 12 minutes at room temperature in the dark. The DAPI stain bound to nucleic acid and appeared blue when using the appropriate filter of a fluorescence microscope. (The excitation wavelength of DAPI is 340 to 380 nm and the excitation wavelength of FITC is 495 to 520 nm, the green fluorescence of FITC was viewed using the appropriate filter).

2.2.5.1.5 Preparation of slides for fluorescent microscopy

After staining of the cells that were attached on the coverslip (section 2.2.5.1.4), the cells were washed twice with dH_2O and a long sharp point forceps was used to extract the coverslip

from the wells. The coverslip was immersed on the slide, the cell side down, over a drop of Vectashield mounting medium to minimize bleaching. Then, the coverslip was fixed to the slide with drops of nail varnish to prevent drying and slipping of the sample.

2.2.5.1.6 Analysis of infected cells

A Nikon Eclipse 400UV light microscope with a Digital camera DXM1200 (2.1.10) at 1000x magnifying power was used for make a random count of 100 cells per replicate. After covering the coverslip with a drop of immersion oil, the slides were viewed under the microscope. Random fields were taken across the area of the coverslip to count the number of examined cells, number of cells associated with one or more bacteria, number of cells with DAPI but not FITC stained bacteria, the DAPI stained bacteria and the total number of FITC stained bacteria. The DAPI stained bacteria revealed both external and internal bacteria, while the FITC stained bacteria revealed external bacteria only. The internal bacteria could be counted by subtracting the FITC stained bacteria from DAPI stained bacteria. The abnormal cells or "Jackpot" cells (the cells which had large numbers of bacteria) were not counted.

Parameters used to measure the difference in Salmonella uptake

Percentage of infected cells (cells with both attached and internalized bacteria) = *Number of cells with bacteria (DAPI stained bacteria) per 100 counted cells*

Percentage of internalization = *(Number of internalized bacteria / Total number of bacteria) * 100*

Number of attached bacteria = *Number of attached bacteria per 100 counted cells*

Number of internalized bacteria = *Number of all bacteria (DAPI Stained) – Number of attached bacteria (FITC stained) per 100 counted cells*

2.2.5.2 Development of a flow cytometry procedure for analysis of *Salmonella* infection

In this assay, the mammalian cells were infected in tubes in suspension, then the cells were fixed using solution A (Fix and Perm™ kit). After fixing, the cells were divided in two groups, one group prepared for staining with FITC-conjugated anti-*Salmonella* polyclonal Abs without cell permeabilisation (which reveals external or attached bacteria only), and the other group was prepared for the same staining with permeabilisation (using permeabilisation solution B from Fix and Perm™ Kit) (which reveals all (external and internal) cell-associated bacteria). After staining, the samples were analysed by flow cytometry (Figure 2.1).

2.2.5.2.1 Mammalian cell preparation

The cells were harvested (2.2.1.5), using cell dissociation solution to detach the adherent cell lines (HEC-1-B and HeLa cell lines) while in semi-adherent cell lines, mechanical harvesting by plastic cell scraper was used. The cells were counted and $1x10^6$ / ml cell suspension in normal cell media was prepared. The cell suspension was aliquoted in to 0.5 – $1x10^6$ per 2ml Eppendorf tubes. The cells were centrifuged and then the cells were treated with 50-100µl of 20µg ml^{-1} tetraspanin antibody or 500-1000nM of recombinant tetraspanin EC2 proteins for 60 min at 37°C.

2.2.5.2.2 Bacteria preparation

Salmonella were prepared as mentioned in 2.2.5.1.2.

2.2.5.2.3 Infection of the cells

Appropriate MOIs of bacteria were used to infect the cells after treatment with anti-tetraspanins antibody or with tetraspanins EC2 domain. 0.5 -1 ml of appropriate MOI was added per tube depending on the cell density to keep the cell-bacteria distribution constant over all the experiments. The tubes were placed in a rotating mixer and the tubes were incubated at 37°C for the time period stated in the experiment. The tubes were then cooled on ice for 5 min and centrifuged at 200g for 5 min. The infected cells were washed twice with B/B/N, then fixed by adding 50µl of solution A (Fix and Perm™ kit) for 15 minutes. The infected cells were washed with 1ml PBS and centrifuged 200g for 5 minutes.

Infection of the cells in 96 wells plate

For analysis of larger numbers of samples, the experiment was carried out using sterile 96 "U" bottom well plates instead of tubes as described in 2.2.5.2.1. Cells were aliquoted at concentration of 0.4-0.5 million for each well, then treated with 20µg ml^{-1} of anti-tetraspanin antibody diluted in normal media for 60 minutes at 37°C. 100µl/well of a suitable MOI of bacteria was added, or 100µl medium for the non-infected cell control was. The plate then sealed using adhesive seals (BioRad) and incubated in a shaking incubator 100rpm, 37°C for 30 minutes. Then the plate was placed on ice for 5 minutes to stop bacterial infection and then centrifuged at 400g for 3 minutes. The cells were washed two times with BBN (Table 2.1). Cells were then fixed with 4% PFA for 15 minutes and stained as described (for non GFP expressing bacteria) or washed once with PBS one time and re-suspend with 1% PFA. The cells were kept on dark and cooled place until analysis.

2.2.5.2.4 Staining protocol

The infected cells (from the previous steps) were re-suspended with 200µl PBS (second wash) and the contents of each tube was divided into two wells in "V" shaped 96 wells plates then centrifuged at 200g for 5 min. The washing solution was removed by suction (one set stained with permeabilisation (with solution B from Fix and Perm™ kit) other set stained without permeabilisation (using B/B/N instead of solution B). Using a multichannel pipette, 25µl of anti-*Salmonella* -FITC conjugate polyclonal antibodies (Table 2.5 B) at 1:500 dilution in PBS was added to each well. This was followed by adding 25µl of solution B to the permeabilised group or 25µl of B/B/N to the non-permeabilised group and the well contents were mixed by pipetting. In permeabilised cells, all bacteria were stained with FITC conjugated anti-*Salmonella* antibody (external and internal bacteria), while in non-permeabilised cells, only the external bacteria were stained. The infected cells were incubated with antibody for 15 minutes at RT, then the stained cells were washed twice with PBS, by adding 100µl of PBS to each well, centrifuging at 200g for 5 min and the washing solution was removed by suction. The plate was then vortexed briefly at low speed, the pellets were re-suspended with 150µl PBS for a second wash. The pellets were re-suspended in 150µl of 1%PFA and the infected cells were transferred in to Micro Test tubes (Table 2.8) and kept at 4°C until were analysis up to 48 hours later.

2.2.5.2.5 FACS analysis of infected cells

An LSR II FACS machine was used to analyse infected cells. The cells were gated depending on forward and side scatter (FSC and SSC). 5,000 -10,000 events were acquired and the data analysed using BD FACSDiva 7.0 software. To calculate the cells with internalized bacteria only, the non-permeabilised cells (cells with attached bacteria) were subtracted from permeabilised cells (cells with attached and internalized bacteria).

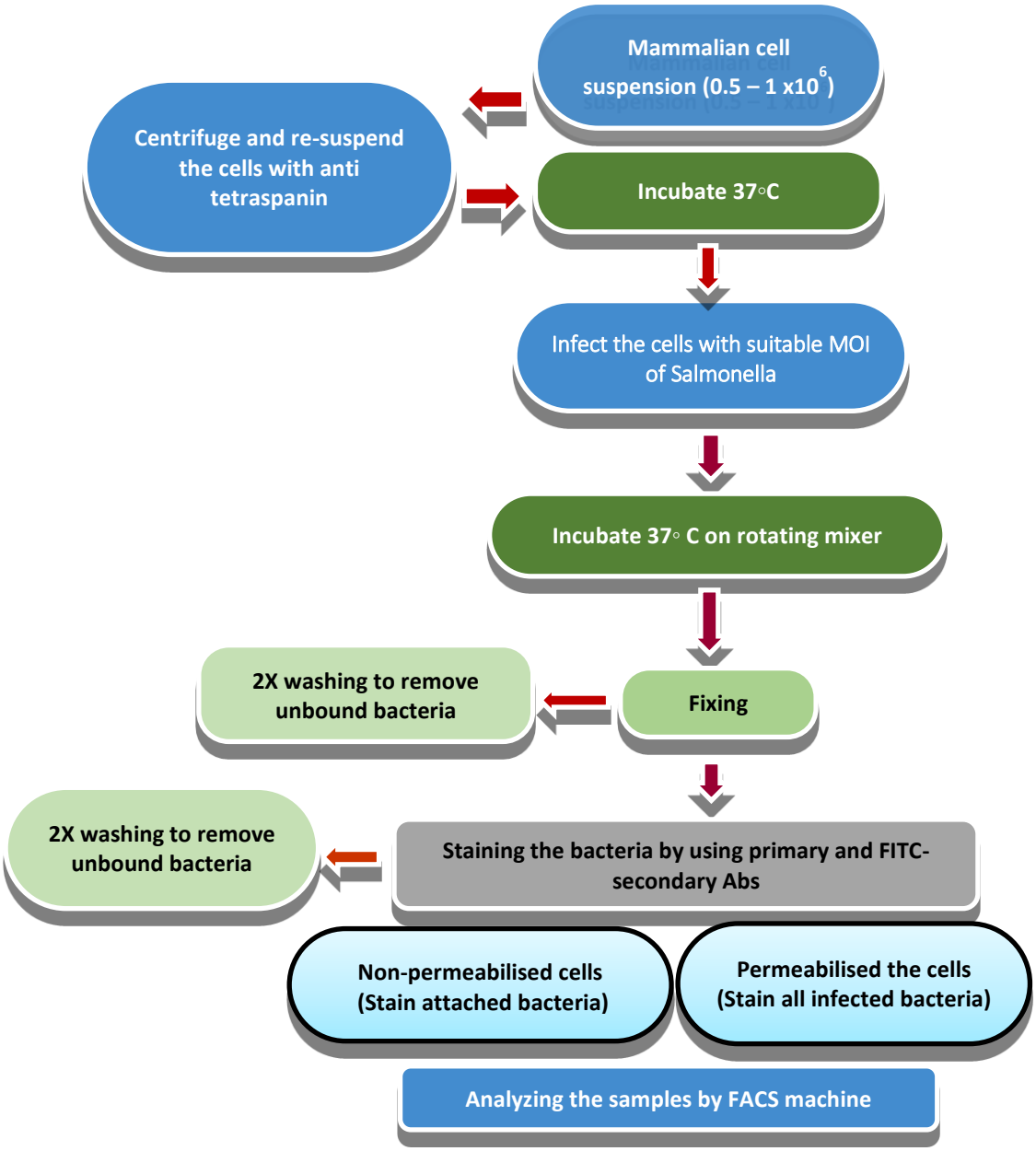

Figure 2.1: Flow cytometry procedure for *Salmonella* infection

2.2.5.3 Flow cytometry analysis of *Salmonella* infection of HeLa syntenin KD and control cells

2.2.5.3.1 Preparing HeLa syntenin and HeLa control cells for infection

The HeLa syntenin KD and WT cells control are human epithelial cells, where the former has been stably transfected with a plasmid encoding shRNA specific for the syntenin gene, whereas control cells contain empty vector (both encoding puromycin resistance) (2.1.8.2.2). Cells were harvested and counted (2.2.1.5) and $3x10^5$ cells were seeded in 12 well culture plates in fresh culture medium supplemented with 1.5µg ml^{-1} puromycin. Cells were cultured overnight before use in the experiment.

2.2.5.3.2 Infection of HeLa syntenin KD and HeLa WT cells

Bacteria were prepared as described in 2.2.4.1.2. Optimization was again carried out to find a suitable MOI to use in infection. After washing once with PBS, the HeLa cells were treated with 5% BSA for 30 minutes prior infection to reduce non-specific binding of bacteria to the well surface, the BSA was removed and after two further washes with PBS, 1ml of media (without puromycin) containing a suitable MOI of bacteria was added for for 1hr before washing to remove unbound bacteria and incubating in medium containing 100µg ml^{-1} kanamycin for the times indicated before harvesting.

After the time course, the cells were washed two times with HBSS (without divalent) followed by the addition of 0.5 ml/well trypsin-EDTA for 5 minutes. Harvested cells from each well were transferred into 5ml tubes followed by centrifugation at 200g for 5 minutes to remove trypsin-EDTA and the cells were washed one time with PBS before fixing the infected cells by re-suspending the pellet with 50µl solution A (Fix and Perm™ kit, 2.1.3) for 15 minutes.

2.2.5.3.3 Staining procedure

The cells were washed 2x with 1ml PBS for the first wash and 200µl PBS for the second wash. In the second wash, the 200µl cells suspension was divided and transferred into two wells from a 96 wells plate ("V" bottomed) to prepare for staining. As described in 2.2.6.2.4, one group of cells was prepared for staining attached bacteria only using FITC-conjugated anti-*Salmonella* polyclonal Abs without cell permeabilisation, and the other group was prepared for the same staining (to stain attached and internalized bacteria) with permeabilisation (cell-associated bacteria). After staining, the samples were analyzed by flow cytometry using the LSR II flow cytometer. 10,000 events were acquired and the gate was adjusted depending on the non-infected cells control.

2.2.6 Confocal microscopy of Hela Syntenin KD and Hela WT cells

HeLa syntenin KD cells and HeLa WT control cells (2.1.8.2.2) were used to investigate any differences in Salmonella co-localization within the SCV. *Salmonella* Typhimurium NCTC-GFP and LT2-GFP were used for these experiments. Alexa fluor® 647-labelled anti-human LAMP-1 was used as an SCV marker and Alexa fluor® 568 phalloidin was used to visualize the cell outline by staining the actin cytoskeleton.

2.2.6.1 Preparation of the HeLa cells

Cells were harvested as described previously and $1.5x10^5$ cells were seeded in culture medium, one day before experiment, in 24 well culture plate over 12mm diameter and thickness number 1.5 sterile glass coverslips.

2.2.6.2 Infection of culture cells

The infection was carried out using an MOI of 100 and times of infection used were 0, 1, 2, 4, 6, 12 and 24 hours. The existent media was removed by suction using a vacuum pump, followed by one wash with PBS. Then, 0.5ml per well of cell media (with no puromycin) containing the MOI was added to each well. The attached bacteria were killed one hour post infection by washing the infected cells twice with pre-warmed PBS followed by adding 1ml per well of normal media containing penicillin and streptomycin (100U penicillin + 100μg streptomycin/ml). After the time course, the cells were washed twice before fixing the infected cells with 4% paraformaldehyde for 15 minutes.

2.2.6.3 Staining procedure

The cells were washed twice with PBS after removing the paraformaldehyde from the wells by suction. 150 μl per well of Alexa Fluor 647-labelled anti-human LAMP-1 was used at 1:100 in 0.1% saponin permeabilising buffer (Table 2.1) for 60 minutes at room temperature in the dark and then the cells were washed twice with PBS. 150 μl/well of the Alexa Fluor 568 phalloidin in permeabilising buffer was then added and incubated for 20 minutes at room temperature in the dark and the cells were washed twice with PBS. The coverslips were extracted from the wells and mounted on microscope slides using Vectashield mounting medium with DAPI as described in 2.2.5.1.5. A Nikon A1 confocal inverted microscope with EM-CCD camera, (Table 2.7), with Nikon elements software was used to visualize and analyse the images.

2.2.7 Mammalian cell lysis

Lysis of mammalian cells was performed prior to detecting cellular proteins by Western blotting. Cells were grown in T175 flasks until they reached 60-70% confluency and then

harvested either by using cell scraper (in semi-adherent cells) or by treating the cells with trypsin-EDTA. Cells were counted, centrifuged for 5 minutes at 200g, then washed with 5 ml HBSS. The pellet was re-suspended with 100µl per 1 x 10^6 cells with lysis solution composed of 0.5% Triton 100 (Sigma) and 0.5% Brij 98 in PBS containing protease inhibitor cocktail (Sigma P8340) at a dilution of 1:100 solution. The mixture was placed on a rotating mixer at 4°C for 6 hours or overnight. The cell lysate was centrifuged for 15 minutes at 13,000 rpm using a micro-centrifuge, then the protein-containing supernatant was removed to pre-cooled 1.5ml Eppendorf tubes and stored at -80°C.

2.2.8 Methods used to sub-clone mouse CD9-EC2 domain

Mouse CD9 EC2 was sub-cloned from the commercially available vector containing full-length CD9-GFP (Origene MG226288, Table 2.9) into the pGEX-KG vector (Guan and Dixon 1991) (Table 2.9) so that it could be expressed as a soluble GST fusion protein, essentially as described previously by our group (Higginbottom, Takahashi et al. 2003).

2.2.8.1 Purification of plasmid DNA

Plasmid DNA was purified by using QIAprep spin Mini Kits (Table 2.4) by following the manufacturer's instructions. Briefly, a single colony of transformed bacteria containing the relevant construct was used to inoculate 5ml LB broth (with selective antibiotics) and incubated in a shaking incubator at 250rpm overnight at 37°C. The bacteria were centrifuged at 5,400g for 10 minutes at 4°C then re-suspended in 250µl of cooled P1 buffer, then transferred to a 1.5 ml microfuge tube and 250µl P2 buffer and then 350µl of N3 buffer added and mixed by inversion. The mixture was centrifuged at 13,000 rpm using a micro-centrifuge for 10 minutes. The supernatant was transferred to a QIA prep spin column and centrifuged for 1 minute as before. The flow through was discarded and the column washed by adding 750µl of PE buffer and then centrifuging as previously for 1 minute. The flow through was discarded and the column was dried by centrifugation for 1 minute. The column was placed into a 1.5 ml sterile microfuge tube and the plasmid DNA was eluted by adding 50µl ddH_2O in the center of the column. The column was left for 1 minute and centrifuged for 1 minute as previously. The concentration of the plasmid DNA was checked using a NanoDrop spectrophotometer at 260nm and the plasmid DNA was stored at -20°C.

2.2.8.2 PCR, digestion and ligation mixture

Table 2.14: PCR, digestion and ligation mixture components. The Q5® High Fidelity Kit from NEB was used for PCR mixture components. * Amounts calculated as described in 2.2.8.11.

PCR mixture	
Component	**Volume (µl)**
Nuclease free water	22.5
5x Q5 buffer	10
10 mM dNTPs	1
DNA 200ng/ml	1
10 µM Forward primer	2.5
10 µM Reverse primer	2.5
Q5 GC enhancer	10
Q5 polymerase	0.5
Total	**50**

Digestion mixture (DNA insert)	
Component	**Volume (µl)**
Nuclease free water	32.85
BSA	0.5
Buffer (2 from NEB)	5
Eco RI-HI (NEB)	1.5
Hind III (Promega)	1.5
PCR reaction (57.8 ng/µl)	8.65 (500ng)
Total	**50**

Digestion mixture (Vector)	
Component	**Volume (µl)**
Nuclease free water	17.75
BSA	0.25
Buffer (2 from NEB)	2.5
Eco RI-HI (NEB)	0.75
Hind III (Promega)	0.75
Vector DNA	3 (250ng)
Total	**25**

DNA ligation mixture	
Component	**Volume (µl)**
Nuclease free water	9
Ligase buffer (10X)	2
*Vector DNA	7.3
*Insert DNA	0.7
Ligase	1
Total	**20**

2.2.8.3 Bacterial glycerol stock preparation

One single colony of transformed bacteria was grown in 5ml of LB media supplemented with selective antibiotics overnight at 37°C in a shaking incubator (250rpm). 250µl of 60% (v/v) of glycerol stock solution (Table 2.1) was transferred into cryovials and mixed with 750µl of the overnight culture. The cryovials tube were placed at -80°C for long term storage.

2.2.8.4 Agarose gel electrophoreses

1% agarose gels were prepared as described (Table 2.1) and allowed to cool slightly before, adding 1µl of ethidium bromide per 100ml of gel and pouring into a gel tray with a comb. When the gel solidified, it was placed in a gel tank containing 1X TAE buffer (Table 2.1) to cover the gel surface. 2x loading buffer (Bioline) was used with the sample DNA at 1:1

dilution (10µl of each) and was loaded into each well. A hyper ladder-1 (Bioline) was loaded into the gel as a DNA size marker. The gels were run for 1 hour at 100V and then the DNA bands were visualized by UV light using a GelDoc-It™ imaging system.

2.2.8.5 mCD9-EC2 determination

The full sequence of mouse CD9 was obtained from a bioinformatics databases (uniProtKB Table 2.12) in a FASTA format and the mCD9-EC2 was identified by the same database.

2.2.8.6 Designation of PCR primers

After determination of the mouse CD9-EC2, primers were designed by taking first 19 to 22 bases from the 5` and 3` ends of mCD9-EC2 and restriction sites were added that were compatible with the expression vector used (pGEX-KG). The primers used are described in Table 2.13).

2.2.8.7 PCR amplification of mCD9-EC2

The PCR reaction mixture was prepared as described in 2.2.8.2 in thin-walled PCR tubes. The mCD9-EC2 was amplified from the full length mouse CD9 in the Origene mCD9-GFP containing vector (Table 2.9). The optimal annealing temperatures for the forward and reverse primers were identified by using the Thermo Fisher Scientific Tm calculator online tool and it was set as the averaged melting temperature (T_m). The setting of thermal cycle reaction was carried out as described in Table 2.15.

Table 2.15: Thermal cycle settings used to amplify mouse CD9-EC2 from the CD9-GFP carrying vector.

Number of cycles	Temperature (°C)	Time
1 Cycle	95	10 minutes
30 Cycle	96	10 second
	60	30 second
	72	30 second
1 Cycle	72	10 minutes
	4	Hold

2.2.8.8 Purification of PCR products

PCR product was purified either after separation on 1% agarose gels and using the QIAquick Gel Extraction Kit (Table 2.4), or by direct purification of DNA fragments using the QIA

PCR purification Kit (mentioned in 2.4). In both methods, a sufficient DNA concentration was obtained.

2.2.8.9 Restriction enzyme digestion

The purified PCR products and the expression vector pGEX-KG were double digested with appropriate restriction enzymes (Table 2.14) to produce 5` and 3` overhang sticky ends for ligation. The mixture of buffer, restriction enzymes and DNA was prepared in thin-walled PCR tubes followed by brief centrifugation. The mixture was incubated at 37°C for 3 hours. The enzymes were deactivated by heating to 80°C for 20 minutes (EcoR I-HF and Hind III-HF). The digested samples were purified after running on 1% agarose gels and then the DNA concentration was determined using a NanoDrop spectrophotometer at 260nm (Table 2.7).

2.2.8.10 DNA ligation

After digestion and purification of both mCD9-EC2 (insert) and pGEX-KG (expression vector), the two fragments were ligated. The concentration of the insert and the vector were determined by NanoDrop (Table 2.14) and all components in the calculated amounts were mixed in small Eppendorf tubes and incubated for 1-3 hours at 25°C.

The amount of insert and the vector DNA were determined according to the following equation:

$$\frac{Vector\ amount\ (ng) x\ Insert\ size\ (bp)}{Size\ of\ vector\ (bp)}\ x\ molar\ ratio\ insert{:}\ vector = Amount\ of\ insert\ (ng)$$

A 3:1 molar ratio of vector: insert was used here.

2.2.8.11 Plasmid amplification

1µl of complete ligation reaction was used to transform 20µl DH5α competent cells following the protocol described in 2.2.9.1. Half of 10 single colonies were picked and grown overnight in 5 ml LB media with selective antibiotics at 37°C and 250 rpm shaking followed by DNA plasmid purification (2.2.8.1) and PCR amplification, as described in 2.2.8.4, using mCD9 EC2 forward and reverse primers (Table 2.13), as well as the forward (pGEX-F2) and reverse (pGEX-R1) primers for the vector (Table 2.13).

2.2.8.12 DNA sequencing

After the results of the PCR described above, DNA from 4 chosen clones were sequenced using forward and reverse vector primers (pGEX-F2 and pGEX-R1 respectively, (Table 2.13). Sequencing was carried out using the Core Genomic Facility, DNA Sequencing

Service at the in University of Sheffield, using an Applied Biosystems 3730 DNA analyser and BigDye v3.1 protocol.

2.2.9 Bacterial protein expression

2.2.9.1 Transformation of DH5α and Rosetta gami competent cells

This method was used for cloning of vector (using DH5α cells) or protein expression (using Rosetta gami B, Novogen). 50µl of competent cells were defrosted on ice and 1µl of plasmid of interest was added and mixed by tapping the tube gently. The mixture was incubated on ice for 30 minutes, then placed in a floating pad in a water bath at 42°C for 45 seconds (heat shock). The cells were left for a further 2 minutes on ice before adding 250µl SOC medium. The cells were then incubated with shaking (150 rpm) for 30 minutes. 50µl from this culture was plated on agar plates containing appropriate selection agents.

2.2.9.2 Expression of protein in Rosetta gami

Rosetta gami cells were transformed with pGEX-GST-CD9-EC2 as described above. One single colony was picked into 5ml LB broth containing carbenicillin (100µg ml^{-1}) using a sterile pipette tip. The cells were incubated overnight at 37°C and 250 rpm in a shaking incubator. Next day, the culture was diluted in 500ml LB broth (in a 2 litre conical flask) containing carbenicillin at 100µg ml^{-1}. The flask was incubated for 5-8 hours until the OD_{600} reached 0.7, and at this point expression was induced by adding 50µl of 1M IPTG solution (0.1mM final concentration) and left for a further 4 hours incubation to express the protein. 500ml tubes were used for centrifugation of the cultures after recording the weight for each tube (to calculate the weight of the bacterial pellet after subtracting the weight of the tube from the total) and filled to a maximum volume of ~330ml per tube. The tubes were centrifuged at 4500g for 20 minutes, the supernatants discarded and the pellets were stored in -80°C until the next step.

2.2.9.3 Bacterial cell lysis

The frozen tubes were defrosted on ice and the pellets were re-suspended with cooled PBS contain 1:100 protease inhibitor cocktail (Table 2.4) at a ratio of 5ml PBS per 1gram of bacterial pellet. The re-suspended pellet was transferred into 20 ml autoclaved pre-cooled Beckman tubes, which were placed in a 500ml plastic beaker containing ice to keep the bacterial suspension cool during sonication. The sonicater was set for 15 micron and the sonication was performed five times for 15 seconds with 2 minute intervals between each round, and the suspension was mixed after two rounds of sonication. The bacterial lysate was

centrifuged at 16,000g for 30 minutes and the supernatant transferred into pre-cooled 15 ml Falcon tubes and kept on ice.

2.2.9.4 Protein purification

Glutathione agarose beads, (Sigma, G4510) were prepared at a concentration of 0.1ml of beads for every 1 gram of bacterial pellet by taking double the volume of the beads from the stock (as 50% of the supplied volume is ethanol). The ethanol was removed by centrifugation at 500g for 5 minutes at 4°C, and the beads were washed 3 times by re-suspending with 5x beads volume of pre-cooled PBS before mixing with the cell lysate.

The mixture of beads and cell lysate was incubated at room temperature on a blood mixer for 2 hours, then centrifuged at 500g for 5 minutes (4°C) and the supernatant discarded. The beads were washed three times with 5 column volumes of pre-cooled PBS (to wash the beads and remove unbound proteins) by re-suspending the beads gently with pre-cooled PBS and then centrifuging as before (one fraction was taken for analysis from each step of the washing). After the final wash, the bound protein was eluted using glutathione elution buffer (Table 2.1) and incubating with gentle rotation for 20 minutes. The beads were centrifuged as previously and the supernatant containing the expressing protein was transferred in to new pre-cooled microfuge tube. The elution process was repeated, as before and fractions were taken at each elution step for analysis by Western blot.

2.2.9.5 Determination of protein concentration and dialysis

The protein concentration was determined by using the NanoDrop spectrophotometer at 280 nm and the purified protein either stored in -80°C or dialyzed the same day. The required length of 16mm SnakeSkin dialysis tubing with 3.5K molecular weight (Life Technologies) (Table 2.8) cut-off with an additional 1-2 inches (for tube closure) was used and the tubing was cleanly cut at a 90° angle. The tubing was briefly dipped into PBS (dialysis buffer) and knotted securely at one end. The eluted protein was added into the open end and it was securely knotted at the other end. An appropriate container and dialysis buffer (about 300 times the volume of samples of PBS) were used for dialysis at 4°C with slow stirring for 8-12 hours (the dialysis buffer was changed twice during dialysis process). After dialysis the dialyzed protein was transferred into sterile 1.5ml pre-cooled tubes and stored at -80°C. The expressed protein and fractions were checked by SDS-PAGE followed by either staining with Coomassie blue or the proteins were transferred onto nitrocellulose membrane for Western blotting.

2.2.9.6 SDS-PAGE electrophoresis

Sodium dodecyl sulphate -polyacrylamide gel electrophoresis (SDS-PAGE) was performed using a Mini-Protein Cell system from BioRad following the manufacturer's instructions. Briefly, EZ-Run™ 12.5% Protein Gel Solution (Fisher BioReagent) was used to prepare the resolving gel after 30µl of freshly made APS and 7.5µl of TEMED for each 5 ml of the gel solution (enough for one gel) were added. A 5% stacking gel was prepared as described in Table 2.1. For non-reducing SDS-PAGE, the protein samples were boiled with 4x non reducing buffer (Table 2.1) at 95°C for 10 minutes using a heating block (Table 2.7). 5-10µl of colored protein marker (all Blue Precision Plus, Biorad) was used and 10-20µl of protein sample was loaded per well. Gels were run using 1x EZ-Run™ running buffer (Table 2.1) at 80V for approximately 20 minutes (until the proteins passed through the stacking gel) and then at 120V for 60-90 minutes.

2.2.9.7 SDS-PAGE staining and de-staining

Gels were extracted from the casting glasses and stained with Coomassie stain (Table 2.1) for 20 minutes on a rocking table. To remove the non-protein bound stain, gels were incubated in de-stain solution (Table 2.1) for 4-6 hours at room temperature then the de-stain solution was replaced with distilled water and incubated overnight on a rocking table at room temperature.

2.2.9.8 Western blotting

After preparing the SDS-PAGE as described above, a wet Western blotting system was used. The gel sandwich was assembled composed of, from negative to positive electrodes, sponge, blotting filter paper, SDS-PAGE gel, 0.45µm nitrocellulose membrane (Amersham™Protran,10600003), blotting filter paper and sponge. All elements of the gel sandwich were soaked with blotting buffer to moisturize before assembly. After that, the sandwich was placed in the blotting module with the nitrocellulose membrane facing the positive electrode. To cool the module, a freezing block was placed in the tank of blotting system. The proteins were transferred at 100V for 1 hour or at 20V overnight. Then the membrane was extracted and placed in a 50ml Falcon tube with 5% blocking solution (Table 2.1) for 30 minutes at RT to block the membrane for any non-specific binding of antibodies.

The blocking solution was replaced with 5ml of an appropriate primary antibody in 5% skimmed milk blocking solution (Table 2.1) and incubated overnight on a rotating mixer at 4°C. The membrane was then washed three times with TBST (Table 2.1) for 5 minutes for each, followed by staining with HRP-conjugated secondary antibodies for 2 hours on a rotating mixer at RT. The membrane was then washed three times as described above. Finally,

the membrane was incubated with Super Signal West Pico Chemiluminescent substrate (from Thermo Scientific or BioRad) for 1-5 minutes at RT, then, the extra reagent was removed by holding the membrane vertically over tissue paper (to absorb the extra amount of the reagent) before placing it in the ChemiDoc™ MP system (BioRad) to visualize and capture the proteins bands.

2.2.10 Mammalian cells transfection

2.2.10.1 Selective reagent kill curve

This method was performed to determine the optimal selective antibiotic concentration for obtaining stable transfected cells. Different concentrations, starting from 0.1 to 2 mg ml^{-1} of G418 in DMEM media were prepared. The cells were seeded in 24 wells plates at 10^5 /well. The next day, the media was removed and replaced with media containing the appropriate G418 concentration in duplicate. The cells were observed every day for 7 days and the media was replaced every 3 days. The optimal antibiotic dose was determined after 7 days and is defined as the lowest antibiotic concentration that is able to kill all the cells after this time.

2.2.10.2 Transfection of J774 cells by electroporation

The transfection of J774 cells with the mCD9-GFP carrying vector (Table 2.9) was carried out using a Gene Pluser® II with capacitance extender plus (BioRad). The cells were grown in a T75 flask overnight 2.2.1.4) then harvested using trypsin-EDTA for 5 minutes (2.2.1.5). 5 $x10^6$ cells were centrifuged and the cell pellet re-suspended with 250µl of DMEM supplemented with 10% HI-FCS. 20µg of plasmid DNA was mixed with the cell suspension in a 0.4cm gap electroporation cuvette. The mixture was incubated on ice for 15 minutes before electroporation. The electroporation system setting was: voltage 0.2 kv, capacitance 950 µF. After the cells were transfected, they were diluted into 30ml DMEM media supplemented with 10% HI-FCS and penicillin streptomycin 100U penicillin + 100µg streptomycin/ml), then separated into 3 10cm culture dishes (Table 2.8) and cultured under standard conditions. The cells were observed using a fluorescence inverted microscope after 24 hours. After 48-72 hours post transfection, the medium was replaced with 10% HI-FCS DMEM supplemented with penicillin, streptomycin and 400µg/ml G418 (selective reagent) for 3 days and thereafter with 200µg/ml G418 containing media for maintaining the transfected cells. The G418 resistant cells were tested by flow cytometry to evaluate the percentage of mCD9-GFP expressing cells. The cells were sorted using a FACS Aria cell sorter depending on their GFP expression.

2.2.11 RNA Microarray analysis

Microarray analysis was performed to compare the mRNA expression profiles of macrophage cell lines derived from CD9 KO or corresponding WT mice (section 2.1.8.2.1)

2.2.11.1 RNA extraction

RNA was extracted using the RNAeasy Mini Kit (Qiagen, Cat. No. 74104) according to the manufacturer's instructions. The total RNA concentration was determined by NanoDrop spectrophotometer and the samples were stored at -80 °C until used for the GeneChip® 3'IVT Express labeling assay.

2.2.11.2 RNA purity and integrity analysis

RNA purity and integrity of extracted RMA were analysed by using Agilent RNA 6000 Nano Kit by microfluidic analysis using the Agilent 2100 bioanalyser following the manufacturer's instructions. The analysis was carried out at the SITraN Microarray facility at the University of Sheffield.

2.2.11.3 RNA amplification and labelling

Amplification was performed using the Affymetrix GeneChip 3' IVT express kit following manufacturer's instructions and will be covered, briefly, in the following section.

Poly-A RNA control: A positive RNA control was prepared to monitor the effectivity of the reagents that were used (all reagents needed were included with the kit). The poly-A RNA controls were also prepared to monitor the whole target labeling procedure. The Poly-A RNA kit included several probe sets of *Bacillus subtilis* genes (*lys, phe, thr* and *dap*); these set of genes are absents in eukaryotic cells and are synthesized *in vitro.* The stock poly-A control was diluted with poly-A control dilution buffer. The poly-A RNA dilution was prepared for 100ng total RNA by adding 2µl of poly-A RNA stock control to 38µl of poly-A control buffer to obtain (1:20) the first dilution and 2µl from this dilution was mixed with 98µl of poly-A control buffer to obtain the second (1:50) dilution. As in the previous step, 2µl from the second dilution was added to 98µl of buffer to obtain the third (1:50) dilution, 2µl from the third dilution was added to 18µl of buffer to have the fourth (1:20) and working dilution.

The total RNA/poly-A RNA control mixer was prepared by adding 100ng (in 1µl) of total RNA to 2µl from fourth dilution (from the previous step) of poly-A RNA control with 3µl of nuclease free water to reach 5µl total volume.

First strand cDNA synthesis: Following the previous step, the first strand cDNA was synthesized following the manufacturer's instruction (GeneChip® IVT Express Kit). Briefly,

to prepare the first strand master mix, 4µl of first strand buffer mix was mixed with 1µl of first strand enzyme mix (for each reaction), the mixture then briefly centrifuged and placed on ice, 5µl of total RNA/poly-A control mixture (from the previous step) was added to 5µl first-strand master mix for 10µl final volume, then mixed, centrifuged and placed on ice. Then the mixture was incubated for 2hr at 42ºC in a thermal cycler, then briefly centrifuged and placed on ice to proceed to the next step.

Second strand cDNA synthesis: The second strand master mix was prepared by mixing 13µl of nuclease free water, 5µl second strand master mix and 2µl second strand enzyme mix (total volume 20µl). This was mixed and briefly centrifuged. 10µl of cDNA (from the previous step) was added to 20µl of second strand master mix and the mixture was mixed, briefly centrifuged and placed on ice. Then the mixture was incubated in thermal cycler at 16ºC for 1 hr followed by 65ºC for 10 minutes. Then, the product was briefly centrifuged (to collect double stranded cDNA). The double stranded cDNA product was placed immediately on ice or stored at -20ºC.

In vitro transcription to synthesize labeled aRNA: In brief, the IVT master mix was prepared for each sample at RT in a nuclease free tube as follows: 4µl of 3` IVT biotin label was mixed with 20µl IVT buffer and 6µl of IVT enzyme. This was briefly mixed and centrifuged. Then, this was mixed with 30µl of double stranded DNA (from the previous step) and the mixture was briefly centrifuged, followed by 16 hr incubation at 40ºC using thermal cycler programmed for Transcription aRNA synthesis. The tubes were either kept on ice for labeled aRNA purification or stored at -20 ºC.

aRNA purification: The aRNA was purified by adding 100µl of purification bead mix for each 60µl aRNA (from the previous step), mixed and transferred to a well of a "U" bottomed 96 well plate, then mixed several times by pipetting followed by 10 minutes incubation at RT. The plate was moved to a magnetic stand for aRNA binding bead capture for about 5 minutes. The supernatant was aspirated and discarded and the beads were washed with 100µl aRNA washing solution for each sample followed by shaking for 1 minute. The plate was returned to the magnetic stand and the washing step was repeated twice more. After washing, the plate was allowed to dry for 5 minute to evaporate the remaining ethanol from the washing buffer. The aRNA was eluted by adding 50µl of pre-warmed (65ºC) nuclease free water to each sample followed by shaking the plate for 3 minutes. Then, the plate was returned to the magnetic stand and the RNA binding bead captured. The eluted aRNA (supernatant) was transferred to a nuclease-free PCR tube and stored at -20ºC. The concentration of aRNA was

determined by measuring (2µl of sample) absorbance at 260 nm using NanoDrop and Agilent Bioanalyser and an RNA6000 nano kit was used to analyse the aRNA size and distribution.

Fragmentation of labeled aRNA: The fragmentation of labeled aRNA was carried out by preparing the fragmentation mixture on ice and adding 15µg aRNA (1-32 µl) to 8µl fragmentation buffer (the volume was adjusted to 40µl by adding nuclease free water). The mixture was briefly centrifuged then incubated for 35 minutes at 95ºC. The tubes was briefly centrifuged and immediately replaced on ice. The Agilent bioanalyser using RNA6000 Nano kit was used to determine the size of fragments.

Hybridization: The array hybridization was carried out by using the GeneChip® Mouse Genome 430.2.0 array (Affymetrix, part. no. 900495). The hybridization cocktail was prepared for single probe array following manufacturer's instruction (GeneChip® 3`IVT Express kit user manual). Briefly, 12.5µg (33.3µl) of fragmented and labeled aRNA was mixed with 4.2 µl control oligonucleotide B2 (3nM), 12.5µl of 20x hybridization controls (bioB, bioC, bioD and cre), 125µl 2x hybridization mix, 25µl DMSO and 50µl nuclease free water. The hybridization cocktail was incubated for 5 minutes at 99ºC then for 5 minutes at 45ºC using the thermal cycler hybridization cocktail program. Meanwhile, the array was wetted with 200µl of pre-hybridization mix and incubated at 60 rpm rotation for 10 minutes at 45ºC. The hybridization cocktail was centrifuged for 5 minutes. Then, the pre-hybridization mix was extracted from the array and re-filled with an appropriate volume of hybridization cocktail and the array was incubated for 16hr at 45ºC with 60 rpm rotation.

After incubation, the hybridization cocktail was extracted from the array chip and the chip was loaded with wash buffer. The chip washing process was carried out using the Affymetrix Fluidics System 450. The GeneChip 30007G scanner was used to scan the chip. The microarray analysis work was carried in collaboration with Dr. Paul Heath in the Microarray facilities in SITraN, University of Sheffield.

2.2.11.4 Data analysis

After obtaining the gene expression data, the difference between CD9 KO mouse macrophages and WT mouse macrophage controls was analysed by using Qlucore Omics. Data from gene expression profiles were analysed using principal component analysis (PCA), a mathematical algorithm which trims data diminutions where the data set retains most variation. This trimming is achieved by determining directions, or so-called principal components (PC), in which a few components could represent thousands of variables that could be visualized as a plot to estimate sample similarity and variation and possible sample clustering (Ringner 2008). In addition to PCA analysis and plots, this software provided other

functions such as investigating any structure in the data by combining PCA with variant filtering and enhancing the results by performing statistical filtering using ANOVA. This classifies data and creates a gene list depending on selected statistical testes such as T-test, F-test or regression; it identifies subgroups by using hierarchical clustering or PCA and finds correlation and networks between selected genes by working with PCA plots (http://qlucore.com/ProdOverviewGeneExpression.aspx?cache=0). Transcriptome Analysis Console v3.0 (Affymetrix) software was also used (http://www.affymetrix.com/estore/browse/level_seven_software_products_only.jsp?productId=prod760001#1_1). This software has the same functionality as in Qlucore Omics except for a few differences in the statistical analysis and data analysis output format, since the fold changes is based on linear values while in Qlucore this value in $\log^2$ format. Multiple T-tests with p values of 0.05, 0.01 and 0.001 were applied in order to evaluate the variably regulated genes and the gene ontology was analysed by using the bioinformatics tool DAVID.

2.2.12 Co-localisation experiments

2.2.12.1 Mouse CD9 and *Salmonella* co-localisation in J774 cells

Both J774 cells and *Salmonella* bacteria were prepared as described in 2.2.5.1.1 and 2.2.5.1.2 respectively, then cells were infected as described in 2.2.5.1.3. After fixation, 5% bovine serum albumin (BSA) blocking solution in PBS was used for 10 minutes to prevent non-specific binding followed by washing twice with PBS. The fixed cells were then stained by adding 150µl/well of primary antibodies anti-mCD9 and anti-*Salmonella* (Table 2.5 A) at concentration of 10 µg ml^{-1} and 50µg ml^{-1} respectively in (0.5 % goat serum in PBS) for 45 minutes. Then, cells were washed twice with PBS and stained with secondary antibodies anti-rat Alexa fluor 546 and anti-rabbit Alexa fluor 647 (Table 2.5 B) at manufacturers recommended concentration (in 0.5% goat serum PBS) to stain cell surface mCD9 and external *Salmonella* respectively for 30 minutes. Cells were then washed twice with PBS followed by staining of cells and bacterial DNA by DAPI stain, 400 µl/well of DAPI solution (Table 2.1) was added for 12 minutes at room temperature in the dark. Cells were then prepared for confocal microscopy as described in 2.2.5.1.5. Images were acquired using 60x objective. A Nikon A1 confocal inverted microscope with EM-CCD camera (Table 2.7), with Nikon elements software was used to visualize and analyse the images.

2.2.12.2 CD9 co-localization in mCD9-GFP J774 transfected cells

The J774 cells were transfected with mCD9-GFP as described in 2.2.10.1. and the transfected cells were infected with pNB57-mCherry (Table 2.9) transformed *Salmonella* Typhimurium NCTC12023 as described in 2.2.2.1.2. at MOI of 50 for 0, 5, 10, 15, 30, 60, 90 and 120

minutes as described in 2.2.5.1.3. The cells were washed and fixed with 4% PFA for 15 minutes RT. Then, the slides were prepared as described in 2.2.5.1.5. using Vectashield mounting medium with DAPI to minimize the bleaching and stain cells and bacterial DNA with DAPI stain (blue). Then, the coverslip was fixed to the slide with drops of nail varnish to prevent drying and slipping of the sample. Samples were analysed and visualized using inverted Nikon confocal microscopy system as mentioned above.

2.2.12.3 Live imaging microscopy

J774 cells transfected with mCD9-GFP grown on glass bottom FluoroDish™ (Table 2.8) at a concentration of 3 x 10^5 were infected with 50 MOI of *Salmonella* Typhimurium NCTC self-expressing of red fluorescent protein (RFP). A Widefield imaging system (Nikon dual cam system) inverted Ti eclipse with Oka-lab environmental control chamber (Table 2.7) controlled by Nikon elements software (NIS) (Table 2.10) was used for live imaging and the 100x objective was used. The microscope and images were adjusted and prepared choosing the appropriate filter for GFP and RFP. The old media was removed and the cells were washed one time with pre-warmed PBS and 1ml of appropriate MOI in phenol red free DMEM media containing 10% FCS was added. Then, the images were acquired every 5-10 seconds, the images then analysed using ImageJ software.

Chapter 3: Investigation of tetraspanin protein expression in mammalian cell lines

3.1 Introduction

Screening of tetraspanin proteins on the cell lines was essential to confirm the presence and distribution of tetraspanin proteins prior to studying the role of tetraspanin proteins in *Salmonella* infection using FACS and immunofluorescence microscopy. In addition, this chapter also details the transformation of fluorescent protein carrying vectors into *Salmonella enterica* serovar Typhimurium NCTC12023 and LT2 strains. These were generated as such strains could enhance and facilitate assessing mammalian cells that associated with bacteria by FACS without needing to stain *Salmonella* and could help to investigate the role of tetraspanins using live or fixed cells microscopic imaging.

3.1.1 Tetraspanin protein expression

Tetraspanin proteins are broadly expressed on mammalian cells, but whilst some members are widely distributed, the expression of others is limited to particular cells (Boucheix and Rubinstein 2001). For example, the uroplakins UP1a and UP1b are expressed specifically in urothelium cells; the photo-receptor tetraspanin peripherin/RDS and ROM-1 is expressed in the photoreceptor outer segment and is required optimum membrane fusion (Boesze-Battaglia, Stefano et al. 2007); tetraspanins CD37 and CD53 are mainly expressed by leukocytes (Virtaneva, Angelisova et al. 1993); tetraspanins Tspan-5 and NET are expressed in mouse macrophages (RAW264.7) and involved in osteoclastogenesis (Iwai, Ishii et al. 2007).

3.1.2 Flow cytometry in tetraspanins screening

Flow cytometry offers a quick method to detect and quantify fluorescent signals of cells labelled with fluorochrome (Van Dilla, Trujillo et al. 1969). Since its development, flow cytometry has been widely used for classifying and studying the expression intensity of different molecules on the cell surface and cytosolic organelles. The synchronised analysis of various fluorescent parameters offers a comprehensive study of signalling, receptor, effector and co-expressed structural molecules (O'Donnell, Ernst et al. 2013).

3.1.3 Cell line models

Different phagocytic and non-phagocytic cell lines were used in this study and screened for tetraspanin expression on the cell surface and associated with intracellular compartments. For macrophages, firstly, the mouse macrophage-like J774 cell line was used, since these cells show an intrinsic ability for phagocytosis (Ralph and Nakoinz 1975). This cell line has been used as an *E. coli* infection model to understand internalized bacterial survival (Stevenson, Baillie et al. 1984) and to understand diarrhogenic *E. coli* in cell toxicity and apoptosis post infection (Lai, Xu et al. 1999). Importantly, J774 cells have also been widely to investigate various aspects of *S.* Typhimurium infection, including studies carried out in this department (Tang, Guest et al. 2004, Gilberthorpe, Lee et al. 2007). Another well-known mouse macrophage cell line was also used: the RAW264.7 cell line that was originally established from a Balb/c mouse by Abelson leukaemia virus transformation (Ralph and Nakoinz 1977). This cell line has also been widely used to investigate *Salmonella* Typhimurium infection (Govoni, Canonne-Hergaux et al. 1999, Lahiri, Das et al. 2008, Ipinza, Collao et al. 2014). However, both of these cell lines are of mouse origin, and few monoclonal antibodies that target the native tetraspanin proteins are commercially available compared with antibodies to the human tetraspanin proteins. The human monocyte cell line, THP-1, derived from a patient with acute monocytic leukaemia (Tsuchiya, Yamabe et al. 1980), can be induced to differentiate into macrophage-like cells by treating the cells with phorbol myristate acetate (PMA) (Tsuchiya, Kobayashi et al. 1982). The cells become adherent, stop dividing and become phagocytic with upregulation of certain cell surface proteins including CD14 and CD11b, and particularly proteins that are associated with cell structure and metabolism after differentiation to macrophages (Schwende, Fitzke et al. 1996, Zhang, Liu et al. 2015). Differentiated THP-1 like macrophage-like cells have also been used for models of *S.* Typhimurium infection (e.g. Sly, Guiney et al. 2002).

As an epithelial cell model, the HEC-1-B cell line was included. This is an adherent human endometrial carcinoma epithelial cell line produced as a sub-strain of HEC-1A that was isolated in 1968 by Kuramoto (Kuramoto, Tamura et al. 1972). Since then, these cells have been used in different infection assays, including those from our group (Griffiss, Lammel et al. 1999, Green, Monk et al. 2011). In addition to HEC-1-B, the well-known human epithelial cell HeLa cell line was also used. This is a human epithelial cell line derived from cervix adenocarcinoma that was the first cultured human cells showing immortality (Gey, Coffman et al. 1952). Later on, these cells were shown to be highly susceptible to poliomyelitis virus infection and first used to develop polio vaccine (Scherer, Syverton et al. 1953) and the full genomic sequences of the cells was firstly published in 2013 (Landry, Pyl et al. 2013). HeLa

cells were suggested for use as a cell model for *Salmonella* invasion based on the fact that *Salmonella* bacteria have the ability to infect non-phagocytic cells (Giannella, Washington et al. 1973) and have been widely used with *S.* Typhimurium.

3.1.4 Fluorescent protein expressing *Salmonella*

The green jelly fish (*Aequoea victoria*) fluorescent protein (GFP) has been developed as a main indicator to observe gene expression by cell transformation, protein tracking and lineages of cells (Sirerol-Piquer, Cebrian-Silla et al. 2012). The fluorescent signal can be detected by flow cytometry in GFP-expressed bacteria, both in bacteria alone or in bacteria associated with different host cells. This provides a potential tool to investigate bacterial pathogenicity either by bacterial visualisation or bacterial quantification (Valdivia, Hromockyj et al. 1996).

The expression of GFP protein can be achieved by transforming bacteria with a plasmid vector encoding the GFP alone or fused with gene of interest that is then inserted into bacterial chromosomal DNA to provide a single copy and stable GFP expression (Hautefort, Proenca et al. 2003, Thone, Schwanhausser et al. 2007, Clark, Martinez-Argudo et al. 2009).

No effect has been observed on bacterial viability and growth rate (Ma, Zhang et al. 2011) or bacterial invasion ability in GFP expressed *Salmonella* Typhimurium (Valdivia, Hromockyj et al. 1996). However, high expression levels of GFP could affect *Salmonella* virulence and it has been suggested that the range of 7000-200,000 molecules per bacterium are enough for detection by FACS and do not affect *Salmonella* pathogenesis (Wendland and Bumann 2002). Nevertheless, others found that the antibiotic resistance gene used for selection could affect *Salmonella* invasiveness; chloramphenicol resistance had the strongest effect on *Salmonella* invasion, whereas the kanamycin resistance gene was the safest to use as an antibiotic marker, it was concluded that increase the size of the plasmid DNA could affect normal bacterial functions (Clark, Martinez-Argudo et al. 2009).

3.2 Aims

The main aim of this chapter, initially, was screening the tetraspanin protein expression that is associated in cells surface and cytoplasmic compartments prior to investigating tetraspanin roles in *Salmonella* uptake. A second aim was generate fluorescent-self-expressing *Salmonella* strains that would facilitate the investigation.

3.3 Results

3.3.1 Expression of tetraspanin proteins on different cell types

Prior to investigating the role of tetraspanin proteins in *Salmonella* infection on cell lines it was important to confirm the presence and expression levels of tetraspanin proteins on the cells that were used. FACS and immunofluorescence microscopy were used for screening. In the FACS method, the population of mammalian cells was gated depending on FSC and SSC parameters (approximately related to cell size and cell granularity, respectively). To confirm presence of tetraspanins immunofluorescence microscopy was carried out by using indirect immunofluorescence staining of cell lines that were seeded on chamber slides.

3.3.1.1 Tetraspanin proteins expression in the J774 cell line

The quantitative estimation of tetraspanin cell surface expression on the mouse macrophage J774 cell line was performed by FACS, as described in 2.2.3.1. The population of cells was gated depending on FSC and SSC parameters (Figure 3.1. A). High surface expression of CD81 and CD9 was observed, whilst the expression of CD63 was not detectable above the isotype control (Figure 3.1 B).

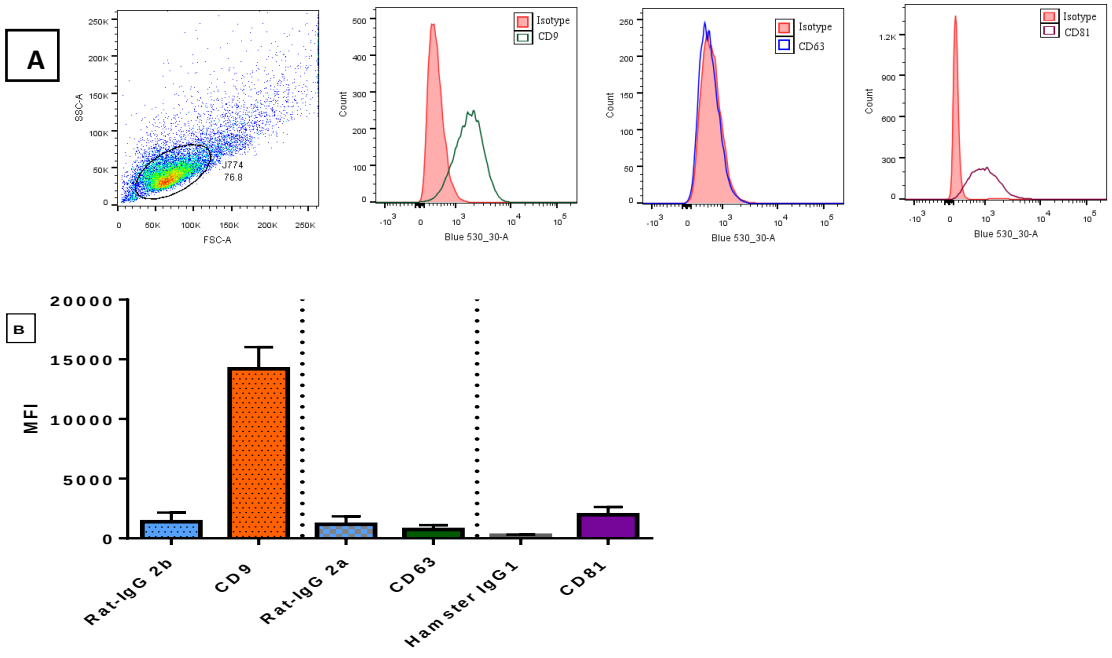

Figure 3.1: Analysis of tetraspanin expression in J774 cells by flow cytometry: The primary monoclonal antibodies used were appropriate isotype controls, anti CD9, anti CD63 and anti CD81 (Table 2.5 A). The secondary antibodies were a FITC-conjugated anti-rat IgG (for CD9 and CD63) and anti-hamster IgG (for CD81) **A:** The dot plot shows J774 cells gated according to forward scatter (FSC) and side scatter (SSC), the histograms plot shows the FCS overlap of isotype and anti-tetraspanins treated cells. **B:** MFI of tetraspanin CD9, CD63 and CD81 expression. Bars describe means, while error bars describe standard error means. n=3 in duplicate, MFI= median of fluorescent intensity.

Immunofluorescence microscopy analysis of tetraspanin expression of J774 cells was consistent with data obtained by flow cytometry. High expression of CD9 and CD81 was observed compared with isotype controls; however, CD63 was poorly expressed in these cells, with staining similar to that obtained with the isotype control (Figure 3.2).

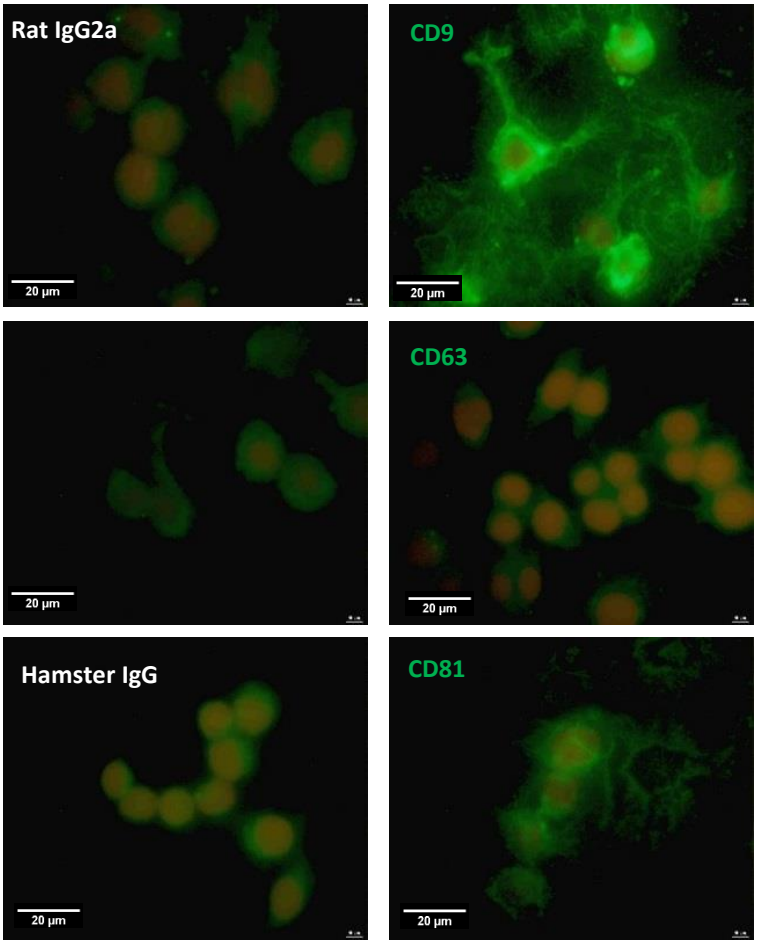

Figure 3.2: Analysis of tetraspanin expression in J774 cells by immunofluorescence microscopy. Cells were cultured on chamber slides and fixed and permeabilised as described in 2.2.4.1, then stained with primary monoclonal antibody anti CD9, anti CD63 and anti CD81 or appropriate isotype controls at 10 µg/ml followed by FITC-conjugated anti-rat IgG (for CD9 and CD63) or anti- hamster IgG (for CD81) as described in 2.1.7.1. Nuclei were counter-stained with propidium iodide. These images were obtained by using the 100x objective.

3.3.1.2 Tetraspanin expression in the RAW247 cell line

Screening of tetraspanin expression on the mouse macrophage RAW247 cell line was performed as described above 3.3.1.1. There is a high expression of tetraspanins CD81 and CD9, while the tetraspanin CD63 expression is lower, but present (Figure 3.3).

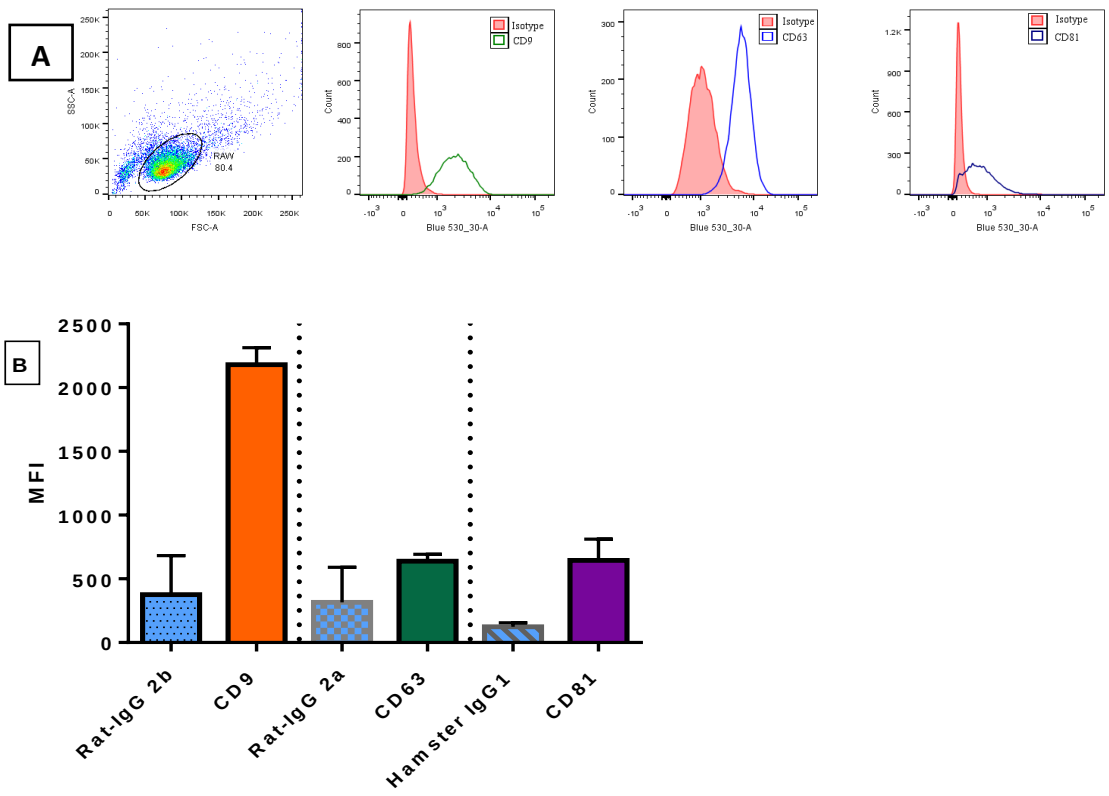

Figure 3.3: Analysis of tetraspanin expression in RAW247 cells by flow cytometry: The primary monoclonal antibody used were appropriate isotype controls, anti CD9, anti CD63 and anti CD81 (Table 2.5 A). The secondary antibodies were a FITC-conjugated anti-rat IgG (for CD9 and CD63) and anti-hamster IgG (for CD81) **A:** The dot plot shows RAW247 cells gated according to forward scatter (FSC) and side scatter, the histograms plot shows the FCS overlap of isotype and anti-tetraspanins treated cells. **B:** MFI of tetraspanin CD9, CD63 and CD81 expression. Bars describe means, while error bars describe standard error of means. n=3 in duplicate, MFI= median of fluorescent intensity.

Indirect immunofluorescence microscopy was used to visualize the tetraspanin proteins as described in 3.3.1.1. The images shows obvious membrane staining of CD9 and high expression of CD9 shows in cell-cell attached membranes. As expected, CD63 (which is known to be associated mainly with intracellular vesicular compartments) showed strong intracellular staining (Figure 3.4).

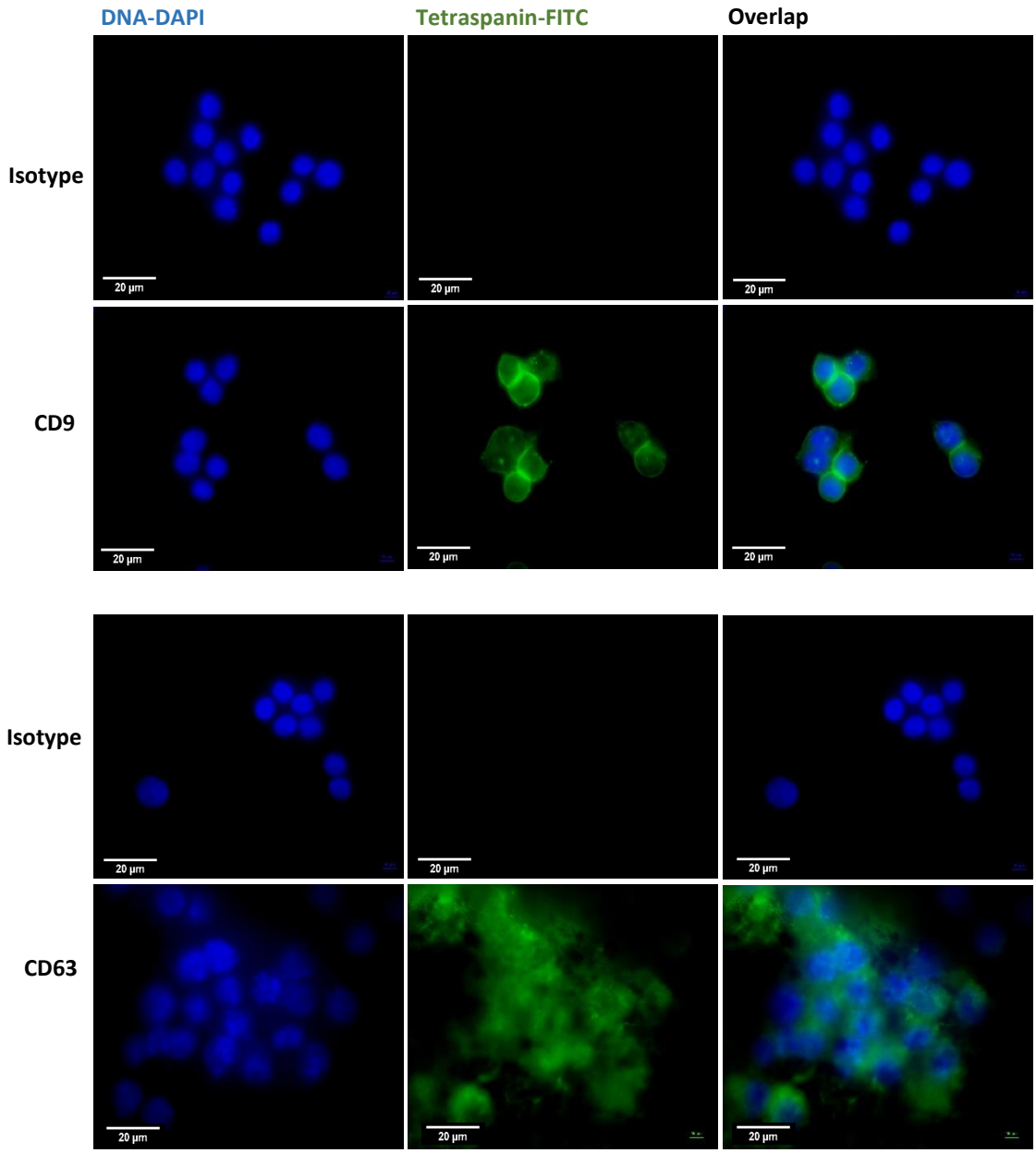

Figure 3.4: Analysis of tetraspanin expression in RAW247 cells by immunofluorescence microscopy. Cells were cultured on chamber slides and fixed and permeabilised as described in 2.2.4.1, then stained with primary monoclonal antibody (mAbs) anti CD9 and anti CD63 or appropriate isotype controls at 10 µg/ml followed by FITC-conjugated anti-rat IgG as described in 2.1.7.1. Nuclei were counter-stained with DAPI. These images were obtained by using the 100x objective.

3.3.1.3 Tetraspanin expression in stimulated and non-stimulated THP-1 cells

As described in 2.1.8.2.1, THP-1 is a human monocyte cell line obtained from a human leukaemia (Tsuchiya, Yamabe et al. 1980). These cells can be differentiated to macrophage-like cells by treating the cells with phorbol ester (PMA), as described in 2.2.1.6. Undifferentiated THP-1 cells were grown in suspension and were stimulated by treating the cells with 20ng ml^{-1} of PMA for 1, 2 and 3 days. After 24 hours in PMA, the cells showed

changes in their phenotype and became adherent. Cells were harvested as described in 2.2.1.5.1. The cell population was gated depending on cell size and granulation revealed by FSC and SSC respectively. Changes in the FSC and SSC profile of the cells showed obvious differences in the properties of the cells after PMA stimulation, with the cells becoming more scattered with changes in their size (Figure 3.5 A). There were also differences in tetraspanin expression compared with non-stimulated cells. A dramatic increase in expression of CD63 and CD81 was apparent, while CD82 showed an increase, but not significant, of surface expression one day post stimulation, but this decreased after two and three days post stimulation. CD9 increased significantly after one day of stimulation, but did not increase further thereafter. CD53 increased up until two days post stimulation. No significant changes were noticed in surface expression of CD37 and CD151 after stimulation (Figure 3.5 B).

Tetraspanin expression was also visualised by immunofluorescence microscopy of permeabilised cells. High total expression of CD63, CD81, CD82 and, to a lesser extent, CD53, was observed in THP-1 derived macrophages after three days PMA stimulation. Low staining of CD9, CD37 and CD151 was observed compared with the isotype control (Figure 3.6). The low staining of CD9 and CD37 was rather unexpected from FACS data. This might be related to high sensitivity of the epitopes recognised by the monoclonal antibodies to the fixative used. As expected, CD63 seen on granular staining, consistent with its known location in the endosomal compartment (Pols and Klumperman 2009).

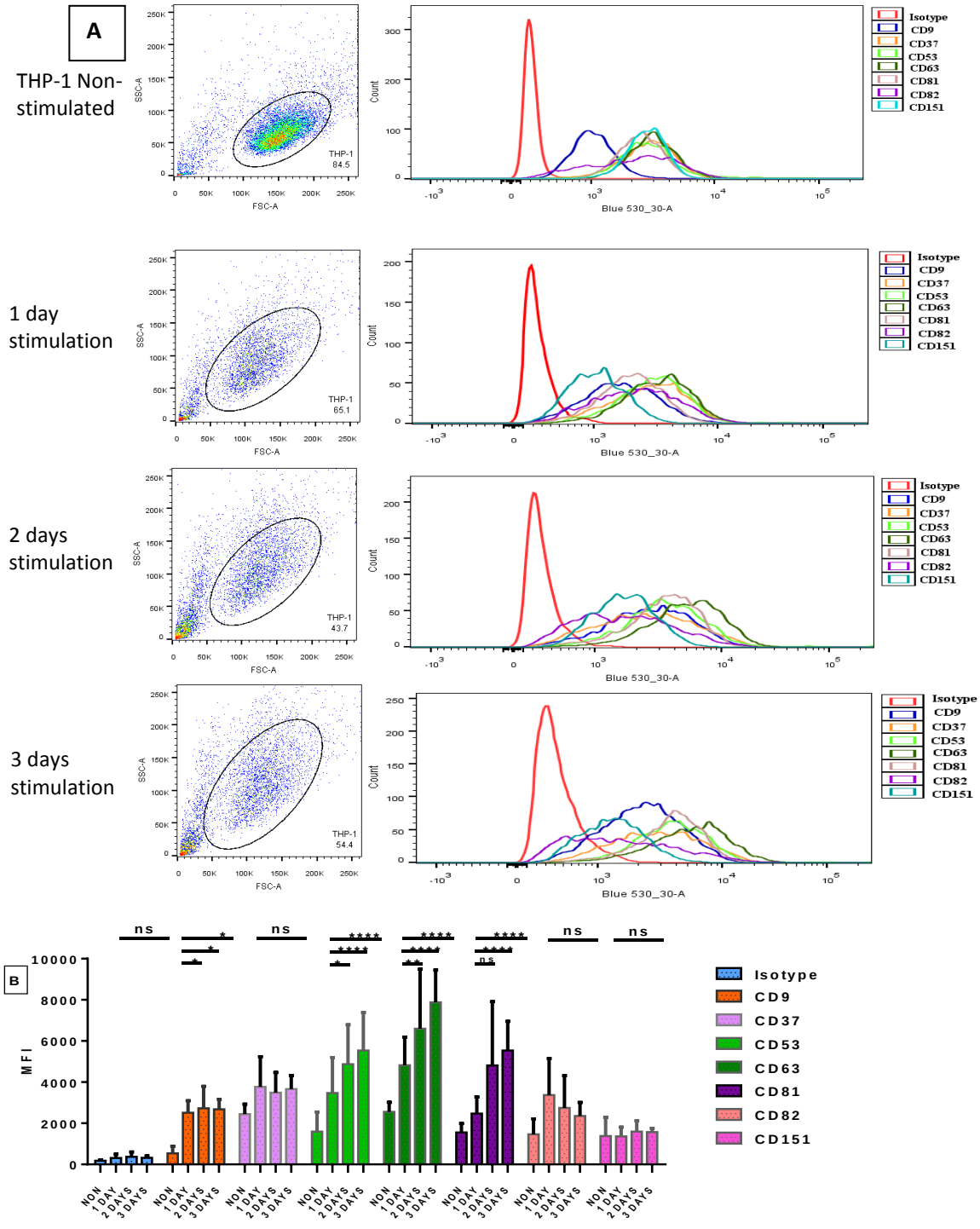

Figure 3.5: Analysis of tetraspanin expression in THP-1 cells by flow cytometry: THP-1 cells were treated with 20ng ml^{-1} PMA for 1-3 days. The primary monoclonal antibody (mAbs) used were JC1 (isotype control), anti CD9 (602.29), anti CD37 (WR17), anti CD53 (MEM-53), anti CD63 (H5C6), anti CD81, anti CD82 and anti CD151 (14 A2) (Table 2.5 A). The secondary Abs was a FITC-conjugated anti-mouse. **A:** The dot plot shows THP-1 cells gated according to forward scatter (FSC) and side scatter, the histograms plot shows the FCS overlap of isotype and anti-troponins treated cells. **B:** MFI of tetraspanins expression. Bars describe means, while error bars describe standard error. n=4 in duplicate, MFI= median of fluorescence intensity. Data was analysed by Two-way ANOVA comparing means for each sample. **** $p \leq 0.0001$ *** $p \leq 0.001$, ** $p \leq 0.01$, * $p \leq 0.05$ and ns is non-significant

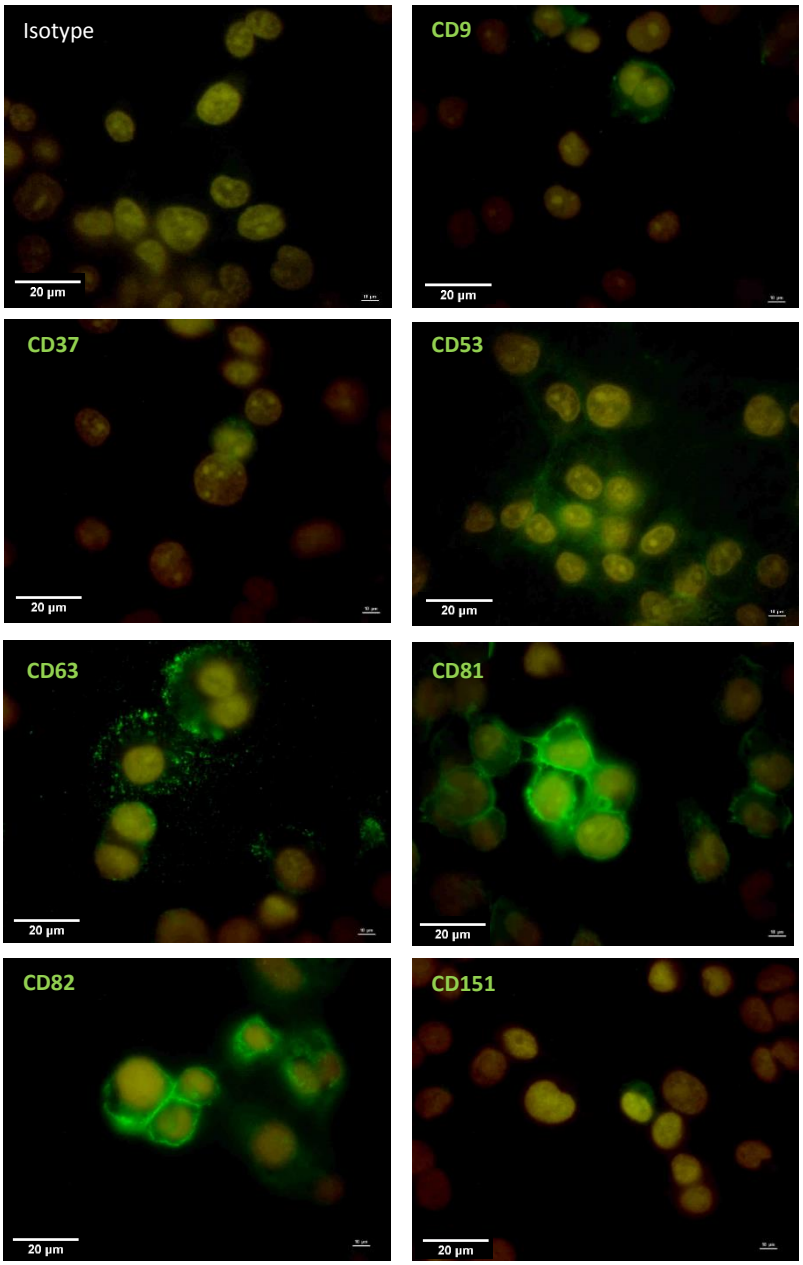

Figure 3.6: Analysis of tetraspanin expression in THP-1 cells by immunofluorescence microscopy. THP-1 cells treated with 20ng ml^{-1} PMA for 3 days. Cells were cultured on 12mm cover slides placed in 24 wells plate and fixed as described in 2.2.4.2. The primary monoclonal antibody (mAbs) used were JC1 (isotype control), anti CD9 (602.29), anti CD37 (WR17), anti CD53 (MEM-53), anti CD63 (H5C6), anti CD81, anti CD82 and anti CD151 (14 A2) (Table 2.5 A) at 10 µg/ml followed by FITC-conjugated anti-mouse IgG as described in 2.1.7.1. Nuclei were counter-stained with propidium iodide. These images were obtained by using the 100x objective.

3.3.1.4 Tetraspanin expression in the HEC-1-B cell line

HEC-1-B cell line is human epithelial cell line model obtained from human endometrial carcinoma (Kuramoto, Tamura et al. 1972) as described in 2.2.3.1. Analysis by flow cytometry showed high expression of CD9 and CD81 with relatively low expression of CD63 and CD151 and little expression of cell surface CD82 (Figure 3.7).

Immunofluorescence microscopy showed high expression of CD63 in patches in the cell cytoplasm as expected since CD63 is known to be associated with intracellular endosomal-lysosomal compartments. High expression of CD81 was observed in contrast to CD9, CD82 and CD151 that were poorly stained in permeabilised HEC-1-B cells (Figure 3.8).

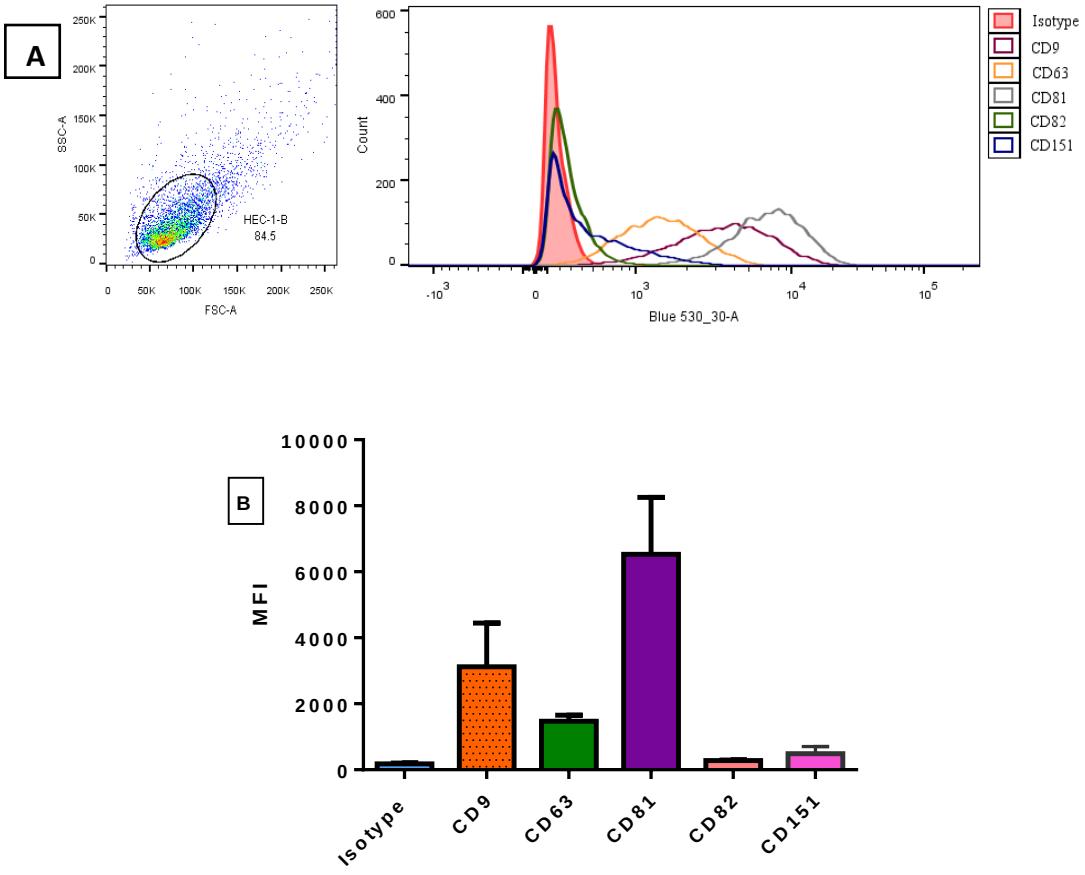

Figure 3.7: Analysis of tetraspanin expression in HEC-1-B cells by flow cytometry: The primary monoclonal antibody (mAbs) used were JC1 (isotype control), anti CD9 (602.29), anti CD63 (H5C6), anti CD81, anti CD82 and anti CD151 (14 A2) (Table 2.5 A). The secondary Abs was a FITC-conjugated anti-mouse. **A:** The dot plot shows HEC-1-B cells gated according to forward scatter (FSC) and side scatter, the histograms plot shows the FCS overlap of isotype and anti-troponins treated cells. **B:** MFI of tetraspanins expression. Bars describe means, while error bars describe standard error. n=3 in duplicate, MFI= median of fluorescent intensity.

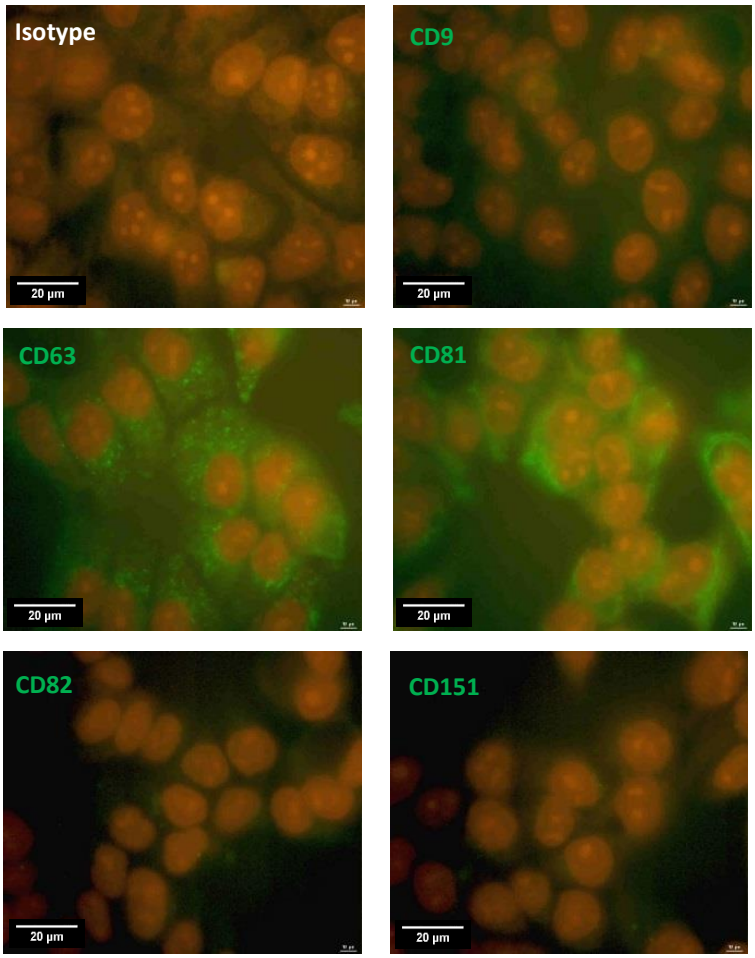

Figure 3.8: Analysis of tetraspanin expression in HEC-1-B cells by immunofluorescence microscopy. Cells were cultured on 12mm cover slides placed in 24 wells plate and fixed as described in 2.2.4.2. The primary monoclonal antibody (mAbs) used were JC1 (isotype control), anti CD9 (602.29), anti CD63 (H5C6), anti CD81, anti CD82 and anti CD151 (14 A2) (Table 2.5 A) at 10 µg/ml followed by FITC-conjugated anti-mouse IgG as described in 2.1.7.1. Nuclei were counter-stained with propidium iodide. These images were obtained by using the 100x objective.

3.3.1.5 Analysis of tetraspanin expression in HeLa cells

In flow cytometry analysis, HeLa cells showed high surface expression CD9, CD63, CD81 and CD151, with slightly lower expression of CD82 (Figure 3.9). Immunofluorescence microscopy of permeabilised cells showed strong staining for CD63, some staining for CD151 and low staining for CD9, CD81 and CD82 (Figure 3.10).

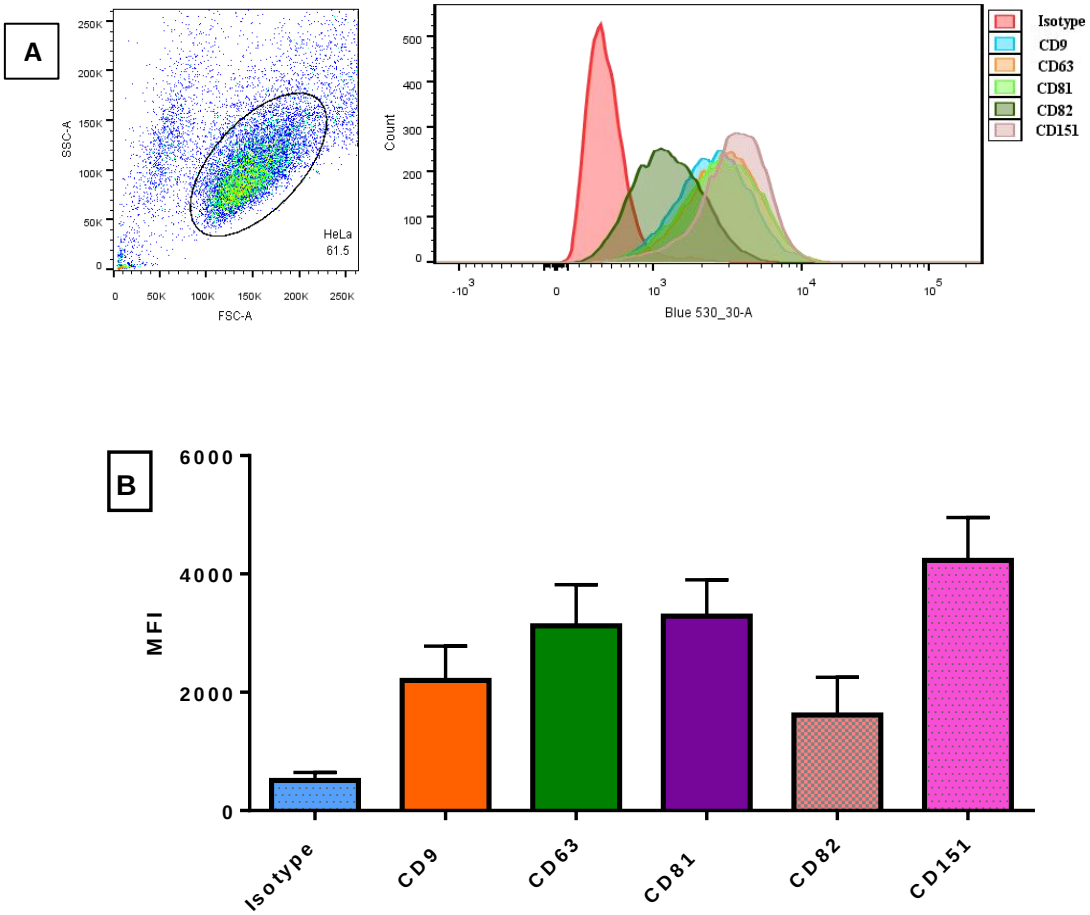

Figure 3.9: Analysis of tetraspanin expression in HeLa cells by flow cytometry: The primary monoclonal antibody (mAbs) used were JC1 (isotype control), anti CD9 (602.29), anti CD63 (H5C6), anti CD81, anti CD82 and anti CD151 (14 A2) (Table 2.5 A). The secondary Abs was a FITC-conjugated anti-mouse. **A:** The dot plot shows HeLa cells gated according to forward scatter (FSC) and side scatter, the histograms plot shows the FCS overlap of isotype and anti-troponins treated cells. **B:** MFI of tetraspanins expression. Bars describe means, while error bars describe standard error. n=3 in duplicate, MFI= median of fluorescent intensity.

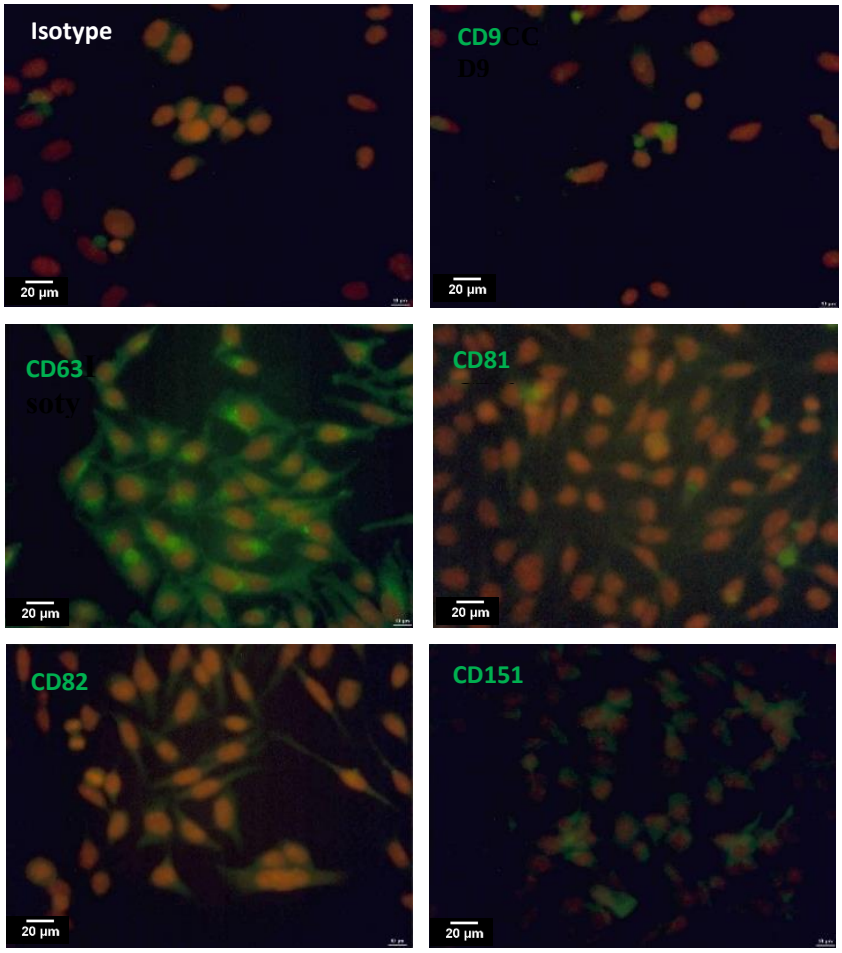

Figure 3.10: Analysis of tetraspanin expression in HeLa cells by immunofluorescence microscopy. Cells were cultured on chamber slides and fixed and permeabilised as described in 2.2.4.1. The primary monoclonal antibody (mAbs) used were JC1 (isotype control), anti CD9 (602.29), anti CD63 (H5C6), anti CD81, anti CD82 and anti CD151 (14 A2) (Table 2.5 A) at 10 µg/ml followed by FITC-conjugated anti-mouse IgG as described in 2.1.7.1. Nuclei were counter-stained with propidium iodide. These images were obtained by using the 40x objective.

3.3.1.6 Tetraspanin protein expression in CD82-KO cell line

Since anti-mouse CD82 is commercially unavailable, CD82 knockout macrophages generated from CD82-KO mice (Risinger, Custer et al. 2014) could offer an alternative to investigate the role of this tetraspanin in infection. The effect of CD82 knockout on expression of tetraspanins CD9, CD63 and CD81 was assessed by flow cytometry. No significant difference was indicated in surface expression of CD9 in CD82-KO cells compared with corresponding WT mouse macrophages; high expression of CD9 was observed in both CD82-KO and WT control. Nevertheless, surface expression of CD63 was significantly upregulated in CD82-KO cells compared with WT control, but was relatively low in WT mouse macrophages, as had previously been observed in J774 and RAW macrophages. Furthermore, CD81 was also significantly upregulated in CD82-KO mouse macrophages compared corresponding WT mouse macrophages (Figure 3.11).

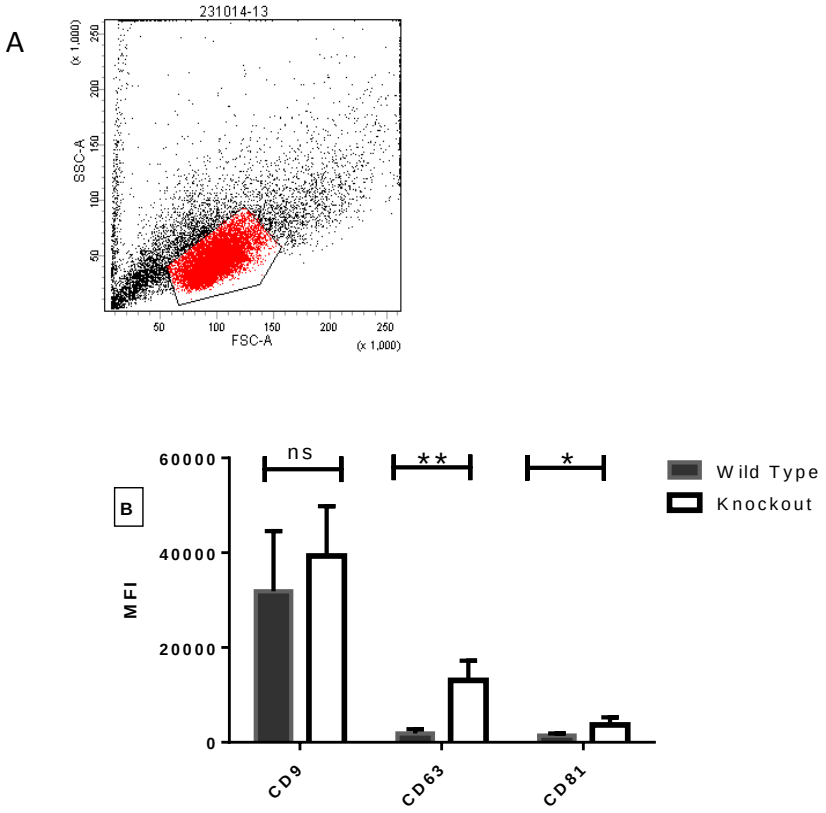

Figure 3.11: Analysis of tetraspanin expression in CD82 KO and WT mouse macrophages by flow cytometry: This work was carried out in our lab by a 3rd year project students S. Howard and V. Rose (under my supervision). The primary monoclonal antibody (mAbs) used were appropriate isotype controls, anti CD9, anti CD63 and anti CD81 (Table 2.5 A). The secondary antibodies were a FITC-conjugated anti-rat IgG (for CD9 and CD63) and anti- hamster IgG (for CD81) **A:** The dot plot shows CD82 KO cells gated according to forward scatter (FSC) and side scatter, the histograms plot shows the FCS overlap of isotype and anti-troponins treated cells. **B:** MFI of tetraspanins. Bars describe means, while error bars describe standard error means. N=4 in duplicate, MFI= median of fluorescent intensity. Data was analysed by T-test comparing means for each sample. ** $p \leq 0.01$, * $p \leq 0.05$ and ns is non-significant.

3.3.2 *Salmonella* Typhimurium expressing green fluorescent protein (GFP)

Salmonella expressing fluorescent proteins have been increasingly employed (Haidinger, Szostak et al. 2001, Thone, Schwanhausser et al. 2007, Robijns, Roberfroid et al. 2014), either in cell infection studies (Thone, Schwanhausser et al. 2007) or to investigate particular virulence associated proteins throughout bacterial infection (Bumann 2002). *Salmonella* cells competent for electroporation transformation were prepared as described in 2.2.2.1.1. and the bacterial transformation using electroporation was carried out as described in 2.2.2.1.2. Optimisation of transformation for *Salmonella* NCTC12023 and LT2 were carried out using different vectors carrying GFP or RFP encoded genes to be expressed in *Salmonella* (Table 2.9). The broad host range (pBHR-1) vector (Szpirer, Faelen et al. 2001) carrying the GFP encoding gene (kindly donated from Dr. Mark Thomas, Medical school, University of Sheffield) was successfully transformed into both *Salmonella* strains and sufficient and stable

GFP protein expression was obtained for detection by flow cytometry and fluorescence microscopy using appropriate filters. In flow cytometry, the GFP positive *Salmonella* population was completely segregated with high percentages (~ 90-99 %) and high fluorescent intensity (Figure 3.12). Fluorescence microscopy visualisation of the GFP and WT *Salmonella* is shown in Figure 3.13. No significant changes in percentage of *Salmonella* expressing GFP was observed in overnight culture compared with 2 hours culture in both strains. No significant MFI difference was also observed in the LT2 strain between overnight culture and 2 hours culture; however, overnight cultures of NCTC12023 expressing GFP seemed to be more highly expressing GFP compared with 2 hours culture, although high expression of GFP was observed here also (Figure 3.12).

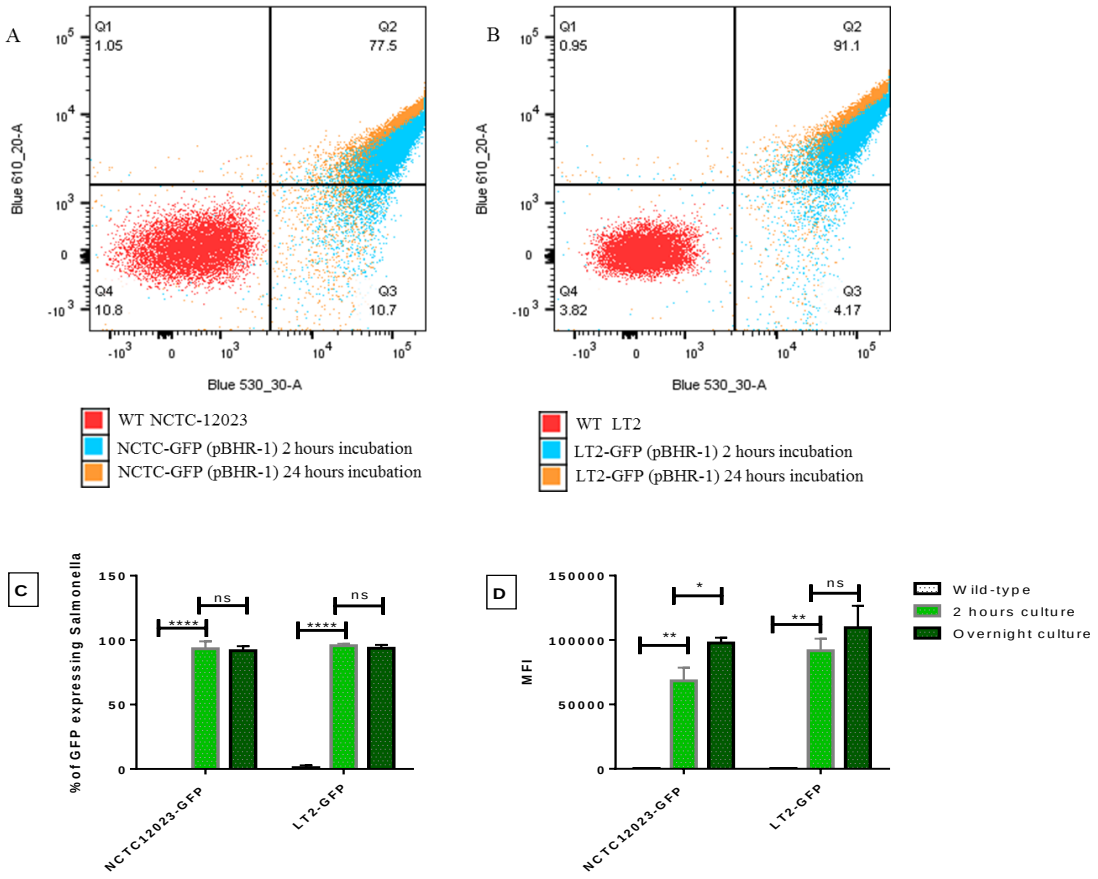

Figure 3.12: GFP expression by *Salmonella* Typhimurium transformed with plasmids encoding GFP. *Salmonella* Typhimurium strains were transformed with the pBHR-GFP vector as described in 2.2.2.1.2. Bacteria were prepared and analysed by LSR-II flow cytometer as described in 2.2.2.1.3. Both FSC and SSC parameters were used to plot the cells on a $\log^{10}$ scale and 10^5 events were acquired. Positive cells were detected using the 530-30 A filter of a LSR-II flow cytometer machine from the FSC-SSC gated cells population. *Salmonella* NCTC12023 and LT2 wild types were included as negative control **A:** Overlap histogram of FSC of *Salmonella* NCTC12023 WT and GFP expressing strain. **B:** Overlap histogram of FSC of *Salmonella* LT2 WT and GFP expressing strains. **C:** Percentage of positive cells compared with non-transformed WT *Salmonella*. **D:** MFI of transformed *Salmonella* compared with WT strain. n=3. MFI= median of fluorescent intensity, data was analysed by Two-way ANOVA comparing between means for each sample. **** $p \leq 0.0001$, ** $p \leq 0.01$, * $p \leq 0.05$ and ns is non-significant.

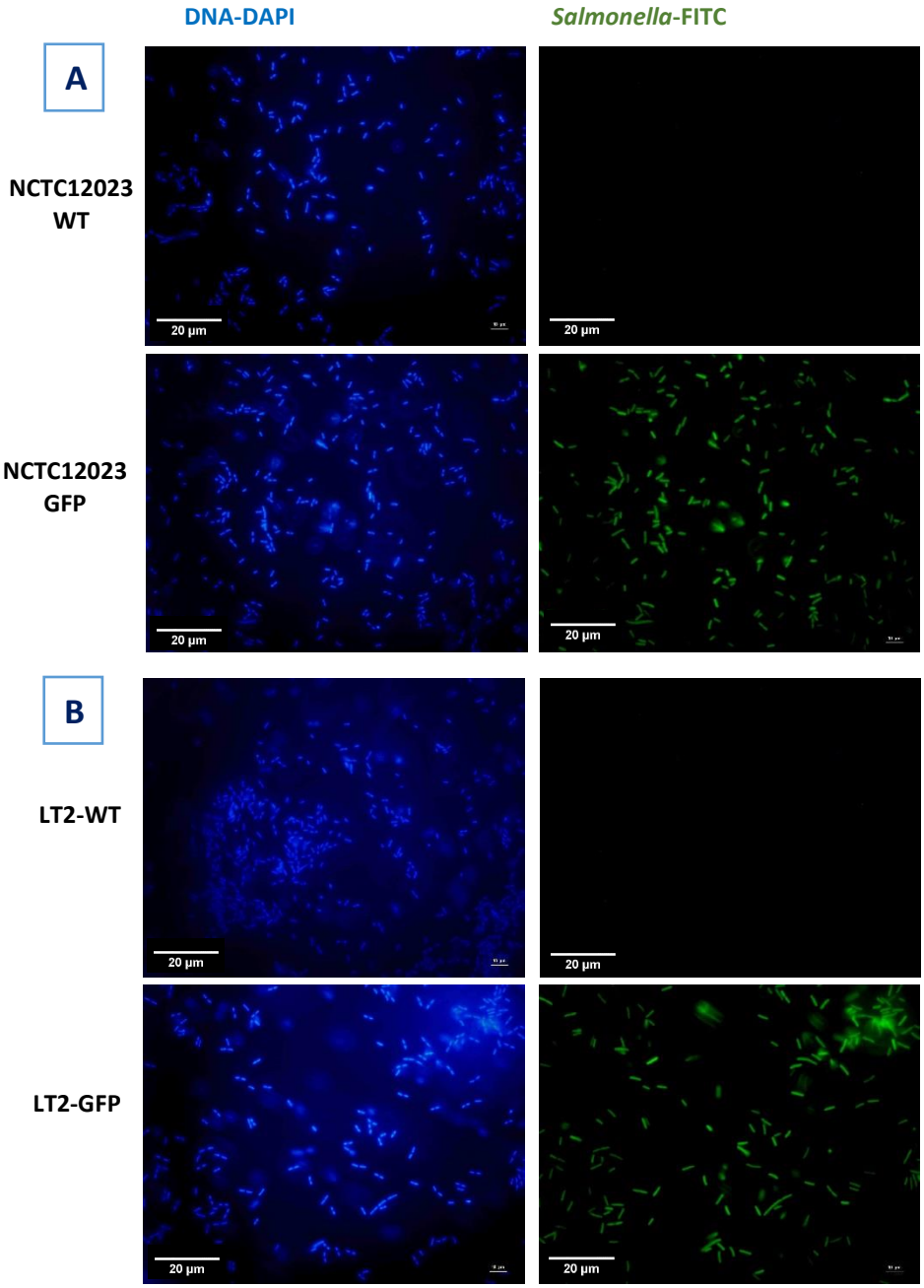

Figure 3.13: Immunofluorescence images of *S.* Typhimurium transformed with pBHR1-GFP plasmid. Bacteria were prepared as described in 2.2.2.1.4 **A:** *Salmonella* Typhimurium NCTC12023 transformed with pBHR1-GFP vector (green), and bacterial DNA stained with DAPI (blue) and visualised using the appropriate filter compared with WT control. **B:** LT2 strain transformed with pBHR1-GFP vector (green), and bacterial DNA stained with DAPI (blue) and visualised using appropriate filter. These images obtained using the 100x objective.

3.3.3 *Salmonella* Typhimurium expressing red fluorescent protein (RFP) protein

As mentioned above, RFP expressing *Salmonella* could provide advantages for investigating bacterial infection either for imaging or quantitative studies (Valdivia, Hromockyj et al. 1996). Furthermore, RFP expressing *Salmonella* could facilitate live imaging when combined with tetraspanin-GFP expressing cells. *Salmonella* were transformed with a DsRed carrying vector pAV49 (Table 2.9). Transformation was successful, as bacteria grew on antibiotic selective plates, but no expression of DsRed in either *Salmonella* strains was found (data not shown). However, successful but unstable expression of DsRed was observed in NCTC12023 strain transformed with another DsRed expressing vector (pDS-Red Expression vector II (Table 2.9)). In addition, the expression of DsRed was affected by the concentration of selective antibiotic used and culture conditions. 200µg ml^{-1} ampicillin gave more stable expression of DsRed grown on LB agar, while weak expression of DsRed was shown in *Salmonella* grown in LB broth containing the same concentration of selective antibiotic (Figure 3.14). Few colonies expressing DsRed in the LT2 strain transformed with pDS expression vector II were observed. In addition, a significant variation in the percentage of positive cells and intensity of fluorescence (MFI) was observed in NCTC12023-pDs-Red in 2 hour bacterial cultures compared with overnight culture (Figures 3.15 and 3.18 A-D). *Salmonella* expressing low levels of DsRed protein are difficult to detect either by fluorescence microscope or by FACS. Since all infection experiments were carried out using bacteria in mid log growth phase (about 2 hours incubation); high DsRed protein expression seems to need a longer incubation time by which the bacteria enter stationary phase. Furthermore, a high percentage of *Salmonella* expressing DsRed protein was also detected in the GFP flow cytometer filter (Figure 3.18 A-D). This high overlap of DsRed protein with the GFP filter could prevent the usefulness of DsRed expressing *Salmonella* with tetraspanin-GFP expressing cells since both GFP and DsRed would show by the same filter. In addition, this overlap was also observed in wide field microscopy, making it difficult to investigate tetraspanin GFP-*Salmonella* localisation using live imaging (data not shown).

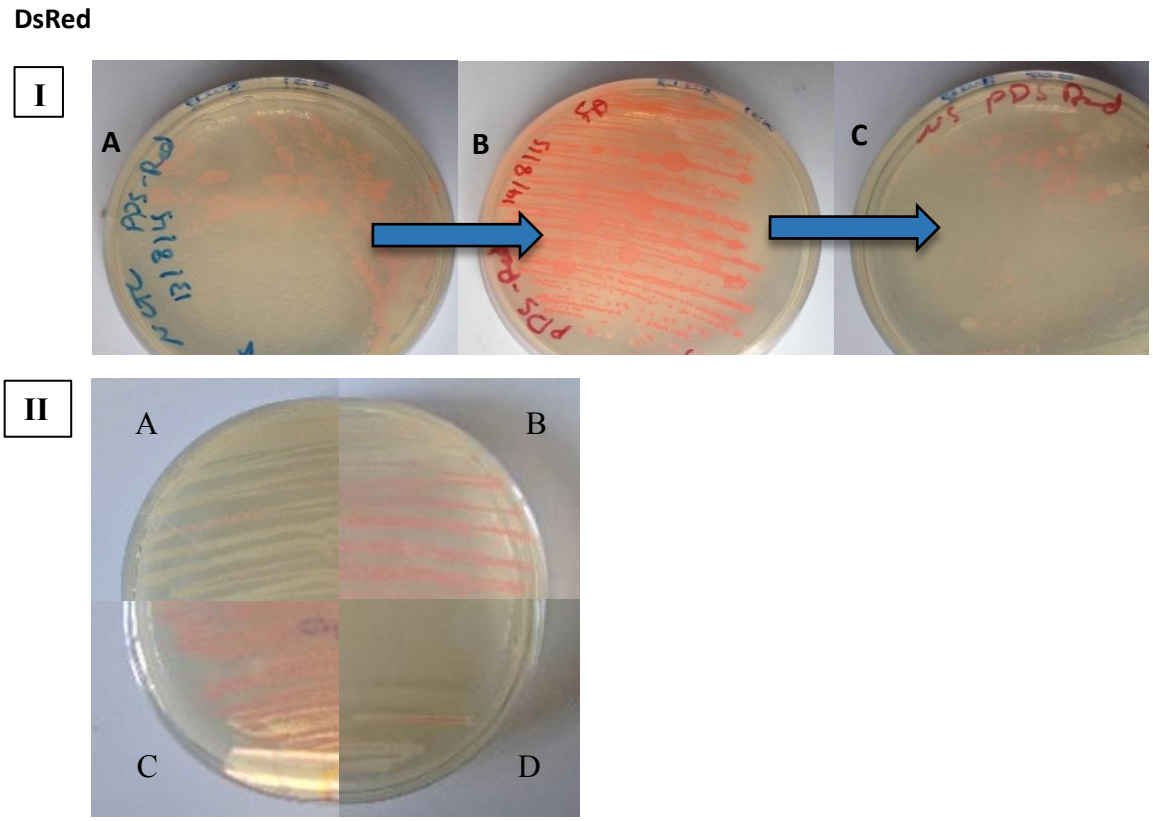

Figure 3.14: Effect of different growth conditions and ampicillin concentration on DS-RED expression. I: NCTC12023-pDS-Red strain subcultured in 200µg ml^{-1} ampicillin LB agar. **A:** Primary culture from frozen glycerol stock. **B:** One colony from "A" sub-cultured into 200µg ml^{-1} ampicillin LB agar. **C:** One single colony from "B" sub-cultured into 200µg ml^{-1} ampicillin LB agar. **II:** NCTC12023-pDS-Red strain grown in different ampicillin concentrations in LB agar. **A:** 50µg ml^{-1} **B:** 200µg ml^{-1}. **C:** 300µg ml^{-1}. **D:** 400µg ml^{-1} overnight culture.

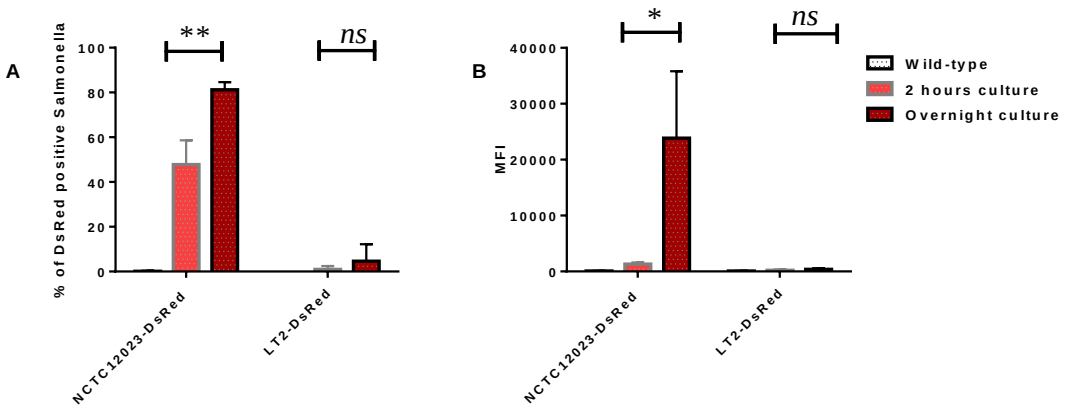

Figure 3.15: Flow cytometry analysis of pDS-Red transformed *Salmonella* Typhimurium. NCTC12023 and LT2 strains were transformed with pDS-Red vector as described in 2.2.2.1.2, and the bacteria were prepared and analysed using LSR-II flow cytometer using 488 blue laser with the 610-20A filter (as recommended for RFP) as described in 2.2.2.1.3. **A:** Percentage of positive cells compared with non-transformed WT *Salmonella*. **B:** MFI of transformed *Salmonella* compared with WT strain. Bars describe means, while error bars describe standard errors. n=3, MFI= median of fluorescent intensity, data was analysed by Two-way ANOVA comparing between means for each sample. ** $p \leq 0.01$, * $p \leq 0.05$ and ns is non-significant.

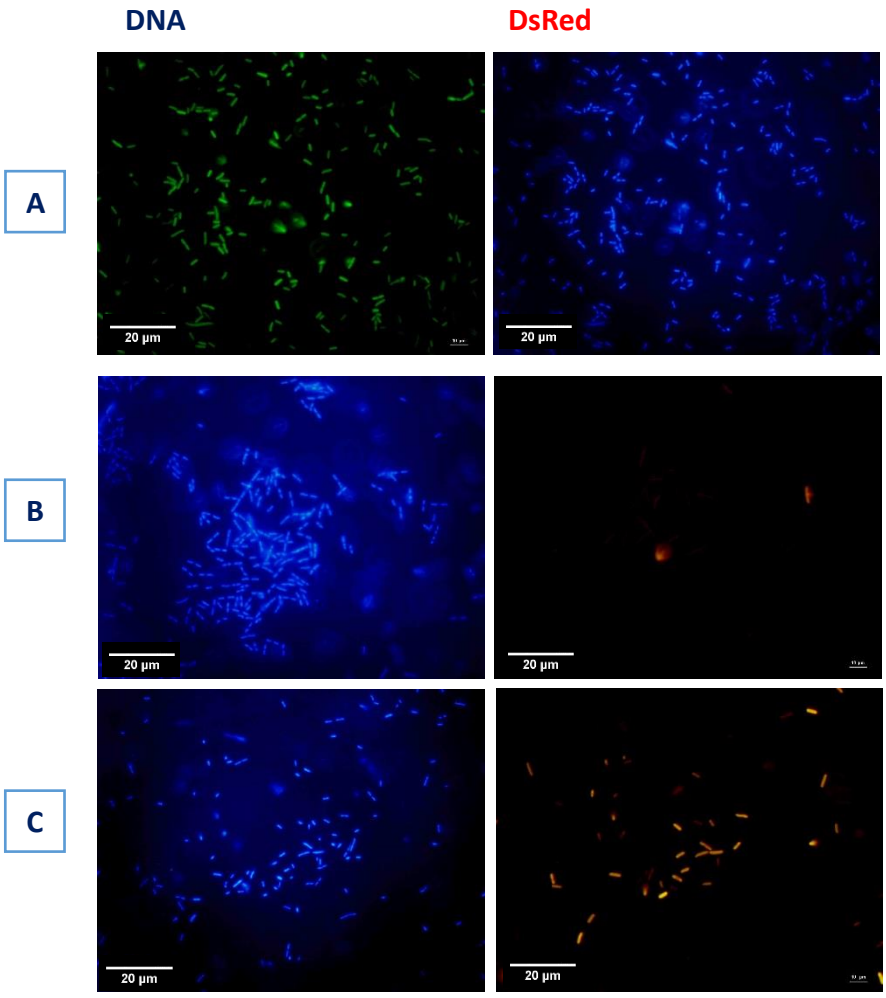

Figure 3.16: Immunofluorescence images of *S.* Typhimurium NCTC12023 transformed with pDS-Red plasmid. Bacteria were cultured and prepared for microscopic imaging as described in 2.2.2.1.4. **A:** NCTC12023-WT control stained with DAPI (blue) visualised using appropriate filter compared with WT control. **B:** NCTC12023-pDSRed (red) 2 hours culture visualised using appropriate filter. **C:** NCTC-12023-pDsRed (red) overnight culture visualised using appropriate filter. These images were obtained using the 100x objective.

Therefore, mCherry expressing *Salmonella* could be better to use with tetraspanin-GFP expressing cells.

A mCherry carrying plasmid pNB57 (Table 2.9) was successfully transformed into both *Salmonella* strains and the mCherry protein was successfully and stably expressed in both strains (Figure 3.17). Flow cytometry analysis showed a high percentage of positive cells, however, as observed for DsRed, both the percentage of mCherry expressing *Salmonella* and MFI was significantly higher in overnight cultures compared with 2 hour cultures (Figure 3.18). In spite of these variations in mCherry expression, the positive population of *Salmonella* expressing mCherry was only detected in the red fluorescence channel, with no overlap in the GFP channel (Figure 3.18 A-D).

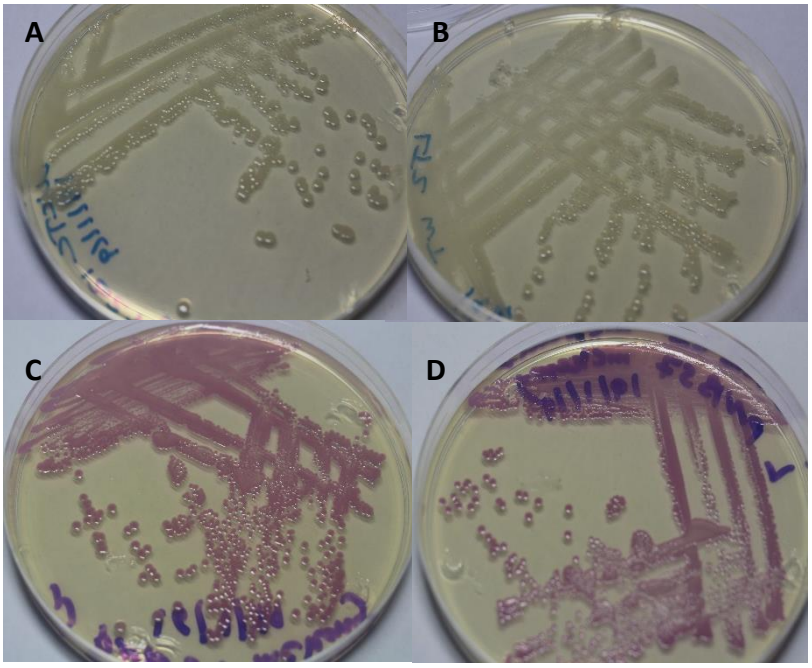

Figure 3.17: *Salmonella* strains transformed with pNB57-mCherry vector. **A:** *S.* Typhimurium NCTC12023 wild type strain grown on LB agar. **B:** *S.* Typhimurium LT2 wild type strain grown on LB agar. **C:** *S.* Typhimurium NCTC12023-pNB57-mCherry strain grown on LB agar with 100µg ml^{-1} ampicillin. **D:** *S.* Typhimurium LT2-pNB57-mCherry strain grown on LB agar with 100µg ml^{-1} ampicillin.

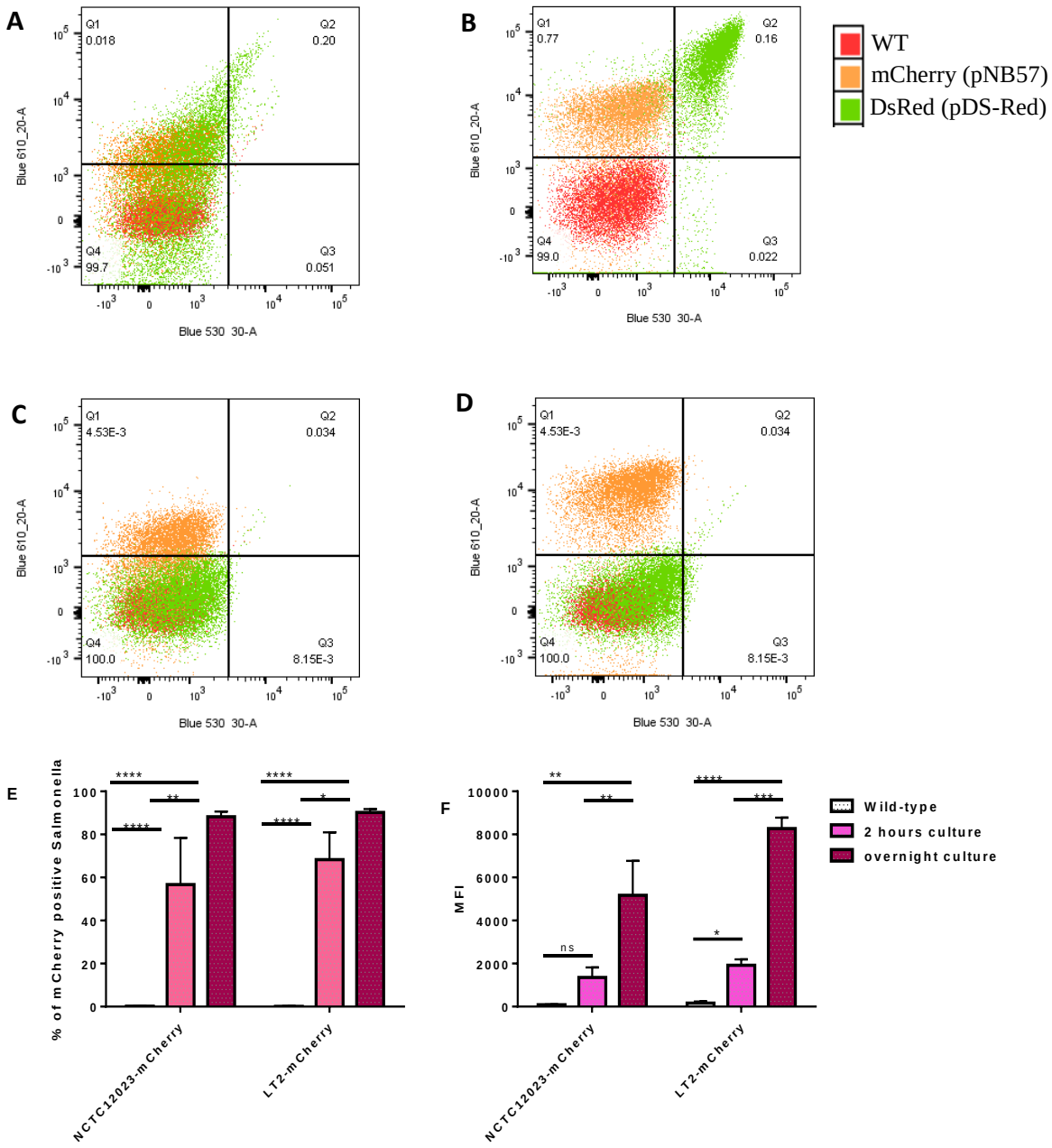

Figure 3.18: Flow cytometry analysis of mCherry transformed *Salmonella* Typhimurium. NCTC12023 and LT2 strains were transformed with pNB57-mCherry vector as described in 2.2.2.1.2, and the bacteria were prepared and analysed using LSR-II flow cytometer using 488 blue laser with the 610-20A filter (as recommended for RFP) as described in 2.2.2.1.3. Both FSC and SSC parameters were used to plot the cells on a $\log^{10}$ scale and 10^5 events were acquired. Positive cells were detected using the 530-30 A and 610-20 A filters of a LSR-II flow cytometer from the FSC-SSC gated cells population. *Salmonella* NCTC12023 and LT2 wild types were included as negative control **A:** Overlap histogram of FSC of *Salmonella* NCTC12023 WT, DsRed and mCherry expressing strain 2 hours incubation culture and overnight incubation culture **(B)**. **C:** Overlap histogram of FSC of *Salmonella* LT2 WT, DsRed and mCherry expressing strain 2 hours incubation culture and overnight incubation culture **(D). E:** Percentage of mCherry positive cells compared with non-transformed WT *Salmonella*. **F:** MFI of pNB57- mCherry transformed *Salmonella* compared with WT strain. n=3. MFI= median of fluorescent intensity, data was analysed by Two-way ANOVA comparing between means for each sample. **** $p \leq 0.0001$, *** $p \leq 0.001$ ** $p \leq 0.01$ and * $p \leq 0.05$.

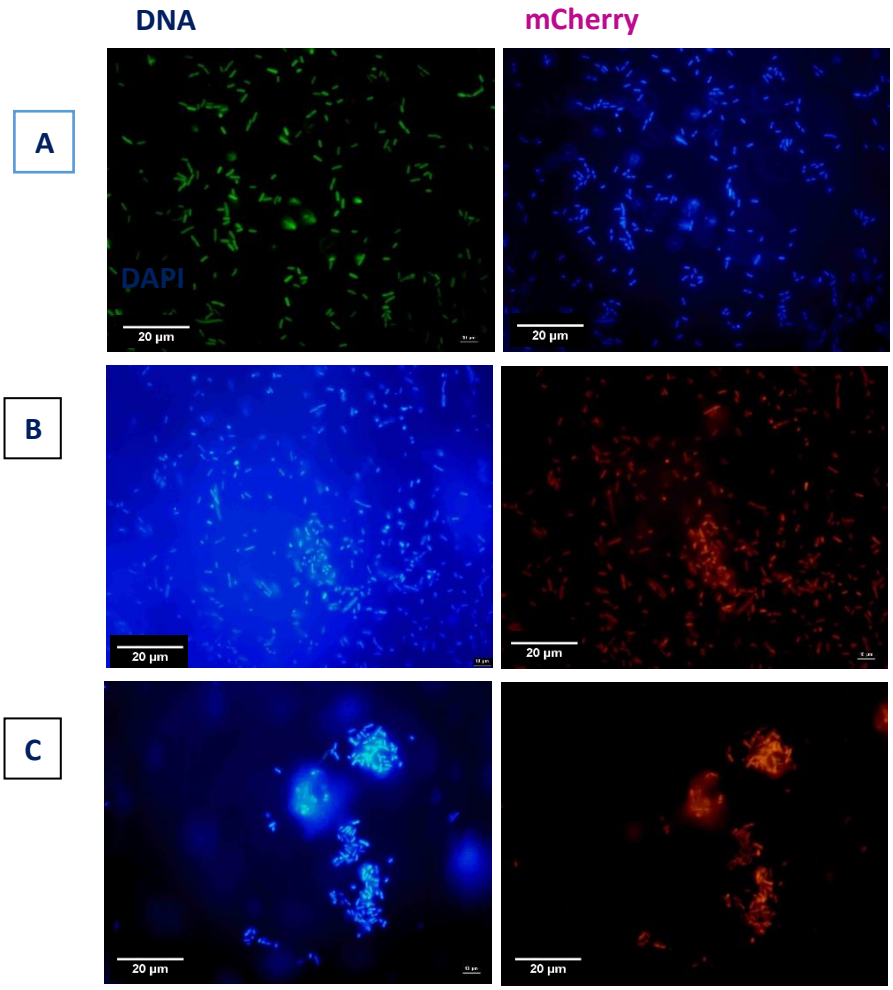

Figure 3.19: Immunofluorescence images of *S.* Typhimurium LT2 transformed with pNB57-mcherry plasmid. Bacteria were cultured and prepared for microscopic imaging as described in 2.2.2.1.4. **A:** NCTC12023-WT control stained with DAPI (blue) visualised using appropriate filter. **B:** NCTC-12023-mCherry (red) overnight culture visualised using appropriate filter. **C:** LT2-mCherry (red) overnight culture visualised using appropriate filter. These images were obtained using the 100x objective.

Similar results were evident from fluorescence microscopy of the pDS-Red transformed NCTC12023 strain. The DsRed expression was observed in overnight bacterial cultures, but only in a few cells after 2 hours culture (Figure 3.16).

3.4 Discussion

The level of tetraspanins expression was screened as an initial step to investigate the role of these proteins in *Salmonella* infection. Two different cell species were used, mouse and human, although few anti-tetraspanin antibodies that recognise the native protein are commercially available for the mouse proteins, in contrast to anti-human tetraspanins. The monoclonal antibodies were used to determine tetraspanins expression, since mAbs provide

a highly specific tool to detect specific antigens (Kohler and Milstein 1975). As reported in many studies, the tetraspanin proteins are expressed in all human cell types, with some tetraspanin members (including CD9 and CD81) expressed in most mammalian cells (Hemler 2005) while others are seen in specific cell types and associated with particular functions, as mentioned previously. CD9, CD53, CD63 and CD81 are expressed in normal MDMs and macrophages (Tippett, Cameron et al. 2013). In RAW and J774, the expression of CD9 and CD81, was observed in using flow cytometry and the results supported by immunofluorescence images. These tetraspanins were found mainly on the cell surface. High expression of CD9 and CD81 was observed with low surface expression of CD63; this could be because the tetraspanin CD63 is associated mostly with intracellular vesicular compartments (late endosomes and lysosomes) (Zhang, Kotha et al. 2009).

The human cell lines derived from human monocytic leukaemia (THP-1) (Tsuchiya, Yamabe et al. 1980) was also used in *Salmonella* infection. These cells could be differentiated to become macrophages by treating the cells with phorbol ester (PMA). Compared with other human monocyte cell lines, this THP-1 cells were shown to be more similar to primary MDMs (Auwerx 1991). The differentiation of THP-1 by phorbol ester could be mediated by protein kinase C (PKC) resulting in suppression of the G1 phase of the cell cycle (Traore, Trush et al. 2005). High concentrations of phorbol ester could lead to affect the differentiated cells responses (e.g. to IL10) therefore a minimum concentration of PMA is required for THP-1 stimulation without affecting macrophage functionality (Maess, Wittig et al. 2014). Different markers have been shown to be expressed post THP-1 differentiation, particularly CD11b and CD14 (Schwende, Fitzke et al. 1996). In the THP-1 cells model, most of the tetraspanins were upregulated within one day of PMA stimulation (apart from CD37, and CD151). The cellular phenotype was changed to become adherent, flat and stopped dividing after stimulation, consistent with previous reported observations (Tsuchiya, Kobayashi et al. 1982). Although CD63 is associated with endosomal-lysosomal compartments (Zhang, Kotha et al. 2009), high surface expression of CD63 was noticed one day after stimulation and dramatically increased to reach the highest level compared with other tetraspanins. Neither CD37 nor CD151 showed changes in expression after THP-1 differentiation, while CD9 was upregulated by one day post THP-1 stimulation and was stabilised by day 2 and 3 of stimulation. This is in contrast to reports that CD9 increased after 24 hours post differentiation by PMA at 40ng/ml and continued to increase until 72 hours of stimulation (Tsukamoto, Takeuchi et al. 2014). Furthermore, human monocyte derived macrophages (MDMs) showed a higher expression of CD9 compared with monocytes while CD81 remained at the same level of expression during maturation and surface CD53 decreased after differentiation,

although intracellular levels increased (Tippett, Cameron et al. 2013), which may relate to the development of the endosomal-lysosomal system in differentiated macrophages (de Winde, Zuidscherwoude et al, 2015). However, THP-1 derived macrophages shown increases in CD53 and CD81 compared with un-stimulated THP-1 cells. Nevertheless, previous studies here also showed that CD53 increased after THP-1 differentiation (Hassuna, 2010, thesis, University of Sheffield).

In the HEC1-B cell line, high expression of CD9 and CD81 was observed by FACS. By contrast, CD63, CD82 and CD151 seem to be lowly expressed compared with isotype control (Figure 3.7). Nevertheless, CD151 showed the highest expression amongst the tetraspanins in another epithelial cell line, HeLa cells (Figure 3.9). CD151 is known to be associated with cancer cells proliferation and high expression of CD151 correlates with bad prognosis in cancer (Hemler 2014). CD63 and CD82 were also shown to be significantly expressed in HeLa cells compared with isotype control. These results demonstrate that, different patterns of tetraspanin expression could be seen depending on the cell type and origin. In HEC-1-B, the immunofluorescence microscopy results shows highly intense staining of CD63 distributed as patches on cells, with more intensive staining localised close to the nucleus, whilst no strong staining was observed for CD9, CD82 and CD151. In contrast, Hela cells present a strong staining of CD151and to a lesser extent CD81 and CD82; however, the CD63 staining localisation shows same pattern observed in HEC-1-B cells. These results support the previous finding using flow cytometry in which low expression of CD151 and CD82 were observed in HEC-1-B in contrast to HeLa cells. Nevertheless, CD63 was highly expressed and showed the same localisation pattern in both cell lines. The presence of patches of staining could be related to the high expression of CD63 in intracellular compartment particularly endosomal lysosomal system (Pols and Klumperman 2009).

Tetraspanin CD82 and also named KAI1 is widely distributed in different cells types including haemopoietic and non-haemopoietic cells (Martin, Roth et al. 2005) and in different cancers (Huang, Taki et al. 1997) acts as a tumour suppressor which supresses cancer cells motility, invasion and metastasis (Liu and Zhang 2006, Hemler 2014, Feng, Huang et al. 2015). Furthermore, it is associated with HTLV-1 (human T-cells leukaemia virus type 1) infection and viral cell-cell transmission (Pique, Lagaudriere-Gesbert et al. 2000). Antibodies targeting mouse CD82 are not commercially available, therefore, CD82-KO mouse macrophages could offer a suitable mouse cell model to study the contribution of CD82 either in cancers (Hemler 2014) or in infections, although many genes shown to be either upregulated or down regulated in mRNA level as a consequence of CD82 gene disruption

(Risinger, Custer et al. 2014). Downregulation of CD63 and CD81 was observed in CD82-KO mouse macrophages compared with corresponding macrophages control (Figure 3.11). In contrast, no change in CD9 expression was noticed in these cells. As for CD63, CD82 is also known to be localised within the endosomal-lysosomal system (Xu, Zhang et al. 2009). In addition, CD82 associates with CD63 and both tetraspanins are found in MHC class-II compartments (Hammond, Denzin et al. 1998). A number of studies have shown association of various integrins, including α3β1, α4β1, α5β1 and α6β1,with CD82 to form CD82-integrins complex in different cells types, reviewed in (Berditchevski 2001), notwithstanding the direct association of CD63 with α3β1 and α6β1 (Berditchevski, Bazzoni et al. 1995). Furthermore, association of CD81 and/or CD82 with α4β1 integrin in hemopoietic cells has also been observed (Mannion, Berditchevski et al. 1996). These tetraspanin-tetraspanin and tetraspanin-integrin association could have a direct or indirect impact in alteration of certain tetraspanins expression in absence of CD82.

Bacteria self-expressing fluorescent proteins such as GFP and RFP offer a good tool to better understand bacterial pathogenesis and bacteria behaviour in a natural environment by employing live cell visualisation (Lagendijk, Validov et al. 2010). GFP has been increasingly used as a fluorescent marker in different applications, in particularly pathogenicity of bacteria to host cells in both imaging and quantification studies (Valdivia, Hromockyj et al. 1996). Two different vectors carrying the GFP gene sequence were used, and although both plasmids expressed GFP in *E. coli*, the pBHR1-GFP vector was most successfully used to express GFP in both *S.* Typhimurium NCTC12023 and LT2 strains. However, the LT2 strain seemed to be express more GFP compared with the NCTC12023 strain. GFP-positive *Salmonella* were detected by flow cytometry (Figure 3.12), since this sensitive and reliable tool has been used to detect different *Salmonella* serotypes using fluorescent-tag mAbs either in food contaminated with *Salmonella* or from cultured bacteria (Pinder and McClelland 1994). Both *Salmonella*-GFP alone and cells associated with *Salmonella* (as described in chapter 4) were detected by flow cytometry using 488nm laser and fluorescence microscopy (Figure 3.13). Therefore, the GFP expressing *Salmonella* could be used to identify *Salmonella* infected host cells and discriminate these cells from non-infected cells by flow cytometry (Salcedo, Noursadeghi et al. 2001). In addition, with high GFP expression, the overall GFP signal could reveal the number of bacteria associated with host cells (Thone, Schwanhausser et al. 2007). However, some studies noted that *Salmonella* infectivity could be affected by either high expression of GFP protein (Wendland and Bumann 2002) or the antibiotic resistance gene used in construction of the GFP carrying plasmid; a GFP-plasmid with the chloramphenicol resistance gene affected *Salmonella* invasion, whereas a kanamycin-resistance gene did not

(Clark, Martinez-Argudo et al. 2009). Since the pBHR1-GFP plasmid used has the kanamycin resistance gene, the GFP expression level is less likely to interfere with *Salmonella*-host cells association.

As it will be described in chapter 6, J774 cells were successfully transfected with a mouse-CD9-GFP vector. The GFP-CD9 was expressed and localised to the cell membrane and detected by both flow cytometry and fluorescent microscopy. These cells offer a valuable tool for live imaging of any CD9-*Salmonella* interactions; however, the self- fluorescent expressing *Salmonella* strains that have been generated in current study have the GFP marker. Hence, it was considered worth trying to generate *Salmonella* self-expressing RFP for dual colour live imaging. This could enhance studying the live imaging of tetraspanin-*Salmonella* associations and also in fixed samples overcome some of the drawbacks of using different primary and secondary antibodies. In that case red fluorescent proteins were thought to be suitable. DsRed is a 28 kDa red fluorescent protein with 583 nm maximum emission that was cloned from the coral genus *Discosoma* and has been shown to be less susceptibility to pH (4.5-12) and more resistant to an acidic environment than GFP, as well as being less sensitive to photo-bleaching (Baird, Zacharias et al. 2000). Nevertheless, different plasmids (Table 2.9) were tested with no success regarding the level of DsRed expression, fluorescent protein maturation and stability, despite these DsRed carrying vectors giving stable and detectable RFP expression in an *E. coli* system, even though both bacterial genuses belong to the same family. It has been reported that a long time is needed to obtain DsRed maturation and also that DsRed shows a high oligomerisation and occurs as a tetramer (Baird, Zacharias et al. 2000). However, Different mutations generated in DsRed fluorescent protein have been shown to enhance its properties (Sorensen, Lippuner et al. 2003) and to decrease the green signal and increase protein solubility (Bevis and Glick 2002).

Thus, a vector carrying the mCherry gene, pNB57-mCherry, was used to generate *Salmonella* expressing mCherry fluorescent protein. The mCherry fluorescent protein was found to be relevant in bacterial investigations and combined with GFP in dual staining to investigate bacterial pathogenicity and live imaging (Lagendijk, Validov et al. 2010). Both *Salmonella* strains expressed stable mCherry that was detected using flow cytometry and fluorescence microscopy. The mCherry transformed *Salmonella* showed a high percentage of positive mCherry bacteria and nicely shifted as a positive population using appropriate filter without overlapping in the GFP channel after incubation of the *Salmonella* for 24 houses in LB broth with selective antibiotic. Nevertheless, NCTC12023-mCherry strain showed a lower percentage of positive cells (about 50%) after two hours culture. In contrast, the transformed

LT2-strain had a higher percentage of positive cells under the same conditions. This suggests that expression of different levels of fluorescent proteins could also be related to incubation time and bacterial strains.

Chapter 4: The effect of tetraspanins on *Salmonella* uptake

4.1 Introduction

The antibiotic resistance of bacteria has become a problematic issue which is increasingly distributed worldwide and a cause of high infection and fatality rates. Many alternative treatments have emerged to target either particular bacterial proteins that are responsible for bacterial virulence and invasion (Gu, Zhou et al. 2015) or targeting certain proteins that act as a bridge between bacteria and host cells to enhance infection (Parker, Sando et al. 2010). In *Salmonella* infection, targeting the effector proteins that are released from bacteria by T3SS could prevent *Salmonella* infection rather than targeting bacteria themselves. For example, a type of salicyliden acylhydrazide, INP0403, showed an inhibitory effect on *Salmonella* T3SS without affecting the viability and growth of the *Salmonella* (Hudson, Layton et al. 2007). This compound reduced the transcription of genes that are involved in T3SS production (Layton, Hudson et al. 2010). Another possibility is to disrupt the bacterial adhesion to the host cells (anti-adhesion therapy), reviewed in (Krachler and Orth 2013). As an example of this strategy, a high glycosylated mucin-1 (Muc-1) in cow's milk was shown to be effective in supressing adhesion of common gastrointestinal disease related pathogens, including *Salmonella* Typhimurium, and *E. coli* to the epithelial cell line, Caco-1, and to some extent Gram positive bacteria including *Bacillus subtilis* and *Staphylococcus aureus*. Sialic acid, D-mannose and L-fucose also inhibited adhesion of *S.* Typhimurium and sialidase abrogated the inhibitory action of Muc-1, showing the importance of sialic acid in bacterial adhesion (Parker, Sando et al. 2010).

The crucial role of host cell pathways recruited by intracellular bacteria to facilitate invasion is reviewed by Bhavsar et al. (2007) and was described in Chapter 1. Different host cell functions have been shown to be recruited by *Salmonella* such as rearrangements of host cell cytoskeleton, signal transduction, and trafficking of *Salmonella* containing vacuoles. Understanding of bacterial-host cell interaction mechanisms could lead to finding new strategies for bacterial treatments, as reviewed in (Finlay and Cossart 1997). Important for our present research is the targeting of particular host proteins that are shown to be involved in bacterial adhesion and invasion such as the tetraspanins (Green, Monk et al. 2011). In bacterial infections, the role of tetraspanins is becoming more obvious, despite relatively few studies, as described in Chapter 1 and reviewed in Monk and Partridge (2012).

Using *Salmonella enterica* serovar Typhimurium as a model of bacterial infection has certain advantages, as the bacterium has a highly sophisticated invasion machinery that allows it to invade both phagocytic and non-phagocytic cells, reviewed in (LaRock, Chaudhary et al. 2015). This therefore offers a good tool to investigate the role of tetraspanin proteins in bacterial infection in different cell lines. Previous studies from this laboratory investigated the role of tetraspanins in *Salmonella* infection of primary human MDMs. The disadvantages of using primary cells are that the cells are subject to donor variation and it may be difficult to obtain sufficient numbers for some experiments (Hassuna, 2010, PhD thesis, University of Sheffield).

Many tools have become available to investigate the functions of tetraspanins such as specific monoclonal antibodies (mAbs), recombinant EC2 proteins, knockdown of tetraspanin expression by siRNA and tetraspanin gene knockout in experimental animals (Hemler 2008). In bacterial infections, anti-tetraspanin antibodies to CD9, CD63 and CD151 reduced *Neisseria meningitides* adhesion to epithelial cells (Green, Monk et al. 2011); anti-CD63 also reduced *Salmonella* Typhimurium uptake by human primary MDMs (Hassuna, 2010, PhD thesis, University of Sheffield).

4.1.1 Flow cytometry and bacterial –host interactions

Flow cytometry analysis has been shown to be useful in investigating bacterial pathogenicity and to study the bacterial-host interaction (Valdivia and Falkow 1998, Pils, Schmitter et al. 2006). It offers a quick and appropriate method to analyse the bacterial-host invasion and has been reported to accurately differentiate between external associated and internalised bacteria; moreover results obtained from flow cytometry were shown to be comparable with other analysis methods (Pils, Schmitter et al. 2006). In most of these studies, groups have labelled bacteria for analysis; a fluorochrome-labelled version of vancomycin was used to label peptidoglycan and to investigate attached and internalised *Staphylococcus aureus* to host cells (Trouillet, Rasigade et al. 2011). However, direct labelling of *Salmonella* may potentially interfere with bacterial binding and invasion, depending on the level of fluorescent protein expression. High GFP expression showed an effect on *Salmonella* invasion (Wendland and Bumann 2002). In contrast, other researchers have suggested that the plasmid construct, not the level of fluorescent protein expression, could has effects on *Salmonella* invasion; and plasmids encoding chloramphenicol resistance seemed to have this impact (Clark, Martinez-Argudo et al. 2009). Other workers have used bacteria expressing chromosomal GFP. For example, this approach was shown to be useful in differentiating

between host cell subpopulations infected with few (1 or 2) or many salmonella, and the accuracy of these results were confirmed by confocal microscopy (Thone, Schwanhausser et al. 2007).

4.2 Aims

The primary aim in this Chapter was to investigate the possible role of tetraspanin proteins in *Salmonella* uptake by phagocytic (mouse and human macrophage) and non-phagocytic (human epithelial) cell lines. Finding a suitable cell line model could overcome the main drawback of a previous study that was dependent on primary human MDMs, which are known to be subject to donor variation and difficult to generate in large numbers for the experiments. The relative merits of human and mouse cell line is more antibody reagents are available for human, but the macrophages derived from these cell line are less mature compared with the more "macrophage- like" murine J774 cell line. The epithelial cell lines were chosen as a model of non-phagocytic cells with different modes of uptake, and these cell lines had not previously been studied. As discussed in Chapter 1, whilst *Salmonella* may be taken up passively by macrophages through phagocytosis, uptake by epithelial cells generally requires expression of the Type 3 secretion system.

The second aim emerged during the experiments that were initially dependent on immunofluorescence microscopy for counting and estimating the rate of cell infection. This method can be subjective and prone to variations arising from human error. We therefore tried to develop a method for assessing bacterial infection by using flow cytometry that would be more objective. In addition such a method is less time consuming, increases the number of infected cells assessed and reduces the amount of expensive antibody reagents that are needed. In brief, instead of infecting, staining and counting cells seeded on coverslips, the cells were infected in suspension, then either fixed (to determine external bacteria) or fixed and permeabilised (to determine total bacteria) before staining with FITC-conjugated anti-*Salmonella* antibody and analysis by flow cytometry (Figure 4.1). As an alternative, potentially faster method, *Salmonella* were transformed with a GFP carrying vector. Successful, stable expression of GFP in both *Salmonella* strains was achieved (as described in Chapter 3) and these GFP strains were investigated in the infection assay and their infection rate was assessed by flow cytometry.

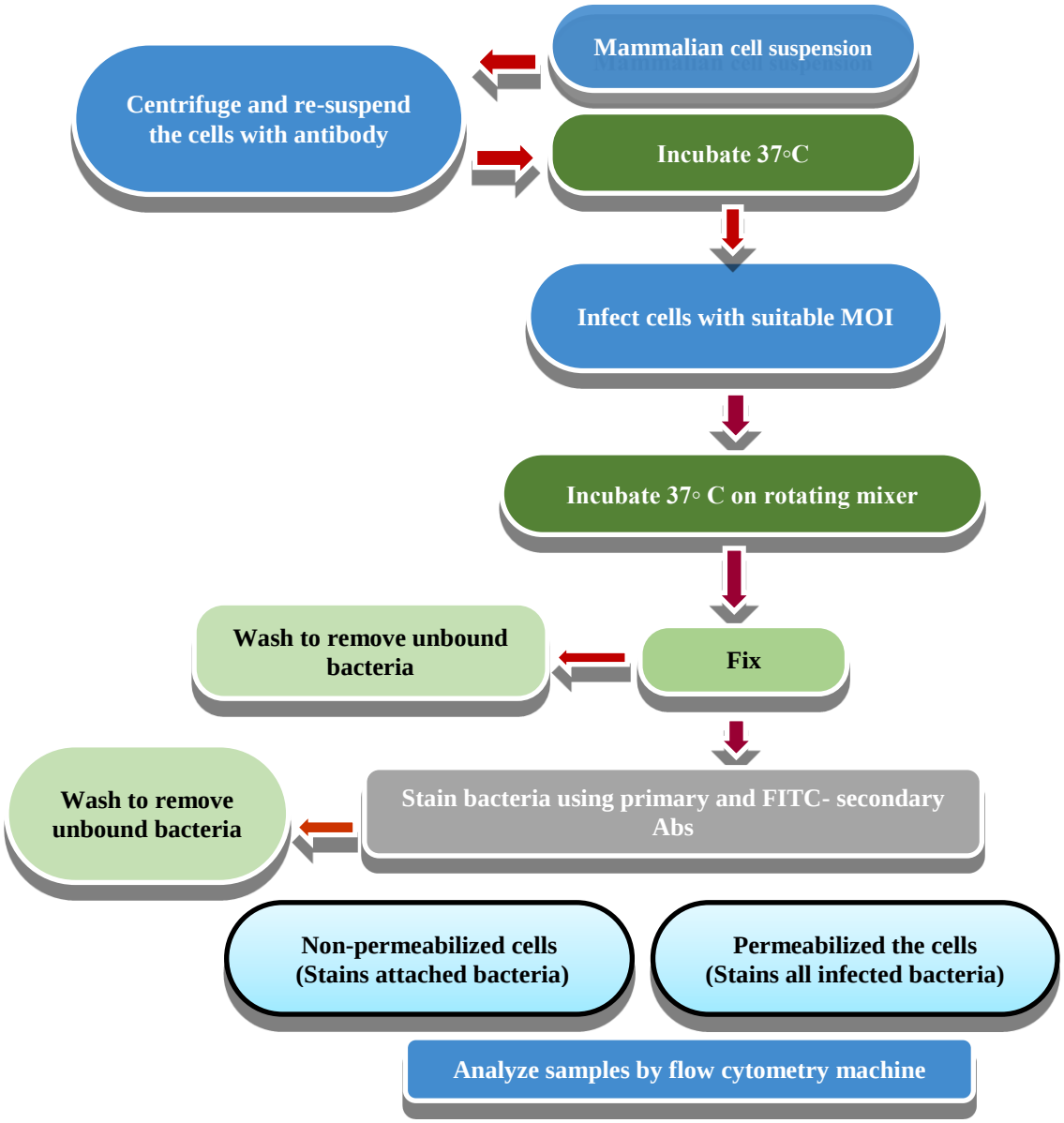

Figure 4.1: Outline of the flow cytometry procedure developed for assessing *Salmonella* infection of mammalian cells.

4.3 Results

4.3.1 Effect of anti-tetraspanin antibodies on *Salmonella* Typhimurium uptake analysed by immunofluorescence microscopy

Tetraspanin expression by the cell lines that would be used in the experiments has been described previously (chapter 3). Other initial experiments included studying the *Salmonella* growth curve to find the log phase that would be used. Different multiplicities of infection (MOI) and infection times were investigated to establish those that were most suitable. A growth curve was plotted by growing *Salmonella* in 20 ml LB broth and measuring both optical density (OD_{600}) and viable bacterial counts (colony forming unit (CFU)) through different time periods (1 - 24 hours). This experiment was repeated three times and the mid-log phase chosen from the average to use for the *Salmonella* infection assay ($OD_{600} \approx$ 0.4-0.5, time $\approx$ 2-2.5 hours and CFU$\approx$ 7-8 x10^7) respectively (data not shown). For further confirmation, the CFU was measured separately for each experiment. To optimise the MOI and infection time, the various mammalian cell lines were infected at different MOIs (30, 50, 100 and 150) and for different infection times (30, 60 and 90 minutes). Cells were fixed, stained and counted, as described in 2.2.5.1. High MOIs and longer infection times gave high infection rates and high numbers of bacteria that made counting difficult, whilst shorter times gave low rates of infection with less bacterial internalisation. Suitable MOIs were chosen therefore as follows: in J774 cell line, a 30 MOI for 30 minutes: in THP-1 derived macrophages, a 30 MOI for 30 minutes; in HEC-1-B, a 100 MOI for 60 minutes (optimisation data not shown).

4.3.1.1 Effect of anti-tetraspanin antibodies on *Salmonella* Typhimurium NCTC12023 uptake by the J774 cell line

The mouse macrophage-like J774 cell line was chosen first to investigate the effect of tetraspanin antibodies in *Salmonella* infection, since this cell line is an immortal cell line and has high expression of surface CD9 and CD81 (Chapter 3, section 3.3.1.1). This cell line has been used successfully here to investigate infection by *Salmonella* Typhimurium (Tang, Guest et al. 2004, Gilberthorpe, Lee et al. 2007). However, few anti-mouse tetraspanin mAbs are commercially available. Furthermore, the anti-tetraspanins mAbs that were used to block the surface tetraspanins antigens will bind non-specifically with Fc receptors (FcR) that are expressed by these cells. To take account of nonspecific binding of mAbs to FcR, appropriate isotype controls were included in all experiments and the results were compared with these. The effect of anti-tetraspanin antibodies on infection of J774 cells with *Salmonella* Typhimurium NCTC12023 was assessed using saturating concentrations of antibody (20µg

ml^{-1}) as described in 2.2.5.1.3. (Figure 4.2). The antibody effects were measured by four parameters: the percentage of cells with associated bacteria, the total number of cell-associated bacteria, the number of attached (external) bacteria and the percentage of internalized bacteria (2.2.5.1.6). The results showed a significant reduction in the percentage of cells with bound bacteria (to ~59% of control) and in the number of bacteria per 100 cells for anti-CD9 pre-treated cells compared with the isotype control. No differences were observed in the number of external bacteria or percentage of bacteria internalised, or for all four infection parameter in the non-treated control compared with the isotype (Figure 4.3).

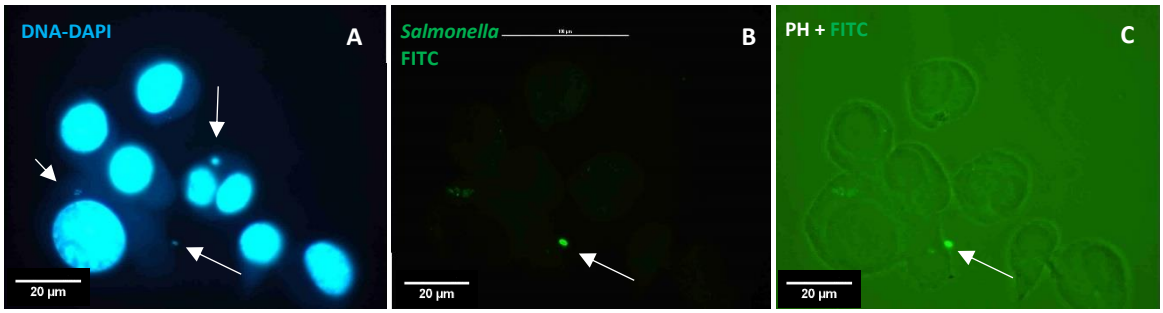

Figure 4.2: Immunofluorescence microscopy of J774 cells infected with *Salmonella* Typhimurium NCTC12023. Following infection at 50 MOI for 30 minutes, cells were fixed and stained, as mentioned in 2.2.5.1.4.using primary rabbit anti-*Salmonella* polyvalent antibody followed by secondary anti-rabbit – FITC and DAPI staining (combined with permeabilising buffer).The cell and bacterial DNA are stained with DAPI (blue) stain and the external bacteria are stained with FITC (green). **A**: J774 cells infected with *S.* Typhimurium, with both bacterial and J774 cell DNA stained blue (DAPI) using correct fluorescence filter **B:** FITC (green) stain that reveals the external bacteria. **C**: Phase contrast image merged with FITC image shows external bacteria stained green (FITC) stain and the outline of the J774 cells. Arrows point to bacteria. Images were captured using a Nikon Eclipse E400 fluorescence microscope using the oil immersion objective (x100).

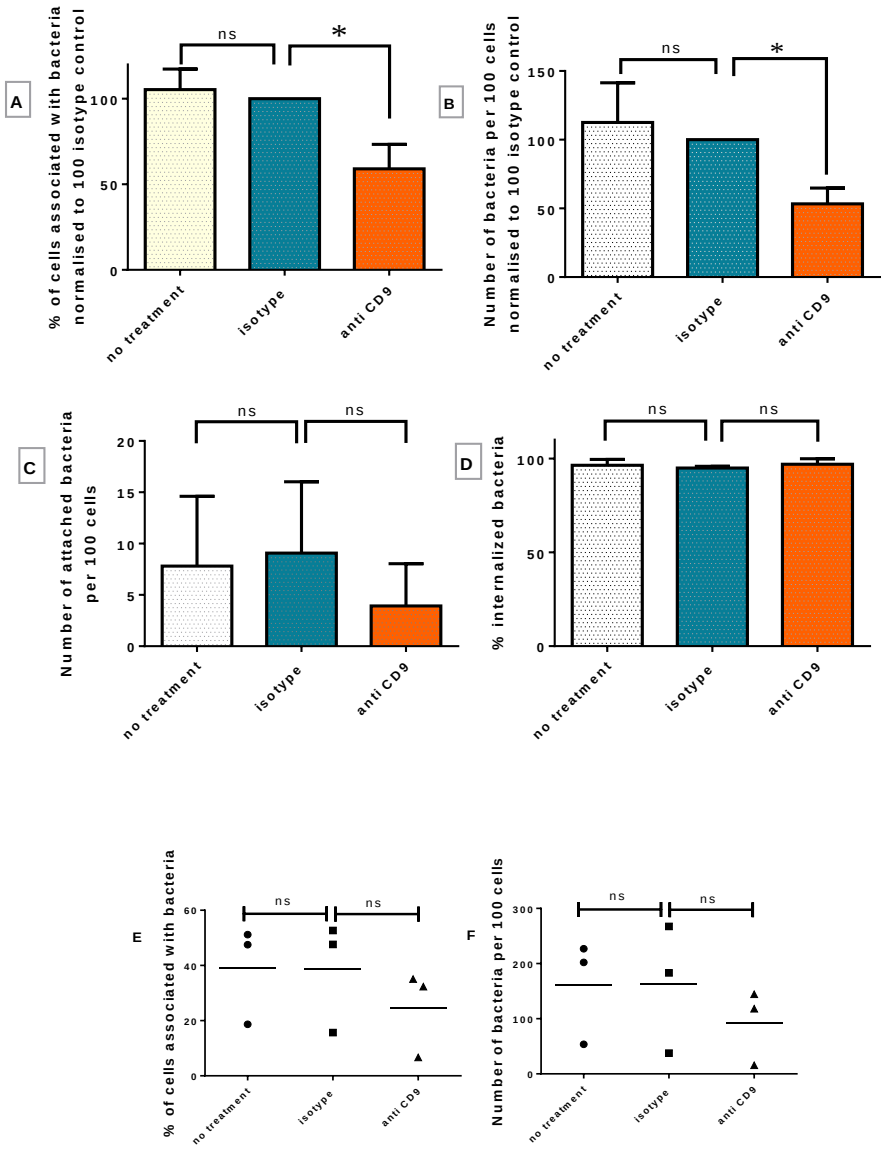

Figure 4.3: Effect of anti-CD9 mAbs on *Salmonella* uptake by J774 cells at 30 MOI for 30 minutes. J774.2 cells were pre-treated with anti-CD9 or isotype control before *Salmonella* Typhimurium NCTC 12023 strain infection as described Figure 4.2. **A:** J774 cells associated with *Salmonella*. **B:** Number of bacteria per 100 cells. **C:** Number of external or attached bacteria**. D:** The percentage of internalized bacteria, **E and F**: Corresponding raw data (average of non-normalised) for normalised **A** and **B** only. Bars show means, while error bars show standard errors. n=3 in triplicate, graphs A and B data was analysed by One Sample T-test comparing with isotype control, graphs C, D, E and F data was analysed by Ordinary one-way ANOVA Holm-Sidak's multiple comparisons test, significance * $P \leq 0.05$ while ns is non-significant.

Work subsequently carried out in our lab by a 4th year project student (under my supervision) investigated the effect of other anti-tetraspanin antibodies (anti-CD63 and anti-CD81) on *Salmonella* NCTC12023 strain uptake by J774 cells. The results showed a significant reduction in the percentage of cells associated with bacteria (to ~ 78%) and in the number of bacteria per 100 cells in anti-CD81 pre-treated cells compared with the isotype control. No differences were observed in the number of external bacteria or percentage of bacteria

internalisation, or for all four infection parameter in anti-CD63 pre-treated cells no significant changes were observed compared with isotype control (Figure 4.4). The lack of an effect with anti-CD63 antibodies may be due to the very low expression levels of this tetraspanin on J774 cells (chapter 3).

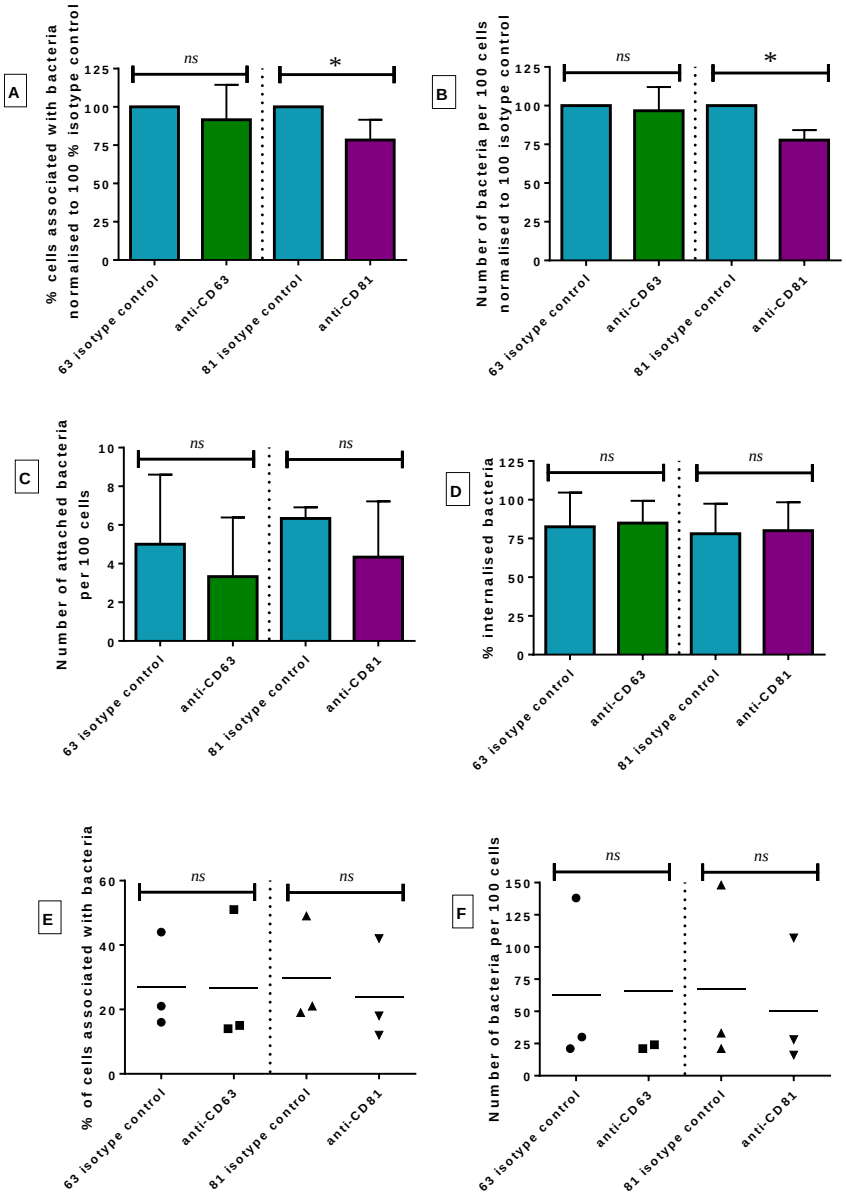

Figure 4.4: Effect of anti-CD63 and anti-CD81 mAbs on *Salmonella* uptake by J774 cells at 30 MOI for 30 minutes. J774.2 cells were pre-treated with anti-CD63, anti-CD81 or corresponding isotype control before *Salmonella* Typhimurium NCTC 12023 strain infection. **A:** J774 cells associated with *Salmonella*. **B:** Number of bacteria per 100 cells. **C:** Number of external or attached bacteria**. D:** The percentage of internalized bacteria, **E and F**: Corresponding raw data (average of non-normalised) for normalised **A** and **B** only. Bars show means, while error bars show standard errors. n=3 in triplicate, graphs A and B data was analysed by One Sample T-test comparing with isotype control, graphs C, D, E and F data was analysed by Ordinary one-way ANOVA Holm-Sidak's multiple comparisons test, significance * $P \leq 0.05$, while ns is non-significant.

4.3.1.2 Effect of anti-tetraspanins antibodies in *Salmonella* Typhimurium uptake by macrophages derived from the human THP-1 cell line

Although the work with the mouse macrophage cell line confirmed a role for tetraspanins in *Salmonella* infection of macrophages, there are some significant differences between the results obtained here and those reported for human MDM (Noha Hassuna, PhD thesis 2010); for example anti-CD9 antibodies had little effect on *S.* Typhimurium uptake by MDM. In addition, there are relatively few antibody reagents for mouse tetraspanins. As human MDM are subject to donor variation and difficult to generate in large numbers (as mentioned before), using macrophages derived from monocyte cell lines such as THP-1 cell line could offer an alternative human macrophage cell model. Undifferentiated THP-1 cells show significant expression of tetraspanins CD37, CD53, CD63 and CD81 and most of these tetraspanins are significantly increased after stimulation of THP-1 cells with phorbol myristate acetate (PMA) to differentiate to macrophages in particular CD9, CD53, CD63 and CD81 (as described in Chapter 3). These cells are non-adherent, making analysis by immunofluorescence microscopy difficult and even when induced to adhere by coating surfaces with poly-L-lysine, take up bacteria inefficiently (Noha Hassuna, personal communication).

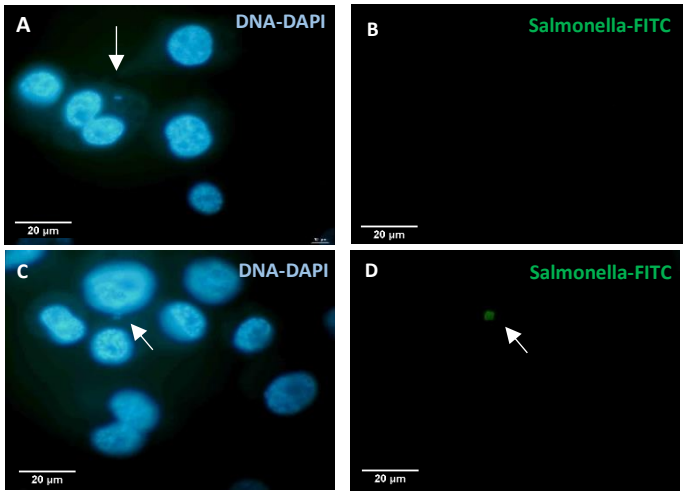

Figure 4.5: Immunofluorescence microscopy of THP-1 derived macrophages cell line cells infected with *Salmonella* Typhimurium at 30 MOI for 30 minutes. THP-1 cells that had been stimulated with 20ng ml^{-1} of PMA for 3 days (Chapter 3.3.1.3) were infected with *Salmonella* Typhimurium NCTC 12023, fixed and stained as described in Figure 4.2. **A and C**: Stimulated THP-1 cells with *S.* Typhimurium, with both bacterial and cell DNA stained blue (DAPI) under the correct fluorescence filter, **B and D:** FITC (green) stain that reveals the external bacteria. Arrows point to bacteria. The images were captured using Nikon Eclipse E400 fluorescence microscope using oil immersion (100x) objective.

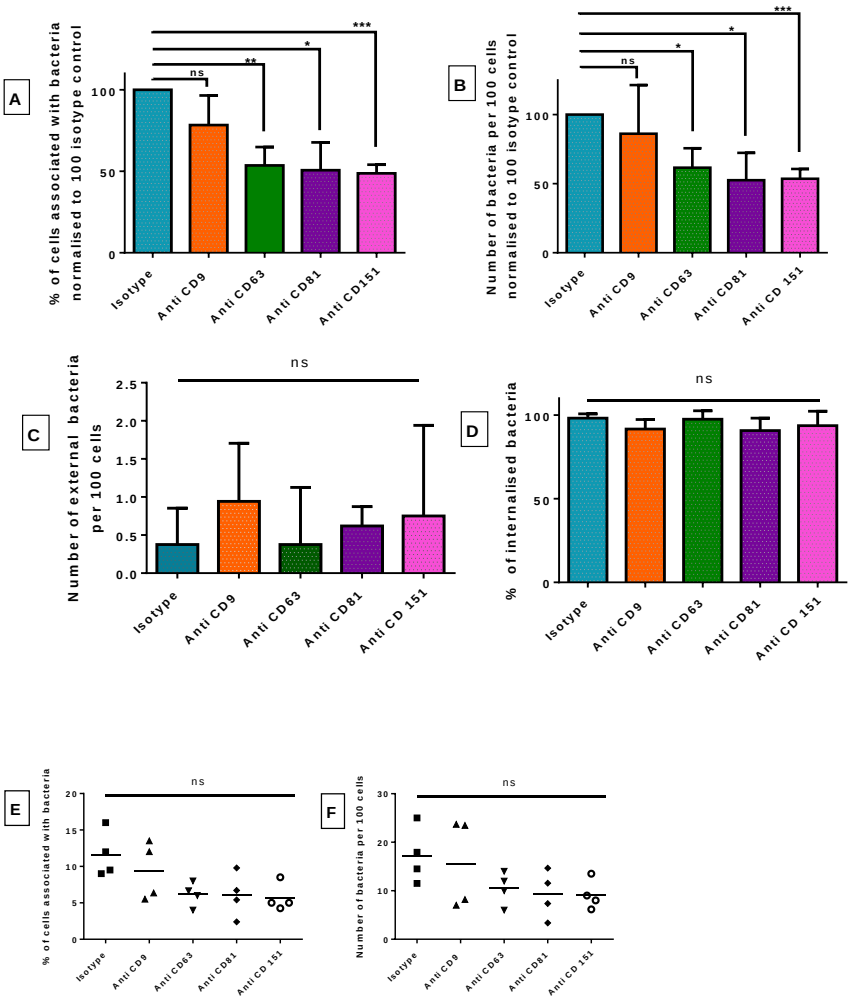

Figure 4.6: Effect of anti-tetraspanin mAbs on *Salmonella* NCTC12023 strain uptake by macrophages derived from THP-1 cells at 30 MOI for 30 minutes. THP-1 cells treated with 20ng ml^{-1} PMA for 3 days and cells were pre-treated with JC1 (control isotype), anti CD9 (602.29), anti CD63 (H5C6), anti CD81 and anti CD151 (14, A2) at 20µg ml^{-1} before *Salmonella* Typhimurium NCTC12023 strain infection as described Figure 4.5. **A:** Cells infected with *Salmonella*. **B:** Number of bacteria per 100 cells. **C:** Number of external or attached bacteria**. D:** The percentage of internalized bacteria, **E and F**: Corresponding raw data (average of non-normalised) for normalised **A** and **B** only. Bars show means, while error bars show standard errors. n=4 in duplicate, graphs A and B data was analysed by One Sample T-test comparing with isotype control, graphs C, D, E and F data was analysed by Ordinary one-way ANOVA Holm-Sidak's multiple comparisons test, significance *** $p \leq 0.001$, ** $P \leq 0.01$ and * $P \leq 0.05$, ns is non-significant.

The same parameters and infection protocol as described in 4.3.1.1 were used to investigate the *Salmonella* infection of phorbol ester treated THP-1 cells. Using 30 MOI for 30 minutes, the percentage of THP-1 derived macrophages cells associated with *Salmonella* Typhimurium NCTC12023 and the number of bacteria per 100 cells showed a significant reduction when the cells were pre-treated with anti-CD63, anti-CD81 and anti-CD151. However, no significant change was observed for cells treated with anti-CD9 before infection. No significant changes were observed in the number of external or attached bacteria and percentage of internalised bacteria for any of the antibody treatments (Figure 4.5 and 4.6).

Since *Salmonella* Typhimurium NCTC12023 strain is a low virulence laboratory strain, a different strain was also introduced in the infection experiments, *Salmonella enterica* serovar Typhimurium LT2 strain. Cells infected with *Salmonella* Typhimurium LT2 strain showed no significant reduction in infection when treated with anti-CD9 and anti-CD63 (Figure 4.7). There appeared to be some obvious reduction with anti-CD81 and CD151 antibodies, but this was not significant. No significant changes were observed in cells treated with isotype control compared with non-treated cells control. No changes were observed in cells treated with anti-tetraspanin mAbs compared with isotype control (JC1) in number of external cells per 100 counted cells and percentage of internalisation.

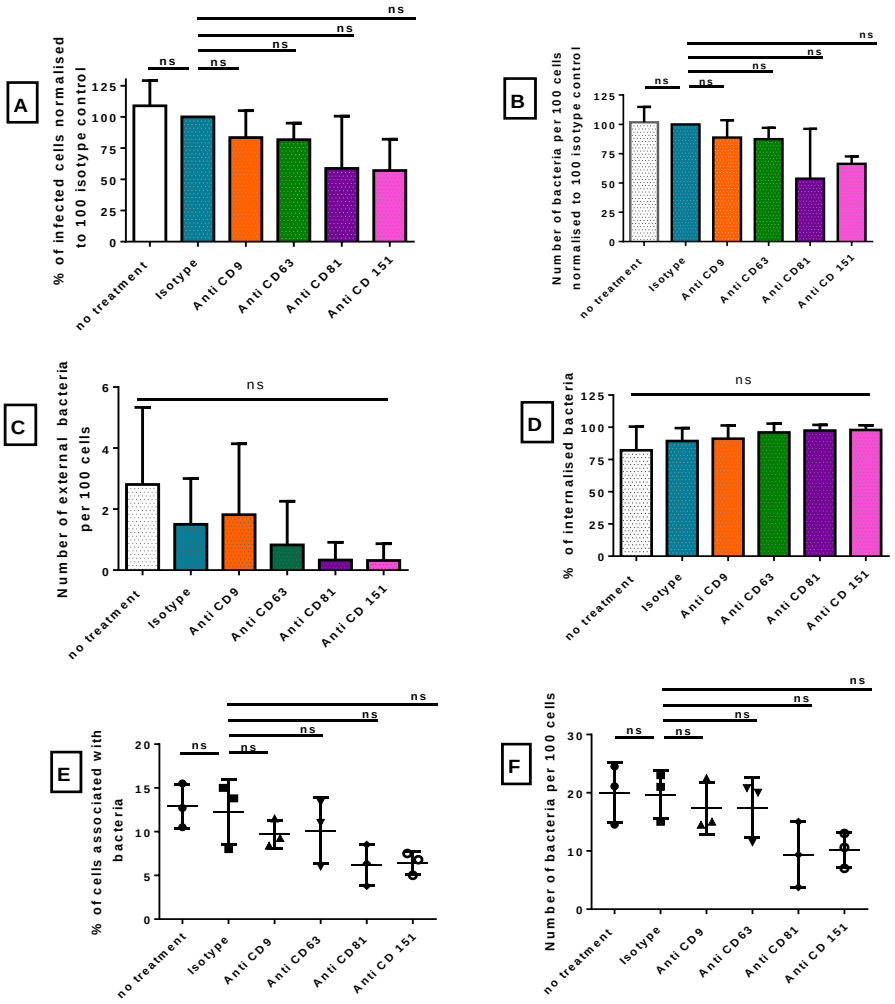

Figure 4.7: Effect of anti-tetraspanin mAbs on *Salmonella* LT2 strain uptake by macrophages derived from THP-1 cells at 30 MOI for 30 minutes. THP-1 cells treated with 20ng ml^{-1} PMA for 3 days and cells were pre-treated with JC1 (control isotype), anti CD9 (602.29), anti CD63 (H5C6), anti CD81 and anti CD151 (14, A2) at 20µg ml^{-1}) before *Salmonella* Typhimurium LT2 strain. **A:** Cells infected with *Salmonella*. **B:** Number of bacteria per 100 cells. **C:** Number of external or attached bacteria**. D:** The percentage of internalized bacteria, **E** and **F:** Corresponding raw data (average of non-normalised) for normalised **A** and **B** only. Bars show means, while error bars show standard errors. n=3 in duplicate, graphs A and B data was analysed by One Sample T-test comparing with isotype control, graphs C,D, E and F data was analysed by Ordinary one-way ANOVA Holm-Sidak's multiple comparisons test, significance ** $p \leq 0.01$ and * $P \leq 0.05$, ns is non-significant.

4.3.1.3 Effect of anti-tetraspanin antibodies on *Salmonella* uptake by the HEC-1-B cell line

Salmonella has the ability to invade and replicate in various cell types within the host (Haraga, Ohlson et al. 2008). It also has the ability to attach to and invade different phagocytic and non-phagocytic cell lines, as shown by many researchers (Finlay, Ruschkowski et al. 1991, Mills and Finlay 1994, Lajarin, Rubio et al. 1996, Rosales-Reyes, Perez-Lopez et al. 2012). The ability to invade non-phagocytic cells can be mediated by T3SS-1 (Rosselin, Abed et al. 2011) (discussed in detail in 1.2.3). The human epithelial cell line, HEC-1-B, was therefore chosen as cell model of non-phagocytic cell line to investigate the tetraspanins effect on *Salmonella* Typhimurium NCTC12023 strain uptake. In addition, when these cells were treated with either anti-tetraspanin antibodies (CD9, CD63 and CD151) or recombinant EC2 domains a reduction in the adhesion of another gram negative bacterium, *Neisseria meningitidis,* was observed (Green, Monk et al. 2011). HEC-1-B cells were infected, fixed and stained as described previously (2.2.5.1) (Figure 4.8). From optimisation experiments, 100 MOI for 60 minutes infection time was chosen as this gave a suitable number of bacteria that could analysed (data not shown). As shown in the previous chapter (3.3.1.4), high surface expression of tetraspanins CD9, CD63, CD81 and CD151were observed in HEC-1-B cells. No significant changes were observed in HEC-1-B cells pre-treated with anti-CD9, anti-CD37, anti-CD63, anti-CD81, and anti-CD82 or anti CD-151 compared with JC1 isotype control in all four parameters used to indicate assess cell infection (Figure 4.8 and 4.9).

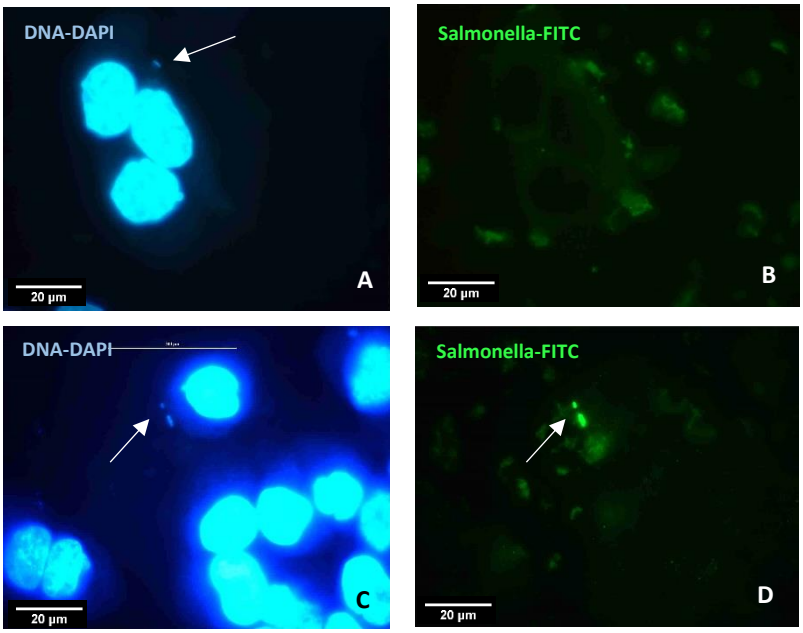

Figure 4.8: Immunofluorescence microscopy of HEC-1-B cell line cells infected with *Salmonella* Typhimurium NCTC12023 at 100 MOI for 60 minutes. HEC-1-B cells were infected with *Salmonella* Typhimurium NCTC 12023, fixed and stained as described in Figure 4.2. **A and C**: HEC-1-B cells with *S.* Typhimurium, with both bacterial and cell DNA stained blue (DAPI) under the correct fluorescence filter, **B and D:** FITC (green) stain that reveals the external bacteria. Arrows point to bacteria. The images were captured using Nikon Eclipse E400 fluorescence microscope using oil immersion (100x) objective.

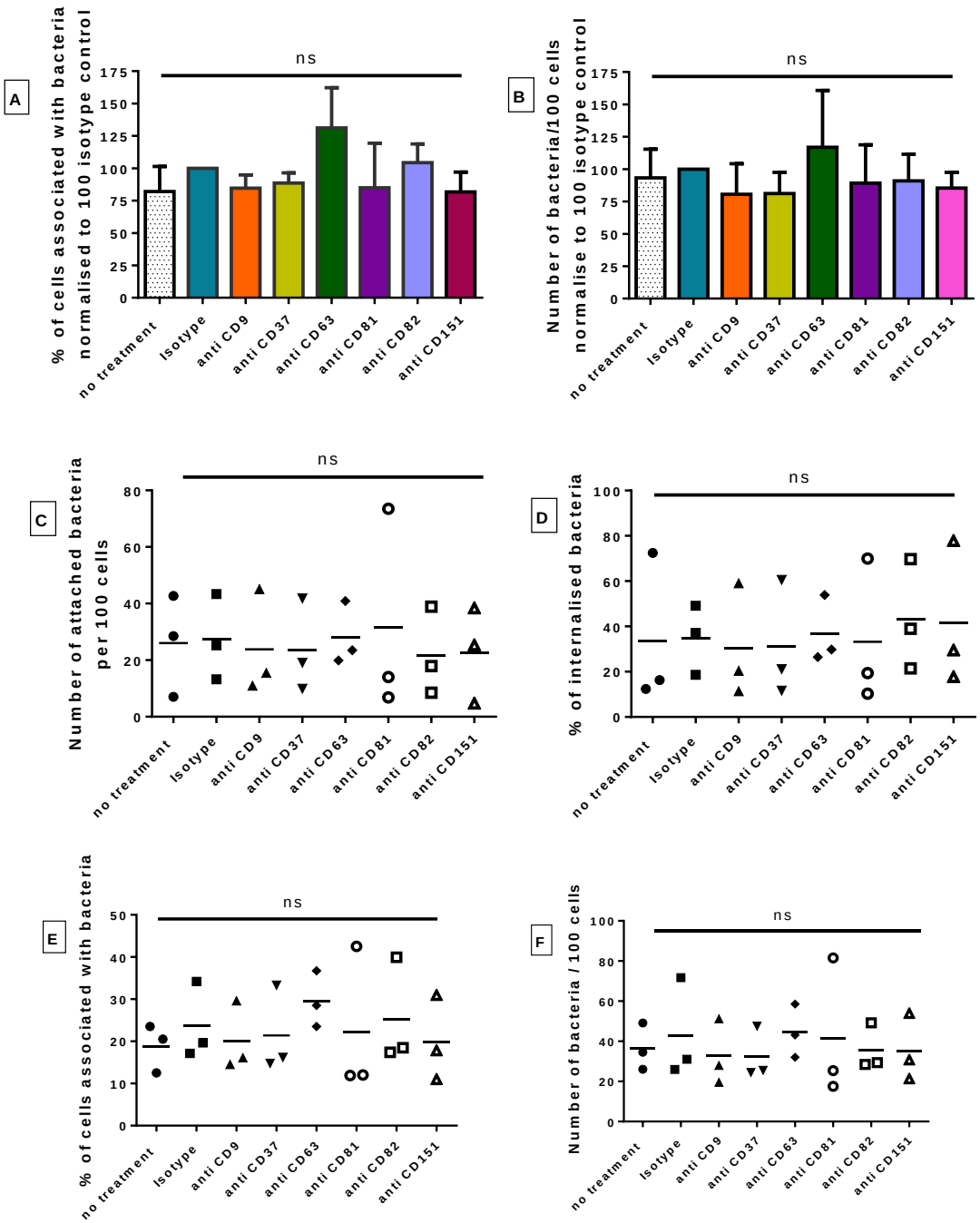

Figure 4.9: Effect of anti-tetraspanin mAbs on *Salmonella* NCTC12023 strain uptake by HEC-1-B cells at 100 MOI for 60 minutes. HEC-1-B cells were pre-treated with JC1 (control isotype), anti CD9 (602.29), anti CD63 (H5C6), anti CD81 and anti CD151 (14, A2) at concentration of (20µg ml^{-1}) before *Salmonella* Typhimurium NCTC 12023 strain infection as described Figure 4.8. **A:** Cells infected with *Salmonella*. **B:** Number of bacteria per 100 cells. **C:** Number of external or attached bacteria**. D:** The percentage of internalized bacteria, **E and F**: Corresponding raw data (average non-normalised) data for **A and B** respectively. Bars show means, while error bars show standard errors. n=3 in duplicate, graphs A and B data was analysed by One Sample T-test comparing with isotype control, graphs C, D, E and F data was analysed by Ordinary one-way ANOVA Holm-Sidak's multiple comparisons test, ns is non-significant.

4.3.2 Effect of anti-tetraspanin antibodies on *Salmonella* Typhimurium uptake analysed by flow cytometry

As described in (4.1), a flow cytometry method was developed to analyse the infected cells instead of using the ordinary immunofluorescent microscopy method (2.2.5.2). Bacteria were prepared for infections as previously (2.2.5.1.2). The main difference in the procedure afterwards was that cells were harvested, and treated with antibody in tubes and then infected with the cells and bacteria maintained in suspension (2.2.5.2.3). Optimisation experiments were carried out for each cell line and for both *Salmonella* strains. Interestingly, the overall optimisation results showed that a lower MOI was needed to give sufficient infected cells for both macrophage and epithelial cell lines using this infection method (optimisation data not shown).

4.3.2.1 *Salmonella* uptake by J774 cell line

J774 cells were infected with *Salmonella* NCTC12023 strain at 5 MOI for 30 minutes after treatment with anti-tetraspanin antibodies using the flow cytometry protocol for infection and staining as described in detail in 2.2.5.2 and outlined in Figure 4.10. The cells were analysed using the LSR-II flow cytometer and 10,000 events were acquired. The cells were gated depending on forward and side scatter (FSC and SSC respectively) and for detecting cells associated with bacteria, the 530-30 filter was used to detect the FITC signal (Figure 4.9 A), which was clearly above the auto-fluorescent background signals from the cells. The percentage of positive cells reveals the cells with associated bacteria whilst the MFI indicates the intensity of bacterial infection. To estimate the percentage of internalised bacteria, the number of infected cells that were stained without permeabilization was subtracted from permeabilized infected cells (total cell associated bacteria). The flow cytometry method shows a significant reduction in infection rate by *S.* Typhimurium of J774.2 cells treated with anti-CD9 antibodies, similar to that observed with the immunofluorescence microscopy method. Anti-CD81 antibodies also showed inhibition, whereas anti-CD63 antibodies showed no significant change in *Salmonella* uptake (Figure 4.10 B). However, no significant changes in MFI was observed (data not shown). No significant changes were observed in the percentage of cells with internal bacteria (subtracting cells associated with attached bacteria (non-permeabilised) from cells associated with bacteria (permeabilised)) or cells associated with external bacteria (Figure 4.10 C and D), despite some reduction in the number of cells associated with internalised bacteria but this was not statistically significant. The results obtained by the flow cytometry assay therefore appear consistent with the data obtained with the microscopy assay described in 4.3.1.1.

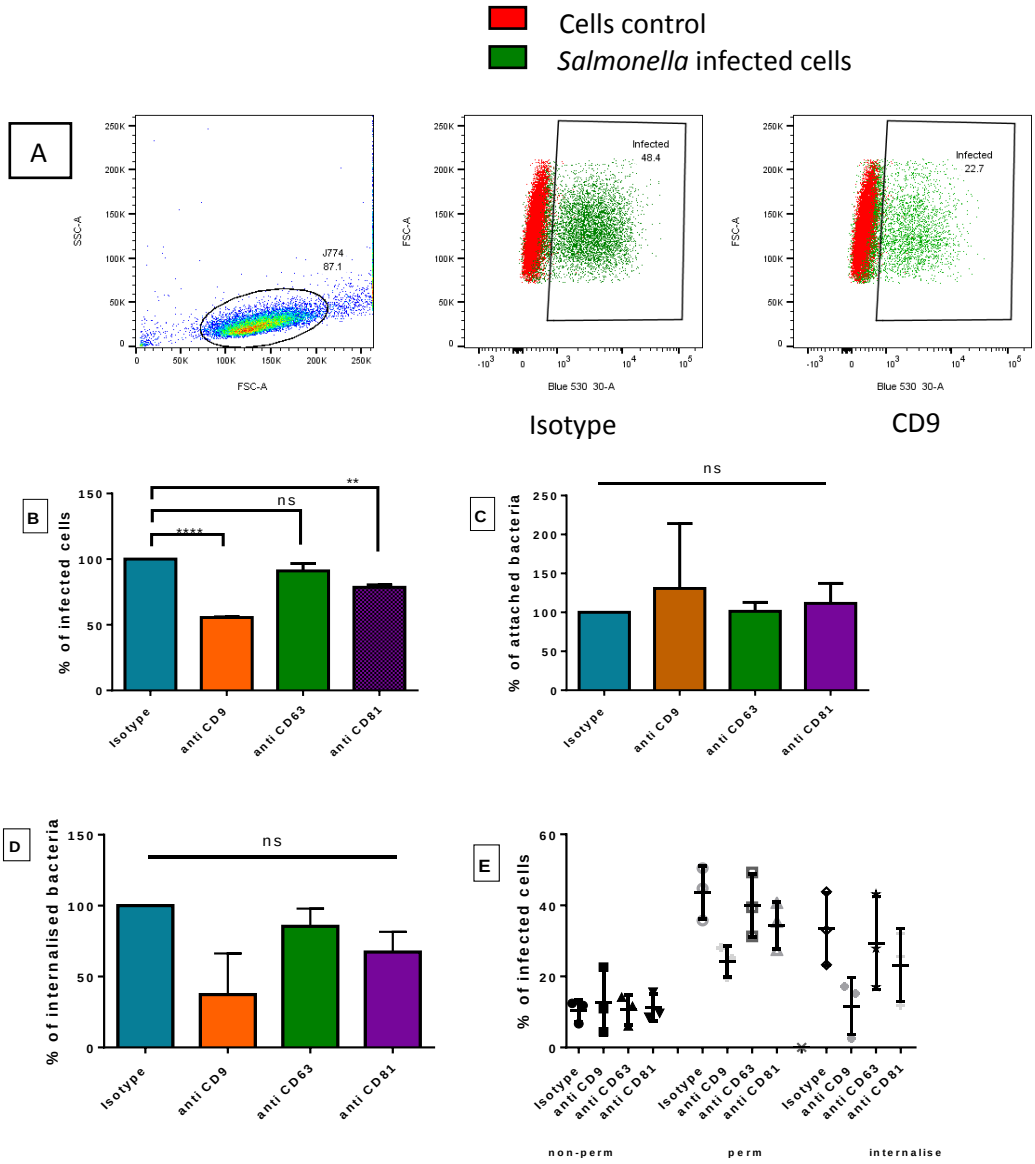

Figure 4.10: Effect of tetraspanin mAbs on *Salmonella* uptake by J774 cells at 5 MOI for 30 minutes analysed by flow cytometry. J774.2 cells were harvested, placed in Eppendorf tubes and pre-treated with anti-tetraspanin mAbs or isotype control (20µg ml^{-1} for 60 minutes) before infection with *Salmonella* Typhimurium NCTC12023 as described in 2.2.5.2.1. The cell-bacteria suspension was placed on a rotating mixer and was incubated at 37°C for 30 minutes. The cells were washed and fixed or fixed and permeabilised as described in 2.2.5.2.4 and stained using primary rabbit anti-*Salmonella* polyvalent antibody followed by secondary anti-rabbit –FITC. Cells were kept in 1% PFA until analysis using an LSR-flow cytometer. **A:** Dot plot from FACS analysis showing how the values shown in B were obtained (LH graph shows the gated population of cells analysed based on forward and right angle scatter, the middle and RH graph show fluorescent staining of infected cells pre-incubated with isotype control and anti-CD9, respectively, with uninfected control cells depicted in red. **B**: Percentage of J774 cells infected with *Salmonella* normalized to 100% isotype control. **C**: Percentage of cells with external bacteria normalised to 100% isotype control. **D:** Percentage of cells with internal bacteria (subtracting the percentage of cells with external bacteria from all infected permeabilized cells). **E:** Raw data before normalisation. Bars describe means, while error bars describe standard error means. n=3 in duplicate, data was analysed by Ordinary one sample T test comparing with isotype control, significance **** $p \leq 0.0001$ and ** $P \leq 0.01$. ns is non-significant.

4.3.2.2 *Salmonella* Typhimurium uptake by HEC-1-B cell line

Since the NCTC12023 strain has been shown to be less invasive to epithelial cells compared with other strains, the LT2 strain was also included here. Both *Salmonella* strains and HEC-1-B cells were prepared and harvested as described in 2.2.5.2. No significant effects were shown in total infected cells, cells with attached bacteria and cells with internalised bacteria in HEC-1-B cells infected with *S.* Typhimurium NCTC12023 strain (Figure 4.11 A and B) and LT2 strains (Figure 4.11 C and D). No significant changes in MFI were observed (data not shown). This result is consistent with that observed by fluorescence microscopy. The LT2 strain did appear to give slightly higher rates of infection, as might be expected (comparing Figure 4.11 E and F and G and H). The results obtained with the flow cytometry assay are consistent with those obtained with the microscopy assay described in 4.3.1.3.

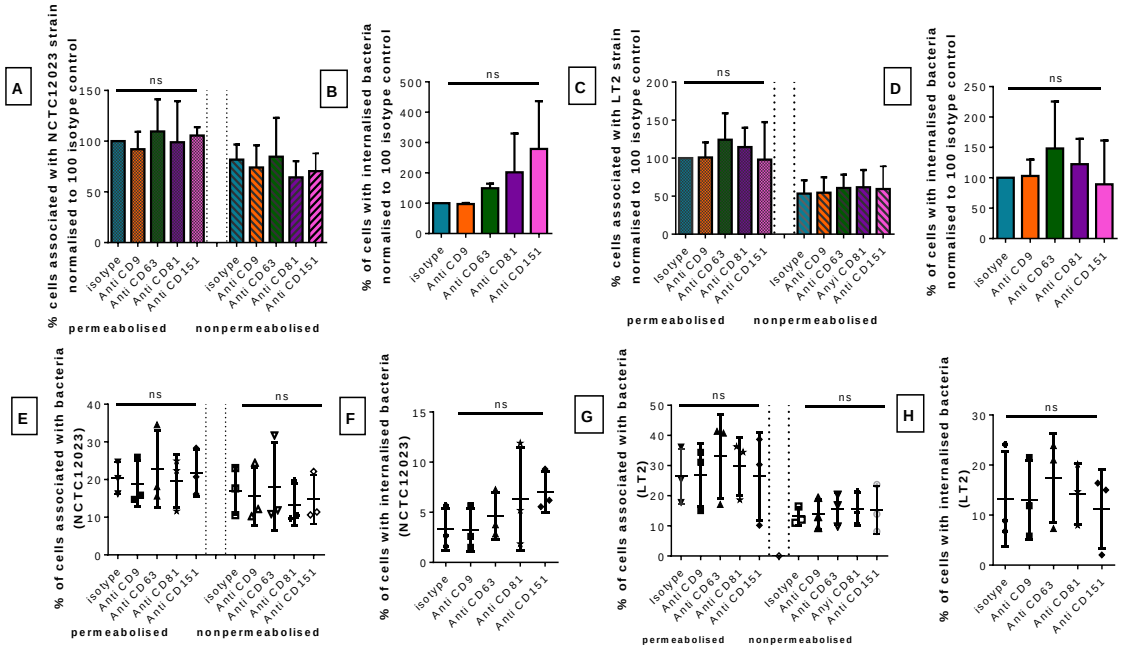

Figure 4.11: Effect of tetraspanin mAbs on *Salmonella* strain uptake by HEC-1-B cells at 50 MOI for 60 minutes analysed by flow cytometry. HEC-1-B cells were harvested non-enzymatically and pre-treated with anti-tetraspanin antibody or isotype control before infection and staining of permeabilised or non-permeabilised cells as described in Figure 4.10. NCTC12023 strain (**A**) or LT2 strain (**C**) normalised to 100% permeabilised isotype control (described in 2.2.5.2). Percentage of cells with internal bacteria, NCTC12023 strain (**B**) or (**D**) LT2 strain normalised to 100 isotype control. **E-H**: Corresponding raw data for **A-D** respectively. Bars show means, while error bars show standard error. n=3 in duplicate, the data was analysed using One Sample T-test (A-D) and Ordinary one-way ANOVA Holm-Sidak's multiple comparisons test (E-H) compared with isotype control, ns is non-significant.

4.3.3 Effect of anti-tetraspanins antibodies on *Salmonella* Typhimurium-GFP uptake analysed by flow cytometry

It was postulated that using GFP expressing bacteria might provide a good tool to allow a more direct, faster method of assessing infections by flow cytometry without the need to stain using anti-*Salmonella* antibodies. As described previously (3.3.2), GFP was successfully expressed in *S.* Typhimurium NCTC12023 and LT2 strains.

4.3.3.1 Effect of anti-tetraspanin antibodies on *S.* Typhimurium-GFP uptake by J774 cells analysed by flow cytometry

Salmonella-GFP strains were prepared as described in (2.2.5.1.2) in media contain 100µg/ml kanamycin and the J774 cells were infected at 5 MOI for 30 minutes as described previously (Figure 4.10). The cells with associated *Salmonella*-GFP were clearly segregated from the non-infected cells (Figure 4.12 A). The results considered represent percentage of total J774 cells with associated bacteria (both attached and internalised *Salmonella*). As previously (Figure 4.10), a significant reduction in percentage of *Salmonella* NCTC12023-GFP strain uptake in cells treated with anti- mouse CD81 prior infection was observed (Figure 4.12 B), although this was less significant than previously (the percentage of cells associated with bacteria). However, unexpectedly, although there appeared to be a slight reduction in uptake by cells treated with anti-CD9 relative to the isotype control, this was not statistically significant. In addition, anti-CD63 mAb had no effect on uptake. No significant reduction in *Salmonella* uptake was apparent with any of the mAb for cells infected with *Salmonella* LT2-GFP strain using normalised data (Figure 4.12 C), but anti-CD81 did show an effect when the raw (non-normalised) data were analysed. It is notable from comparing the raw flow cytometry data for WT NCTC12023 (Figure 4.10 E) with GFP-NCTC12023 (Figure 4.12 E) that the infection rate of the GFP strain is lower (~ 40% of J774 cells are associated with WT bacteria compared with ~ 20% for the GFP bacteria).

Control samples of *Salmonella*-GFP strain and wild type bacteria were included in each experiment, confirming that GFP was highly expressed (over 90% of bacteria were GFP positive for both strains used) indicating that GFP expression was stable (data not shown). As noted previously, the LT2 strain showed higher GFP expression, as indicated by a higher MFI, as shown previously (3.3.2).

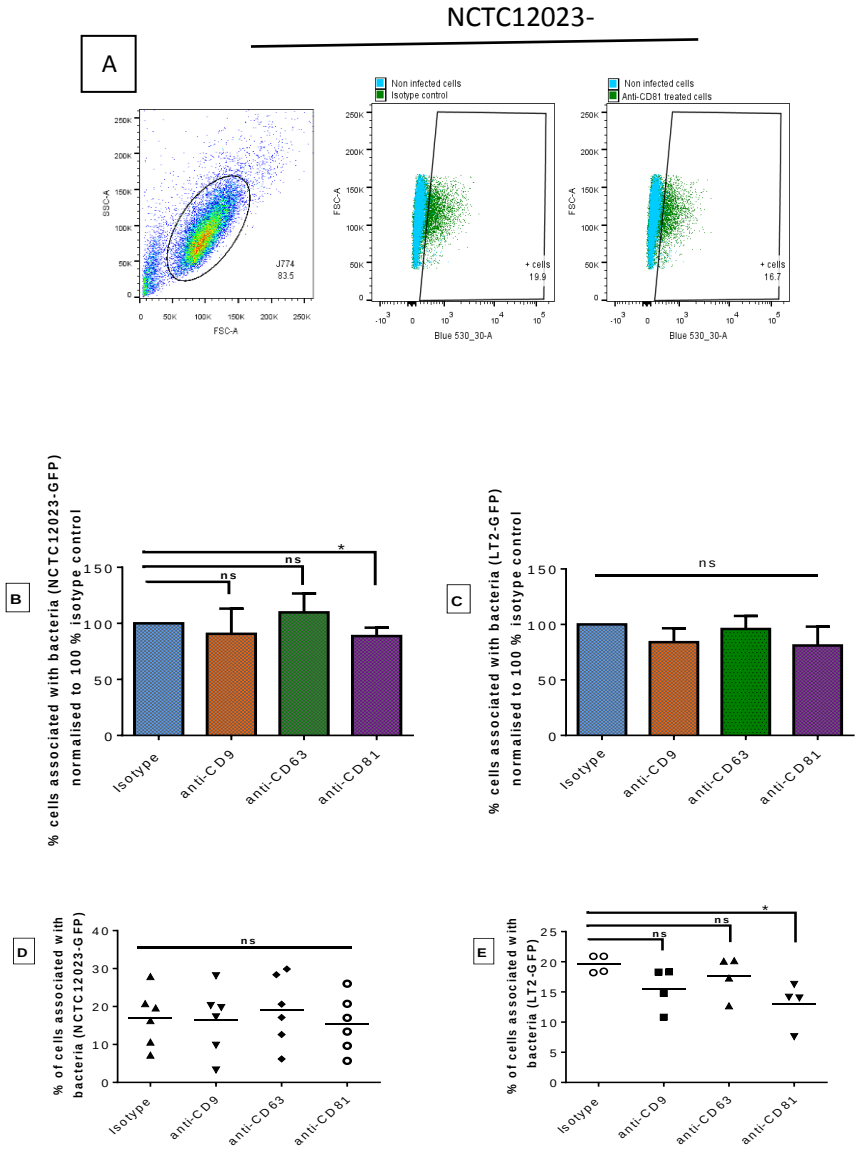

Figure 4.12: Effect of tetraspanin mAbs on *Salmonella*-GFP uptake by J774 cells at 5 MOI for 30 minutes analysed by flow cytometry. J774.2 cells were harvested and pre-treated with mAbs or isotype control before infecting with GFP-expressing *Salmonella* as described in 4.10. After washing the infected cells were fixed with 4% PFA for 15 minutes, washed once with PBS and suspended in with 1% PFA before analysis using the LSR-II flow cytometer (2.2.5.2.3). 10,000 events were acquired and the cells were gated according to FSC and SSC parameters. The GFP signal was detected using 530-30A filter and 530nm maximum emission 488nm blue laser. **A:** Dot plot from FACS analysis showing how the values shown in **B-E** were obtained. Percentage of J774 cells infected with *S.* Typhimurium normalized to isotype control (**B**) NCTC12023-GFP or (**C**) LT2-GFP. **D and E:** Raw data for **B and C** respectively. Bars describe means, while error bars describe standard errors. n=6 in **(B)** and n=4 in **(C),** in duplicate. The data was analysed by One sample T test comparing with isotype control in **B** and **C** and Ordinary one-way ANOVA Holm-Sidak's multiple comparisons test compared with isotype control in **D** and **E**, significance * $P \leq 0.05$, ns is non-significant.

4.3.3.2 *Salmonella* Typhimurium uptake by RAW264 cell line

Alongside the experiments with J774 cells, uptake of *Salmonella*-GFP strains by another mouse macrophage cell line, the semi-adherent RAW264 cell line, were carried out. Optimisation experiments indicated that an MOI of 20 and an infection time of 30 were suitable. The results considered represent the total RAW264 cells with associated bacteria (both attached and internalised *Salmonella*). Here, a significant reduction in the cells

associated with *Salmonella*-GFP was observed on pre-treatment with anti-CD9 and anti-CD81, but not anti-CD63, for both *Salmonella*-GFP strains (Figure 4.13 A and B).

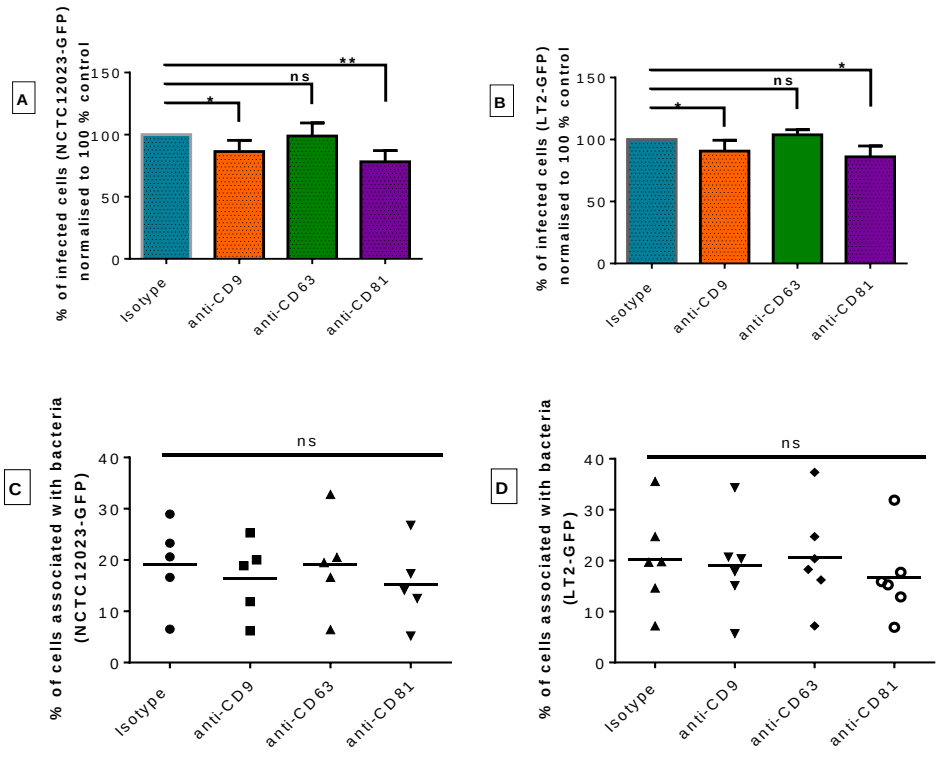

Figure 4.13: Effect of tetraspanin mAbs on *Salmonella* expressing GFP uptake by RAW264 cells at 20 MOI for 30 minutes analysed by flow cytometry. RAW264 cells were harvested and pre-treated with antibodies in U-bottomed 96-well plates prior to infection with bacteria on a shaking incubator then washed and fixed as described in 2.2.5.2.3 and Figure 4.12. Cells were analysed using the LSR-II flow cytometer, as previously and 5,000 events were acquired. Percentage of RAW264 cells infected with *S.* Typhimurium normalized to isotype control (**A**) NCTC12023-GFP or (**B)** LT2-GFP. **C and D:** Raw data for **A and B** respectively. Bars describe means, while error bars describe standard errors. n=5 in **(A)** and n=6 in **(B),** in duplicate. The data was analysed by One sample T-test comparing with isotype control in **A** and **B** and Ordinary one-way ANOVA Holm-Sidak's multiple comparisons test compared with isotype control in **C** and **D**, significance ** $P \leq 0.01$,* $P \leq 0.05$, ns is non-significant.

4.3.3.3 *Salmonella* Typhimurium uptake by non-differentiated THP-1 cell line

The human monocyte cell line (THP-1) was also used to investigate the effect of anti-tetraspanins antibodies on *Salmonella*-GFP strain uptake. The undifferentiated cells were used in the flow cytometry method because it was too difficult to harvest sufficient numbers of viable cells, as they become more adherent. From optimisation experiments 50 MOI and infection for 60 minutes was chosen as showing sufficient numbers of cells with associated bacteria for analysis; this compares with 30 MOI and 30 minutes infection for PMA-stimulated THP-1 (4.3.1.2), indicating that the undifferentiated cells are more difficult to infect. The cells were harvested, pre-treated with antibodies and infected with *Salmonella*-GFP as described in the preceding section, before analysis by flow cytometry. Variations in

the effects of anti-tetraspanin antibodies on uptake of GFP-transfected bacteria were observed depending on the *Salmonella* strain used. Anti-CD81 reduced bacterial association of cells infected with the NCTC12023-GFP strain, whilst no significant effects were noticed with any other anti-tetraspanin treatments (Figure 4-14 A and C). However, none of the anti-tetraspanin antibodies tested reduced association of cells infected with LT2-GFP strain (Figure 4.14 B). By contrast, THP-1 cells pre-treated with anti-CD151 appeared to show some increase in bacteria association, with a high median of fluorescent intensity (MFI) compared with isotype cells control. (Figure 4-14 D).

4.3.3.4 *S.* Typhimurium-GFP strains uptake by HeLa cell line

As described in 4.3.2.2. no effect of tetraspanin antibodies were observed in the human epithelial cell line HEC-1-B. Here, another epithelial cell line was introduced, since Hela cells offer a useful epithelial cell model to investigate *Salmonella* infection (Giannella, Washington et al. 1973, Jones, Richardson et al. 1981). This cell line was used to investigate the effect of anti-tetraspanins antibodies on *Salmonella*-GFP strain uptake. The tetraspanin expression of these cells was described previously in Chapter (3.3.1.5) and high expression of CD151 was observed in addition to that of other tetraspanins including CD9, CD63 and CD81. From initial optimising experiments the 50 MOI for 60 minutes was chosen (data not shown). Cells were harvested, pre-treated with antibody, infected with GFP-expressing strains of *Salmonella* as described previously (4.3.2.2). The anti-CD81 treated cells were shown to have more associated *Salmonella* NCTC12023-GFP compared with the isotype control, whereas no significant changes were noticed for the other anti-tetraspanin treatments (Figure 4-15 A). None of the anti-tetraspanins antibodies affected association of the cells with the LT2-GFP strain (Figure 4.15 B). No significant changes in MFI was observed (data not shown).

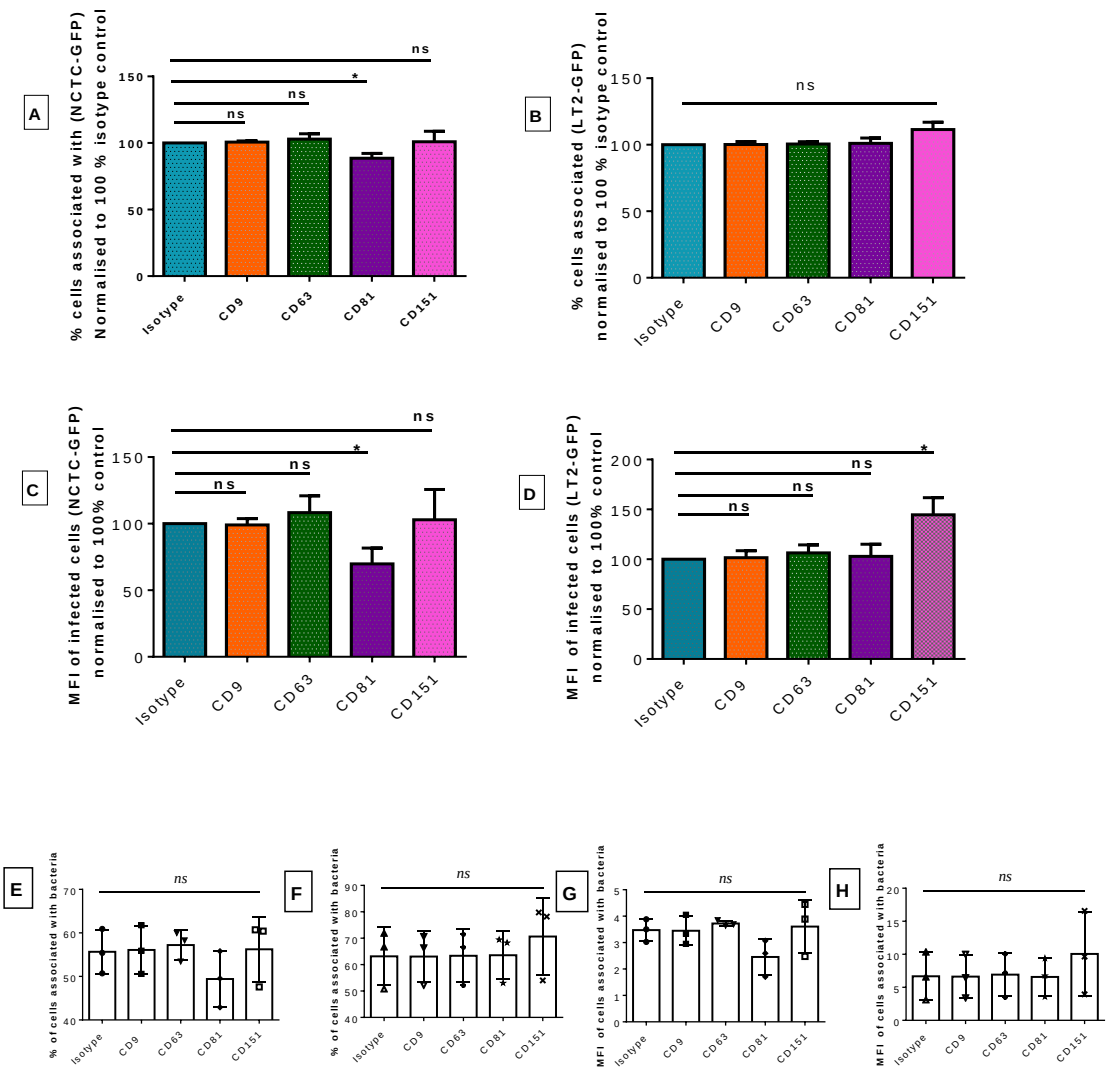

Figure 4.14: Effect of tetraspanin mAbs on *Salmonella* expressing GFP uptake by THP-1 cells at 50 MOI for 60 minutes analysed by flow cytometry. THP-1 cells were harvested and pre-treated with antibodies in U-bottomed 96-well plates prior to infection with bacteria on a shaking incubator then washed and fixed as described in 2.2.5.2.3 and Figure 4.12. Cells were analysed using the LSR-II flow cytometer, as previously and 5,000 events were acquired. Percentage of THP-1 cells infected with *S.* Typhimurium normalized to isotype control (**A**) NCTC12023-GFP or (**B**) LT2-GFP. And median of fluorescent intensity (MFI) **(C)** NCTC12023-GFP or **(D)** LT2-GFP. **E-H:** Corresponding raw data for **A-D** respectively. Bars describe means, while error bars describe standard errors. n=3 in duplicate. The data was analysed by One sample T-test comparing with isotype control in **A-D** and Ordinary one-way ANOVA Holm-Sidak's multiple comparisons test compared with isotype control in **E-H**, significance * $P \leq 0.05$, ns is non-significant.

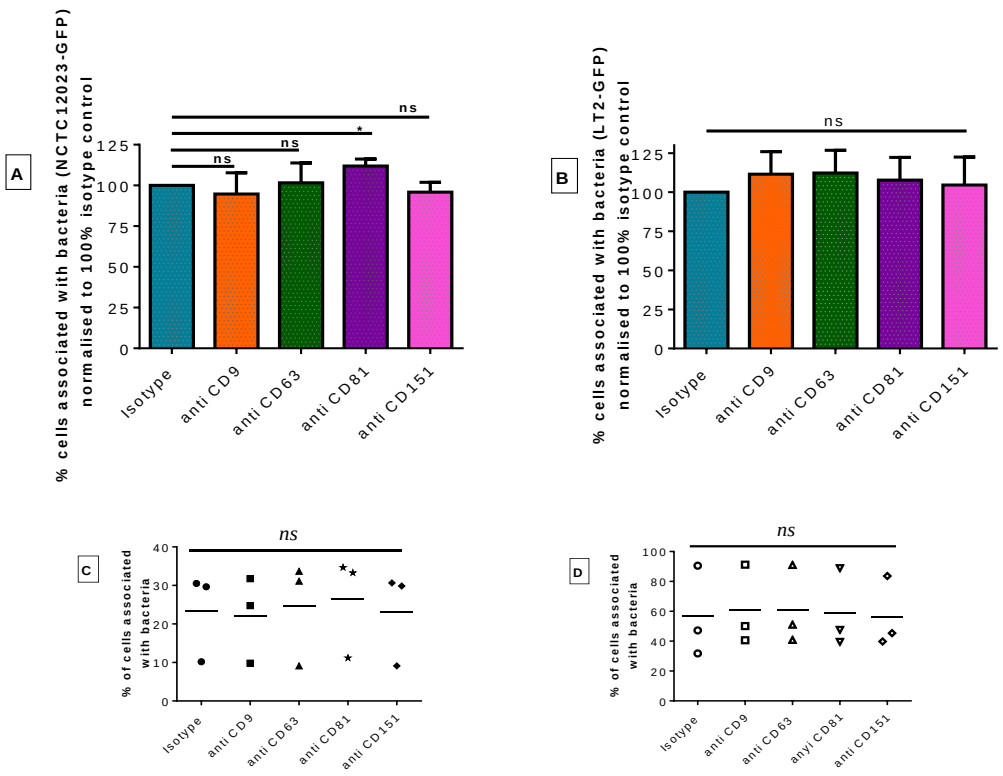

Figure 4.15: Effect of tetraspanin mAbs on *Salmonella* expressing GFP uptake by HeLa cells at 50 MOI for 60 minutes analysed by flow cytometry. HeLa cells were harvested and pre-treated with antibodies in U-bottomed 96-well plates prior to infection with bacteria on a shaking incubator then washed and fixed as described in 2.2.5.2.3 and Figure 4.12. Cells were analysed using the LSR-II flow cytometer, as previously and 5,000 events were acquired. Percentage of HeLa cells infected with *S.* Typhimurium normalized to isotype control (**A**) NCTC12023-GFP or (**B**) LT2-GFP. **C and D:** Corresponding raw (non-normalised) data for **B and C** respectively. Bars describe means, while error bars describe standard errors. n=3 in duplicate. The data was analysed by One sample T-test comparing with isotype control in **A** and **B** and Ordinary one-way ANOVA Holm-Sidak's multiple comparisons test compared with isotype control in **C** and **D**, significance * $P \leq 0.05$, ns is non-significant.

4.4: Discussion

Previous work from our lab has indicated that tetraspanins are involved in *S.* Typhimurium infection of human monocyte-derived macrophages (MDMs). The initial aim of this work was to develop cell line models to investigate the role of tetraspanins in *Salmonella* infection. In this study, different cell lines including mouse macrophage cell lines (J774.2 and RAW247), human macrophage-like cells (derived from human monocytes THP-1) and a human epithelial cell lines (HEC-1-B and HeLa cell lines) were infected with *Salmonella* strains. Initial infection experiments were carried out to optimise the conditions for infection of cell lines with *Salmonella* including the multiplicity of infection (MOI) and the time of infection.

Salmonella can infect and replicate in various cell types within the host (Haraga, Ohlson et al. 2008). As well, it has the ability to attached and invade different phagocytic and non-phagocytic cell lines (Finlay, Ruschkowski et al. 1991, Mills and Finlay 1994, Lajarin, Rubio et al. 1996, Rosales-Reyes, Perez-Lopez et al. 2012). In the present study, the results show the ability of *Salmonella* to invade non-phagocytic cells (HEC-1-B, HeLa epithelial cell lines) as well as phagocytic cell lines (RAW, J774 mouse macrophages and THP-1 derived macrophages). The ability to infect non-phagocytic cells can be mediated by T3SS-1 (Rosselin, Abed et al. 2011).

The mouse like macrophages J774 and RAW cell lines were used as a macrophage models to investigate the effect of anti-tetraspanin antibodies on *Salmonella* uptake. Furthermore, THP-1 derived macrophages were also used, since this cell line is of human origin and might more closely resemble the primary human MDM used in the previous study. The THP-1 cells were differentiated to macrophages – like cells using phorbol ester (PMA) as mentioned in chapter 3. As reviewed in (Auwerx 1991), the THP-1 cell line offers a close human model for MDMs. Initially a conventional immunofluorescence microscopy manual counting technique was used to investigate the effects of anti-tetraspanins on *Salmonella* infection. This method has routinely been used in our lab to indicate bacterial infection in both human macrophages (Hassuna, 2010, PhD thesis, University of Sheffield) and epithelial cell lines (Green, Monk et al. 2011); (Cozens, 2015, PhD thesis, University of Sheffield).

As shown in (Figure 4.3), a significant reduction in *Salmonella* NCTC12023 uptake was shown in J774 cells treated with anti-mouse CD9 prior *Salmonella* infection compared with isotype control. This is in contrast to previous studies on human MDM, where no inhibition with anti-CD9 mAbs was observed; however recombinant soluble CD9 EC2 proteins inhibited association of *Salmonella* with human MDM, suggesting involvement of CD9 in this process (Hassuna, PhD thesis, University of Sheffield 2010). Anti-CD81 antibodies showed a more modest inhibitory effect, consistent with previous data on human MDM. However anti-CD63 antibodies showed no effect; this may relate to the extremely low levels of CD63 on the surface of J774 cells (chapter 3). In contrast, the THP-1 derived macrophages and human MDMs both showed high levels of CD63 (Chapter 3) and (Hassuna, 2010, PhD thesis, University of Sheffield).

By contrast, for human cells, no inhibition by anti-CD9 mAb in THP-1 derived macrophages was noticed when using the same anti-CD9 antibody that blocked adhesion in the human MDM experiments. The differences in the effects of the anti-CD9 antibodies between mouse and human cells may relate to differences in the particular antibodies used, or differences in

CD9 between the mouse and human cells. Also in agreement with previous studies on human MDM, anti-CD63 and anti-CD81 antibodies inhibited association of *Salmonella* NCTC12023 to THP-1 derived macrophages. However anti-CD151 antibodies caused inhibition of infection of THP-1 macrophages, whereas no effect was seen with human MDM. The differing effects the antibodies here may relate to differences in expression of the tetraspanins, as human MDM were shown to express low levels of CD151 (only slightly higher than the isotype control (Hassuna, PhD thesis, University of Sheffield 2010). No significant effects were seen on the number of internalised bacteria, so it appears that the antibodies are acting at a stage prior to this. The infection of THP-1 derived macrophages by another *Salmonella* strain, LT2, which is reported to be more virulent (Professor Jeff Green, personal communication) and suggested in the present study (when the bacteria were used at mid log phase of growth) was also investigated. This difference could probably relate to differences in SPI-1 expression of certain T3SS components depending on *Salmonella* strains. It has been found that *Salmonella* Typhimurium NCTC12023 has less ability to invade epithelial cell lines, which may relate to low expression of prgH that is shown to be important to instruct needle complex formation in other *Salmonella* Typhimurium strains (Clark, Perrett et al. 2011). With the LT2 strain, anti-CD9 and anti-CD63 antibodies had no significant effect on adhesion to THP-1 macrophages and although some reduction was observed with anti-CD81 and anti-CD151 antibodies, this did not reach significance. Interestingly, anti-CD151 antibodies were previously found to reduce *Neisseria meningitidis* adhesion to human epithelial cells (Green, Monk et al. 2011).

It was of interest to investigate any potential role for tetraspanins in the infection of non-phagocytic cells by *Salmonella*, as the uptake of bacteria by these cells is likely to be primarily through the Type 3 secretion system (Finlay, Ruschkowski et al. 1991, Mills and Finlay 1994, Lajarin, Rubio et al. 1996, Rosales-Reyes, Perez-Lopez et al. 2012). As shown in (Figure 4.8) *Salmonella* were attached to and internalised into HEC-1-B cells after one hour incubation. Nevertheless, no significant effects were observed in these cells after treatment with anti-tetraspanins antibodies, either for the total cells associated with bacteria or in attached and internalised bacteria (Figure 4.9). This finding was in contrast to the reduction that was found in cells associated with attached *Salmonella* NCTC12023 in HEC-1-B cells that had been pre-treated with recombinant EC2 proteins corresponding to CD9, CD63 or CD151 prior to infection (Green, 2010, PhD thesis, University of Sheffield). The effect of antibodies was not assessed individually in the previous study. It could be that EC2 proteins have an effect whereas antibodies do not; in retrospect, it would have been useful to see if the previous

findings with EC2 proteins could be replicated here. Alternatively, it could be that tetraspanins are not involved in *Salmonella* uptake that is mediated by T3SS. Interestingly, infection of MDMs by *Salmonella* induced to express high level of T3SS was less affected by anti-CD63 antibodies (Noha Hassuna, PhD thesis 2010).

As stated previously, another aim of the work described in this Chapter was to develop a flow cytometry assay for assessing infection, which would be comparable with the microscopy assay but should be faster, permit analysis of more events and give more objective results. As mentioned earlier in this chapter (4.1.1), flow cytometry has been applied to study bacterial pathogenicity to host cells and bacterial-host interaction (Valdivia and Falkow 1998, Pils, Schmitter et al. 2006). Additionally, it was reported to be comparable with other ordinary infection assays and provide a quick and appropriate method to differentiate between external associated and internalised bacteria (Pils, Schmitter et al. 2006, Trouillet, Rasigade et al. 2011). The J774 cell line infection results that were obtained from this method, where bacteria were stained using antibodies after infection, were very comparable with the results from the fluorescence microscopy method (Figures 4.3, 4.4 and 4.10). In both methods anti- CD9 and anti CD81 antibodies similarly reduced *Salmonella* uptake significantly. Additionally, anti-mouse tetraspanins CD63 showed no effect on *Salmonella*/cells association, as in the microscopy assay. Interestingly, a lower MOI was necessary to achieve similar level of infections in the flow cytometry assay; it is possible that incubation of cells with bacteria in suspension may facilitate greater binding compared to cells adhered to coverslips. Also as found in the microscopy based method (Figure 4.9), no significant changes in total cells associated with bacteria, cells associated with external bacteria and cells associated with internal bacteria was found in HEC-1-B human epithelial cell line infected with *Salmonella* Typhimurium NCTC12023 and LT2 strains.

It was speculated that the generation of stable GFP expressing *Salmonella* strains could have advantages for both flow cytometry and for confocal microscopy. After optimising experiments using different vectors carrying either GFP or RFP proteins (as mentioned in chapter, 3.3.2), a broad host range plasmid (pBHR-1) carrying the GFP expression sequence was used to induce a stable, highly expressed GFP that was detected by flow cytometry and fluorescent microscope using appropriate filters. The pBHR1vector is derived from pBBR1 (Szpirer, Faelen et al. 2001) that was firstly isolated from *Bordetella bronchiseptica*-S87 (Antoine and Locht 1992). Bacteria expressing GFP have been employed in bacterial pathogenicity studies (Valdivia, Hromockyj et al. 1996) and it has been reported that GFP expression does not interfere with *Salmonella* invasion (Valdivia, Hromockyj et al. 1996, Ma,

Zhang et al. 2011). In contrast, high expression levels of GFP seems to affect *Salmonella* virulence (Wendland and Bumann 2002). In the present study, the *Salmonella*-GFP strains were successfully detected by flow cytometry using appropriate filter either alone (described in previous chapter, Figure 3.12) or associated with host cells in different cell lines. Also the population of bacteria infected cells was nicely segregated from the non-infected cell population by FACS analysis (Figure 4.12 A). Unexpectedly, J774 cells treated with anti-CD9 antibodies showed no significant change in cells associated with *Salmonella* NCTC12023-GFP and LT2-GFP strain, although some reduction was still seen with anti-CD81 antibodies. This could be related to the sensitivity of detecting fluorescence signal by flow cytometry which seems to be lower in GFP-expressing bacteria compared with bacterial immunostaining. To further investigate CD9 and CD81 in mouse macrophages, another mouse macrophages cell line was introduced. With the RAW 264.7 cell line, a small but significant reduction in *Salmonella* uptake in cells treated with anti-mouse CD9 and CD81 (but not in CD63) prior *Salmonella* NCTC and LT2 strains infection was observed. However a higher MOI was required to obtain sufficient cell infection (20 MOI), which could be because the RAW cells are less phagocytic than J774 cell line. Attempts to use the flow cytometry method to assess infection in THP-1 derived macrophages cells (stimulated for three days stimulation using PMA) were unsuccessful. This could be because these cells seem to become more fragile after harvesting, as a high concentration of cells debris was apparent in flow cytometry when the cells were infected in suspension; this could affect the flow cytometry analysis accuracy. PMA-stimulated THP-1 cells are very strongly adherent, and may have been damaged during harvesting prior to infection. Therefore, undifferentiated THP-1 cells were also assessed using the flow cytometry method. A high MOI was required to achieve infection of these cells, similar to that used for the epithelial cell lines. Interestingly, the undifferentiated THP-1 cells behaved differently depending on the *Salmonella* strains used. Cells treated with anti-human CD81 prior to *S.* Typhimurium NCTC12023-GFP infection showed a slight but significant reduction in cells associated with bacteria, but this was not observed with the LT2-GFP strain. None of the other antibodies used reduced infection. In contrast, a significant increase in the fluorescence (MFI) of cells treated with CD151 prior to infection with the LT2 strain was observed (Figure 4.14), suggesting that in this case the antibody may actually enhance bacterial uptake. The differences in anti-tetraspanin mAb action between non-differentiated and differentiated THP-1 cells might be related to the differences in tetraspanins expression and/or non-differentiated THP-1 cells are weakly phagocytic compared with high phagocytic activity of differentiated THP-1. A higher MOI was needed to obtain sufficient infection rate in non-differentiated THP-1 cells. Another epithelial cell model, the well-known HeLa cell line was

also used to assess infection by the GFP-expressing strains. Again no inhibition of infection was observed with any of the anti-tetraspanin antibodies used, but anti-CD81 treated Hela cells seemed to show slightly enhanced infection with *Salmonella*-NCTC12023-GFP, but not with the LT2-GFP. This contrasts with studies by Tham, et al (2010), where the anti-CD81 treated HeLa cells showed lower susceptibility to infection by another Gram negative bacteria *Listeria monocytogenes,* and CD81 has been shown to be regulated immunity against this bacterial infection (Martinez del Hoyo, Ramirez-Huesca et al. 2015). This diversity in tetraspanin mAb response could be related to the differences in bacterial types and strains that used, where some bacterial strains seem to be more dependent on cell surface proteins than others.

Overall, the results obtained in this Chapter are consistent with previous studies showing that tetraspanins are involved in *Salmonella* infection of mononuclear phagocytes (mouse or human), although some differences were observed in the involvement of individual tetraspanins; this may relate to varying expression levels of the tetraspanins or differences in the immortalised cell lines used here. However, in the studies using specific antibodies, there was little evidence to suggest that tetraspanins are involved in *Salmonella* infection of non-phagocytic cells.

A flow cytometry assay was developed for monitoring *Salmonella* infection that gave very comparable results with the microscopy assay when antibody staining was used to detect bacteria. However, a flow cytometry assay using GFP-expressing bacteria gave rather different results, with generally no or less effects being seen when using anti-tetraspanin antibodies. It could be that expressing GFP protein affected the infectivity of the bacteria in some way or that the GFP bacteria were not as well detected by FACS. Is it possible that if bacteria were internalised, the GFP signal may have been lost/reduced. Because of this, thereafter in this work, the antibody-staining method was used to detect *Salmonella* infection by flow cytometry.

Chapter 5: Effect of soluble tetraspanins EC2 proteins on *Salmonella* Typhimurium uptake by J774 cells and generation of soluble mouse CD9 EC2.

5.1 Introduction

The large extracellular loop (LEL or EC2 domain) of tetraspanins has the most variable sequence between family members, but contains a highly conserved CCG motif that indicates the tetraspanin signature, together with another 2, 4 or 6 cysteine residues that form 2, 3 or 4 disulphide bonds respectively (Seigneuret, Delaguillaumie et al. 2001). The EC2 regions of tetraspanins have been shown to be involved in many cell functions including fusion (Fanaei, Monk et al. 2011), egg-sperm fertilisation (Zhu, Miller et al. 2002, Hemler 2003), migration (Powner, Kopp et al. 2011), multinucleated giant cell formation (Takeda, Tachibana et al. 2003, Hulme, Higginbottom et al. 2014) and adhesion (Reyes, Monjas et al. 2015).

5.1.1 Tetraspanins EC2 and infections

Soluble recombinants EC2 proteins of several tetraspanins including CD9, CD63, CD81 and CD151 were shown to inhibit CXCR4-HIV-1 viral invasion in to macrophages (Ho, Martin et al. 2006). Also, as motioned previously (Chapter 1, Chapter 4) cells treated with tetraspanin EC2 recombinant proteins prior to infection reduced bacterial adhesion to epithelial cells (Green, Monk et al. 2011) and *Salmonella* Typhimurium uptake by MDMs (Noha Hassuna, 2010. PhD Thesis).

5.1.2 Recombinant proteins expression systems

Success in achieving a high level of recombinant protein expression is subject to different factors including the characteristics of cell growth, level of expression, endogenous or exogenous expression, post-translational protein modification and functional activity of expressed proteins and the overall cost of expression system (Makrides 1996, Yin, Li et al. 2007). Recombinant protein expression system is chosen according to the size and complexity of expressed proteins; the bacterial system is useful for expressing relatively small proteins, while eukaryotic systems such as yeast, mammalian cells, insect cells and plant cells are relevant to express large, complex and glycosylated proteins (Demain and Vaishnav 2009). Two main yeast systems are commonly used to express recombinant proteins including

Saccharomyces cerevisiae and *Pichia pastoris*. A high level of recombinant proteins (of more than 50 kDa) could be produced by this system with many advantages, in particular of glycosylated proteins, with the advantage of low cost (Demain and Vaishnav 2009). The mammalian cell system, however, is another popular system to express recombinant proteins, specifically glycosylated proteins, and the Chinese hamster ovary cells (CHO) cells have become the most widely used here. These cells can produce a high level of recombinant protein, with correct post-translational modifications for mammalian proteins, reviewed in (Kim, Kim et al. 2012). For more complex proteins, mainly proteins that require post translational modification, the baculoviral-insect system could also be a choice (Demain and Vaishnav 2009). Nevertheless, the high cost of this system compared with other eukaryotic recombinant protein expression systems could be considered as a main disadvantage (Gecchele, Merlin et al. 2015). In addition to all of the eukaryotic systems that are described above, plants have been shown to be important and effective expression system for recombinant proteins production (Wilken and Nikolov 2012), with advantages of flexibility, costs and protein quality; however, not all recombinant proteins are suitable for this system (Gecchele, Merlin et al. 2015). The plant *Arabidopsis thaliana* and other plants are commonly used to produce recombinant proteins (Demain and Vaishnav 2009).

The prokaryotic recombinant protein expression by *E. coli* offers a low cost, high level of recombinant protein production. Despite the advantage of *E coli*, it is not the system of choice for certain genes, which could relate to many factors such as complex structural features, mRNA stability and translation efficiency, miss-folding of proteins, protein degradation by host enzymatic activity and the toxicity of the expressed protein to host cells (Makrides 1996, Yin, Li et al. 2007). Understanding the basics of *E. coli* transcription, translation and folding of proteins and genetic improvement led to enhancing the efficiency of this system to express complicated eukaryotic proteins (Baneyx 1999). Folding of recombinant proteins, particularly complex and cysteine rich proteins, are the main issue of concern to obtain host native protein features. The size and complexity of host proteins affects their folding and formation of functional native proteins. Generally, large and complex recombinant proteins are less likely to reach the native conformation efficiently, and assistance is usually needed compared with small (<100 residues) and single host proteins. The unfolded or misfolded recombinant proteins are therefore often aggregated in inclusion bodies or degraded by the action of host cells enzymes (Baneyx and Mujacic 2004). This aggregation could be as a result of the presence of a strong promoter and high concentration of inducer that leads to the production of high levels of recombinant protein and, consequently, aggregation of insoluble proteins to form inclusion bodies (Baneyx and Mujacic 2004, Sorensen and Mortensen 2005).

A strong promoter is required in an expression vector to regulate the high levels of gene expression and the presence of a repressor leads to decreased basal transcription in the absence of an inducer. The promoter could be induced thermally or chemically, and the main chemical that is used for promoter induction is isopropyl-beta-D-thiogalactopyranoside (IPTG) (Sorensen and Mortensen 2005), which binds to the *lac* repressor, allowing transcription from the lac operon. The formation of inclusion bodies could be considered as main disadvantage of using *E coli* systems compared with other expression systems (Gecchele, Merlin et al. 2015). As much as 50-95% of insoluble proteins have been found in inclusion bodies that are usually degraded by host cell proteases, reviewed in (Sorensen and Mortensen 2005). One strategy that could prevent aggregation of recombinant proteins is by using a molecular chaperone that regulates the protein folding processes and prevents aggregation of misfolded proteins, reviewed in (Schlieker, Bukau et al. 2002). Alternatively re-solubilisation of the insoluble recombinant proteins can be carried out by using urea and guadinium hydrochloride detergent (Sorensen and Mortensen 2005).

Since the N-linked glycosylation system of *Campylobacter jejuni* has been successfully transferred into *E. coli*, it has now become possible to produce glycosylated proteins in *E. coli* even though there is structural variation between bacterial and eukaryotic glycans (Wacker, Linton et al. 2002). More recently, the glycosyltransferase pathway from yeast *Saccharomyces cerevisiae* was also transferred into the glycosylation modified *E. coli* system to enable this modified bacteria to produce lipid linked trimannosyl-chitobiose (Man3-GlcNAc2) and mannosyl-chitobiose (Man-GlcNAc2) that are seen essential in eukaryotic glycosylation (Srichaisupakit, Ohashi et al. 2015).

A polypeptide fusion protein called an affinity tag is widely used to enhance recombinant proteins purification and detection, and is also used to increase protein production, folding and solubility. As well it can used to express toxic proteins and it could save the tagged proteins from degradation, reviewed in (Costa, Almeida et al. 2014). Different tags have been commonly used depending on the protein of interest and popular choices include His-tag, thioredoxin, Strep-tag, SBP-tag, Nus-tag, Arg-tag, cellulose-binding domain, calmodulin-binding peptide, c-myc-tag, DSb A and glutathione S-transferase (GST) (Terpe 2003). A 26 kDa GST of *Schistosoma japanicum* was cloned into an *E. coli* expression plasmid and the expressed proteins could be purified from host cell lysates using affinity chromatography on fixed glutathione. Binding GST protein could be eluted using 10mM reduced glutathione under non-denaturation conditions and the expressed GST protein is commonly found soluble in aqueous solution and forms dimers and it could be detected easily by enzymatic

and immunological methods. However, the GST-tagged proteins can be insoluble and this could be associated with the presence hydrophobic regions in the tagged protein. GST can be inserted either at the C or N terminus of proteins and can be used in different expression systems (Terpe 2003). The GST tag has been shown to stabilise the linked protein better compared with His-tag. It has been shown that the *E. coli* acetohydroxyacid synthase-I isozymes large subunit (AHAS-I-LSU) that is tagged with GST (GST-LSU) was more stable compared with the His-tagged protein (His-LSU) that was unstable (Li, Liu et al. 2015).

In our group, the *E. coli* system has been shown to be competent to produce tetraspanins extracellular domains, EC2s tagged with GST. As described before, the tagged proteins were shown to be stable and the GST did not interfere with fused protein functions as indicated in previous study in our group. The system reliably expresses EC2 domains with correct folding and formation of the disulphide bonds that are crucial to EC2 function. Despite this, a high proportion of the proteins may be in inclusion bodies as insoluble form that could be as result of high levels of recombinant proteins expression (Fanaei, PhD thesis, University of Sheffield, 2013).

5.2 Aims

In present study, targeting tetraspanins CD9 and CD81with specific antibodies in the mouse macrophage cell line J774 reduced *Salmonella* uptake. There was no effect with anti-CD63 antibodies, which is not surprising as these cells express very low levels of CD63 on their surface (Chapter 3). From a previous study in our lab, MDMs treated with antibodies to CD63 and recombinant CD63-EC2 showed a significant reduction in *Salmonella* uptake (Hassuna, PhD thesis, University of Sheffield 2010). In the same study, CD9-EC2 also inhibited bacterial adhesion. Furthermore, another study showed a significant reduction in adhesion of various bacteria to epithelial cells that treated with tetraspanins EC2-GST recombinant proteins prior infection (Green, PhD thesis, University of Sheffield 2010) (Green, Monk et al. 2011). Here, we investigated the effect of human tetraspanins EC2 recombinant protein on mouse J774 cells prior to *Salmonella* infection. In addition, mouse CD9-EC2 was generated, and its effects on *Salmonella* uptake by J774 cells investigated.

5.3 Results

5.3.1 Effects of recombinant EC2 fragments on J774 cells infected with *S.* Typhimurium NCTC 12023 (flow cytometry)

Previous studies using human monocyte-derived macrophages (MDM) showed that recombinant versions of the large extracellular domains (EC2s) of tetraspanins CD9 and CD63 inhibited *S.* Typhimurium uptake by approximately 50% (Hassuna, PhD thesis, University of Sheffield 2010). The recombinant proteins also inhibited adhesion of *N. meningitidis* and other bacteria to human epithelial cell lines (Green et al., 2011). Since antibodies to CD9 and CD81 had an inhibitory effect on *S.* Typhimurium infection of J774 cells, it appeared appropriate here to test the effect of the corresponding soluble EC2 proteins. The human versions of these recombinant proteins were expressed as GST-fusion proteins in *E. coli* and had been prepared by another member of the laboratory (Marzieh Fanaei). These proteins were shown to be correctly folded in Western blots with conformation-sensitive antibodies (Marzieh Fanaei, PhD thesis University of Sheffield, 2013) and also showed biological activity in a number of other assays carried out concurrently with the experiments described here, including inhibition of adhesion of bacteria to epithelial cells lines and inhibition of multinucleated giant cell formation in J774 cells induced by infection with *Burkholderia thailandensis* (D. Cozens PhD thesis University of Sheffield 2015, A. Elgawidi, personal communication).

The effect of tetraspanin EC2 proteins was tested by flow cytometry as described in 2.2.5.2 using direct staining with FITC conjugated anti-*Salmonella* polyclonal antibody (Figure 5.1). No significant changes in the percentage of cells infected or in the median fluorescence intensity (MFI), which gives an indication of the level of infection, were shown when recombinant human CD9 EC2 and CD81 EC2-GST fragments were used to pre-treat J774 cells prior to infection with *S.* Typhimurium at 500 and1000 nM protein concentrations compared with the GST control., However, a minor significant change in MFI was observed with CD9-EC2 for cells treated with 500nM of recombinant EC2 protein compared with non-treated cells.

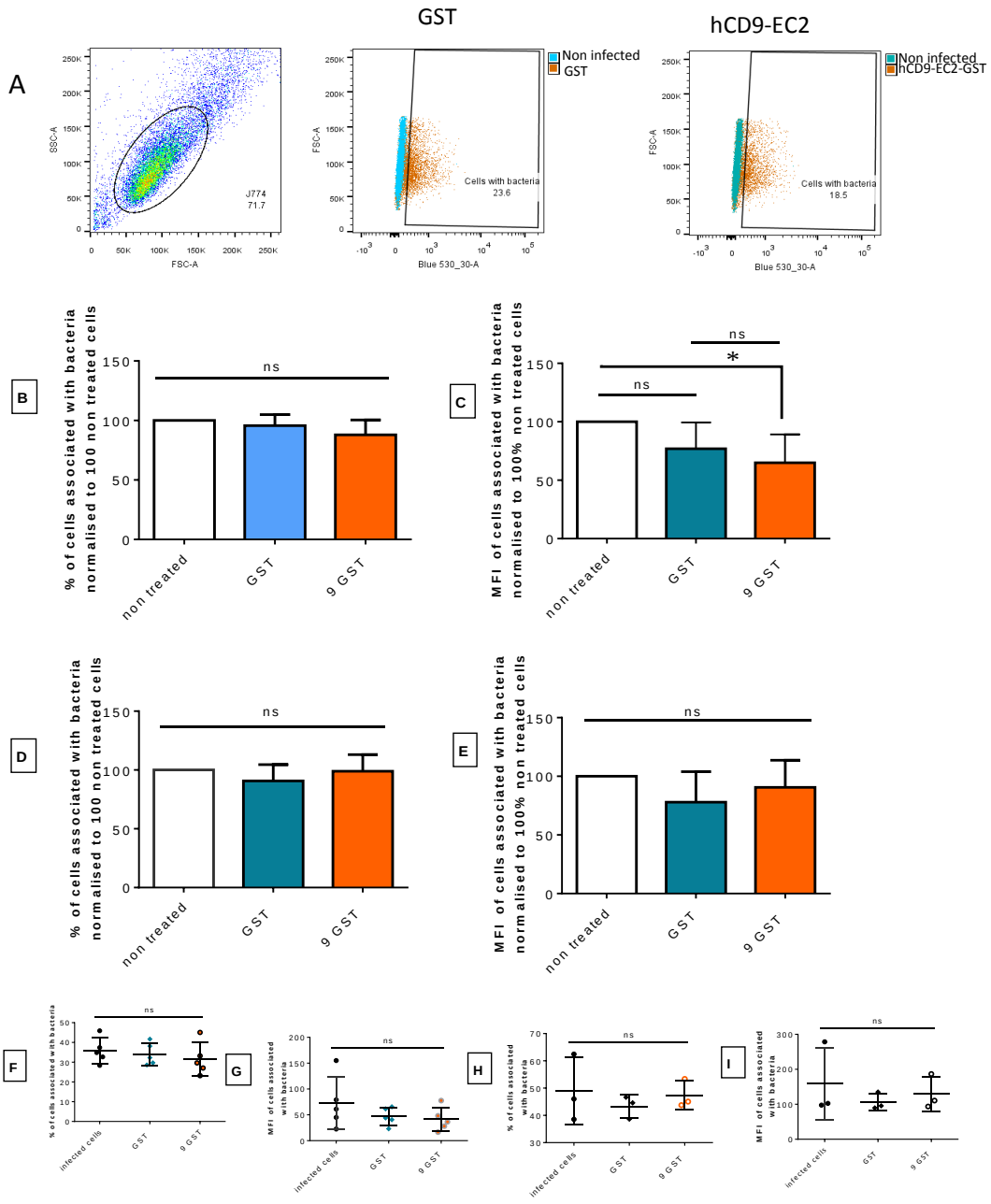

Figure 5.1: Effect of tetraspanin EC2 recombinant protein on *Salmonella NCTC-12023* uptake by J774 cells analysed by flow cytometry. J774.2 cells were harvested, placed in Eppendorf tubes and pre-treated with CD9 and CD81 EC2-GST at concentration of 500nM (B and C) and 1000nM (D and E) for 60 minutes before infection with *Salmonella* Typhimurium NCTC12023 at 5 MOI for 30 minutes as described in 2.2.5.2.1. The cells-bacteria mixture was placed on a rotating mixer and was incubated at 37°C for 30 minutes. The cells were washed and fixed or fixed and permeabilised as described in 2.2.5.2.4 and stained using FITC conjugated anti-*Salmonella* polyvalent antibody. Cells were kept in 1% PFA until analysis using an LSR-II flow cytometer. **A:** Dot plot from FACS analysis showing how the values shown in B-E were obtained **B**: Percentage of J774 cells infected with *Salmonella* normalized to 100% isotype control. **C**: MFI of J774 cells infected with *Salmonella* normalized to 100% isotype control. **D:** Percentage of cells infected with *Salmonella* NCTC12023 **E:** MFI of J774 cells infected with *Salmonella* normalized to 100% isotype control. **F-I:** Raw data before normalisation. Bars describe means, while error bars describe standard error means. MFI is the median of fluorescence intensity, n=5 in **B** and **C** and n=3 in **D** and **E** in duplicate, data was analysed by Ordinary one sample T-test comparing with non-treated cells and GST treated control (B-E), graphs (F-I) data was analysed by Ordinary one-way ANOVA Holm-Sidak's multiple comparisons test, significance * $P \leq 0.05$. ns is non-significant.

.

5.3.2 Generation of soluble mouse CD9-EC2

Human tetraspanin EC2s have previously been shown to be active on mouse cells in other types of assay (sperm: egg fusion (Higginbottom et al 2003; *B. thailandensis*-induced fusion of J774 cells, Atiga Elgawidi, personal communication). However, their lack of an effect on *Salmonella* infection might be due to sequence differences between the human and mouse CD9 EC2 proteins, which show 76% identity.

5.3.2.1 Mouse CD9-EC2 sequence and alignment

The full length of the CD9 protein sequences were obtained from online bioinformatics database UniProt (http://www.uniprot.org/), and the domain sequences were chosen as indicated in this online tool. The sequences were aligned using online multi-sequences alignment, MultAline, (http://multalin.toulouse.inra.fr/multalin/) and BoxShade (http://www.ch.embnet.org/software/BOX_form.html) where the sequences identities expressed as percentages were obtained using BLAST 2 sequences alignment (http://blast.ncbi.nlm.nih.gov/Blast.cgi?CMD=Web&PAGE_TYPE=BlastHome).The mouse, rat and human CD9 protein sequence were aligned using a combination of these tools (Figure 5.2). The tetraspanin mouse CD9 shown about 95% identity to rat CD9 and 89% with Homo sapiens CD9. However, the mouse EC2 shows about 87% homology with rat CD9-EC2 and 77% homology with Homo sapiens CD9.

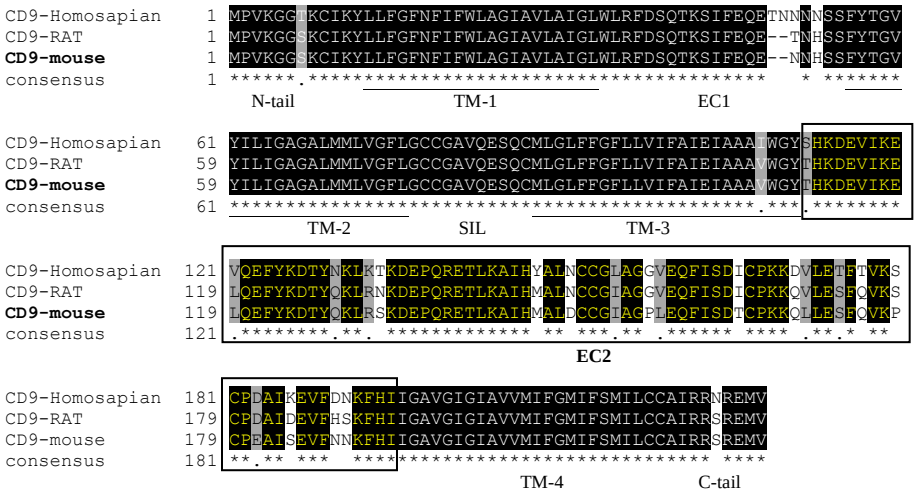

Figure 5.2: Mouse, rat and human CD9 proteins sequence alignment. All three full CD9 sequence were obtained from UniProt (http://www.uniprot.org/). The large extracellular domain (EC2) sequences is shown boxed and in yellow letters. The transmembrane domains (TMs) are underlined. EC1: Is the small extracellular domain. SIL: Is the small intracellular loop. All domains sites were chosen as it indicated in UniProt. MultAline, (http://multalin.toulouse.inra.fr/multalin/) and BoxShade (http://www.ch.embnet.org/software/BOX_form.html) were used to align these sequences.

5.3.2.2 Mouse CD9-EC2 theoretic structure alignments

The online protein structure prediction tool, Phyr2, was used to build a 3D model protein structure and shows the putative ligand binding sites and amino acid differences (Kelley, Mezulis et al. 2015) of mouse, rat and human CD9, since these protein structures have not yet been solved . A combination of this online tool with the PyMOL Molecular graphic system, Version 1.7.4 Schrödinger, LLC. Software (https://www.pymol.org/), was used to visualised the 3D structure predicted using the Phyr2 tools. The CD9-EC2 of mouse was predicted and aligned with the predicted rat and human CD9-EC2 structures (Figure 5.3). And as described previously, the online tools MultAline and BoxShade were used also to show differences and homology of mouse CD9-EC2 compared with rat and Homo sapient (Figure 5.2).

1

Mouse CD9-EC2

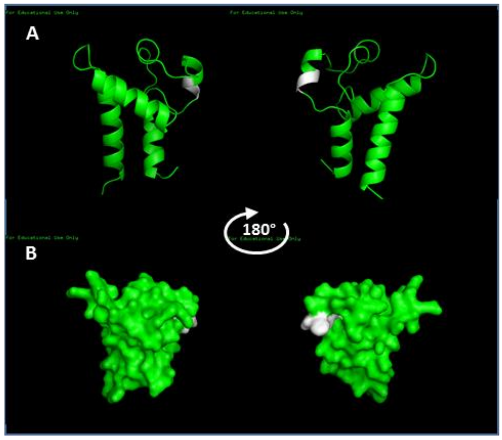

2

```
Mouse     1 THKDEVIKELQEFYKDTYQKLRSKDEPQRETLKAIHMALDCCGIAGPLEQFISDICPKKQ
Human     1 SHKDEVIKEVQEFYKDTYNKLKIKDEPQRETLKAIHYALNCCGLAGGVEQFISDICPKKD

Mouse    61 LLESFQVKPCPEAISEVFNNKFHI
Human    61 VLETFTVKSCPDAIKEVFDNKFHI
```

HUMAN CD9-EC2

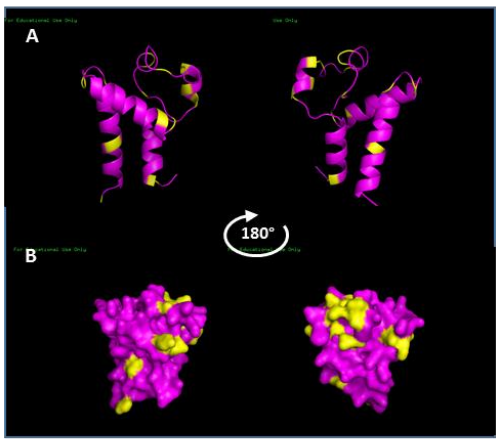

C

Mouse and Human CD9-EC2 structures alignment

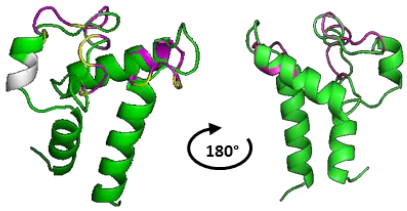

3

```
Mouse     1 THKDEVIKELQEFYKDTYQKLRSKDEPQRETLKAIHMALDCCGIAGPLEQFISDICPKKQ
Rat       1 THKDEVIKELQEFYKDTYQKLRNKDEPQRETLKAIHMALNCCGIAGGVEQFISDICPKKQ

Mouse    61 LLESFQVKPCPEAISEVFNNKFHI
Rat      61 VLESFQVKSCPDAIDEVFHSKFHI
```

RAT CD9-EC2

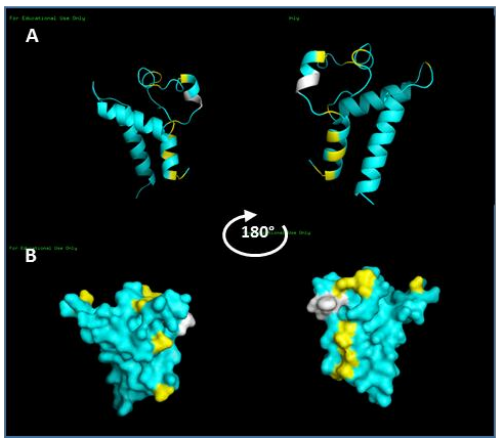

C

Mouse and Rat CD9-EC2 structures alignment

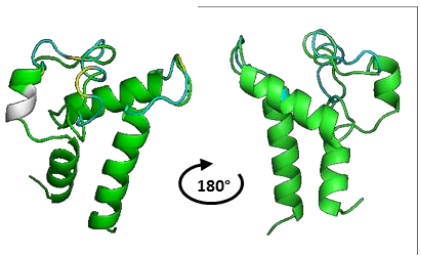

Figure 5.3: The predicted structure, sequence comparison and alignment of mouse, human and rat CD9-EC2 (large extracellular domain). The grey colour in (1) shows the position of SFQ residues found in mouse and rat but not in human CD9-EC2 and shown to be needed in mouse gametes fusion (Zhu, Miller et al. 2002). The yellow colour in (3) represents the sites of differences between human or in rat compared with mouse. **1A:** The predicted structure of mouse CD9-EC2 obtained by Phyre2 (Kelley, Mezulis et al. 2015), the structure was edited and visualised using The PyMOL Molecular Graphics System, Version 1.7.4 Schrödinger, LLC (https://www.pymol.org/). **1B:** Space-filling model of the predicted mouse CD9-EC2 structure. **2:** Mouse and human sequence alignment, both full length sequences obtained from the UniProt online database (http://www.uniprot.org/uniprot/P40240) (http://www.uniprot.org/uniprot/P21926) and aligned using MultAline (http://www.sacs.ucsf.edu/cgi-bin/multalin.py) and BoxShade (http://embnet.vital-it.ch/software/BOX_form.html). **2A:** The predicted structure of human CD9-EC2. **2B:** Space-filling model of the predicted human CD9-EC2 structure. **2C:** Mouse and human aligned structures of predicted CD9-EC2 showing the structural homology. **3:** Mouse and rat aligned sequences, the rat full length sequence was obtained from UniProt (http://www.uniprot.org/uniprot/P40241). **3A:** The predicted structure of rat CD9-EC2. **3B:** Space-filling model of predicted rat CD9-EC2. **3C:** Mouse and rat predicted CD9-EC2 aligned structures showing the structural homology.

5.3.2.3 Cloning of Mouse recombinant CD9-EC2

The expression of mouse CD9-EC2-GST was therefore undertaken to find out the role of mouse CD9-EC2 in *Salmonella* uptake. The sequence corresponding to the EC2 was PCR-amplified from a full-length mouse CD9-GFP construct (Origene) (Figure 5.4) using forward and reverse primers designed to be complementary to 5` and 3` of mCD9-EC2 and incorporating EcoR-l and Hind-lll restriction sites to allow cloning in to corresponding sites of the pGEX-KG vector, as described in 2.2.8.6 The PCR products were analysed by agarose gel electrophoresis (Figure 5.5).

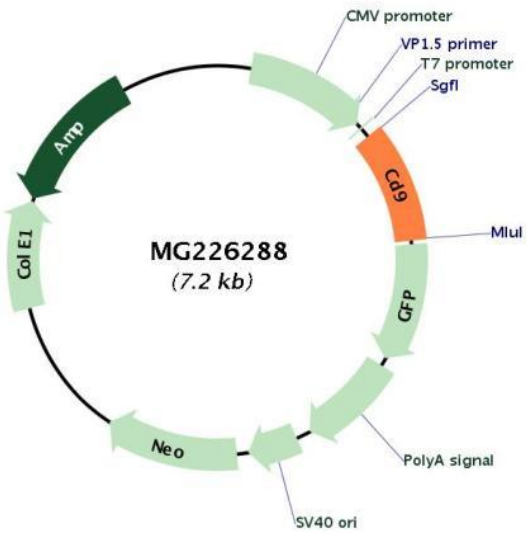

Figure 5.4: Mouse CD9 in pCMV6-AV-GFP (MG226288) vector. The image was obtained from the plasmid supplier's website (http://www.origene.com/mouse_orf_clone/NM_007657/MG226288/Cd9.aspx) showing the vector construct and the inserted mouse CD9 fused with GFP DNA sequence and the cloning sites.

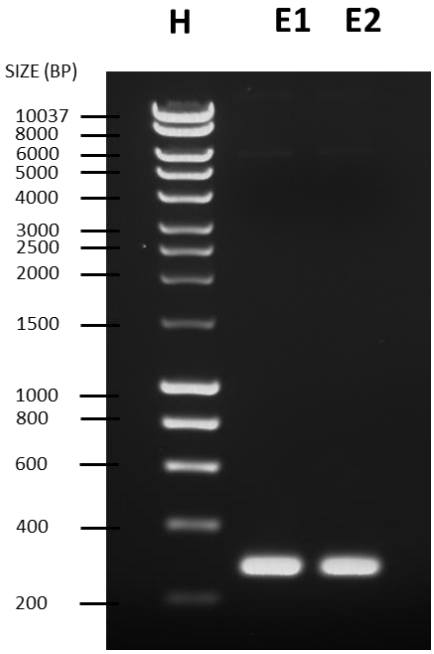

Figure 5.5: PCR amplification of mouse CD9-EC2 from pCMV-AC-GFP mouse CD9. The mCD9-EC2 was amplified from CD9-GFP using the conditions described in 2.2.8.7. 4µl of PCR product was mixed with 1µl of 5x DNA loading buffer (BioRad) and loaded for each well of a 1% agarose gel, 5µl of DNA ladder (hyper ladder 1, Bioline) was used as a marker to indicate the DNA size (**H**). **E1** and **E2**: Amplified mCD9-EC2 DNA segments [252 bp] taking into consideration the extra bp in forward and reverse primers and the restriction sites

The amplified mCD9-EC2 DNA was shown to be pure and the expected size in relation to the DNA ladder. The amplified mCD9-EC2 was extracted from the gel (2.2.8.8) then double digested by EcoR-l and Hind-III restriction endonuclease enzymes (2.2.8.9). The same procedure was applied to the pGEX-KG plasmid to produce overhanging ends, then the restricted PCR purified product was ligated with the pGEX-KG vector to generate a mouse CD9-EC2-GST construct, as described in 2.2.8.10 and shown in (Figure 5.6). The ligation product was transformed into DH5α cells which were grown in selective media contain 100µg carbenicillin to select transformed bacteria.

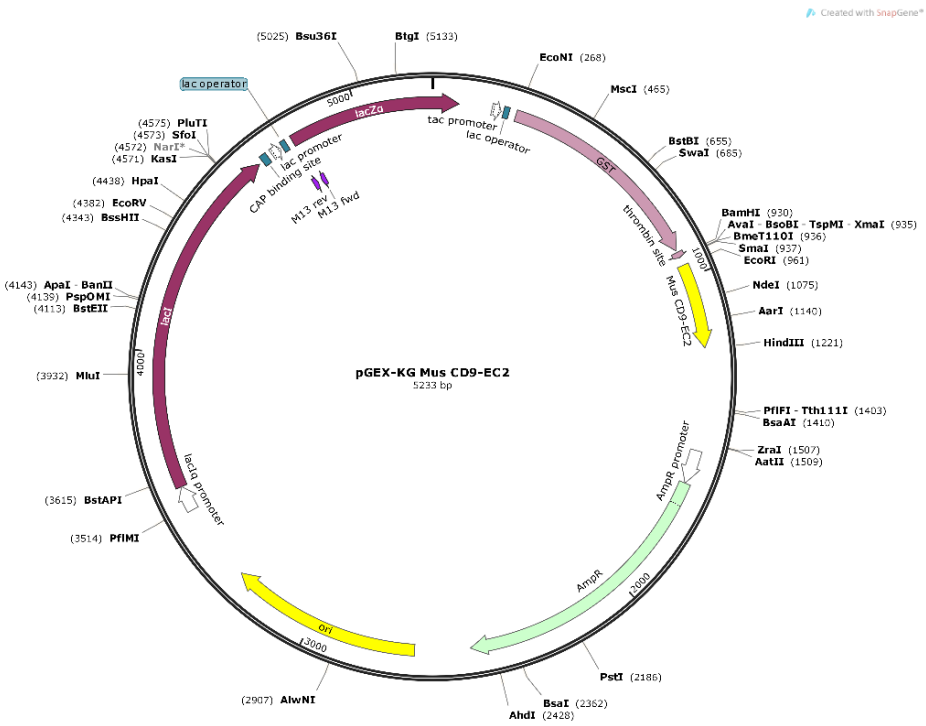

Figure 5. 6: Plasmid map for mouse CD9-EC2 in pGEX-KG-GST vector. SnapGene® 2.8 software was used to draw the plasmid map.

To confirm the presence the mCD9-EC2 in the pGEX-KG vector, different transformed colonies were taken and grown in selective LB broth followed by plasmid extraction (2.2.8.1). The extracted plasmids were double digested with *EcoR-l* and *Hind-III* to excise the EC2 segment from the plasmid and also PCR amplification was carried out using the same primers used previously to amplify the mCD9-EC2 as well as using primers designed to amplify the mCD9-EC2 along with the GST-tag (2.1.14.3). Plasmids obtained from two colonies were shown to be contain the full length inserted DNA fragment by both restriction digest and PCR amplification. Other colonies analysed gave fragments of unexpected size on double digestion, but appeared to contain mCD9-EC2 as determined by PCR (Figure 5.7).

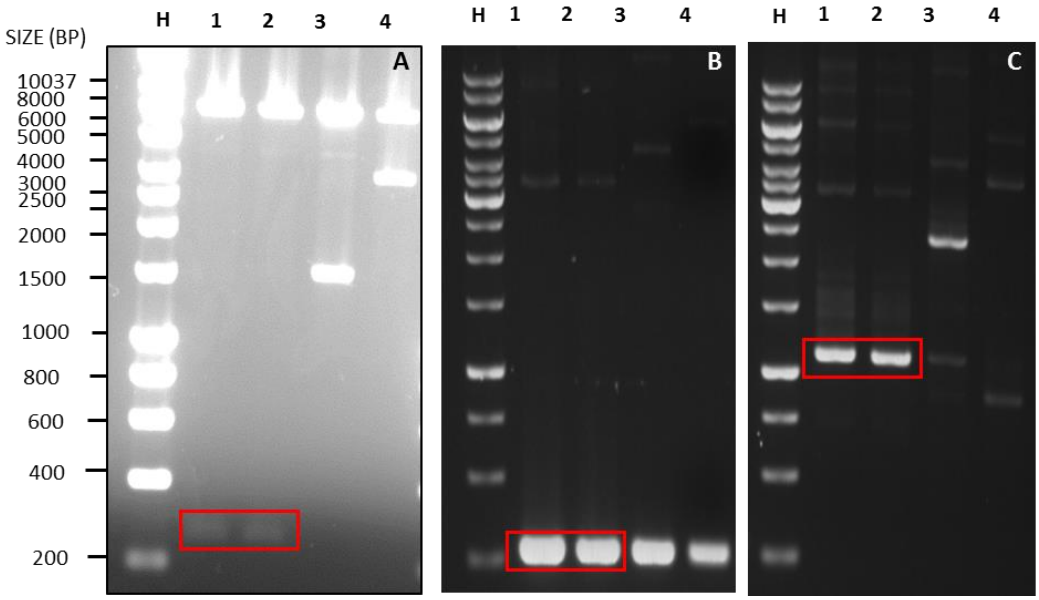

Figure 5.7: Detection of the presence of mCD9-EC2 DNA fragment in the pGEX-KG plasmid: A: Double digestion of plasmid DNA extracted from different colonies transformed with pGEX-KG mCD9EC2 ligation products to excise the inserted mCD9-EC2 (shown in **1** and **2** in red box). **B:** PCR amplification of mouse CD9-EC2 from plasmid DNA extracted as for (**A**). **C:** PCR amplification of mouse CD9-EC2-GST from plasmid DNA extracted as for (A). Samples were run on a 1% agarose gel as described in Figure 5.5. H=Hyper ladder (Bioline), 1-4 = colony number selected post ligation.

Colonies 1 and 2 were expanded and DNA from these sequenced to confirm presence of the correct mCD9-EC2 construct using the foreword and reverse primers, pGEX-F2 and pGEX-R1 respectively described in 2.2.8.12. The sequencing confirmed the presence of mCD9-EC2 and that no mutation had been introduced.

5.3.3 Expression and purification of recombinant mouse CD9-EC2 protein in *E. coli* Rosetta-Gami strain

The confirmed pGEX-mCD9-EC2 and pGEX-GST control vectors were separately used to transform Rosetta Gami competent cells (2.2.9.1) followed by expression of recombinant protein in 500ml bacterial cultures (2.2.9.2). After induction of protein expression, the bacteria were harvested, lysed and the mCD9-GST and GST control proteins were purified from the soluble lysate fraction as described in 2.2.9.3 (Figure 5.8), essentially following the methods described previously (Higginbottom, Takahashi et al. 2003) as described in (2.2.9.4). Fractions taken from each step of the protein purification were checked by SDS-PAGE and western blotting using primary rat anti-mouse CD9 antibodies followed by HRP conjugated anti-rat secondary antibodies (Figure 5.9) or HRP tagged anti GST (Figure 5.10). The protein concentration was estimated by measuring the absorption at 280 nm using a Nano drop (2.2.9.5).

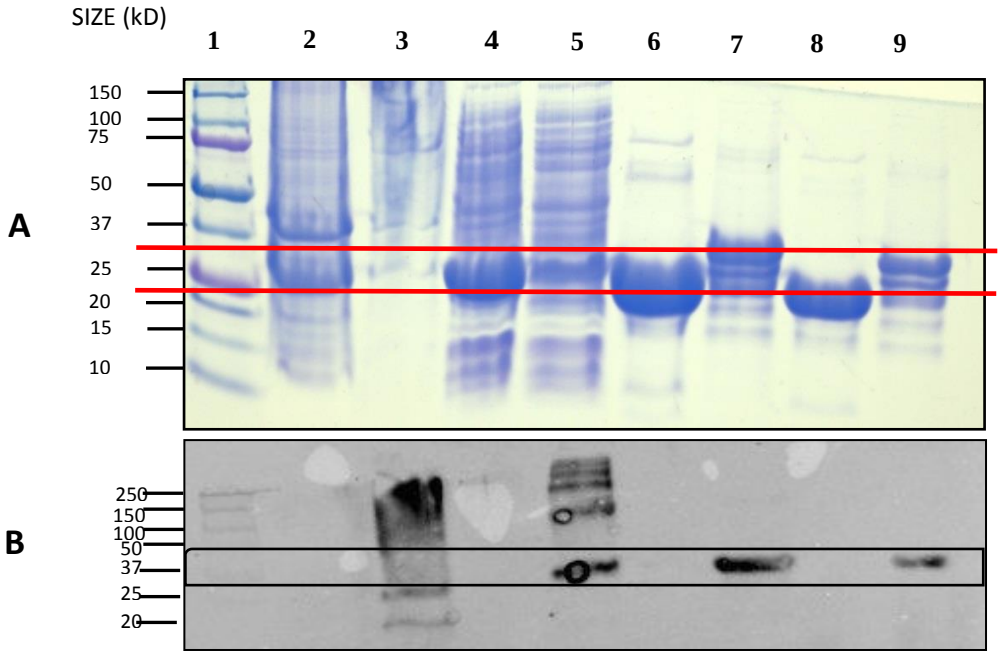

Figure 5.8: **Analysis of purification of mCD9-GST and GST control by SDS-PAGE and Western blotting.** Lysates were prepared from *E. coli* cells transformed to express GST-mCD9 or GST control as described in 2.2.9.1. The insoluble fractions were retained after lysis and re-suspended in PBS buffer for analysis by SDS-PAGE. Soluble lysate fractions were used for glutathione affinity chromatography. Samples were taken at each stage of the purification and run on a 12.5% PAGE gel under non-reducing conditions before staining with Coomassie blue (**A**). **1**: precision plus protein standards. **2,4:** GST expression: insoluble and supernatant fractions, respectively, **3,5 :** CD9-EC2-GST expression : insoluble and supernatant fractions, respectively, **6,8:** GST: first and second elution of bound protein from glutathione beads, respectively, **7,9:** CD9-EC2: first and second elution of bound protein from glutathione beads, respectively. **B:** Western blot of the proteins described in **(A)** detected using anti-mouse CD9 primary Ab followed by anti-rat-HRP secondary Ab (2.2.9.8).

The exposure time in Western blot was increased to visualise the protein bands and see if mCD9 multimers could be detected (Figure 5.9). The results show the presence of one small band at the higher exposure time. A relatively high level of insoluble proteins was shown after treatment of the insoluble fraction with 2M urea solution to re-solubilise the insoluble proteins.

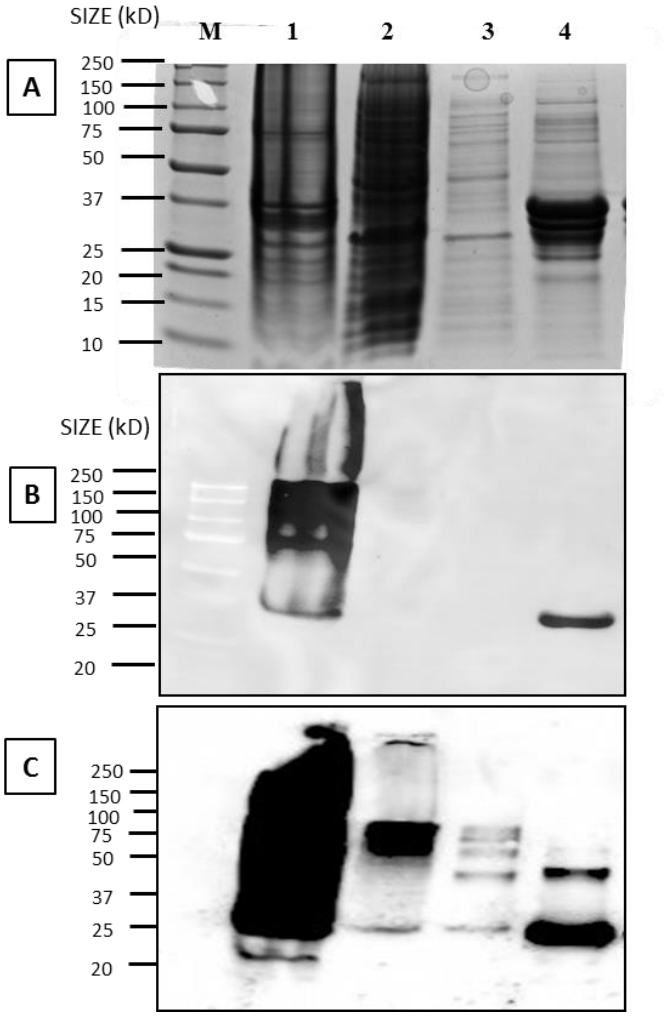

Figure 5.9: Expression and purification of t GST-mCD9-EC2 analysed by SDS-PAGE and Western blotting. Lysates from *E. coli* induced to express pGEX GST-mCD9 were used in glutathione affinity chromatography (2.2.9.4). Fractions from each step were selected for analysis by SDS-PAGE and western blot. Samples were run on 12.5% SDS-PAGE gels. **A;** Total protein stained with Coomassie stain. **B:** Western blot using anti-mouse CD9 and anti-rat-HRP secondary Abs (2.2.9.8), exposure time (5 second exposure). **C:** (9.5 second exposure) high exposure time period. **M:** Protein marker, **1:** Insoluble fraction obtained post-lysis (re-suspended with 2M urea buffer). **2:** Soluble fraction obtained post-lysis (applied to glutathione column. **3:** second wash flow through after application of soluble lysate to column, **4:** protein eluted with glutathione.

As shown by Western blotting (Figure 5.10) the purified mCD9-EC2 was successfully detected with anti-GST-HRP; however, different bands were present in the mCD9- GST preparation compared with one single band in the GST protein control. The band at 25 kD corresponds to some free GST, whereas the band at 37 kD is the expected size for CD9EC2-GST. The higher molecular weight bands could be due to the presence of CD9 multimers and this has been noted by other workers (Higginbottom et al 2003). Interestingly, the Western blot obtained using anti-mCD9 antibody (Figure 5.9) showed a clear single band of mCD9 located in correct position; this could be because the anti-GST antibody gave a stronger signal and bound more strongly to GST. Overall the results of Western blotting show the mCD9

was successfully expressed and has correct disulphide bond formation (the mCD9-EC2 was specifically identified by specific anti-mouse CD9 mAb under non-reducing condition), GST tagged and purified.

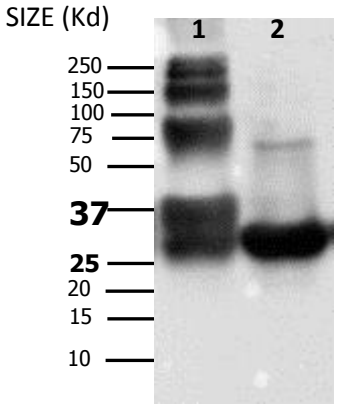

Figure 5.10: **Analysis of recombinant GST-tagged mouse CD9-EC2 protein and GST control by western Blotting after affinity purification** Samples of purified mouse CD9EC2-GST and purified GST were run under non-reducing conditions on 12.5% SDS-PAGE gels and then transferred to nitrocellulose membrane. GST was detected using primary HRP conjugated anti-GST antibody. **1**: mCD9-GST. **2**: GST.

Further investigation was carried out to determine whether there is any cross reactivity between mouse, rat and human CD9-EC2. Different primary antibodies were used targeting mouse, rat and human CD9 against mouse and human CD9-EC2 recombinant proteins (Figure 5.11). No cross reactivity between mouse and human CD9-EC2 was observed by using anti-mouse CD9 and anti-human CD9, while anti-rat CD9 reacted with human CD9-EC2 but not mouse CD9-EC2 recombinant proteins. Taken together, the results show that mouse CD9-EC2 recombinant protein was identified successfully by anti-mouse CD9 antibody and was not identified by anti-rat or anti-human CD9 antibodies.

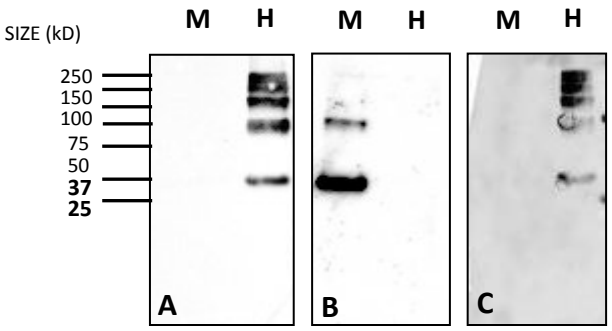

Figure 5.11: **Detection of recombinant GST-tagged mouse and human CD9-EC2 protein by Western blot using anti-human, anti-mouse and anti-rat primary Abs. A:** Western blotting using anti-rat CD9 primary Abs and anti-mouse HRP tagged secondary Abs. **B:** Western blotting using anti-mouse CD9 primary Abs and anti-rat HRP tagged secondary Abs. **C:** Western blotting by using anti-Human CD9 primary Abs and anti-Mouse HRP tagged secondary Abs. **M**, purified mouse CD9-EC2-GST, **H**, human CD9-EC2-GST. Purified recombinant proteins were run on 12% SDS-PAGE gels under non-reducing conditions prior to transfer to nitrocellulose prior to Western blotting.

5.3.4 Effect of Mouse CD9-EC2 domain in *Salmonella* Typhimurium uptake

The mouse version of CD9-EC2 recombinant protein was successfully produced and used in infection experiments. Infection by *Salmonella* NCTC12023 and LT2 strains of J774 cells pre-treated with mouse CD9-EC2 showed no significant reduction in *Salmonella* uptake compared with the GST control, using 500 and 1000nM of recombinant proteins; however a slight but significant reduction in the percentage of cells pre-treated with 1000nM CD9-EC2 with *S.* Typhimurium NCTC12023 compared with non-treated cells were observed (Figure 5.12). No significant changes were observed for the same cells treated with mouse CD9-EC2 infected with *S.* Typhimurium LT2 strain. The infected cells were analysed by the flow cytometry method as previously described (Figure 5.13).

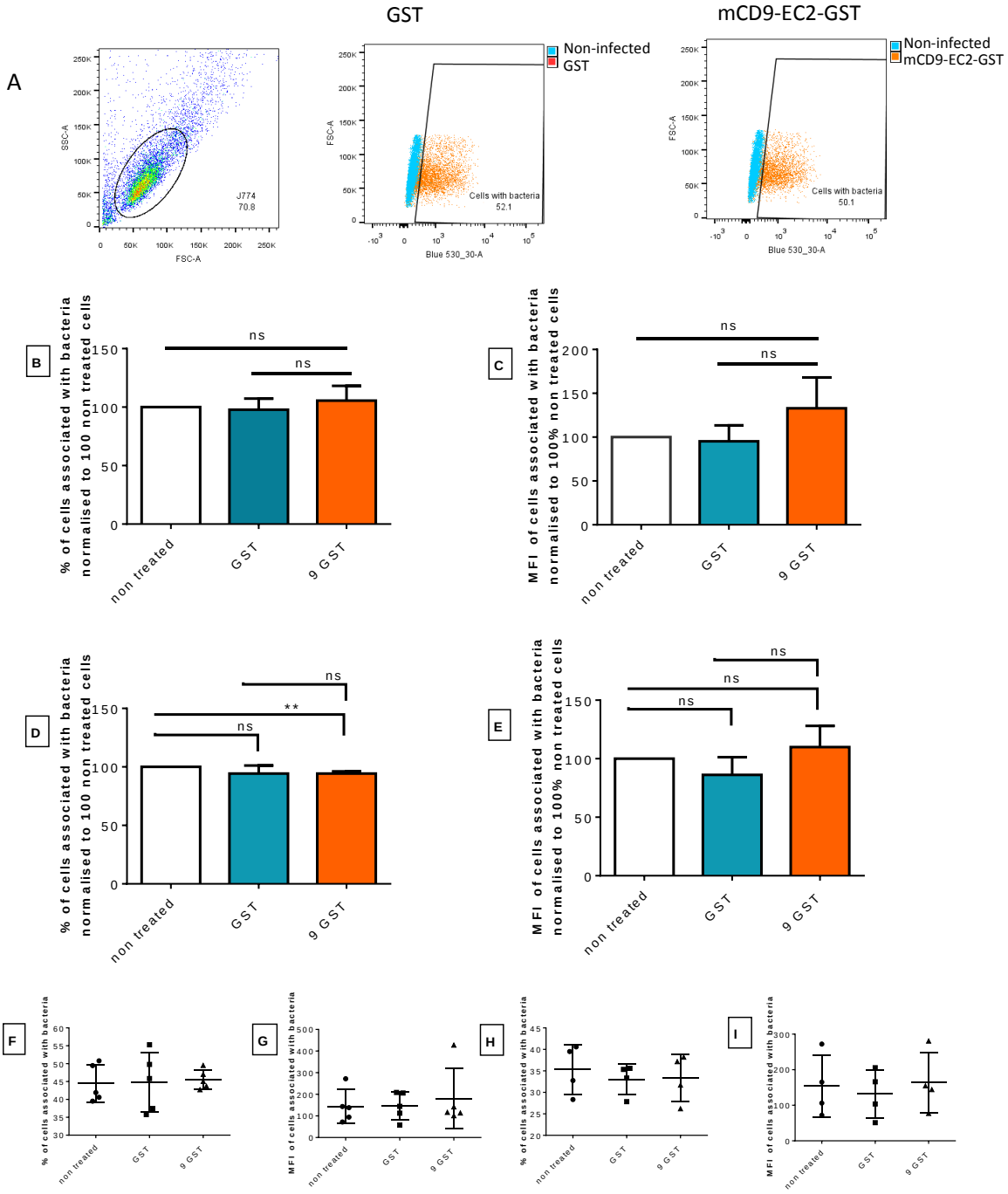

Figure 5.12: Effect of mouse tetraspanin CD9-EC2 recombinant protein on *Salmonella* NCTC12023 uptake by J774 cells analysed by flow cytometry. J774.2 cells were harvested, placed in Eppendorf tubes and pre-treated with mCD9 EC2-GST at concentration of 500nM (B and C) and 1000nM (D and E) for 60 minutes before infection with *Salmonella* Typhimurium NCTC12023 at 5 MOI for 30 minutes as described in 2.2.5.2.1. The cells-bacteria mixture was placed on a rotating mixer and was incubated at 37°C for 30 minutes. The cells were washed and fixed or fixed and permeabilised as described in 2.2.5.2.4 and stained using FITC conjugated anti-*Salmonella* polyvalent antibody. Cells were kept in 1% PFA until analysis using an LSR-II flow cytometer. **A:** Dot plot from FACS analysis showing how the values shown in B-E were obtained **B**: Percentage of J774 cells infected with *Salmonella* normalized to 100% isotype control. **C**: MFI of J774 cells infected with *Salmonella* normalized to 100% isotype control. **D:** Percentage of cells infected with *Salmonella* NCTC12023 **E:** MFI of J774 cells infected with *Salmonella* normalized to 100% isotype control. **F-I:** Raw data before normalisation. Bars describe means, while error bars describe standard error means. MFI is the median of fluorescence intensity, n=5 in **B** and **C** and n=4 in **D** and **E** in duplicate, data was analysed by Ordinary one sample T-test comparing with non-treated cells and GST treated control, significance ** $P \leq 0.01$. Ns is non-significant.

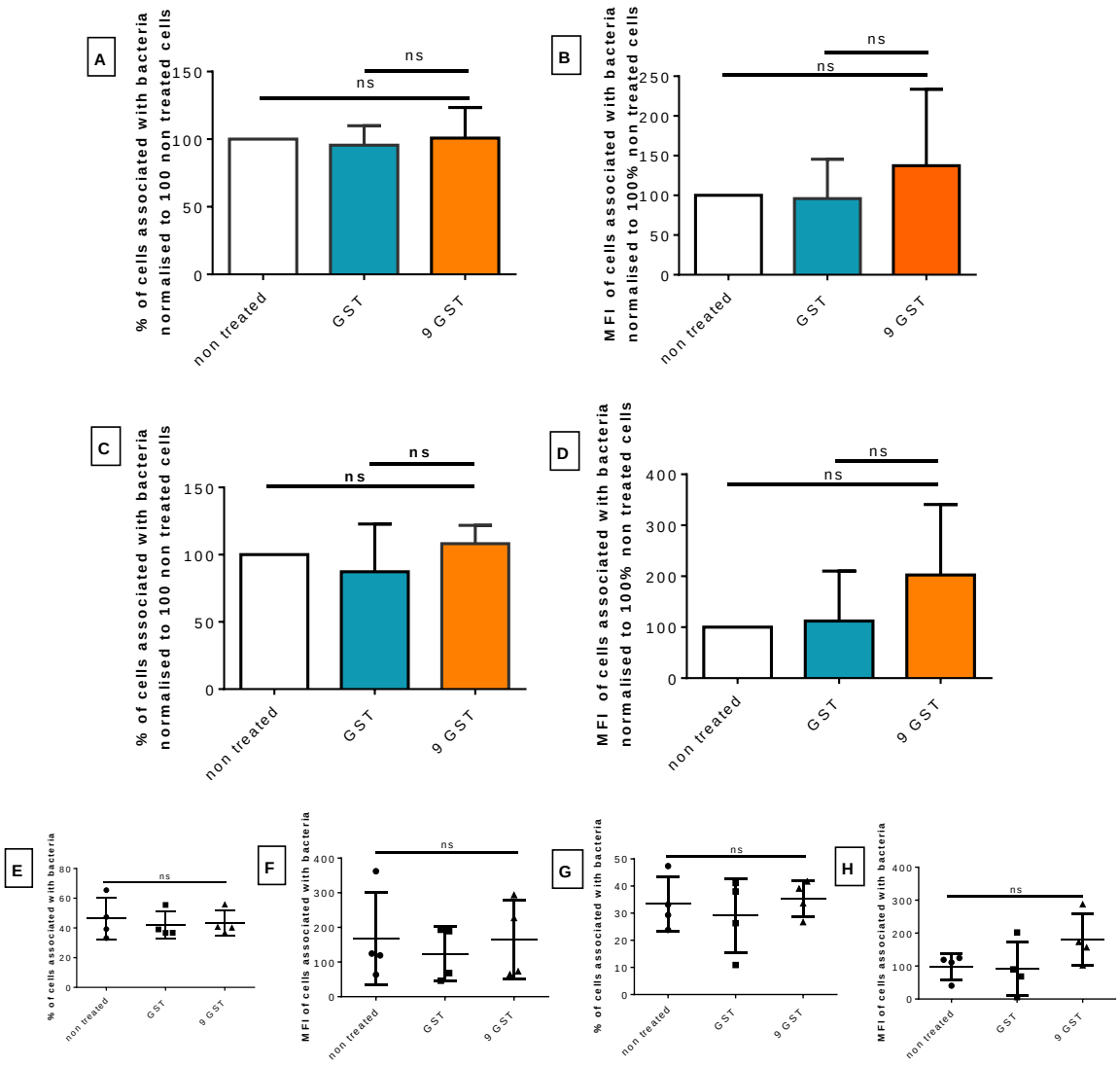

Figure 5.13: Effect of mouse tetraspanin CD9-EC2 recombinant protein on *Salmonella* LT2 uptake by J774 cells analysed by flow cytometry. J774.2 cells were harvested, placed in Eppendorf tubes and pre-treated with mCD9 EC2-GST at concentration of 500nM (A and B) and 1000nM (C and D) for 60 minutes before infection with *Salmonella* Typhimurium LT2 at 5 MOI for 30 minutes as described in 2.2.5.2.1. The cells-bacteria mixture was placed on a rotating mixer and was incubated at 37°C for 30 minutes. The cells were washed and fixed or fixed and permeabilised as described in 2.2.5.2.4 and stained using FITC conjugated anti-*Salmonella* polyvalent antibody. Cells were kept in 1% PFA until analysis using an LSR-II flow cytometer. **A**: Percentage of J774 cells infected with *Salmonella* normalized to 100% isotype control. **B**: MFI of J774 cells infected with *Salmonella* normalized to 100% isotype control. **C:** Percentage of cells infected with *Salmonella* LT2. **D:** MFI of J774 cells infected with *Salmonella* normalized to 100% isotype control. **E-H:** Raw data before normalisation. Bars describe means, while error bars describe standard error means. MFI is the median of fluorescence intensity, n=3 in **A** and **B** and n=4 in **C** and **D** in duplicate, data was analysed by Ordinary one sample T test comparing with non-treated cells and GST treated control (A-D) and graphs (E-H) data was analysed by Ordinary one-way ANOVA Holm-Sidak's multiple comparisons test, significance. ns is non-significant.

5.4 Discussion

This chapter details studies investigating the role of the large extracellular domain of tetraspanins CD9 and CD81 in *Salmonella* uptake by mouse macrophages cell line model J774. Soluble, recombinant human versions of both tetraspanins that had previously been produced in our lab were first used at two different concentrations (500nM and 1000nM) to treat J774 cells prior to *Salmonella* infection. Despite the reduction by antibodies to both tetraspanins on *Salmonella* uptake by J774 cells (chapter 4), no clear effect of either tetraspanin recombinant protein on *Salmonella* infection was seen when compared with the GST control (Figure 5.1). As mentioned previously, the recombinant EC2s used here had been shown to be correctly folded using conformation sensitive antibodies and had shown biological activity in other assays, including inhibition of adhesion of *N. meningitidis* to human HEC-1B epithelial cells (Daniel Cozens, PhD thesis, University of Sheffield 2015). Human CD9-EC2 is highly homologous with the mouse version (77%) and the recombinant protein used here was effective in inhibiting giant cell formation induced by *Burkholderia thailandensis* in J774 cells (Atiga Elgawidi, personal communication). However, species differences may be important in some functions; for example human but not mouse CD9-EC2 reduced giant cell formation in human MDMs induced by Con-A (Parthasarathy, Martin et al. 2009, Hulme, Higginbottom et al. 2014). The mechanism of action of recombinant CD9-EC2 proteins is not fully understood as yet. However, a previous study indicated that the CD9-EC2 could be associating with leukocyte integrin receptors VCAM-1 and ICAM-1 that were shown to be included in TEMs that act as a "docking structure" on endothelial cells during leukocyte firm adhesion (Barreiro, Zamai et al. 2008). Soluble GST tagged CD9-EC2 proteins inhibited leukocyte adhesion to endothelial cells and were shown to decrease the clustering of ICAM-1 and VCAM-1 receptors and interrupt their scattering pattern. It was suggested that the CD9-EC2-GST competed with the native membrane CD9-EC2 for its heterophilic and homophilic protein associations, interfering with its action (Barreiro, Zamai et al. 2008). The EC2 domain of CD9 also exhibited an inhibitory effect on adhesion mediated by LFA-1 and LFA-1 dependent leukocyte cytotoxicity. The effect of CD9 on LFA-1appeared to be through altering its aggregation (Reyes, Monjas et al. 2015). Furthermore, the human recombinant EC2 fusion proteins for CD9, CD63 and CD151 showed a strong effect in inhibiting adhesion of bacteria to human epithelial cells (Green, Monk et al. 2011). Here it was also speculated that the soluble EC2s were acting by disrupting interactions of native membrane tetraspanins in TEMs, which were proposed to form "adhesion platforms" for the bacteria. In contrast, in HCV infections, a study showed the mouse CD81 EC2-GST recombinant protein failed to suppress viral infection, whilst cells expressing the full length

mouse CD81 supported infection, leading to suggestion that CD81-EC2 lacks the ability to fully mimic the native CD81 (Flint, von Hahn et al. 2006). Taken together, it was postulated that the lack of effect of human CD9 and CD81 soluble EC2 proteins on *Salmonella* infection of J774 might be due to the fact that we were using mouse cell line, although the EC2s of human and mouse CD9 are 77% identical, while mouse and human CD81-EC2 are 80.2% identical.

To investigate if this lack of an effect was due to species differences, mouse CD9-EC2 was cloned and successfully expressed as a GST fusion protein. However, J774 cells treated with mCD9-EC2-GST prior to *Salmonella* NCTC12023 strain showed no significant effect on *Salmonella* infection relative to the GST control. The mouse CD9-EC2 produced here was detected using specific monoclonal antibodies in immunoblotting and has been shown to be biologically active in another system as it inhibited fusion of J774 cells induced by *Burkholderia thailandensis* (Atiga Elgawidi, personal communication).

As mentioned before, a previous study in our lab showed that human CD9 EC2-GST reduced *Salmonella* uptake by MDMs, whereas no reduction in uptake, was observed with anti-CD9 antibody. This difference in results could be subject to different mechanism of action between antibodies and recombinant proteins. It is known that the antibody binds directly to antigen, whilst the mechanism of tetraspanin recombinant proteins is not fully understood yet. It has been suggested that it could compete with the native proteins or disrupted its association within TEMs (Noha Hassuna, 2010, thesis). This will be discussed further in Chapter 8.

The generated mCD9-EC2-GST was expressed in *E. coli* (Figure 5-8 to 5-9) an important host system for protein expression (Baneyx 1999, Baneyx and Mujacic 2004). A relatively thick and clear band of about 35kD molecular weight (predicted size of CD9-GST) was observed with lower molecular weight band down to 26 kDa that bound with anti-GST antibody but not anti mCD9. This band corresponded to free GST that had been in some way cleaved or degraded from the full length protein or possibly production of the full length protein was terminated early in protein translation (Fanaei, PhD thesis, 2013, University of Sheffield). In addition, degradation by bacterial proteases has been observed, particularly, on misfolded or partial folded proteins (Baneyx and Mujacic 2004, Sorensen and Mortensen 2005), or aggregated insoluble forms particularly as inclusion bodies. Furthermore, proteins that have several disulphide bonds seems to be more affected (Georgiou and Valax 1996). Although the recombinant proteins was identified by a specific anti-CD9 monoclonal antibody, the recombinant CD9-EC2 protein was not glycosylated as native CD9-EC2, since *E. coli* lacks the protein glycosylation machinery present in eukaryotic cells. As mentioned previously (5.1) the glycosylation machinery from *Campylobacter jejuni* was successfully

transferred to *E. coli* expression system, and this system seems to be promising although this molecularly engineered *E.coli* system was relatively inefficient for complicated and large proteins (Jaffe, Strutton et al. 2014). Hence, the eukaryotic expression system such as mammalian cells, yeast and baculoviral system seems to be more compatible to produce proteins that need glycosylation. Amongst these more complex systems, yeast appears to be more similar to *E. coli*, yielding sufficient amounts of protein at low expense (Demain and Vaishnav 2009). Using mammalian cells seems to be more relevant for CD9-EC2 expression. Nevertheless, attempts to express GST-CD9-EC2 and other tetraspanins using Chinese hamster kidney (CHO) and mammalian human embryonic kidney cells (HEK293) by our group were unsuccessful (John Palmer, 2016, thesis, University of Sheffield). More recently, the yeast, *S. cerevisiae*, expression system was successfully used to express tetraspanin proteins and the expressed protein was aggregated in endoplasmic reticulum membrane or in yeast cells as granules or present in cell membrane (Skaar, Korza et al. 2015).

Chapter 6: *Salmonella* uptake by CD9 knockout macrophages

6.1 Introduction

Tetraspanin CD9 or Tspan29, also known as p24, is a 24 kD molecular weight protein originally identified as a protein expressed on leukocytes and the expression of p24/CD9 was also observed in normal platelets and several neoplastic cell types (Hercend, Nadler et al. 1981, Jones, Borowitz et al. 1982). An antibody to CD9 appeared to cause platelet activation (Jennings, Crossno et al. 1994).

CD9 is now known to be widely expressed on a variety of cell types and tissues (Charrin, Jouannet et al. 2014) CD9, together with CD81 and CD151, was recently shown to be highly expressed on blood and lymphatic endothelial cells (Iwasaki, Takeda et al. 2013). CD9 is also expressed on haematopoietic stem cells and different levels of CD9 expression could be used as a tool to separate haematopoietic stem cell into different sub-population (Karlsson, Rorby et al. 2013). Tetraspanin CD9 has also been shown to be expressed in different types of tumour; it is expressed in basal and squamous cell carcinomas in the skin and actinic keratosis. Different levels of CD9 expression were observed by using immuno-histochemical staining of the cell membrane and cytoplasm, with differences in CD9 localization according to the type of tumour (Ach, Ziemer et al. 2010).

CD9 has been shown to be involved in various cell functions; notably it has been shown to play an important role in mouse egg fertilization (Rubinstein, Ziyyat et al. 2006), and described in more detail in Chapter 1.

6.1.1 CD9 and partner proteins

Partner proteins that interact directly with CD9 are described in Yanez-Mo M., et al. 2009. Of note, integrins are known to be a close CD9 partner (Radford, Thorne et al. 1996, Halova, Draberova et al. 2013). CD9 was shown to be associated directly to β_2 integrin (LFA-1) in a variety of leukocytes (Reyes, Monjas et al. 2015), and with α_3, α_5 integrins (Hirano, Higuchi et al. 1999), β1integrin (Kohmo, Kijima et al. 2010) and α6 β1 integrins (Park, Inoue et al. 2000). It has been shown the CD9 and CD81 associated directly with α3β1 integrin without needing this integrin to be connected with other tetraspanins. As the integrin β1 is linked directly with the membrane cofactor protein, CD46, this protein has been detected as an indirectly associated partner to CD9 (Lozahic, Christiansen et al. 2000, Gustafson-Wagner

and Stipp 2013). Tspan-4 (previously known as NAG-2) also associates with CD9 and CD81 in an interaction that also includes α6β1 integrin protein (Tachibana, Bodorova et al. 1997).

A direct and strong interaction of CD9 and CD81 has been observed with the human EWI-2 Ig superfamily protein (which shows 91% homology with mouse EWI-2 protein) (Stipp, Kolesnikova et al. 2001). A clear association with another Ig superfamily member (prostaglandin F2α receptor regulatory protein (FPRP), also known as CD9P-1 or EWI-F) with CD9 and/or CD81 also has been reported (Charrin, Le Naour et al. 2001, Stipp, Orlicky et al. 2001).

CD9 also interacts with the metalloprotease, ADAM17, and negatively regulated the sheddase enzyme (Gutierrez-Lopez, Gilsanz et al. 2011). ALCAM also associated with CD9 in surface protein complexes in leukocytes that also contain ADAM17/TAGE (Gilsanz, Sanchez-Martin et al. 2013). Furthermore, LR11 (low density lipoprotein receptor family candidate) mediated shedding by ADAM17 was shown to be modulated by tetraspanin CD9 in different leukocyte tumour cell lines, where CD9 suppresses LR11 shedding mediated by ADAM17 (Tsukamoto, Takeuchi et al. 2014). By using co-immunoprecipitation, an association between CD9 and CD10, another metalloprotease, has recently been identified. The C- terminal region of CD9 and EC2 domains were required for the CD9 -CD10 association, and CD9 was shown to enhanced the amount of release of CD10 in exosomes (Mazurov, Barbashova et al. 2013).

A physical association of CD9, CD63 and CD81 with c-kit receptor tyrosine kinase has been observed (Anzai, Lee et al. 2002) and it was suggested that the tetraspanins may modulate its activity. As mentioned in Chapter 1, the tetraspanin proteins have also been shown by co-immunoprecipitation to be associated with protein kinase C (PKCs) and may recruit PKC to integrins. In Jurkat T cells, PKCα has been shown to be strongly associated with CD9, CD81 and CD82 (Zhang, Bontrager et al. 2001).
The type 2 scavenger receptor, CD36, has also shown to be directly associated with CD9 in platelets (Miao, Vasile et al. 2001) and macrophages (Huang, Febbraio et al. 2011), and integrins were also involved in this interaction.

6.1.2 CD9 Knockout mouse macrophages

The CD9 gene was knocked out at the embryonic stage to generate CD9 +/- mice by the Boucheix researcher group (Le Naour, Rubinstein et al. 2000). Following the method that was described in (Capecchi 1989), the CD9 gene was disrupted by CD9 gene targeting in embryonic stem cells in which the CD9 promoter and exon-1 were replaced by a G418

(Neomycin) resistance gene and southern blotting was used to confirm this Flow cytometry and immunohistochemistry analysis confirmed absence of surface CD9 in homozygote mice (Le Naour, Rubinstein et al. 2000). J2 transforming retrovirus (Cox, Mathieson et al. 1989) was used to generate the immortal CD9KO and wild type macrophage cell lines used in the present study by Ha and co-workers. Briefly, bone marrow derived macrophages (BMDM) were collected and purified from the femur and tibia of CD9-KO and wild type C5BL/6 mice and transfected with J2 transforming retrovirus to generate immortal cell lines. The CD9KO and corresponding WT control were kindly donated by Dr. Gabriela Dveksler, Dept. Pathology, Uniformed Services University of Health Sciences, Bethesda, MD, US (Ha, Waterhouse et al. 2005).

6.1.3 Microarray analysis method

Microarray analysis of mRNA provides analysis of thousands of gene expression sets, leading towards a better understanding of cell physiology. This technique has been used to investigate different diseases and tumour mechanisms, with support provided from bioinformatics data bases and statistical analysis (Margalit, Somech et al. 2005, Jeffery, Higgins et al. 2006).

6.2 Aims

Since CD9 antibodies appeared to show a significant effect on *Salmonella* uptake in J774 cells (Chapter 4), it was of interest to examine uptake in a macrophage cell line derived from a mouse in which the CD9 gene had been knocked out, with the corresponding wild macrophage cell line as a control (Ha et al, 2005).Therefore the aims of this chapter were to investigate the uptake of *Salmonella* Typhimurium NCTC and LT2 strains by CD9-KO mouse macrophages compared with corresponding WT cells. In addition, the expression of tetraspanins by these cells was studied. Differences in the expression of a wide range of proteins at the mRNA level in CD9-KO and WT mouse macrophages control were investigated by microarray analysis. Attempts were also made to rescue the CD9-/- macrophages and to establish a stable macrophage cell line expressing GFP-CD9.

6.3 Results

6.3.1 Tetraspanin protein expression in CD9KO and wild type mouse macrophages

6.3.1.1 Western blot analysis

Initially, Western blotting was used to verify that the macrophage cell line derived from the CD9KO mouse did not express CD9 protein (Figure 6.1). As expected, no CD9 expression was detected in lysates prepared from CD9-KO mouse macrophages whilst CD9 protein band (at 24kd) was clearly detected in WT mouse macrophages.

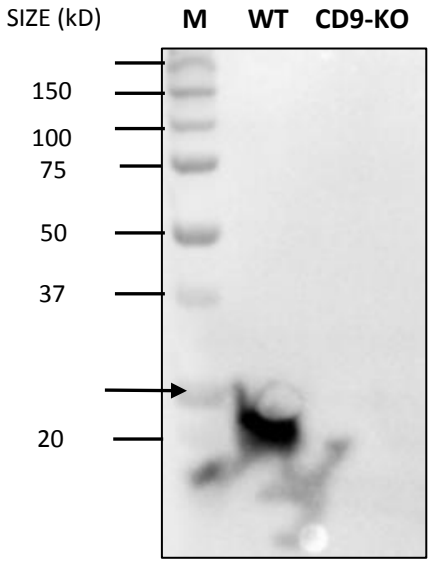

Figure 6.1: Western blot analysis of lysates prepared from CD9 KO mouse macrophages and WT control. Cells were lysed with cell lysis solution (2.2.7) and the lysate was run on 12.5% SDS gels under non-reducing condition and transferred to nitrocellulose as described in 2.2.9.6. The blot was developed using rat anti-mouse CD9 primary Ab followed by anti-rat-HRP conjugated secondary Abs as described in 2.2.9.8. **M**: Protein marker (Table 2.1).

6.3.1.2 Immunofluorescence Microscopy analysis

Immunofluorescence microscopy was also performed on the CD9KO cells and corresponding WT mouse macrophages. As expected, no surface expression of CD9 in CD9KO cells was observed compared with high surface expression of CD9 in WT mouse macrophages. In addition, low expression of CD63 in CD9KO compared with WT control was observed. CD81 showed little surface expression on either cell type, possible due to sensitivity of the epitope to the fixation process (Figure 6.2). These results are further confirmed by FACS as described in the following section.

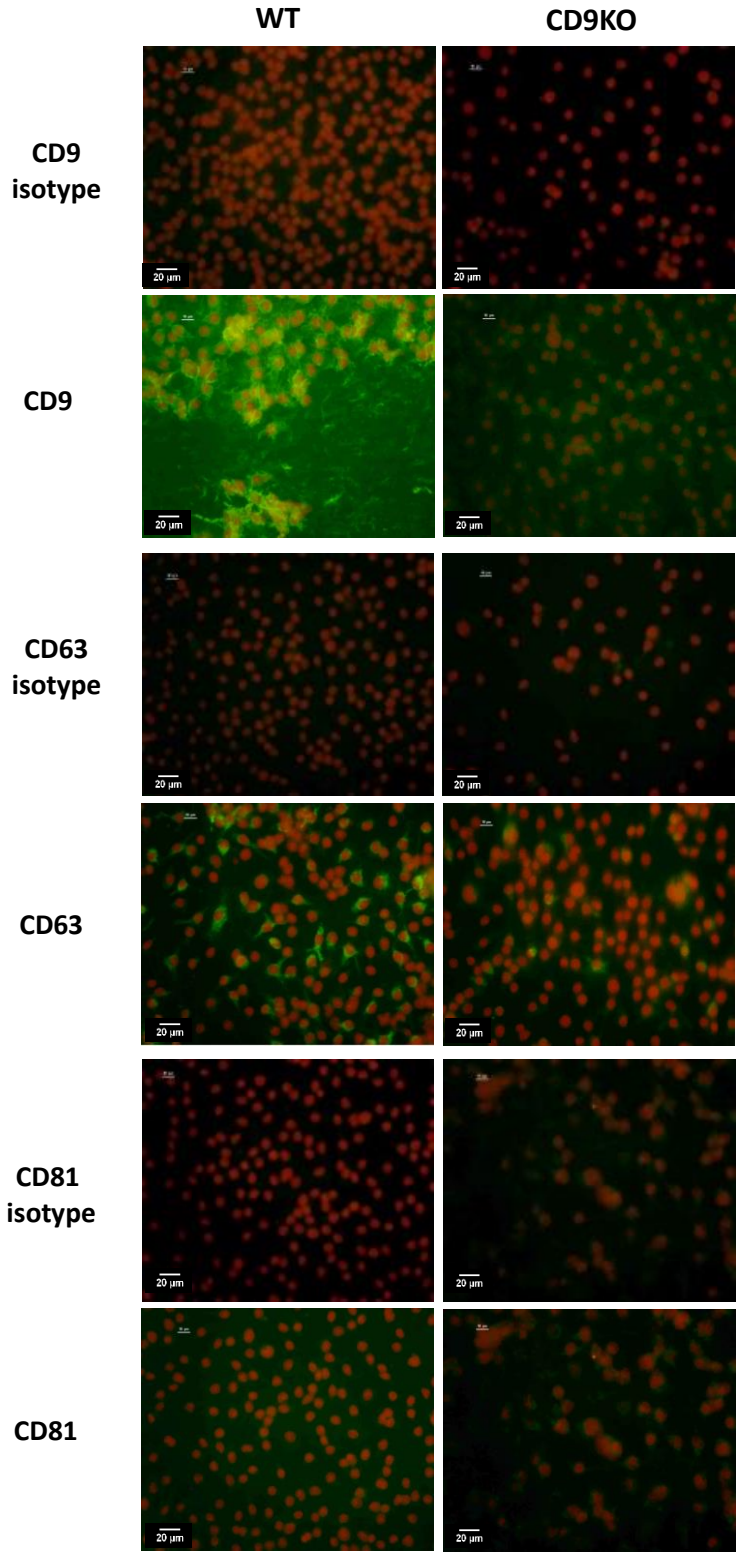

Figure 6.2: Immunofluorescence microscopy of mouse CD9 -/- and WT control macrophages. Cells were cultured on chamber slides and fixed as described in 2.2.4.1, then stained with primary monoclonal antibody (mAbs) anti CD9, anti CD63 and anti CD81 or appropriate isotype controls at 10 µg/ml as described in 2.1.7.1. The secondary Abs was a FITC-conjugated anti-Rat Ab (for CD9 and CD63) and anti-Hamster Abs (for CD81primary anti-tetraspanin antibodies). Nuclei were counter-stained with propidium iodide, Rat IgG2a and IgG2b were used as an isotype controls for CD9 and CD63 respectively, hamster IgG was used as a control for CD81. These images were obtained by using the 40x objective.

6.3.1.3 Flow cytometry (FACS analysis)

Immunofluorescence microscopy showed a clear difference in CD9 expression in WT and CD9 KO cells, but the differences in CD63 and CD81 levels were less clear. Therefore, FACS analysis was used to investigate total levels of tetraspanins (permeabilised cells) and cell surface levels (non-permeabilised) cells. As shown in figure 6.3, high expression of CD9 was observed in WT cells compared with CD9KO cells. Most of the CD9 is found on the cell surface as there is little difference in levels between permeabilised and non-permeabilised cells. Both CD9KO and WT show considerable CD63 expression in permeabilised cells by FACS, as expected since CD63 is known to predominantly associate with intracellular vesicles. Relatively low, but not significantly, expression of CD63 was observed in CD9KO cells. Significant changes were observed in CD81 expression between CD9KO and WT mouse macrophages, in both permeabilised and non permeabilised cells; the percentage of positive cells and the median of fluorescent intensity (MFI) were significantly lower in CD9KO compared with WT control cells. To summarise, CD9 and CD81 were highly expressed on cell surface of WT mouse macrophages, whereas most of the CD63 was intracellular. CD81 was shown to be significantly downregulated in the absence of CD9.

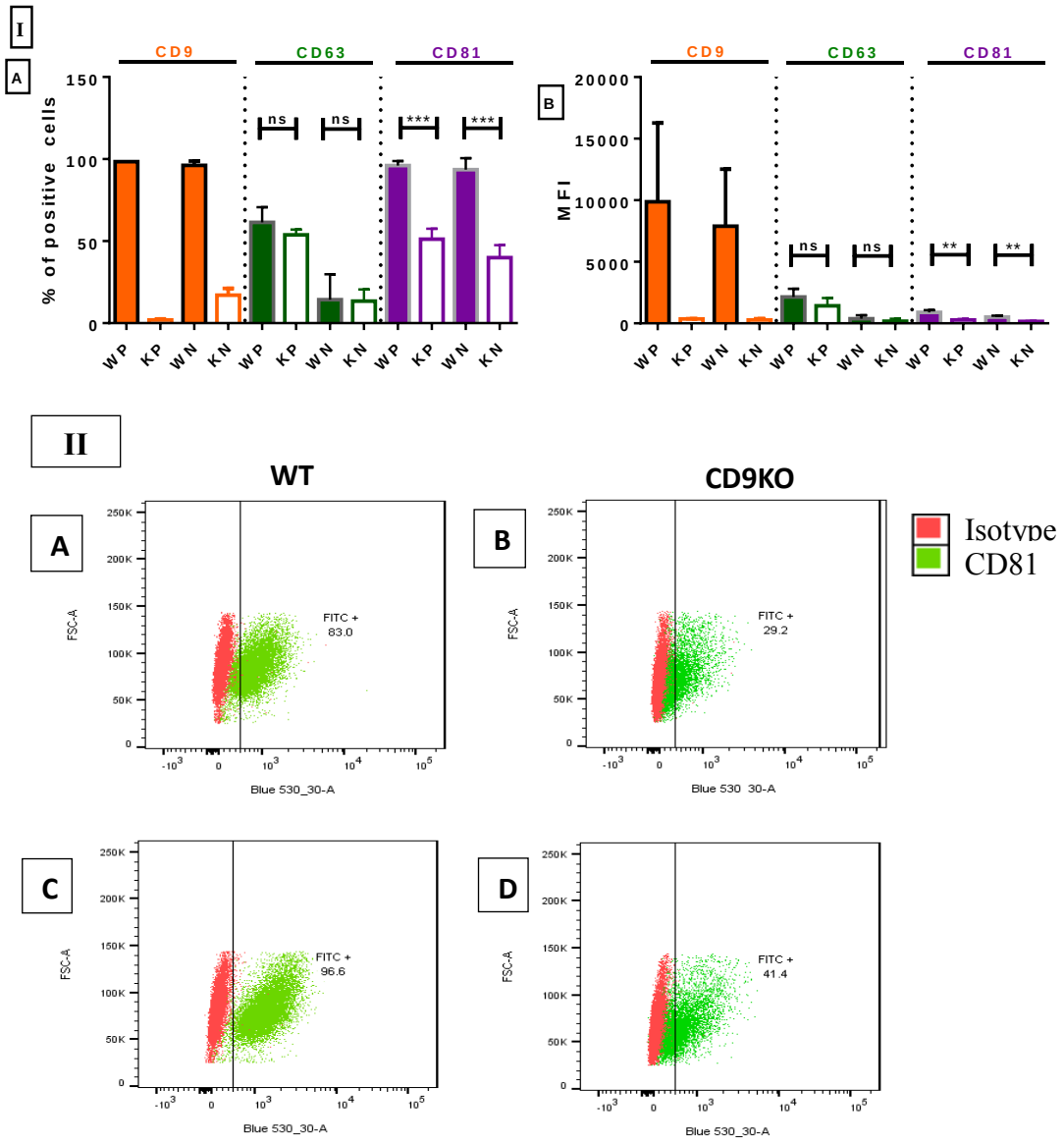

Figure 6.3: Tetraspanin expression in CD9KO and WT mouse macrophages by flow cytometry: The primary monoclonal antibody (mAbs) used were isotype (control) anti CD9, anti CD63 and anti CD81. The secondary Abs was a FITC-conjugated anti-Rat Ab (for CD9 and CD63) and anti- Hamster Abs (for CD81, **I:** Shows tetraspanins expression in CD9KO and WT control (isotype control values were subtracted) **A:** Percent of positive cells expressed tetraspanins .**B:** MFI of tetraspanins expression. Bars describe means, while error bars describe standard error means. **II**: Shows the raw FACS data in the form of dot plots for isotype control and anti-CD81 that were used to obtain the values shown in (**A** and **B**), line segregate between negative and positive cells, **A and B:** cells were stained without permeabilisation**. C and D:** cells were stained with permeabilisation. **W** and **K** reveals to wild type and CD9-KO mouse macrophage respectively, **P** and **N** reveals to permeabilised and non-permeabilised respectively)**.** n=2 (CD9) and n=3 (CD63 and CD81) in duplicate, the significant difference was analysed by T test compared between means for each sample. *** $p \leq 0.001$, ** $p \leq 0.01$, * $p \leq 0.05$ and ns is non-significant.

6.3.2 *Salmonella* uptake by wild type and CD9-KO mouse macrophages

6.3.2.1 Immunofluorescence Microscopy

Using the immunofluorescence microscopy assay (2.2.5.1), no difference in infection of the CD9 KO macrophage cell line was shown for the NCTC12023 strain (at MOIs of 10 and 30) compared to the wild type in any of the categories used to assess infection (Figures 6.4 and 6.5). However, the CD9 KO macrophages showed some increase in the percentage of cells associated with the LT2 strain at an MOI of 30 and this became significant after the data was normalised to 100% WT cells control (Figure 6.4). No significant differences were apparent in the other parameters used to assess infection after such normalisation (data not shown). Interestingly, the LT2 strain was less associated with WT macrophages than the NCTC12023 strain and this became significant at 10 MOI (Figure 6.5 A and B).

6.3.2.2 Flow cytometry method

Since there appeared to be a slight but significant difference in infection of CD9KO and WT mouse macrophages by the LT2 strain, infection was also analysed using the flow cytometry method, (2.2.5.2), as this method is more objective than microscopy. After optimisation, 5 MOI for 30 minutes infection time was chosen for these experiments since this gave a sufficient number of infected cells. As noted previously in Chapter 4, it seems that a lower MOI is needed when the cells are infected in suspension compared to when they are adherent to coverslips. Again, no significant differences were observed in CD9KO compared with WT control for the NCTC12023 strain. However, CD9KO cells again were more susceptible to *Salmonella* infection with the LT2 strain (Figure 6.6). Also, as noticed in previously (Figure 6.4 and 6.5), the LT2 strain was significantly less associated with macrophages than the NCTC12023 strain (Figure 6.6).

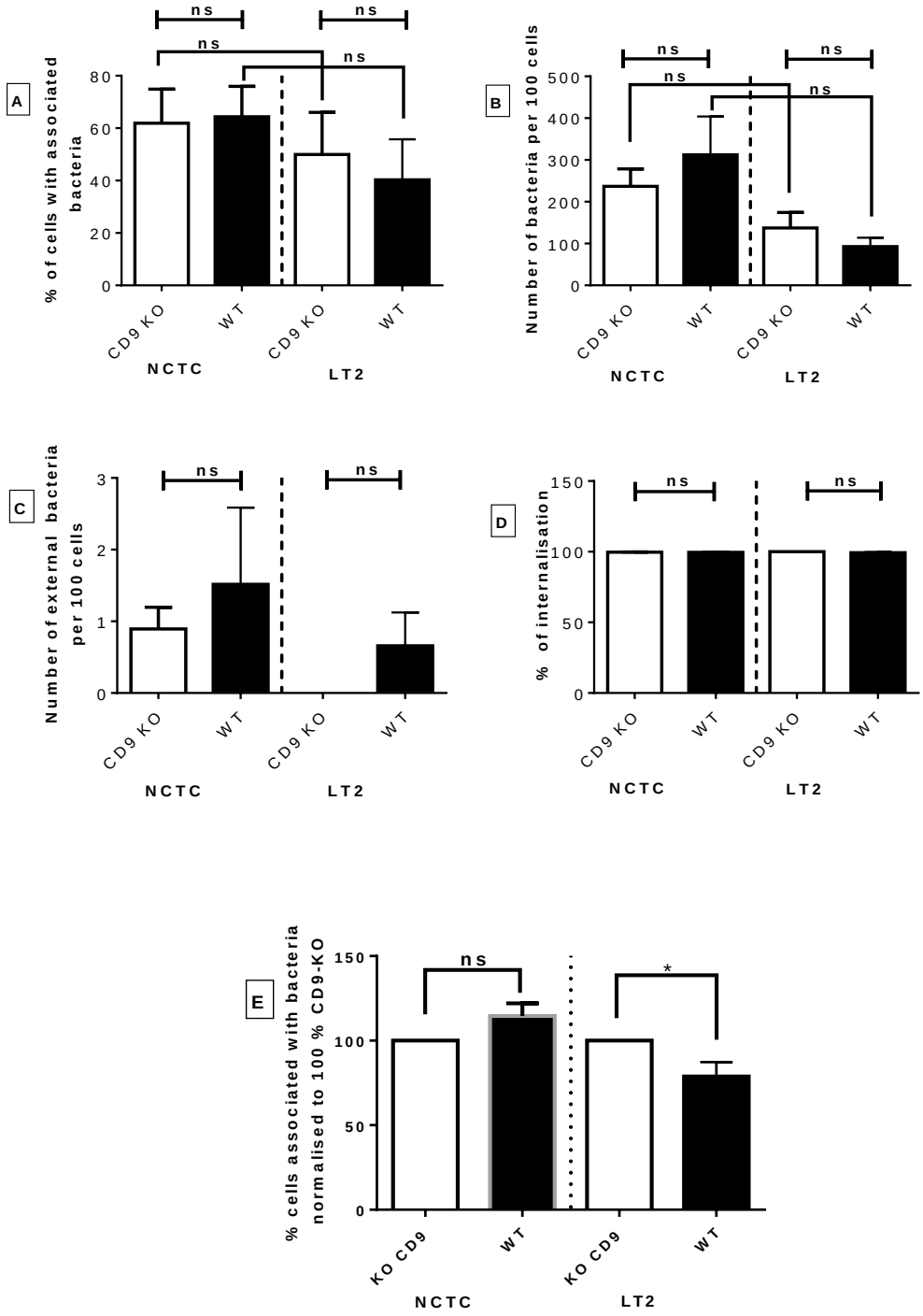

Figure 6.4: *Salmonella* Typhimurium uptake by CD9 KO (-/-) and wild type mouse macrophage at 30 MOI analysed by fluorescent microscopy. Cells were infected with *S.* Typhimurium strains NCTC12023 and LT2 for 30 minutes as described in 2.2.5.1.3. **A:** Percentage of cells with associated bacteria. **B:** Number of bacteria per 100 cells **C:** Number of external or attached bacteria per 100 cells. **D:** The percentage of internalized bacteria **E:** Percentage of cells with associated bacteria normalised to 100 CD9-KO cells, Bars describe means, while error bars describe standard error .n=3, performed in triplicate Data were analysed by T-test **(A-D)** and One Sample T-test in **E**, * $p \leq 0.05$ and ns is non-significant.

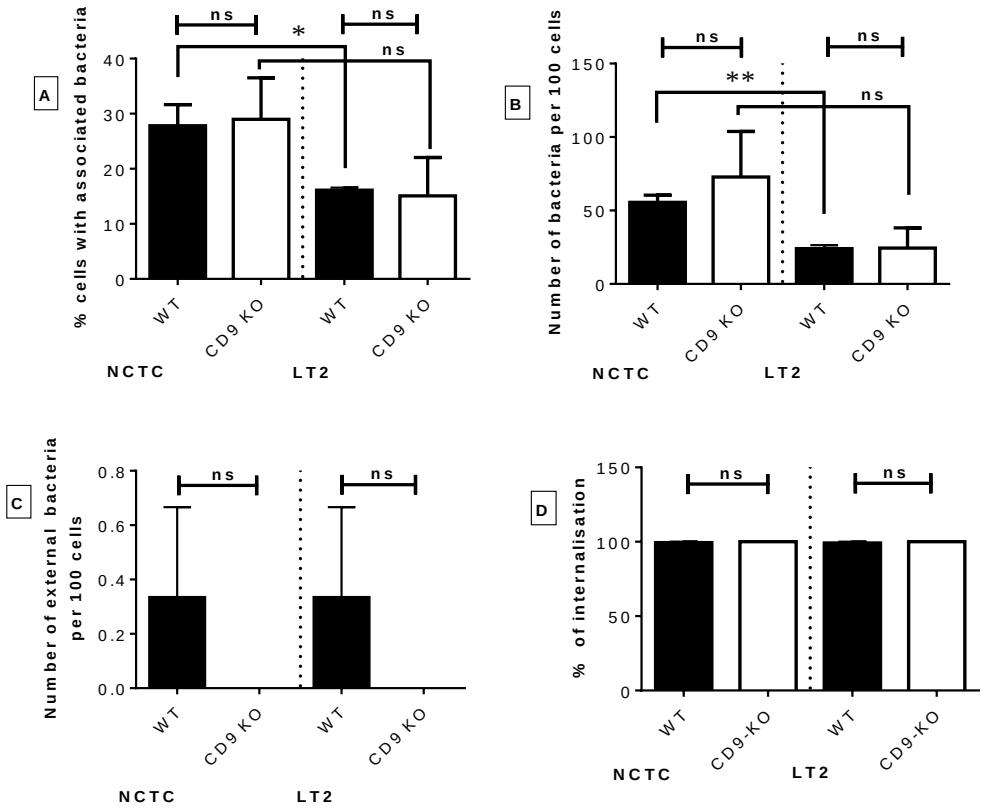

Figure 6.5: *Salmonella* Typhimurium uptake by CD9 KO (-/-) and wild type mouse macrophage at 10 MOI analysed by fluorescent microscopy. Cells were infected with *S.* Typhimurium strains NCTC12023 and LT2 for 30 minutes as described in 2.2.5.1.3. **A:** Percentage of cells with associated bacteria. **B:** Number of bacteria per 100 cells **C:** Number of external or attached bacteria**. D:** The percentage of internalized bacteria. Bars describe means, while error bars describe standard error .n=3, performed in triplicate. Data were analysed by T-test, ** $p \leq 0.01$, * $p \leq 0.05$ and ns is non-significant.

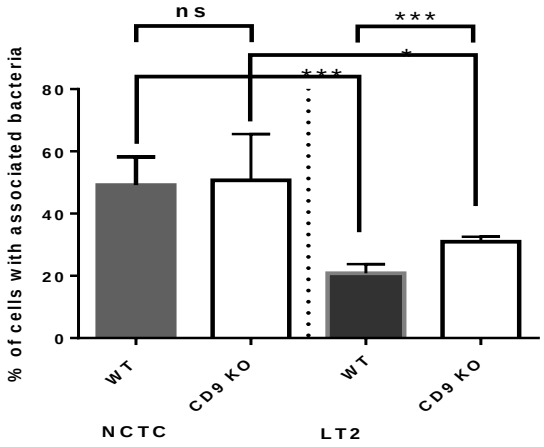

Figure 6.6: *Salmonella* Typhimurium uptake by CD9 KO (-/-) and wild type mouse macrophages analysed by flow cytometry. Cells were infected at 5 MOI with *S.* Typhimuriu*m* strains NCTC12023 and LT2 for 30 minutes as described in 2.2.5.2 and analysed using an LSRII flow cytometer, capturing 10,000 events per sample. The graph shows percentage of cells with associated bacteria. Bars describe means, while error bars describe standard error means. n=7 in **NCTC** and n=4 in **LT2** in duplicate. Data were analysed by T-test, ***$p \leq 0.001$, * $p \leq 0.05$ and ns is non-significant.

As expected, anti-CD9 antibodies showed no effect on infection of CD9KO macrophages, but inhibited infection of WT cells significantly (Figure 6.7). Overall the results of this section show *Salmonella* uptake in CD9KO mouse macrophages differed compared with WT, but this was dependent on the *Salmonella* strain. Surprisingly the CD9KO cells appeared more susceptible to the LT2 strain.

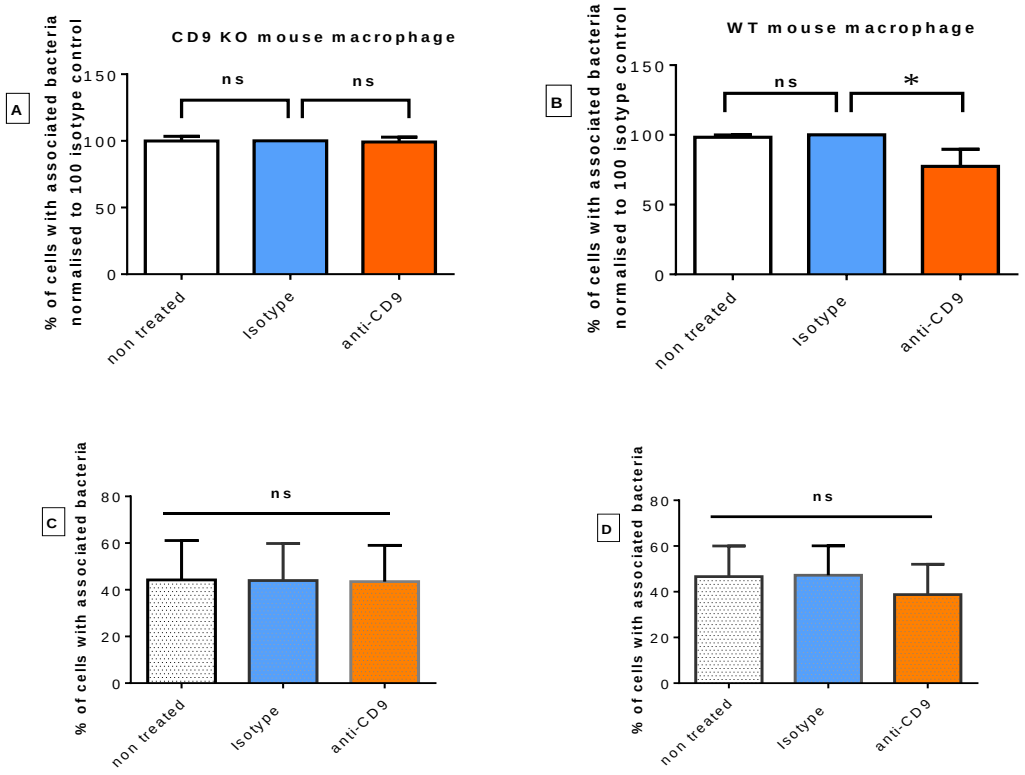

Figure 6.7: Effect of anti-CD9 antibodies on *Salmonella* Typhimurium NCTC12023 uptake by CD9 KO (-/-) and wild type mouse macrophages. Cells were treated with rat IgG2a (isotype control) or anti-CD9 antibody at 10µg ml^{-1} for 60 minutes prior to infection with an MOI of 5 for 30 minutes and analysed by flow cytometry as described in Figure 6.6. **A:** Percentage of CD9 KO cells infected with NCTC12023 (normalised to isotype control). **B:** Percentage of WT cells infected with NCTC12023 (normalised to isotype control). **C and D**: Raw data for **A** and **B** respectively. Bars describe means, while error bars describe standard error. n=4 in duplicate, the data was analysed by One Sample T-test (A and B) and One way ANOVA (C and D), * $p \leq 0.05$ and ns is non-significant.

6.3.3 CD9-KO and WT mouse macrophages RNA microarray analysis

As mentioned in 6.1, microarray analysis is widely used to investigate the broad spectrum of gene expression in different types of cells including mouse macrophages (Eskra, Mathison et al. 2003, Cheng, Liu et al. 2010). Since there appeared to be changes in expression of proteins other than CD9 in the KO macrophage cell line, it was of interest to compare mRNA expression between the cell lines. It was thought that this might also give information on the apparent differences in susceptibility of the CD9KO and wild type macrophages to infection by the LT2 strain of *Salmonella*. Microarray analysis was carried out on RNA extracted from

each cell line in three independent experiments. The expression profiles of 45101 genes for CD9 KO cells were compared with that of WT mouse macrophages; this work was carried out in collaboration with Dr. Paul Heath, Sheffield Institute for Translation Neuroscience (SITraN), University of Sheffield.

6.3.3.1 RNA Quality

Testing RNA purity and integrity was carried out in all samples of extracted RNA as this can affect the efficiency of RNA amplification. RNA quality was analysed by using Agilent RNA 6000 Nano Kit as described in 2.2.11.2. The results that were obtained for extracted RNA for all 6 samples (3 preparations from CD9KO and WT cells) showed high integrity with an RNA integrity number (RIN) of greater than 9.9 in all cases (Schroeder, Mueller et al. 2006). The RNA was of a sufficiently a high concentration and the level of contaminants was very low (Figure 6.8). The electropherograms indicate that the 28S rRNA was full length in a single peak that corresponds to high integrated non-degraded RNA and double the intensity of 18S rRNA band. Based on the 28S and 18S rRNA ratio, the mRNA was likely to be intact and full length.

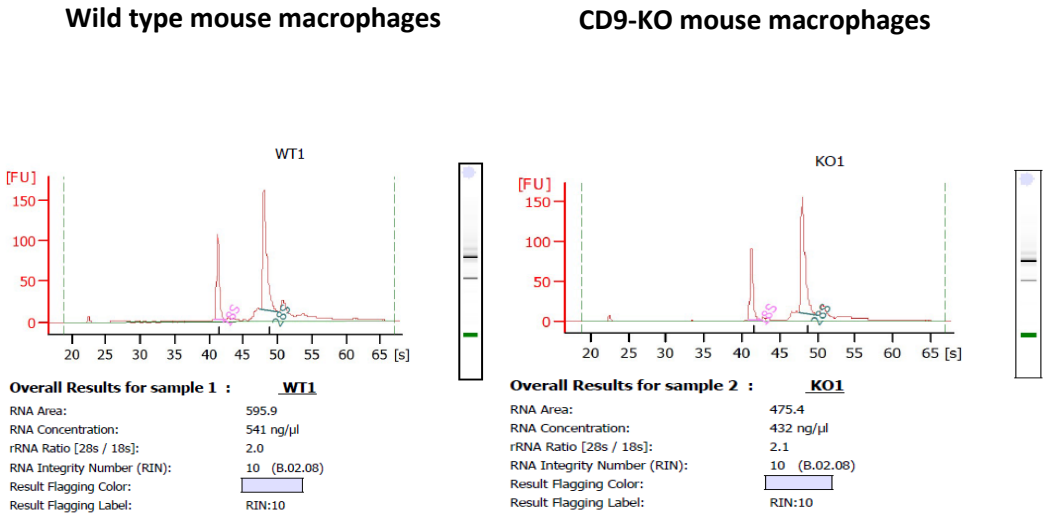

Figure 6.8: Analysis of total RNA extracted from mouse CD9-KO and WT macrophage cell lines. Electropherograms were obtained using the Agilent RNA 6000 Nano Kit. Graphs show the total RNA analysis from CD9 KD and WT cells. The total RNA concentration and integrity are shown in the tables attached to the graphs. The two small peaks to the left of the graphs reveal to marker used, while the two large peaks reveal 18S and 28S rRNA.

6.3.3.2 Comparison of gene expression in CD9-KO and WT mouse macrophage cell lines

The GenChip® Mouse Genome 430 2.0 arrays from Affymetrix were used to examine gene expression in the two macrophage cell lines. The profiles showed some significant consistent

changes in expression for CD9-KO cells compared with WT control. By using QLUCORE OMICS explorer software to analyse and cluster the variable gene expression, principle components analysis (PCA) of all three experiments (three arrays of WT and three arrays of CD9-KO cells) demonstrated a clear separation between the two groups of samples. The variables of all three arrays of WT and the three arrays of CD9-KO showed high interrelationship with 77% in PCA analysis (2.2.11.5) (Figure 6.9). At a significance value of $P \leq 0.05$, 1037 genes show either higher expression (252 genes) or lower expression (787 genes) in CD9-KO compared with WT cells. Furthermore, at $P \leq 0.01$, 194 genes showed changes in expression, with up-regulation (47 genes) or down-regulation (147 genes) in CD9 KO macrophages compared to WT. (Table 6.1). 9 genes were either downregulated in CD9KO (6 genes) or upregulated in CD9KO (3 genes) compared with WT considering 1.5 fold-changes and $p \leq 0.05$.

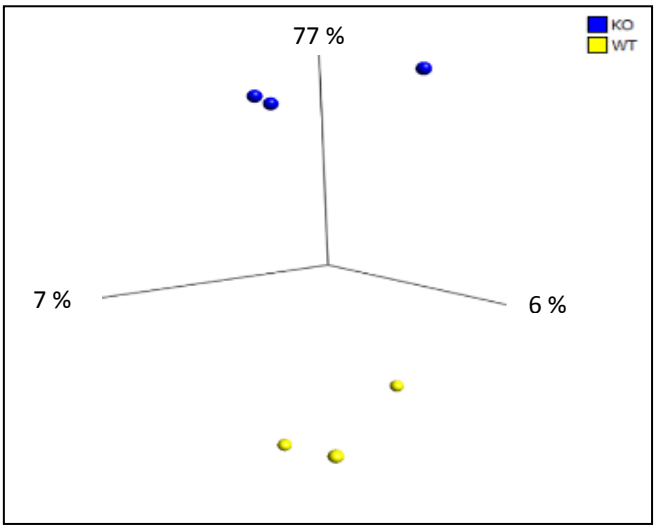

Figure 6.9: Principle Component Analysis (PCA) of mRNA microarray expression results. The analysis was performed using QLUCORE OMICS explorer in RMA normalised data. The blue and yellow spheres show 3 separate arrays for CD9-KO and WT mouse macrophages, respectively. The PCA of the variables was analysed by multi comparison T-test compare the variable of three separate arrays of CD9-KO cells with WT mouse macrophage cells control. n=3, $p \leq 0.05$.

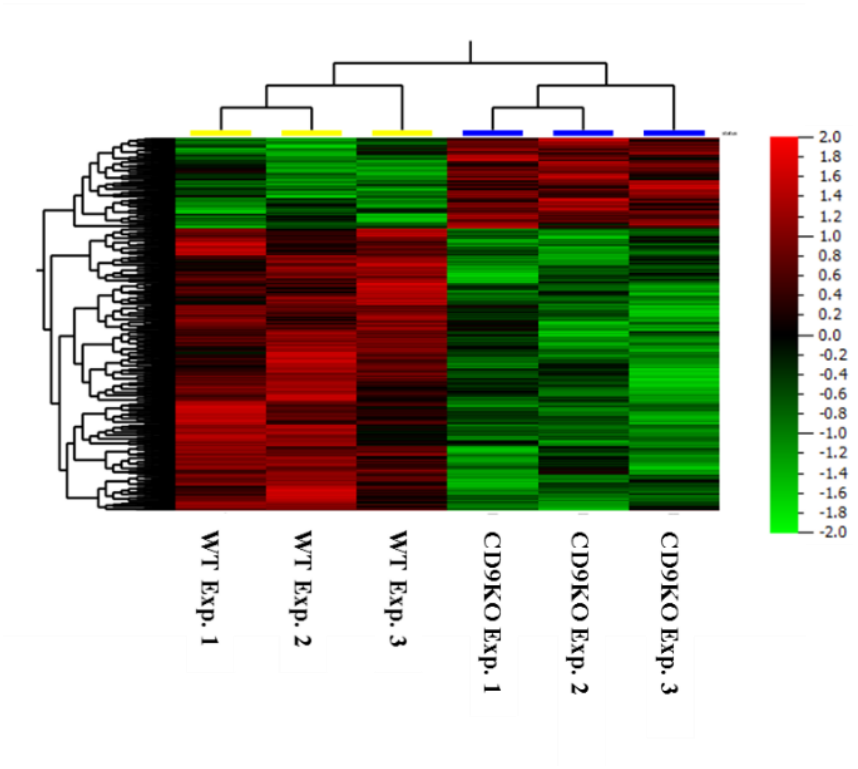

Figure 6.10: The hierarchical clustering and heat map of gene expression of CD9-KO and WT mouse macrophage cell lines. Hierarchical cluster analysis was performed using 6 arrays (3 for CD9 KO and 3 for WT). The data were analysed using QLUCORE OMICS explorer on RMA normalised data. Red indicates upregulated gene expression and green indicates downregulated gene expression.

Table 6.1: Summary of significant differences in gene expression between CD9 KO and WT macrophage cell lines.

		Two groups comparison by WT mouse macrophages			
Fold changes	**P Value**	**Number of genes analysed**	**Number of genes with changed expression**	**Number of up-regulated genes**	**Number of down-regulated genes**
Fold changes 1	**P ≤ 0.05**	**45101**	**1037**	**252**	**787**
	P ≤ 0.01		**194**	**47**	**147**
	P ≤ 0.001		**19**	**6**	**13**
Fold changes 1.5	**P ≤ 0.05**		**9**	**3**	**6**

Genes whose expression was up-regulated or down-regulated in CD9KO compared with WT mouse macrophages were analysed using QLUCORE OMICS explorer, n=3, multiple comparison T test. The fold-change in gene expression is also shown.

Table 6.2 describes genes that show a 1.5 fold change in expression between CD9KO and WT macrophage cell lines at $p \leq 0.05$. As expected, CD9 is significantly downregulated in CD9KO macrophages, along with other genes including inactive X specific transcripts (Xist), cyclin-dependent kinase inhibitor 2A (Cdkn2a), sphingomyelin phosphodiesterase acid like 3A (Smpdl3a).

Table 6.2: List of genes with significant changes in expression at p ≤ 0, 05 and Fold changes greater than 1.5 (log2).

Cluster ID	Gene Symbol	Gene Title	Mean (gene expression (log 2) WT	Mean (gene expression log 2) CD9KO	p-value (T test)	differences
1427263_at	**Xist**	inactive X specific transcripts	8.771663333	3.536686667	0.00340875	**expression in CD9-KO Low**
1416066_at	**Cd9**	CD9 antigen	11.92996667	6.679943333	0.009066419	
1436936_s_at	**Xist**	inactive X specific transcripts	10.27028667	5.590026667	0.014852971	
1427262_at	**Xist**	inactive X specific transcripts	7.97583	3.265586667	0.02585763	
1416635_at	**Smpdl3a**	sphingomyelin phosphodiesterase, acid-like 3A	9.593803333	5.10127	0.028010708	
1450140_a_at	**Cdkn2a**	cyclin-dependent kinase inhibitor 2A	10.62583	5.919296667	0.041311694	
1437534_at	**--- ***	---	3.71228	6.01991	0.039206261	**High expression in CD9-KO**
1423331_a_at	**Pvrl3**	poliovirus receptor-related 3	4.157093333	6.969106667	0.045487168	
1430567_at	**Spink5**	Serine protease inhibitor kazal-type 5	4.53532	7.037873333	0.045806818	

Genes whose expression was up-regulated or down-regulated in CD9KO compared with WT mouse macrophages were analysed using QLUCORE OMICS explorer, multiple comparison T test, n=3. The mean of WT and CD9-KO values correspond to normalised expression levels expressed as log to the base 2 (log 2).* Mouse hypothetical protein full sequence cDNA target probe identified from whole body cDNA.

Tables 6.3 and 6.4 show the top 20 genes with lower and higher expression in CD9KO cells compared with WT control, respectively.

Table 6.3: List of top 20 downregulated genes in CD9KO compared with WT mouse macrophages.

Gene id	Gene Symbol	Gene Title	p-value (T test)	Fold change	Mean WT (log 2)	Mean CD9 KO (log 2)
1427263_at	**Xist**	inactive X specific transcripts	0.0034088	0.410772	8.7716633	3.5366867
1427262_at	**Xist**	inactive X specific transcripts	0.0258576	0.431587	7.97583	3.2655867
1416635_at	**Smpdl3a**	sphingomyelin phosphodiesterase, acid-like 3A	0.0280107	0.529539	9.5938033	5.10127
1436936_s_at	**Xist**	inactive X specific transcripts	0.014853	0.554648	10.270287	5.5900267
1450140_a_at	**Cdkn2a**	cyclin-dependent kinase inhibitor 2A	0.0413117	0.557509	10.62583	5.9192967
1416066_at	**Cd9**	**CD9 antigen**	**0.0090664**	**0.559064**	**11.929967**	**6.6799433**
1449195_s_at	**Cxcl16**	chemokine (C-X-C motif) ligand 16	0.0384578	0.766257	9.1632133	6.9701733
1438498_at	**N/A**	N/A	0.038851	0.784942	6.5227133	5.09923
1428367_at	**Ndst1**	N-deacetylase/N-sulfotransferase (heparan glucosaminyl) 1	0.0226324	0.78663	7.07705	5.5451233
1443783_x_at	**N/A**	N/A	0.0063796	0.793061	3.29521	2.6150667
1438858_x_at	**N/A**	N/A	0.0268185	0.840707	6.7662	5.6961367
1430672_at	**N/A**	N/A	0.0367112	0.849284	7.46829	6.3399767
1455741_a_at	**Ece1**	endothelin converting enzyme 1	0.0300922	0.849423	7.80457	6.6259233
1442218_at	**N/A**	N/A	0.0148969	0.850929	4.92839	4.19017
1440413_at	**N/A**	N/A	0.0364437	0.851115	3.7763433	3.2087833
1452388_at	**Hspa1a**	heat shock protein 1A	0.0117909	0.85863	7.9276267	6.8083233
1439475_at	**N/A**	N/A	0.041715	0.85957	6.6055333	5.66356
1452431_s_at	**H2-Aa**	histocompatibility 2, class II antigen A, alpha	0.0305783	0.862184	6.3508767	5.4692933
1447494_at	**D7Bwg0826e**	DNA segment, Chr 7, Brigham & Women's Genetics 0826 expressed	0.0131046	0.867507	3.85747	3.3472
1432723_at	**N/A**	N/A	0.0020257	0.872652	3.78802	3.3045367

The expression value data were analysed using T test, QLUCORE OMICS explorer software, n=3, P ≤ 0, 05.

Table 6.4: List of top 20 upregulated genes in CD9KO compared with WT mouse macrophages.

Gene id	Gene Symbol	Gene Title	p-value	Fold change	Mean WT (log2)	Mean KO (log2)
1423331_a_at	**Pvrl3**	poliovirus receptor-related 3	0.045487	1.69633	4.157093	6.969107
1437534_at	**---**	---	0.039206	1.63258	3.71228	6.01991
1430567_at	**N/A**	N/A	0.045807	1.58347	4.53532	7.037873
1417398_at	**Rras2**	related RAS viral (r-ras) oncogene homolog 2	0.034543	1.4263	5.082387	7.237393
1455869_at	**---**	---	0.036756	1.41965	6.37495	9.062807
1415965_at	**Scd1**	stearoyl-Coenzyme A desaturase 1	0.045557	1.40215	5.70242	7.950387
1425708_at	**Rnf17**	ring finger protein 17	0.030104	1.34886	4.214657	5.682737
1449484_at	**Stc2**	stanniocalcin 2	0.045969	1.34773	4.94744	6.718833
1456226_x_at	**Ddr1**	discoidin domain receptor family, member 1	0.030232	1.30163	3.40317	4.431883
1427673_a_at	**Sema3e**	sema domain, immunoglobulin domain (Ig), short basic domain, secreted, (semaphorin) 3E	0.025358	1.29009	5.069307	6.508393
1436501_at	**N/A**	N/A	0.015441	1.26409	4.001333	5.069983
1419417_at	**Vegfc**	vascular endothelial growth factor C	0.029201	1.2509	3.761343	4.707927
1440739_at	**N/A**	N/A	0.003451	1.23823	4.548617	5.638523
1425906_a_at	**Sema3e**	sema domain, immunoglobulin domain (Ig), short basic domain, secreted, (semaphorin) 3E	0.048039	1.22191	4.91507	6.00677
1429462_at	**N/A**	N/A	0.028464	1.21682	4.095197	4.968653
1421193_a_at	**Pbx3**	pre B cell leukemia homeobox 3	0.039064	1.21246	5.637947	6.816113
1439489_at	**N/A**	N/A	0.039913	1.21164	5.04427	6.121793
1426411_a_at	**Strbp**	spermatid perinuclear RNA binding protein	0.037228	1.20429	6.137743	7.37052
1428402_at	**Zcchc3**	zinc finger, CCHC domain containing 3	0.025575	1.2038	5.644963	6.780513
1426605_at	**Brcc3**	BRCA1/BRCA2-containing complex, subunit 3	0.03085	1.19821	4.11993	4.925937

Data were analysed using T test, QLUCORE OMICS explorer software, n=3, $P \leq 0.05$.

As expected, the CD9 gene expression is significantly lower in CD9-KO cells compared with WT macrophages and the CD9 expression showed the highest up-regulated fold change in WT cells. In contrast, no significant changes were seen with other tetraspanins (Figure 6.11 and Table 6.5). In particular CD81, which was significantly reduced in protein expression as determined by flow cytometry in CD9-KO (Figure 6.3), showed no significant change at the mRNA level. The data were collected manually from the main microarray expression data set for all three experiments and the mean expression levels were taken to represent the mRNA levels of the tetraspanins. These results show the highest mRNA expression were for CD53 and CD9 followed by tetraspanin SAS (Tspan 31), CD81, CD63, Tspan 4, Tspan 3, CD82, Tspan 32, Tspan 13 and CD37. As previously described (6.3.1.1) the CD9, CD81 and CD63 protein expression level look compatible with mRNA expression level (in terms of the level of expression). As expected, CD53 shows a high level of expression in these cell lines as this protein is particularly expressed in white blood cells, along with CD37 (Figure 6.11). It was not possible to observe the expression of other tetraspanins at the protein level due to the lack of availability of monoclonal antibodies specific for mouse tetraspanins.

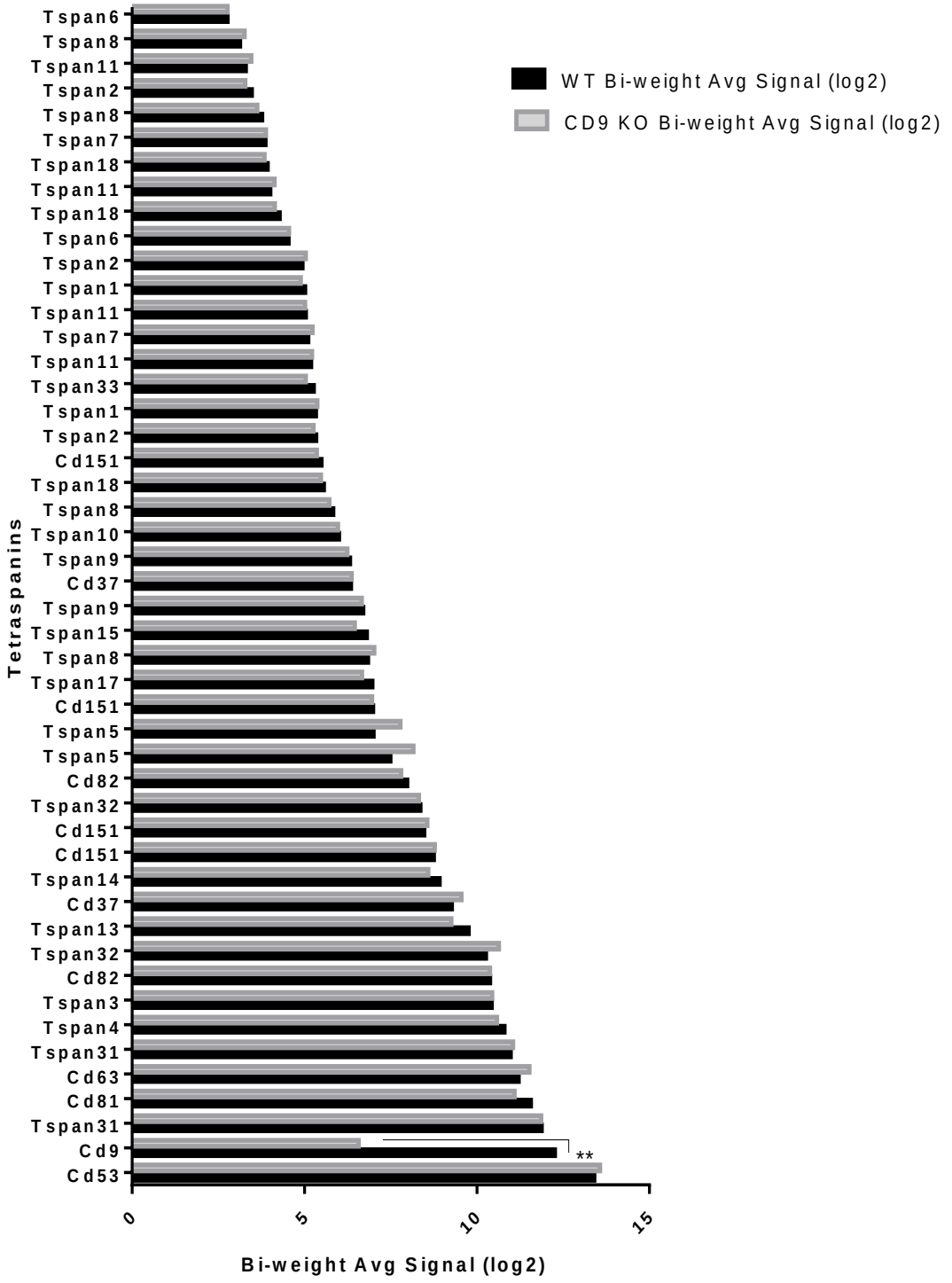

Figure 6.11: Tetraspanin mRNA expression in CD9 KO mouse macrophages and WT control as determined by RNA microarray analysis. The graph shows the level of mRNA expression in both CD9-KO and WT mouse macrophages. CD9 was significantly down regulated in CD9KO cells compared with WT cells control. Data were analysed using multiple comparison T test, **$p \leq 0.001$, Qlucore Omics explorer software, n=3.

Table 6.5: Tetraspanin mRNA expression in CD9 KO mouse macrophages and WT control as determined by RNA microarray analysis.

Transcript Cluster ID	Gene Symbol	WT Bi-weight Avg Signal (log2)	CD9KO Bi-weight Avg Signal (log2)	WT Standard Deviation	CD9KO Standard Deviation	Fold Change (linear) (WT vs. CD9KO)	ANOVA p-value (WT vs. CD9KO)
1448617_at	Cd53	13.4	13.57	0.93	0.54	-1.12	0.562474
1416066_at	Cd9	12.26	6.57	1.66	1.06	51.34	0.009897
1416556_at	Tspan31	11.88	11.86	0.54	0.47	1.01	0.961661
1416330_at	Cd81	11.56	11.09	0.55	0.5	1.38	0.148905
1417057_a_at	Cd63	11.21	11.52	0.45	0.74	-1.25	0.403789
1430029_a_at	Tspan31	10.98	11.05	0.34	0.29	-1.04	0.971217
1448276_at	Tspan4	10.8	10.58	0.5	0.37	1.16	0.818489
1416009_at	Tspan3	10.43	10.44	0.56	0.38	-1	0.793574
1416401_at	Cd82	10.38	10.38	0.43	0.6	1.01	0.782086
1418398_a_at	Tspan32	10.26	10.64	1.2	1	-1.3	0.620637
1418643_at	Tspan13	9.76	9.26	1.09	1.6	1.42	0.68876
1419206_at	Cd37	9.27	9.55	1.75	1.23	-1.21	0.883932
1423924_s_at	Tspan14	8.92	8.59	0.26	0.08	1.26	0.119316
1437670_x_at	Cd151	8.75	8.78	0.32	0.49	-1.02	0.838355
1424093_x_at	Cd151	8.47	8.56	0.23	0.28	-1.06	0.79979
1431289_at	Tspan32	8.36	8.32	0.39	0.03	1.03	0.575533
1449611_at	Cd82	7.98	7.8	0.28	0.13	1.13	0.708419
1417179_at	Tspan5	7.49	8.16	0.36	0.46	-1.6	0.286094
1431530_a_at	Tspan5	7	7.78	0.44	0.54	-1.72	0.269263
1427525_at	Cd151	6.99	6.96	0.21	0.15	1.02	0.236338
1424334_at	Tspan17	6.97	6.67	0.1	0.35	1.23	0.633919
1424649_a_at	Tspan8	6.84	7.02	1.39	0.81	-1.13	0.51709
1424653_at	Tspan15	6.81	6.46	0.41	0.22	1.28	0.282095
1428197_at	Tspan9	6.7	6.66	0.06	0.14	1.03	0.638838
1425736_at	Cd37	6.35	6.37	0.3	0.04	-1.01	0.870017
1441968_at	Tspan9	6.32	6.24	0.14	0.05	1.06	0.567916
1426588_at	Tspan10	6	5.97	0.05	0.13	1.03	0.305498
1420017_at	Tspan8	5.83	5.72	0.24	0.46	1.08	0.612396
1442174_at	Tspan18	5.56	5.48	0.12	0.13	1.06	0.505433
1420921_at	Cd151	5.49	5.36	0.17	0.05	1.09	0.30413
1432417_a_at	Tspan2	5.34	5.26	0.14	0.23	1.06	0.124232
1417957_a_at	Tspan1	5.33	5.37	0.04	0.06	-1.02	0.238855
1425157_x_at	Tspan33	5.27	5.04	0.22	0.18	1.17	0.575588
1441776_at	Tspan11	5.19	5.22	0.12	0.04	-1.02	0.674501
1417502_at	Tspan7	5.11	5.23	0.24	0.16	-1.09	0.74318
1430310_at	Tspan11	5.04	5.02	0.16	0.23	1.01	0.767338
1417958_at	Tspan1	5.02	4.89	0.19	0.01	1.09	0.301564
1424568_at	Tspan2	4.94	5.04	0.09	0.12	-1.07	0.675034
1416872_at	Tspan6	4.54	4.55	0.13	0.28	-1.01	0.953296
1429856_at	Tspan18	4.28	4.14	0.11	0.23	1.11	0.081541
1436626_at	Tspan11	4.01	4.13	0.1	0.12	-1.08	0.650124
1437095_at	Tspan18	3.93	3.84	0.33	0.18	1.06	0.409074
1448737_at	Tspan7	3.87	3.88	0.02	0.18	-1	0.482717
1420019_at	Tspan8	3.77	3.63	0.27	0.13	1.1	0.163325
1424567_at	Tspan2	3.47	3.28	0.14	0.15	1.14	0.371873
1445860_at	Tspan11	3.3	3.46	0.17	0.04	-1.12	0.524847
1420018_s_at	Tspan8	3.13	3.26	0.23	0.27	-1.1	0.963114
1448501_at	Tspan6	2.77	2.77	0.04	0.04	1	0.275909

The table shows the level of mRNA expression in both CD9-KO and WT mouse macrophages. CD9 is significantly down regulated in CD9KO cells compared with WT cells control. Data were analysed using multiple comparison ANOVA test, Transcriptome Analysis Console v3.0 (Affymetrix) software, n=3.

CD9 is known to be involved in cell adhesion and cell:cell fusion and studies by another member of the laboratory have shown that the CD9 KO macrophages show an enhanced ability to fuse when infected with *Burkholderia thailandenesis* (Atiga Elgawidi, personal communication). It was therefore of interest to examine changes in expression of genes related to adhesion and cell-cell fusion. The Database for Annotation, Visualization, and Integrated Discovery (DAVID) was used to identify, annotate, and summarise a list of significantly variable genes that were obtained from Qlucore Omics explorer microarray data analysis software to summarise adhesion related proteins (Table 6.6). Some proteins that are involved in adhesion show changes in their expression, either up- or down-regulated,

particularly integrin β3 that has been shown to be associated with CD9 (Indig, Diaz-Gonzalez et al. 1997) and was downregulated in CD9KO cells. In addition, the integrin β6, another tetraspanin partner protein, was also downregulated in CD9KO mouse macrophages. Claudin-1, another CD9 partner protein (Kovalenko, Yang et al. 2007), was also downregulated in CD9KO cells.

Table 6.6: Expression of adhesion related genes in CD9 KO and WT macrophages.

Gene id	Gene Symbol	Gene Title	p-value (T test)	Difference	Fold change (Log2)	average CD9KO (log2)	Average WT (Log2)
1456226_x_at	Ddr1	discoidin domain receptor family, member 1	0.0302315	0.380319	1.30163	4.43	3.40
1449764_x_at	Ssx2ip	synovial sarcoma, X breakpoint 2 interacting protein	0.0386983	0.166595	1.12241	3.01	2.68
1431611_a_at	Cadm1	cell adhesion molecule 1	0.0434334	0.166575	1.12239	8.58	7.65
1421614_at	Zan	zonadhesin	0.0433298	0.107517	1.07737	5.52	5.13
1416133_at	Efr3a	EFR3 homolog A (S. cerevisiae)	0.0396587	0.059217	1.0419	9.74	9.35
1446332_at	Pcdhgc	protocadherin gamma subfamily A, 8; protocadherin gamma subfamily A, 9; protocadherin gamma subfamily B, 4; protocadherin gamma subfamily C, 3; protocadherin gamma subfamily C, 5; protocadherin gamma cluster; protocadherin gamma subfamily C, 4; protocadherin gamma subfamily A, 2; protocadherin gamma subfamily A, 3; protocadherin gamma subfamily A, 11; protocadherin gamma subfamily A, 12	0.0131914	0.0304663	1.02134	3.54	3.46
1444317_at	Pcdh15	protocadherin 15	0.0031688	-0.037897	0.974074	2.82	2.89
1429072_at	RIKEN cDNA 1110001D15 gene	RIKEN cDNA 1110001D15 gene	0.0252886	-0.0399849	0.972665	5.46	5.61
1441706_at, 1432196_a_at	dscam1	Down syndrome cell adhesion molecule-like 1	0.0298455	-0.0521435	0.964502	4.01	4.16
1435349_at	Nrp2	neuropilin 2	0.0245295	-0.0531348	0.96384	10.17	10.55
1450922_a_at	Tgfb2	transforming growth factor, beta 2	0.0440474	-0.0549237	0.962645	2.97	3.09
1426997_at	Thra	thyroid hormone receptor alpha	0.0346426	-0.056231	0.961773	7.10	7.38
1416357_a_at	Mcam	melanoma cell adhesion molecule	0.0160792	-0.0621606	0.957829	4.25	4.44
1422590_at	Cdk5	cyclin-dependent kinase 5	0.0415928	-0.0695461	0.952938	5.94	6.23
1432281_a_at	Itgb6	integrin beta 6	0.0262944	-0.0703539	0.952404	3.55	3.72
1438662_at	ajap1	adherens junction associated protein 1	0.032503	-0.0730263	0.950642	4.34	4.57
1447825_x_at	Pcdh8	protocadherin 8	0.0060953	-0.0786623	0.946935	3.07	3.24
1433413_at	Nrxn1	neurexin I	0.0016809	-0.0798047	0.946186	5.96	6.30
1435190_at	N/A	N/A	0.0347286	-0.0804348	0.945773	2.97	3.14
1419423_at	Stab2	stabilin 2	0.0342327	-0.0836406	0.943673	5.28	5.59
1445798_at	dlg1	discs, large homolog 1 (Drosophila); similar to Discs, large homolog 1 (Drosophila)	0.0290769	-0.0857195	0.942315	2.92	3.10
1460412_at	Fbln7	fibulin 7	0.0370743	-0.0857738	0.942279	3.77	4.01
1421511_at	Itgb3	integrin beta 3	0.0423281	-0.0872572	0.941311	5.09	5.41
1450341_at	Pcdhb8	protocadherin beta 8	0.0328162	-0.0905556	0.939161	4.75	5.06
1437932_a_at	Cldn1	claudin 1	0.0034232	-0.0965702	0.935254	3.52	3.76
1421633_a_at	Hapln1	hyaluronan and proteoglycan link protein 1	0.0259266	-0.0973429	0.934753	3.08	3.30
1418664_at, 1441361_at	Mpdz	multiple PDZ domain protein	0.0003761	-0.112017	0.925293	4.65	5.02
1449586_at	Pkp1	plakophilin 1	0.0461386	-0.117819	0.92158	3.95	4.29
1445731_at	N/A	N/A	0.0385795	-0.119602	0.920442	4.65	5.05
1450199_a_at	Stab1	stabilin 1	0.0242771	-0.133711	0.911484	7.41	8.13
1419527_at	Comp	cartilage oligomeric matrix protein	0.0425262	-0.13966	0.907733	5.32	5.87
1421723_at	Pcdhb18	protocadherin beta 18	0.022168	-0.145366	0.90415	3.05	3.38
1416066_at	Cd9	CD9 antigen	0.0090664	-0.838915	0.559064	6.68	11.93

Variably expressed genes were annotated using DAVID online annotation software from analysed $p \leq 0.05$ significant value by multiple T test in Qlucore Omix explorer software. n=3.

6.3.4 Transfection of mCD9-GFP in J774 mouse macrophage cells

The pCMV6-AV construct obtained from Origene (Table 2.9) carrying mouse CD9-GFP was used initially to try to rescue mCD9 in CD9-KO cells. This would also provide the opportunity to visualise CD9 by microscopy without the need for antibody staining. However, despite using different transfection techniques (including chemical transfection, conventional and nucleofector electroporation, data not shown) the transfections were unsuccessful. The pCMV6-AV vector carries G418 resistance, but the CD9-KO mouse macrophages already have the G418 resistance gene from the CD9 knock down experiment (Le Naour, Rubinstein et al. 2000, Ha, Waterhouse et al. 2005). Attempts to select for transfectants by co-transfection using a second plasmid carrying puromycin resistance were therefore also carried out but were unsuccessful.

Instead, attempts were made to over express mCD9 in J774 cells by transfecting the cells with the CD9-GFP vector using electroporation as described in 2.2.10.2. mCD9-GFP was successfully expressed and localised in cell membrane of transfected J774 cells (Figure 6.12), with most cells shown to be expressed mCD9-GFP after cell sorting.

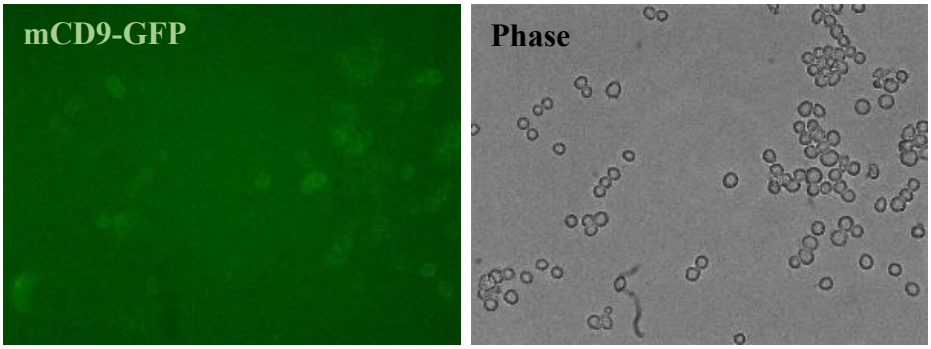

Figure 6.12: Expression of mCD9-GFP transfected J774 cells. Cells were transfected with the mCD9-GFP construct (Table 2.9) by electroporation as described in 2.2.10.2. followed by selection of transfected cells using G418 containing media. GFP expressing cells were sorted by flow cytometry. The sorted cells were visualised using an inverted florescent microscope.

Screening for expression of tetraspanins CD9 and CD81 was carried out using appropriate antibodies labelled with Alexa fluor and flow cytometry. CD9 expression was about two times higher in mCD9-GFP transfected cells compared with non-transfected cells (Figure 6.13 B). As described previously in fluorescence microscopy, most transfected cells expressed CD9-GFP (Figure 6.13 A). A significant reduction in CD81 expression was detected in mCD9-GFP transfected cells compared with non-transfected cells (Figure 6.13 C).

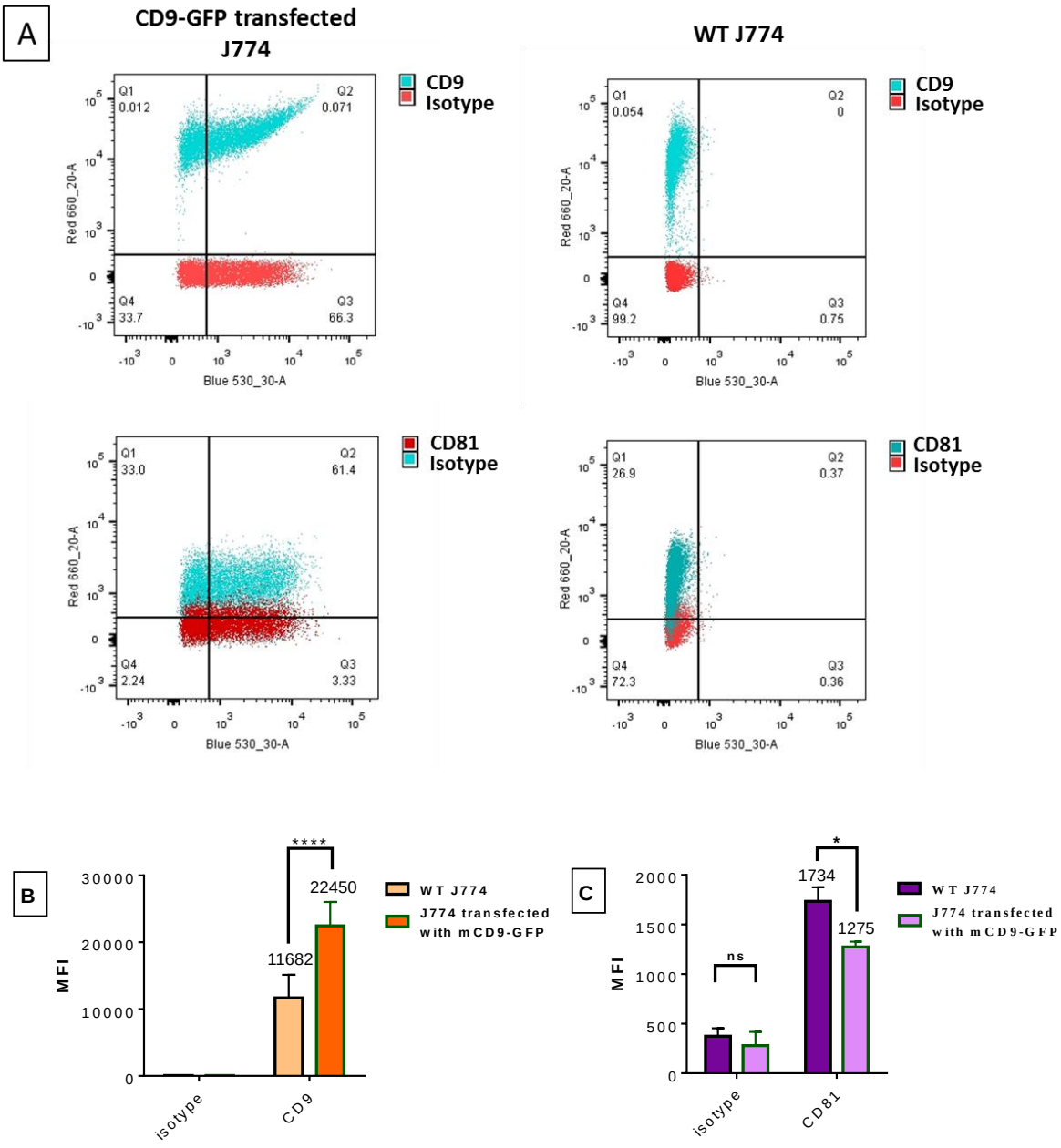

Figure 6.13: Tetraspanin CD9 and CD81 expression in mCD9-GFP transfected J774 cells. **A:** Dot plot showing the main parameters that were used in the experiments. **B, C:** Surface expression of CD9 and CD81, respectively, in CD9-GFP transfected J774 compared with non-transfected cells. Anti-mouse tetraspanin primary mAbs or appropriate isotype controls conjugated with Alexa fluor® 647 were used (**Table** 2.5.B). Data were analysed by BD FACSDiva 8.0.1. The gate was set depending on the non-treated cells control (washing buffer was added to the cells instead of antibody). The experiment was done in duplicate, MFI =Median fluorescent intensity. N=3 in duplicate, the significant difference was analysed by Two ways ANOVA, Sidak`s multiple comparisons test, significance **** $p \leq 0.0001$ and * $P \leq 0.05$, ns is non-significant.

6.3.5 Localisation of CD9 during *Salmonella* infection in mCD9-GFP transfected J774 cells

A permanent mCD9-GFP transfected cell line was successfully generated, which provides an important tool to study CD9 localisation during *Salmonella* infection by taking advantage of having mCherry expressing *Salmonella*. The mCD9-GFP transfected J774 cells were prepared and infected with *Salmonella* NCTC12023-mCherry and then fixed and prepared for confocal microscopy at different time points. The results showed that CD9-GFP was aggregated and surrounded *Salmonella* at phagocytosis sites and some CD9 appears to be present on the membrane of the phagosomes containing internalised *Salmonella* at 15 minutes post- infection. By 120 minutes post infection, internalised bacteria do not co-localise CD9 (Figure 6.14).

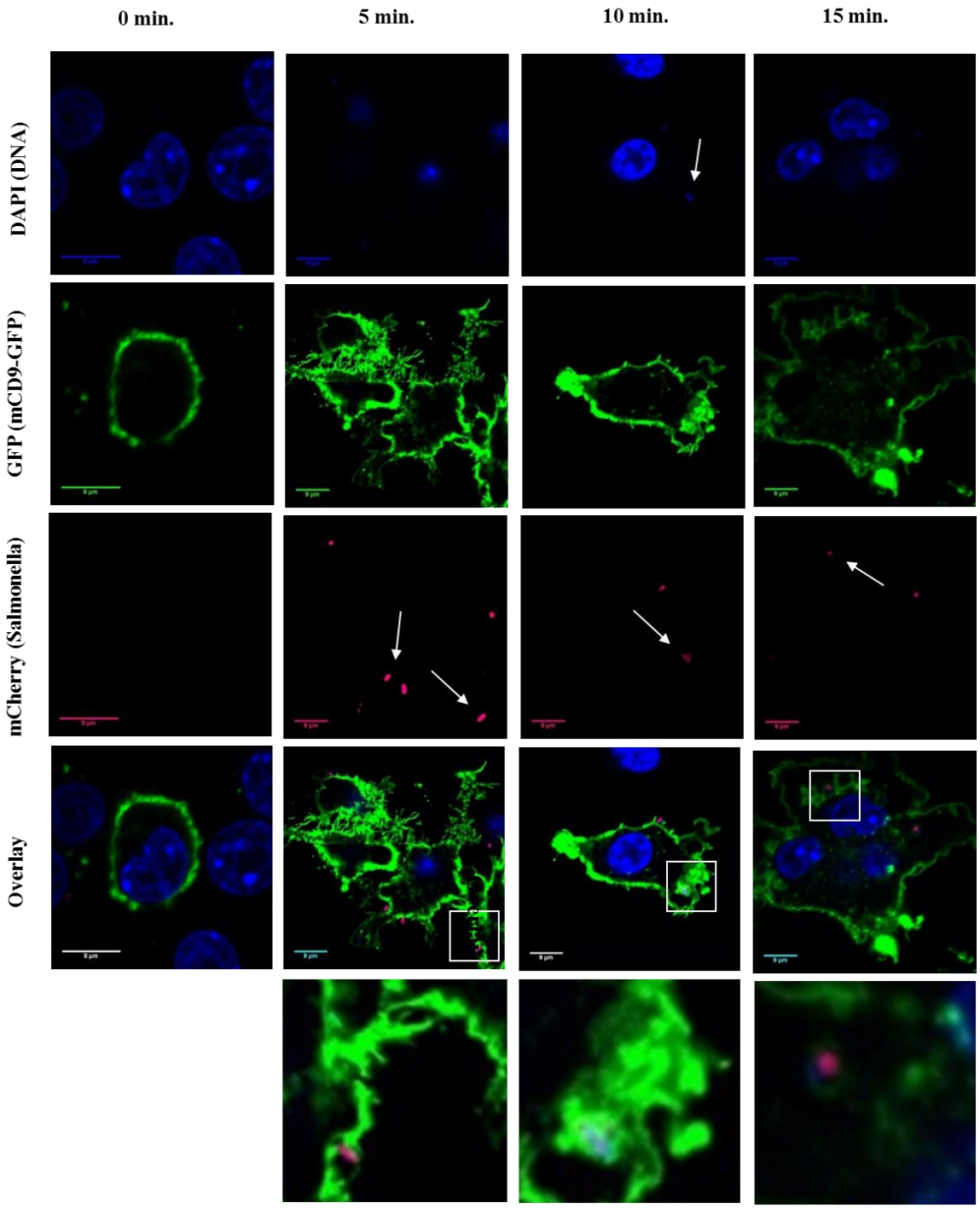
0 min.
5 min.
10 min.
15 min.
DAPI (DNA)
GFP (mCD9-GFP)
mCherry (Salmonella)
Overlay

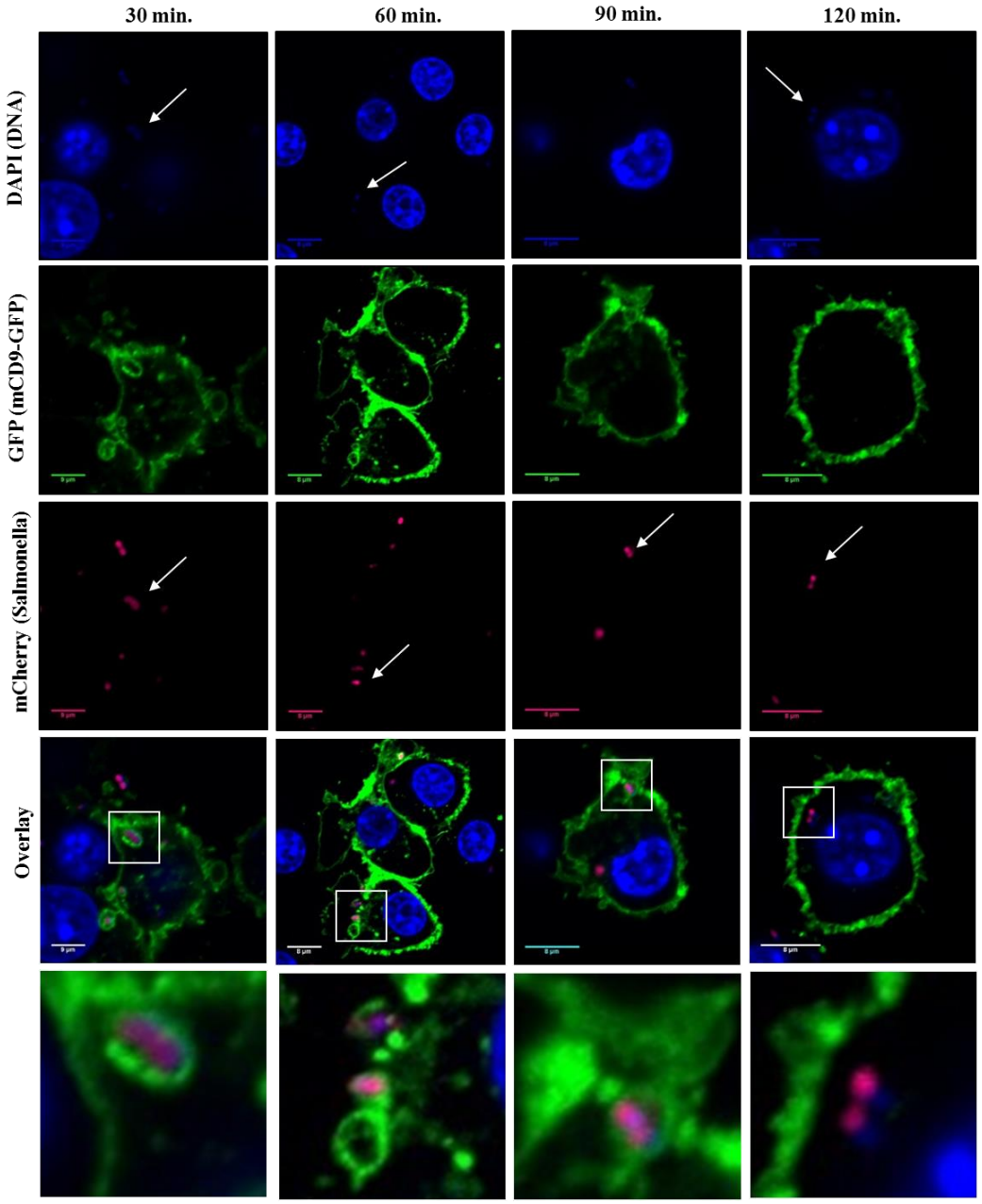

Figure 6.14: Confocal microscopy of mCD9-GFP transfected J774 cells infected with *Salmonella* Typhimurium NCTC12023-mCherry. J774 cells were infected with NCTC12023-mCherry strain (magenta) at 50 MOI for 0, 5, and 10. 15, 30, 60 and 120 minutes, as described in (2.2.12.2). The cells then were fixed then cellular and bacterial DNA were stained blue (DAPI) stain (blue). Images were visualised using Nikon A1 Confocal inverted system with EM-CCD camera and 60x objectives.

6.4 Discussion

CD9 is one of most important tetraspanin family members encoded by a gene that was found on chromosome12 in humans (Maecker, Todd et al. 1997) and chromosome 6 in mouse (Elliott and Moore 1996). Tetraspanin CD9 (Tspan29) has been detected in a variety of mammalian cells such as basophils, macrophages, eosinophils, epithelial cells, fibroblasts, neurons, oocytes, different cancer cells and cancer cell lines (Zhang, Kotha et al. 2009).

In the current study, we have shown high expression of CD9 in mouse macrophages at both mRNA (microarray analysis results) and protein expression level (immunofluorescence and flow cytometry). CD9 has been shown to be involved in bacterial adhesion to human epithelial cell lines (Green, Monk et al. 2011) and mouse macrophages cell lines (Chapter 4). To further investigate the role of CD9 in infection of mouse macrophages by *Salmonella*, macrophage cell lines derived from CD9KO and corresponding wild type mice were used. There was no difference in the infection of CD9KO or WT macrophages by the NCTC12023 strain of *Salmonella*, but surprisingly, CD9KO macrophages were more susceptible to infection by the LT2 strain. This might also relate to the effects of CD9 gene knock out on other tetraspanin members (as there was significant reduction in expression of CD81 in CD9 KO cells) or on other proteins relevant to infection. It has been found that *Salmonella* Typhimurium NCTC12023 is less able to invade epithelial cell lines compared with *Salmonella* Typhimurium SL1344 strain because it is deficient in some of the T3SS proteins (Clark, Perrett et al. 2011). Furthermore, T3SS is also important for *Salmonella* survival after uptake by macrophages (Cirillo, Valdivia et al. 1998). In addition, the differences in *Salmonella* strains uptake could relate to differences in uptake mechanism, with LT2 seeming to be more resistant to phagocytosis than *Salmonella* strain NCTC12023, as described in 6.3.2.

Western blot, immunofluorescence and FACS analysis with anti-CD9 antibodies showed strong expression of CD9 in wild type control and no expression of CD9 in CD9KO. However, a very slight shifting of the cells to the positive gated region (based on the isotype control) was observed for the CD9KO cells in flow cytometry analysis. As no expression was apparent by Western blotting, it is likely that this was due to slightly higher non-specific binding of the anti-CD9 antibody to the cells compared to the isotype control. CD81 showed a significant reduction at the protein level, but not in mRNA expression, in the CD9KO cells. CD63 protein expression also appeared lower in the CD9KO cells, although this was, not statistically significant from flow cytometry analysis and high levels of CD63 mRNA were

observed in both cell types in microarray analysis. CD9 and CD81 are known to interact at the protein level, but the effect of knock down or knock out of CD9 on expression of other tetraspanins seems to vary depending on cell type. Knockdown of CD9 or CD81 in human dermal lymphatic endothelial cells (HDLEC) led to increased protein expression of the other tetraspanin without affecting the CD151 expression levels (Iwasaki, Takeda et al. 2013). However, in the same study, siRNA knockdown of CD9 in human umbilical vein epithelial cells (HUVEC) had little effect on CD81 expression and blood or lymphatic endothelial cells from CD9 KO mice showed little change in CD81 protein expression compared to wild type. In another study, no changes in CD81 and CD151 mRNA and protein expression levels were noticed after knocking down CD9 by lentiviral shRNA in vascular smooth muscles, although the CD9-KD cells showed a different phenotype (Herr, Mabry et al. 2014). It is possible that knockdown of CD9/CD81 leads to compensatory changes in expression of the other tetraspanin in some cell types but not others. Interestingly, CD81 protein expression was also down regulated in mouse macrophage J774 cells transfected to over-express CD9, as described in 6.3.4. As far as we are aware, the expression of other tetraspanins on macrophage cell lines derived from CD9KO mice has not been investigated at the protein expression level because of the limited number of anti-mouse tetraspanin antibodies available. The fact that CD81 expression seems to be downregulated either in CD9KO macrophages or CD9 overexpressing J774 mouse macrophages may be related to the role of CD9 in the proper trafficking of CD81 in these cells.

Microarray analysis has emerged and developed since it was used for graphic evaluations of results, to more sophisticated algorithmic comparisons of gene expression used in many types of biological research (Allison, Cui et al. 2006). The quality of the extracted RNA in gene expression experiments has a vital role in microarray analysis and high sensitivity of several microRNAs to the method of RNA isolation used has been demonstrated (Podolska, Kaczkowski et al. 2011). The extracted RNA should not contain any contaminants such as proteins, cell debris and DNA; in addition, the RNA samples should not contain RNA extraction related materials such as salts, phenol and ethanol. These contaminants could lead to a decrease in the efficiency of reverse transcription and reduce amplification levels. The RNA full length integrity is another important factor that affects RNA quality as a degraded RNA will produce cDNA with missing portions of the transcripts that are complemented with probes in the array (Podolska, Kaczkowski et al. 2011). Testing RNA purity and integrity were carried out in all samples of extracted RNA (Figure 6.8), confirming that it was of high quality.

Different methods have been developed to evaluate the significance of changes in gene expression; T test analysis was shown to be powerful in microarray analysis of a range of different sizes of gene sets (Jeffery, Higgins et al. 2006). Here, two different software analyses were used: QLUCORE OMICS explorer that uses T-Test analysis, and Affymetrix® Transcriptome Analysis console (TAC) software that uses the ANOVA test. Despite some differences in the results that were obtained from these two types of microarray analysis tools , a highly significant reduction of CD9 mRNA in CD9KO cells was shown ($p \leq 0.01$combined with 1.5 $\log^2$ fold change). Three genes shown to be also highly down regulated in CD9KO mouse macrophages were Xist, Cdkn2a and Smpl3a. The Xist gene (X-inactive specific transcript) is an RNA gene that has a role X chromosomal inactivation (XCI), and mainly functions to genetically suppress one of two feminine X chromosomes (Brockdorff, Ashworth et al. 1991). It is expressed in both somatic and germ cells (McCarrey and Dilworth 1992) and has also been shown to be involved in embryo development (Hartshorn, Rice et al. 2002).

Cdkn2a (cyclin-dependent kinase 2a) was firstly identified as being mutated in melanoma, but mutations in this gene were soon shown to be related to different non melanoma tumors. Cdkn2a codes for two different tumor suppressors p16 (INK4a) and p19 (ARF) that have roles in regulating cell proliferation and cancer malignancy, reviewed in (Aoude, Wadt et al. 2015). It has been shown that p19 (ARF) is important in the p53 tumor suppressor pathway (Herzog, Noh et al. 1999); furthermore, p53 is involved in cancer adhesion and metastasis. CD9 is shown to be upregulated in $p53^{R248}$ mutants of ovarian cancer cells in both whole genome sequence microarray and RT-PCR along with several adhesion related proteins (Lee, Ahn et al. 2015). The p53 gene was also shown to be significantly downregulated ($p \leq 0.05$ and fold change not considered) in CD9KO mouse macrophages compared with WT control.

The Smpdl3a (encoding the sphingomyelin phosphodiesterase, acid-like 3A protein) was another gene that was shown to be downregulated at the mRNA level, in CD9KO cells. In primary human macrophages Smpdl3a expression is shown to be regulated by cholesterol and by liver X receptor (LXR and cyclic AMP (cAMP) (Traini, Quinn et al. 2014). Regulation of CD9 expression by the cAMP/PKA signaling pathways has been observed (Muroi, Sakurai et al. 2009).

Three genes were shown to be upregulated in CD9KO cells ($p \leq 0.05$ and 1.5 fold changes). Of note, the poliovirus receptor-related 3 (Pvrl3) gene encodes the poliovirus receptor-related 3 protein (also known as Nectin 3) and is known to be associated in cell-cell adhesion (Satoh-Horikawa, Nakanishi et al. 2000). The Pvrl3 gene was shown to be associated in human eye development through its involvement in cell-cell adhesion that mediated by Nectin (Lachke, Higgins et al. 2012). Nectin is thought to co-operate with E-cadherin in the development of

cell: cell adhesion junctions, in human epithelial cells (Peng, Mandai et al. 2002). Interestingly, tetraspanins including CD9 have been reported to co-localise with E-cadherin (Yanez-Mo, Mittelbrunn et al. 2001).

In contrast to the results reported here for macrophage cell lines, embryonic stem cell (ESC) lines established from CD9-/- (3 cell lines) and WT (2 cell lines) mouse ESCs were shown by microarray analysis to have globally similar (but not identical) expression patterns. The cell lines were phenotypically similar and no difference in CD81 protein expression was observed. Also, no differences were observed in predicted tetraspanins expression (mRNA level) or CD9 associated proteins between CD9KO ESCs and WT control (Akutsu, Miura et al. 2009).

The online tools DAVID (The Database for Annotation, Visualization and Integrated Discovery) were used to cluster, annotate and extract functional genes from gene list to understand functional analysis and annotation of variable genes (Huang da, Sherman et al. 2009). The CD9 associated proteins, integrin α3 (Indig, Diaz-Gonzalez et al. 1997) and claudin-1(Kovalenko, Yang et al. 2007) were down regulated in CD9KO cells (Table 6.6).

Attempts to rescue the CD9 -/- macrophages with CD9-GFP were unsuccessful, but a stable J774 cell line expressing CD9-GFP was established, which is useful for fluorescence microscopy. The results showed that transfected CD9 behaved, in term of distribution, similarly to cells expressing native CD9. As shown in (Figure 6.12), CD9-GFP was correctly distributed on the plasma membrane while no obvious cytoplasmic CD9 was detected. An obvious co-localisation of CD9 and *Salmonella* was observed during the phagocytic process by J774 macrophages; however, this co-localisation was not clear after *Salmonella* internalisation. It could be that the CD9 was affected by degradation in internalised bacterial phagosome or could it be that CD9 is not present in the endosomal compartments where *Salmonella* is found at the later stages of infection. Attempts were made to visualise the CD9 distribution and association with *Salmonella* during infection in live imaging using J774 overexpressing CD9-GFP and mCherry expressing *Salmonella*. However, it was difficult to analyse the results using available imaging analysis software because of high background signals that made it difficult to observe any association.

Other workers have reported that cancer cell motility was decreased after introducing CD9-GFP in small cell lung cancer (SCLC) (Funakoshi, Tachibana et al. 2003). Overexpression of CD9-GFP was also used to investigate cell membrane fusion induced by HIV-1 virus

infection (Gordon-Alonso, Yanez-Mo et al. 2006). The stably transfected GFP-CD9 J774 macrophage cell line generated here may be useful for further functional studies in the future.

Chapter 7: Investigation of the effects of syntenin knockdown on *Salmonella* Typhimurium uptake

7.1 Introduction

Previous studies from this laboratory indicated an important role for tetraspanin CD63 in the association of *Salmonella* Typhimurium with human MDMs (Noha Hassuna, PhD, thesis, University of Sheffield, 2010). Binding of *S.* Typhimurium to MDM was shown to be inhibited by antibodies to CD63, which induced internalisation of cell surface CD63, and by siRNA knockdown. During the course of present studies, a HeLa cells that had been stably knocked-down for the expression of syntenin, a partner of CD63 involved in its trafficking (Latysheva et al, 2006), became available; it was therefore of interest to investigate *S.* Typhimurium uptake by these cells.

7.1.1 Syntenin-1

Syntenin-1 is a scaffolding protein containing two PDZ domains, which was originally shown to link syndecan (a family of transmembrane heparin sulphate proteoglycans) to the cytoskeleton. It co-localised with syndecan at the plasma membrane and at intracellular vesicles (Grootjans, Zimmermann et al. 1997). The PDZ domain shows homology with domains found in yeast, plant and bacteria (Ponting 1997) (Kennedy 1995). Syntenin is expressed in various cell types and cell lines and is found at sites of cell-cell adhesion, microfilaments and the nucleus (Stier, Totzke et al. 2000, Zimmermann, Tomatis et al. 2001, Meerschaert, Bruyneel et al. 2007). It is also known as melanoma differentiation association gene-9 (mda-9) because of its role in regulating melanoma metastasis (Boukerche, Su et al. 2005).

7.1.2 Syntenin functions

As a scaffolding or adaptor protein, syntenin is involved in various cell functions including membrane-cytoskeletal organisation (Grootjans, Zimmermann et al. 1997), adhesion, where it was originally shown to play a role in adherence junction formation by regulating cell membrane kinetics (Zimmermann, Tomatis et al. 2001) and protein trafficking (Zimmermann, Zhang et al. 2005). Mice knocked out for the syntenin-1 gene appeared normal but had elevated levels of intestinal immunoglobulins, suggesting that syntenin negatively regulates their production. (Tamura, Ikutani et al. 2015). In the nervous system, syntenin is involved in regulating nerve cell maturation and formation of synapses in central nervous system (CNS) (Hirbec, Martin et al. 2005). In cancers, syntenin promotes angiogenesis (Das, Bhutia et al. 2013) and metastasis, migration and invasion (Lee, Kim et al. 2011, Das, Bhutia

et al. 2012, Das, Bhutia et al. 2012, Zhong, Ran et al. 2012, Hwangbo, Tae et al. 2015) and is upregulated in metastases in a number of cancers including melanoma (Helmke, Polychronidis et al. 2004) (Boukerche, Su et al. 2005). Syntenin is also expressed in exosomes and has been implicated in their biogenesis (Friand, David et al. 2015, Roucourt, Meeussen et al. 2015). It has also been shown to negatively regulate HIV-1 invasion of T cells (Gordon-Alonso, Rocha-Perugini et al. 2012).

7.1.3 Syntenin structure

The PDZ domains are the main feature of syntenin structure, consisting of 80-100 residues organized in six β strand and two α helices (Kegelman, Das et al. 2015). The functional syntenin-1 is made up of 298aa consisting of 2 PDZ domains, with PDZ-1 positioned at a.a. 114-193 and PDZ-2 positioned at a.a.198-273 and N and C-terminal tails (http://www.uniprot.org/uniprot/O00560). The human syntenin crystal structure has been solved, showing that the two PDZ domains are structurally quite similar (Figure 7.1) (Kang, Cooper et al. 2003). Both PDZ domains are required for syntenin functions (Zimmermann, Tomatis et al. 2001) and it has been suggested that PDZ_2 acts as the main syndecan binding domain while PDZ_1 acts as an auxiliary binding domain to syndecan (Grootjans, Reekmans et al. 2000). Nevertheless, both PDZ domains in syntenin have a crucial role in mediating the interaction between syntenin and syntenin-associated proteins (Sarkar, Boukerche et al. 2004).

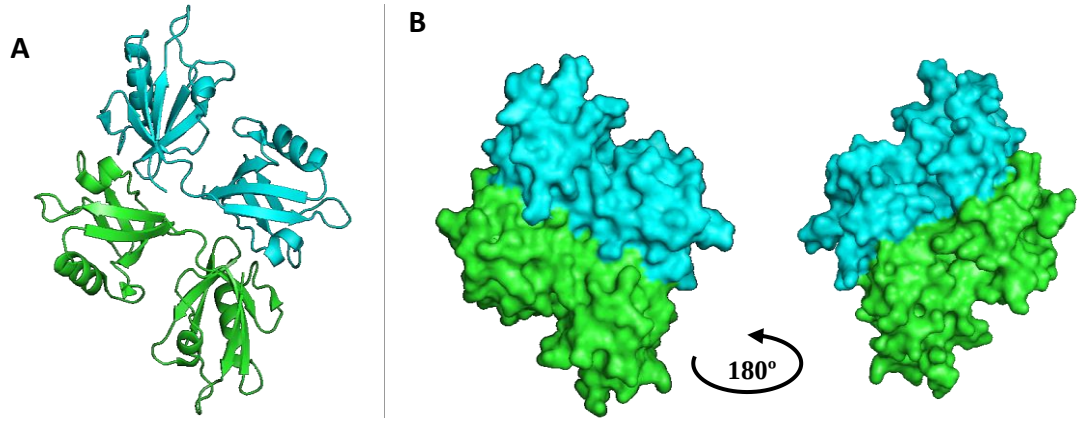

Figure 7.1: Structure of PDZ tandem of Syntenin-1. The structure 1N99 (Kang, Cooper et al. 2003) was obtained from PDB data base (http://www.rcsb.org/pdb/explore/explore.do?structureId=1N99) and was visualised using the PyMOL molecular graphic viewer. **A:** A cartoon diagram shows the two PDZ domains. **B:** A surface diagram showing the two PDZ domains that compose syntenin-1 protein.

7.1.4 Syntenin protein associations

Syntenin was initially shown to interact with the heparin sulphate proteoglycan syndecan through the FYA sequence in the C-tail of syndecan (Grootjans, Zimmermann et al. 1997). It also interacts with a wide range of other proteins including schwannomin (sch-1) (Jannatipour, Dion et al. 2001), the glycine transporter protein2 (GlyT2) (Ohno, Koroll et al. 2004), the type I membrane glycoprotein CD6 (Gimferrer, Ibanez et al. 2005), the c-Src proto-oncogene (Boukerche, Su et al. 2008), type 1 membrane protein NG2 (Chatterjee, Stegmuller et al. 2008), TRAF6 (Chen, Du et al. 2008), frizzled 7 receptor (Luyten, Mortier et al. 2008), lysyl-tRNA synthetase (Meerschaert, Remue et al. 2008), PIP2 (Zimmermann, Meerschaert et al. 2002, Zimmermann, Zhang et al. 2005), IL-5 receptor (Beekman, Verhagen et al. 2009) and Notch ligand Delta-1 (Estrach, Legg et al. 2007). Importantly for this study, it has also been shown to interact with tetraspanin CD63 and was suggested to be a component of TEM (Latysheva, Muratov et al. 2006). The interaction between tetraspanin CD63 with syntenin-1 was direct and no association of CD9 or CD81 was detected by immunoprecipitation. The tetraspanin CD63 C-terminus is crucial to the association with Syntenin-1 as deletion of the last two C-terminal amino acids abolished the interaction. The interaction occurred through the PDZ domain of syntenin but the syntenin C-terminus also stabilized this association as removing this abolished the interaction. Over-expression of syntenin slowed internalisation of CD63, and CD63 internalisation was arrested in cells expressing mutant syntenin-1 lacking the N-terminal 100 amino acids (Latysheva, Muratov et al. 2006). As mentioned previously (Chapter 1) CD63 has an internalization/lysosomal targeting motif at its C-terminus that facilitates interaction with AP-2 complexes that promote its internalisation (Rous, Reaves et al. 2002). It has therefore been suggested that syntenin competes with AP-2 mediated internalisation of CD63 to regulate endocytosis (Latysheva, Muratov et al. 2006).

7.1.5 HeLa syntenin –KD cells

The Hela syntenin knock down cell line was generated using a pLKO-sh Syntenin clone, while the control cell line was transfected with pLKO-puro vector (Fedor Berdichevski, personal communication). Both Hela syntenin-KD and control cell lines were kindly provided by Fedor Berditchevski (Institute for cancer studies, the University of Birmingham, Birmingham, United Kingdom).

7.2 Aims

Since syntenin directly associates with CD63, which has previously been implicated in association of *S.* Typhimurium with human MDM, it was of interest to investigate association of the bacteria with cells that had been stably knocked down for syntenin expression. Furthermore, as mentioned previously, anti-CD63 antibody inhibition of this association was mediated by CD63 internalisation, which may be affected by syntenin (Latysheva, Muratov et al. 2006).

7.3 Results

7.3.1 Investigation of expression of syntenin-1 protein in syntenin-1 KD and control HeLa cells

Syntenin-1protein has been shown to be expressed in different cell types and cell lines (Meerschaert, Bruyneel et al. 2007), including HeLa cells (Latysheva, Muratov et al. 2006). Western blot and immunofluorescence microscopy were performed to investigate differences in syntenin protein expression on HeLa syntenin KD cells and HeLa cells control.

7.3.1.1. Western blot of HeLa-syntenin KD and control cell lysates

To independently verify knock-down of syntenin-1 expression in the cell line provided by Professor Berditchevski, Western blotting was used to detect syntenin-1 in syntenin KD and control HeLa cells. As expected, no expression of syntenin was shown in HeLa syntenin KD cells compared with a clear protein band in HeLa control cells (Figure 7.2) at ~33kd, the expected size of syntenin.

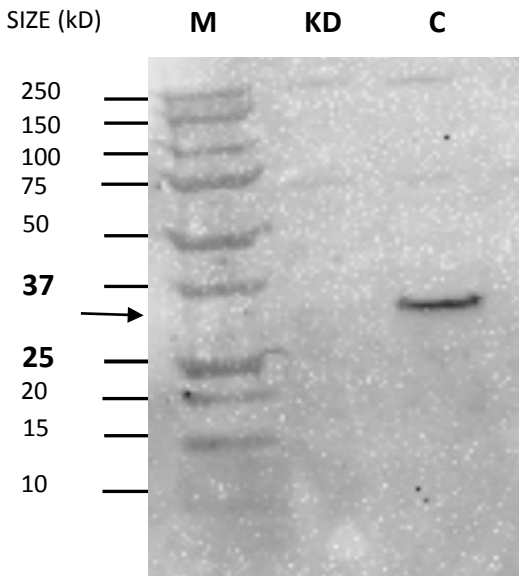

Figure 7.2: Western blot of lysates prepared from HeLa Syntenin KD and control cells. Cells were lysed with 0.5% Brij 98 and 0.5% Triton 100X as described in 2.2.7 and the lysate was run on 12.5% SDS-PAGE gels under reducing conditions before transfer to nitrocellulose membrane. The membrane was probed with anti-human syntenin followed by anti-rabbit-HRP. **M**, protein markers; **KD** and **C**, lysate from syntenin KD and control cells respectively.

7.3.1.2 Immunofluorescence microscopy analysis of syntenin expression in KD and control HeLa cells

Immunofluorescence microscopy was performed to investigate the total level of syntenin-1 protein expression and distribution in HeLa syntenin-KD cells and control cells as described in 2.2.4.1. The results showed low expression of syntenin protein in syntenin-KD HeLa cells compared with WT cells control (Figure 7.3). Slight background staining was observed in isotype treated cells control indicating some non-specific binding of the rabbit IgG or the secondary antibody.

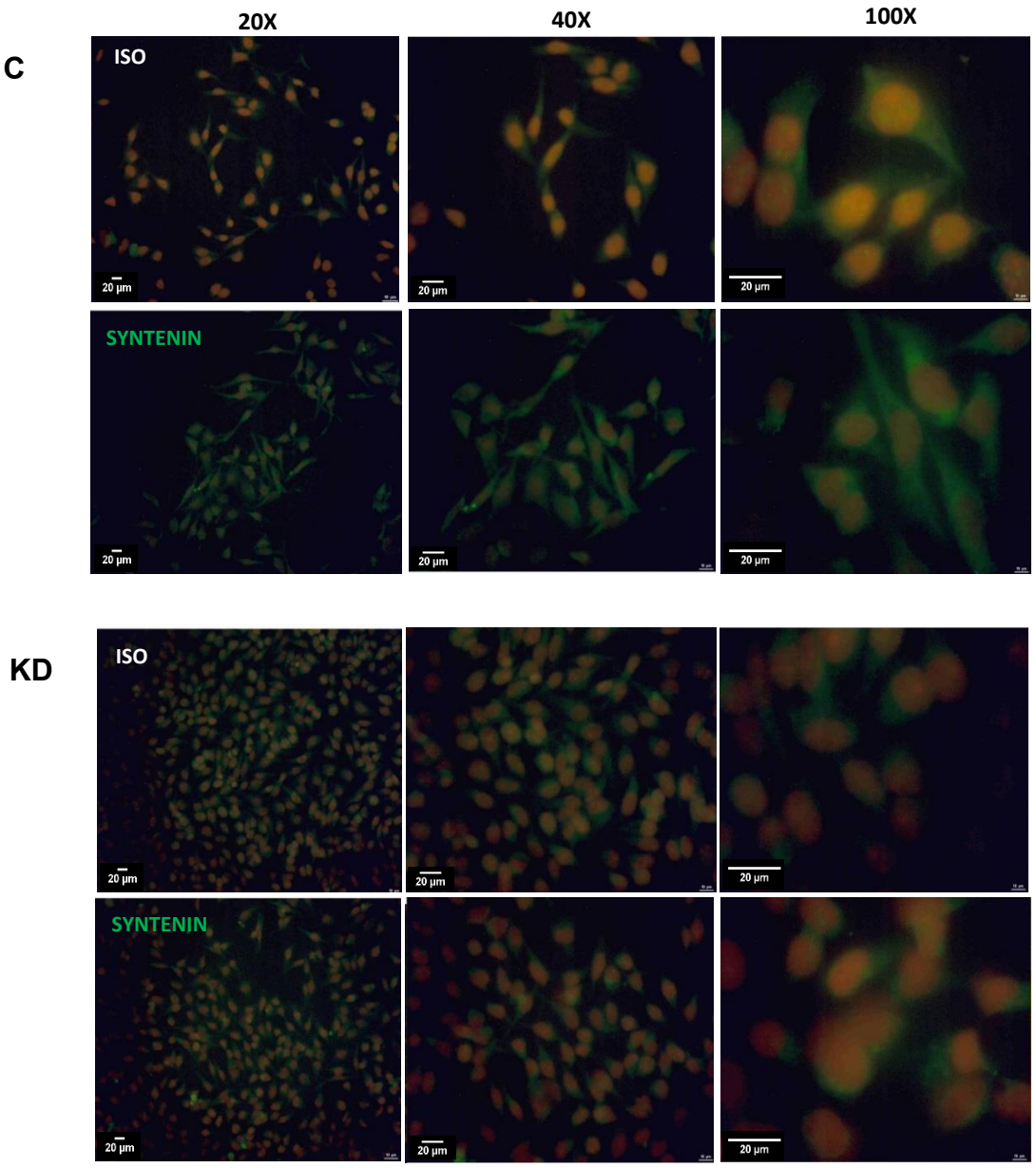

Figure 7.3: Immunofluorescence microscopy of syntenin KD and control HeLa cells stained for syntenin. Hela cells were seeded in 8-well chamber slides, fixed and permeabilised and stained with primary anti-syntenin or rabbit IgG control (10µg ml^{-1}) (Sigma) followed by anti-rabbit-FITC as described in 2.2.4.1 Nuclei were counter-stained with propidium iodide. These images obtained using 20 x, 40x and 100x oil immersion objective lenses.

7.3.2 Investigation of tetraspanin protein expression in syntenin-KD and control HeLa cells

The expression of tetraspanin proteins was investigated in syntenin-KD cells and control HeLa cells by flow cytometry and immunofluorescence microscopy. The flow cytometry was carried out on both live, fixed (for surface expression only) and fixed and permeabilised cells (for surface and cytoplasmic protein expression). Staining was also carried out on live cells here to address the possibility that the fixation reagent used (paraformaldehyde) might be itself be causing some permeabilisation. In live cell staining,

the surface expression (MFI) of CD151 showed a significant reduction in syntenin KD cells compared with control cells. No significant changes were observed for other tetraspanins (Figure 7.4, A and B). Nevertheless, the tetraspanin protein expression showed some differences after fixing and permeabilising the cells prior to staining. A significant increase in total CD63 expression and, to a lesser extent CD81, was observed in syntenin-KD cells compared with control cells (Figure 7.4, C). The percentage of CD63 and CD81 positive cells also increased. Although the MFI did not increase, the percentage of CD9 and CD151 positive cells was increased in fixed and permeabilised syntenin KD cells (data not shown).

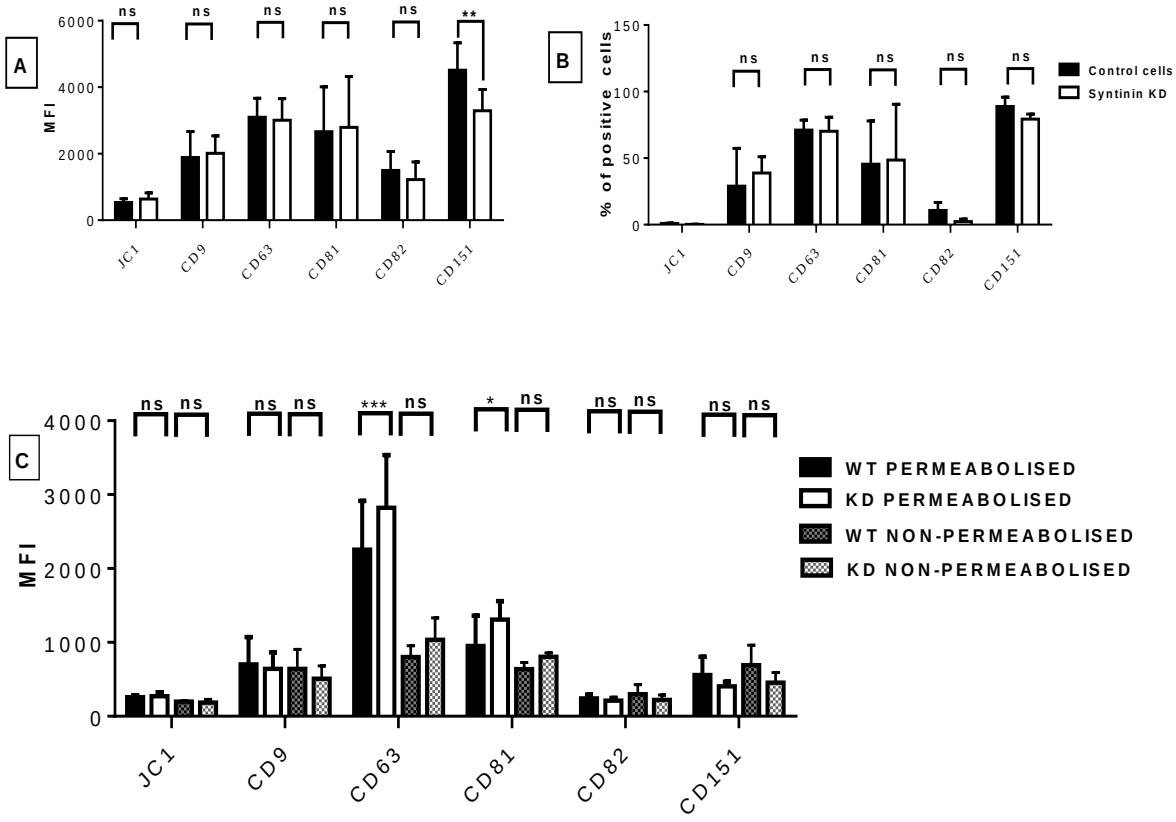

Figure 7.4: Tetraspanin expression in syntenin KD and control HeLa cells determined by flow cytometry. HeLa cells were stained with primary anti-tetraspanin mAbs or isotype control (JC1) as described in 2.2.3.6 followed by FITC-conjugated anti mouse antibody. MFI =Median fluorescent intensity. **A:** MFI of live cell stained. **B**: The percentage of live cells stained, Figure A and B work was carried out in our lab by a 3rd year project students S. Howard and V. Rose (under my supervision). **C:** MFI of fixed or fixed and permeabilised cells stained. n=4 in duplicate, the data was analysed by Two ways ANOVA Tukey's multiple comparisons test comparing with isotype control, significance *** $P \leq 0.001$, ** $p \leq 0.01$ and * $P \leq 0.05$, ns is non-significant.

In immunofluorescence microscopy, the tetraspanins CD9, CD63 and CD81 staining of fixed, permeabilised cells also appeared stronger in the syntenin-KD cells compared with control cells (Figure 7.5).

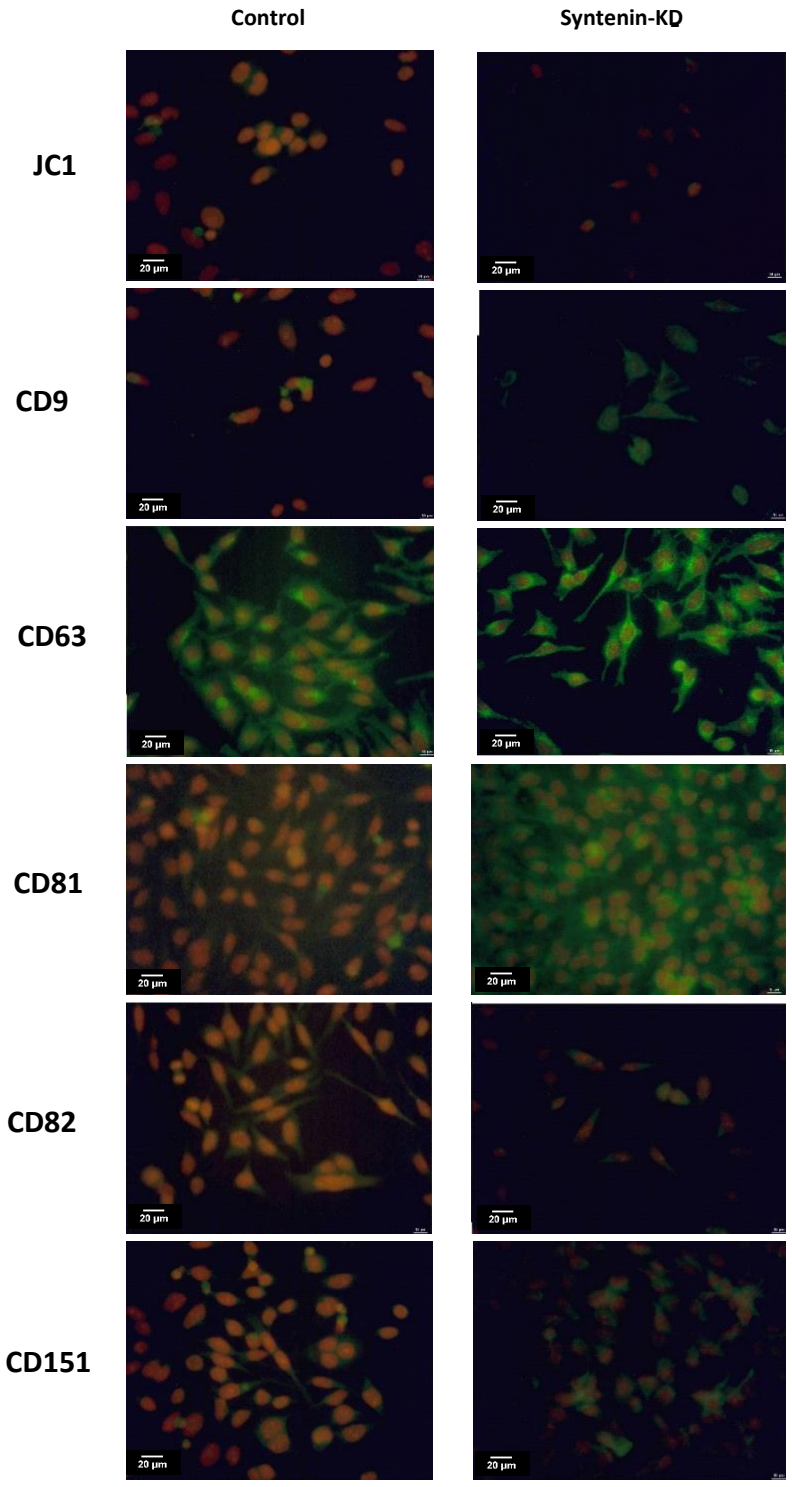

Figure 7.5: Immunofluorescence microscopy of syntenin KD and control cells stained for tetraspanins. Cells were prepared and fixed as described in Figure 7.3 before staining with anti – tetraspanin antibodies or isotype control Nuclei were counter-stained with propidium iodide. These images were obtained by fluorescence microscopy using the 40x objective.

7.3.3 HeLa cells integrin expression

The expression of integrin proteins α_3, α_6 and β_1 was also investigated in syntenin-KD cells and control HeLa cells by flow cytometry, since CD151 expression on syntenin-KD cells was significantly reduced and CD151 is known to associate with integrins (Figure 7.4 A). This work was carried out by a 4th year project student under my supervision. The flow cytometry was carried out using live cells to investigate the surface expression of these proteins. The surface expression (MFI) of β_1 integrin showed a significant reduction in syntenin KD cells compared with control cells. No significant changes were observed for other integrins (α_3 and α_6) (Figure 7.6).

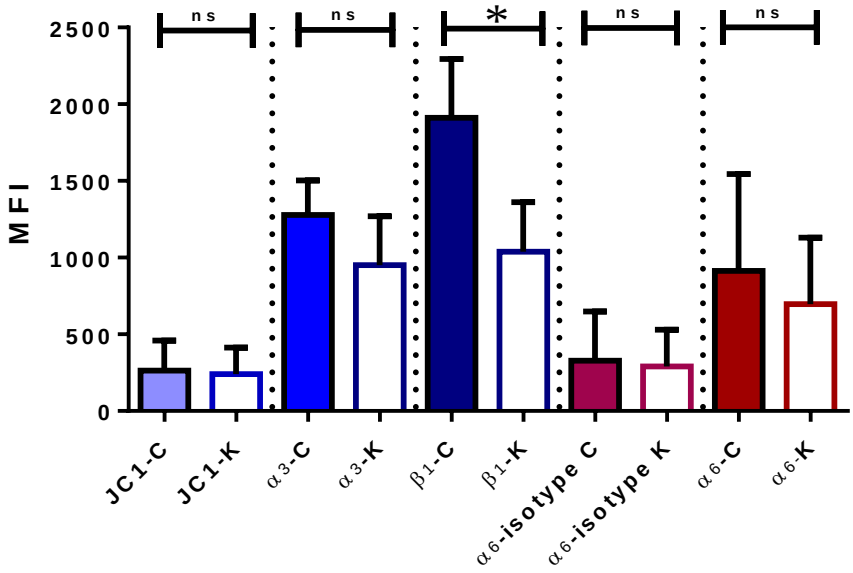

Figure 7.6: Integrins expression in syntenin KD and control HeLa cells determined by flow cytometry. Integrin expression assay carried out by M. Jones. Briefly, HeLa cells were stained with primary anti-α3, anti-β1 and anti-α6 mAbs or corresponding isotype control followed by FITC-conjugated anti mouse antibody. MFI =Median fluorescent intensity. n=3 in duplicate, the data was analysed by T- test comparing Syntenin-KD HeLa cells (**K**) with cells control (**C**), significance * $P \leq 0.05$, while ns is non-significant.

7.3.4 *Salmonella* uptake by HeLa-Syntenin KD cells compared with WT control

HeLa syntenin KD and WT control were infected by *Salmonella* Typhimurium NCTC12023 and LT2 strains at MOI 100 for 1 hr. The cells were then washed and incubated in antibiotic containing medium to kill extracellular bacteria before analysis at various time periods post-infection, as described in (2.2.5.3.2). As noticed in chapter 4 (Figure 4.15), the HeLa cells were more susceptible to infection by the LT2 strain compared to NCTC12023 strain (comparing figure 7.7. A and B, E and F). It was noticeable that at all time points and for both

strains, the syntenin KD cells appeared to have more bacteria associated with them than the control cells, although this only reached significance at certain time points when considering total cell associated bacteria and cells with internalised bacteria for the LT2 strain. However, for the NCTC12023 strain, the percentage of cells with internalised bacteria was significant at all time points.

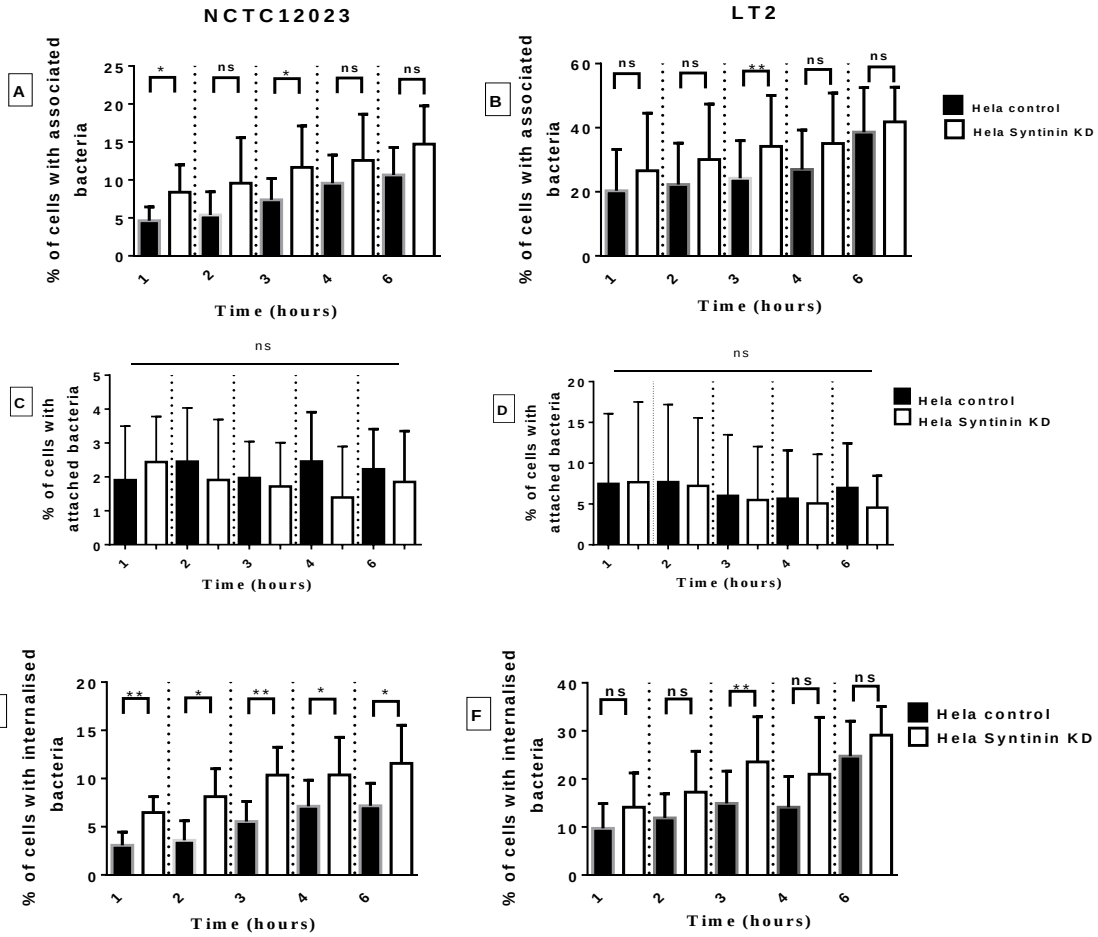

Figure 7.7: *Salmonella* Typhimurium uptake by syntenin KD or control HeLa cells at 100 MOI for different time periods analysed by flow cytometry. HeLa cells were infected with *S.* Typhimurium as described in 2.2.5.3.2 for 1hr before washing to remove unbound bacteria and incubating in medium containing 100µg ml^{-1} kanamycin for the times indicated before harvesting, fixing and permeabilising and staining with FITC-conjugated anti-*Salmonella* antibodies and analysis by flow cytometry as described in 2.2.5.3.2. **A:** Total percentage of cells infected with NCTC12023 strain (permeabilised cells) or **B:** LT2 strain (permeabilised cells). **C:** Percentage of cells with attached bacteria NCTC12023 strain or **D**: LT2 strain. **E:** Percentage of cells with internalised bacteria NCTC12023 strain or **F**: LT2 strain. (The percentage of cells with internalised bacteria was determined by subtracting the value obtained for non-permeabilised cells form that of permeabilised cells). Bars describe means, while error bars describe standard errors. n=5 in **A, C** and **E** and n=3 in **B, D** and **F** in duplicate, the data was analysed by T test to compare the mean between WT and KD infected cells, ** $p \leq 0.01$, * $p \leq 0.5$ and ns is non-significant.

To investigate possible differences in bacterial adhesion to syntenin KD and control cells, both cell lines were infected at MOI 100 for shorter time periods and the number of non-

permeabilised cells with attached bacteria determined (Figure 7.8). (In the experiments described above, the principle aim had been to investigate any differences in internalisation of bacteria. In the previous protocol it would be expected that most attached bacteria would be killed by the antibiotic treatment used after infection and removed during washing and harvesting as described in 2.2.5.3.2 and (Figure 7.7). The present experiment was carried out to observe cells with attached bacteria infected in suspension as described in 2.2.5.2. There was no significant difference in adhesion of the NCTC12023 strain to KD or control cells but at the earlier time points, the percentage of KD cells with attached LT2 bacteria was lower than for the control cells.

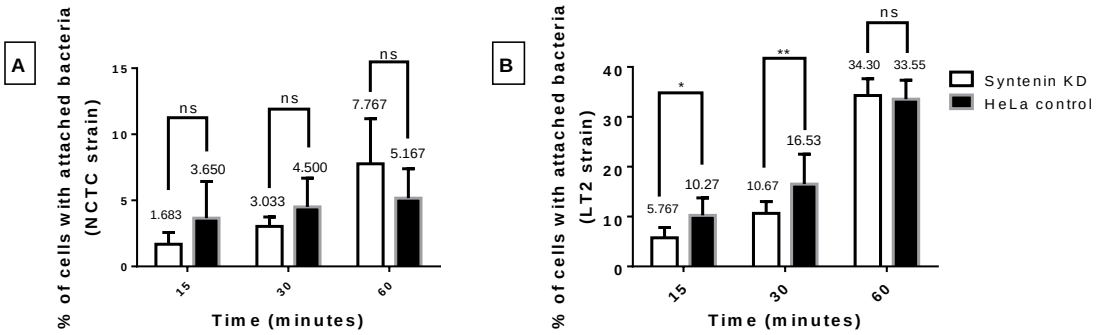

Figure 7.8: Adhesion of *Salmonella* Typhimurium to syntenin KD and control HeLa cells at 100 MOI for different time periods (analysed by flow cytometry). HeLa cells infected with *S.* Typhimurium. NCTC12023 and LT2 strains *in tube* and stained with anti-*Salmonella*-FITC conjugated antibody, as described in (2.2.5.2) without permeabilisation to observe attached bacteria only. **A:** Percentage of cells with attached NCTC12023 or **B:** LT2 strain. Bars describe means, while error bars describe standard errors. n=3 in duplicate, the data was analysed by two ways ANOVA test Sidak's multiple comparison test to compare the mean between WT and KD infected cells, ** $p \leq 0.01$, * $p \leq 0.5$ and ns is non-significant.

7.3.5 Confocal microscopy analysis of Syntenin KD cells and WT cells control infected with *Salmonell*a

Syntenin KD cells appeared to be more susceptible to infection by both strains of *Salmonell*a, but this did not appear to correlate with any difference in bacterial adhesion. Confocal microscopy studies were therefore undertaken in an attempt to see if there were any obvious differences in trafficking of *Salmonella* between the cell lines. The confocal microscopy was performed as described in (2.2.6). Different fluorescent stains were used to indicate *Salmonella*-containing vacuoles (SCVs), the nucleus, and the cell boundary and to investigate *Salmonell*a localisation within the cells cytoplasm. LAMP-1 (or CD107a) is described as a SCV marker (Brumell, Tang et al. 2002) and it co-localises with SCV at different stages of *Salmonella* infection (Rajashekar, Liebl et al. 2014). Anti-LAMP-1-AF®647 conjugate was

therefore used to detect SCV within the cytoplasm and give a good indication of *Salmonella* internalisation, survival and replication inside the infected cells. To track *Salmonella* bacteria inside infected cells, a GFP expressing *Salmonella* strain was used as described in 2.2.6. Cellular actin was stained by Alexa Fluor®568 phalloidin, to indicate the cell boundary. Preliminary experiments using flow cytometry showed similar, but slightly lower expression of LAMP-1 in syntenin-KD cells compared with controls (Figure7.9).

The LAMP-1-*Salmonella* co-localisation experiment showed an obvious increase in *Salmonella* with time after infection, as shown previously by flow cytometry (7.3.4). Syntenin KD cells showed relatively more bacteria within the cytoplasm niche compared with control cells in both *Salmonella* strains, particularly at the 24 hours post-infection time point. LAMP-1 started to co-localise with *Salmonella* at 2 hours post infection, indicating SCV biogenesis. This LAMP-1-*Salmonella* association decreased from 6 hours post infection, correlating with intracellular bacterial replication. Most of the bacteria accumulated in one place within the cell cytoplasm and no obvious differences were observed between HeLa syntenin-KD and control cells in terms of bacterial accumulation and distribution. At earlier time points (1 hour infection time point) it was difficult to determine whether the bacteria were simply attached to cells or internalised. However, localisation of LAMP-1 with bacteria revealed internalised *Salmonella,* although this could not be observed in earlier stages of infection (Figure 7.10, 7.11 and 7.12). Attempts were made to quantitate co-localisation of GFP-bacteria with LAMP-1 using Fiji software (Figure 7.12). For the LT2 strain, there was significant co-localisation at 2- 6 hr post-infection in both cell lines. The same pattern was apparent for NCTC strain in the syntenin-KD cells, but co-localisation was not significant at 2 hr for control cells and was also slightly reduced at 4 hr. This suggests that knock-down of syntenin may promote uptake of the NCTC strain, which is broadly in agreement with the observations made previously from flow cytometry (Figure 7.7).

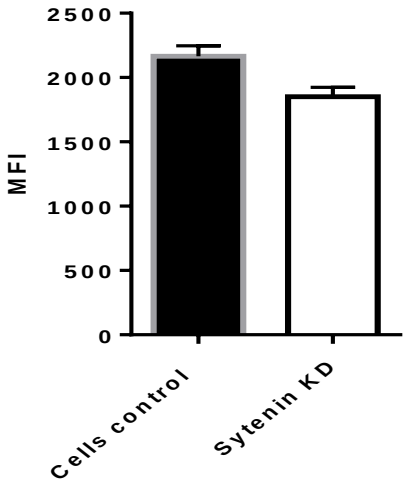

Figure 7.9: LAMP-1 expression in syntenin KD and control HeLa cell lines determined by flow cytometry. Permeabilised cells were incubated with anti-LAMP-1 AF® 647 antibody before analysis by flow cytometry using LSR-II flow cytometer as described in 2.2.3.5. Bars describe means, while error bars describe standard errors.

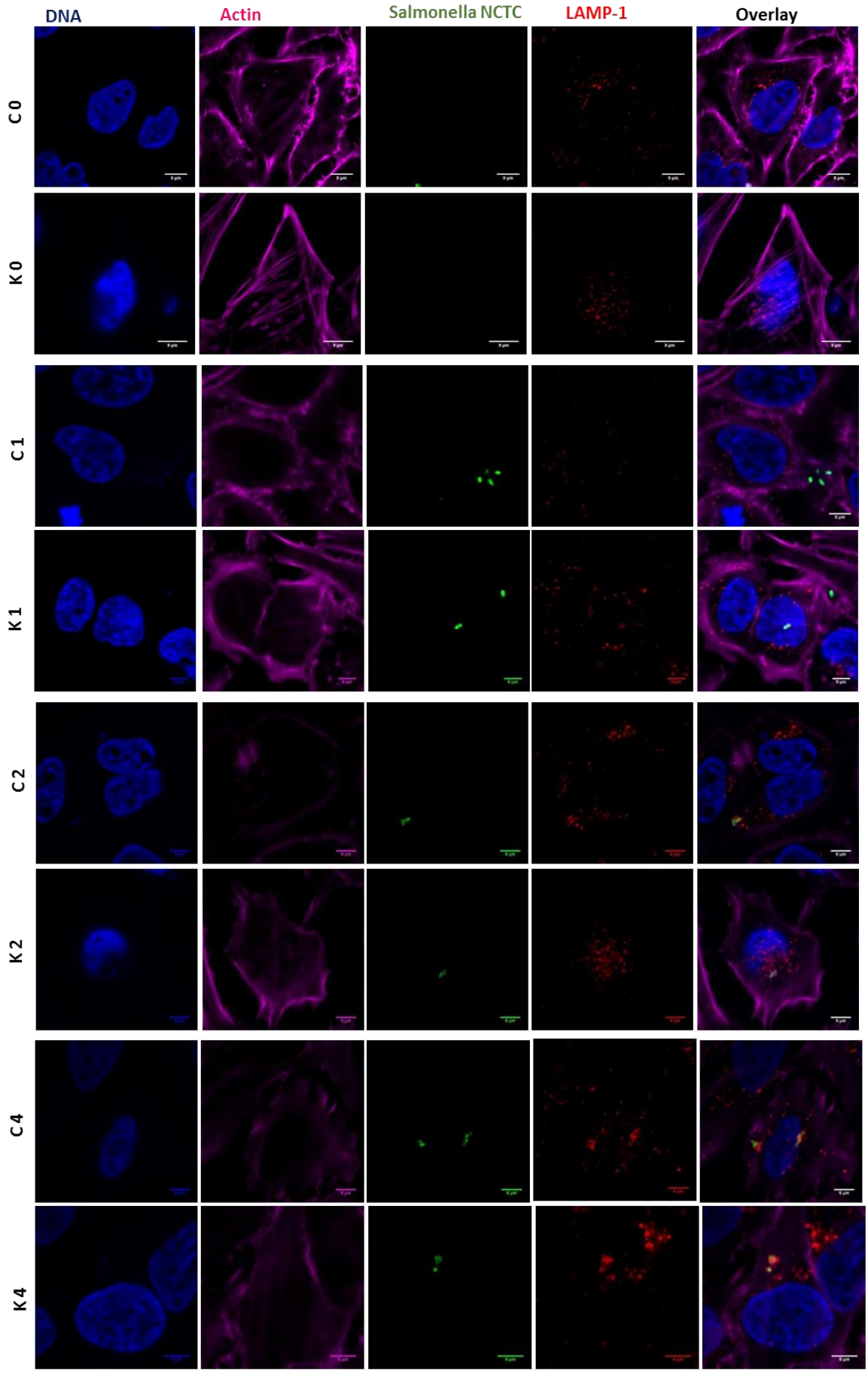
DNA
Actin
Salmonella NCTC
LAMP-1
Overlay
C 0
K 0
C 1
K 1
C 2
K 2
C 4
K 4

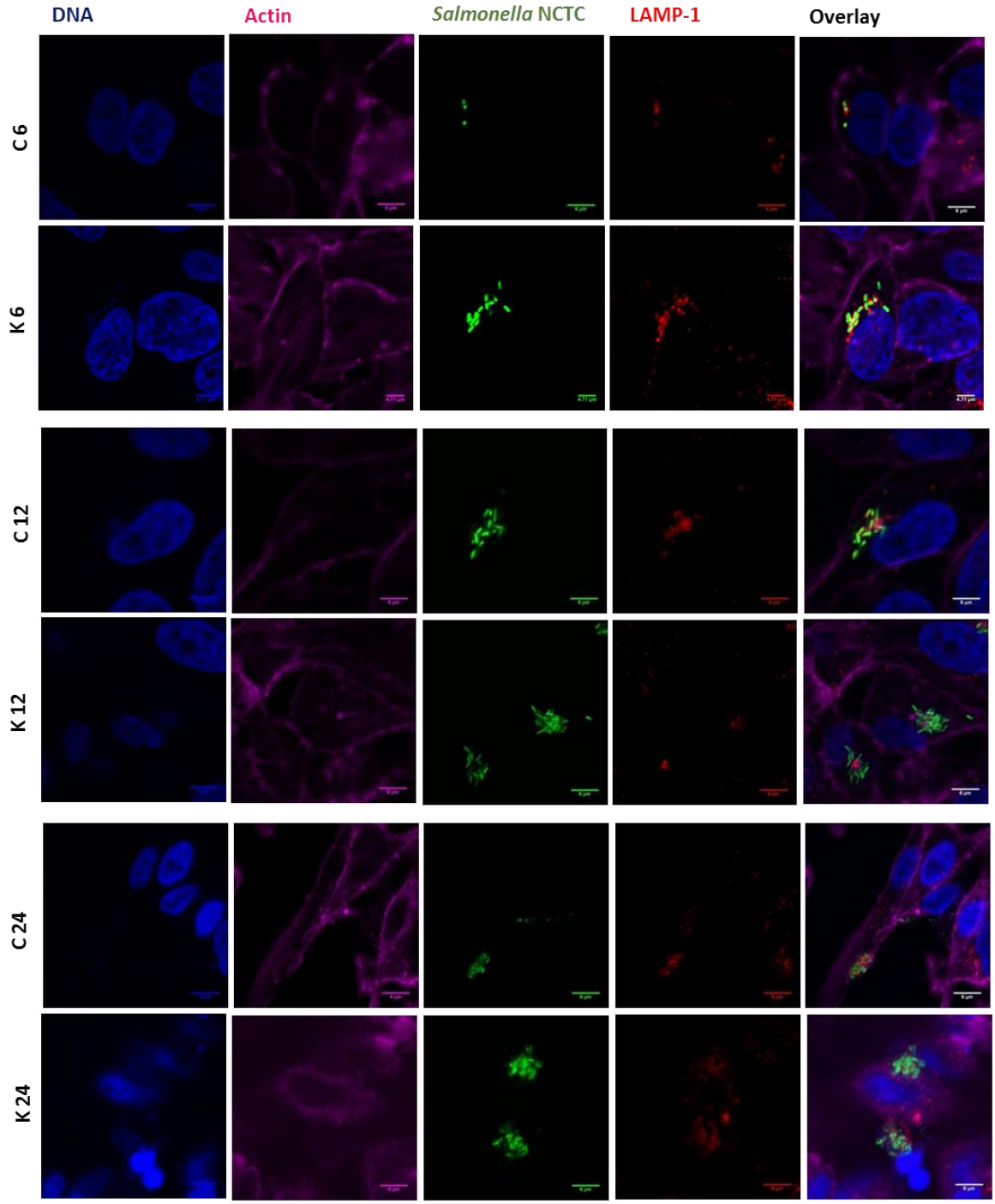

Figure 7.10: Confocal microscopy of syntenin KD or control HeLa cells infected with *Salmonella* Typhimurium NCTC12023-GFP. HeLa cells were infected at 100 MOI for 1 hour, as described in (2.2.6), then incubated with 100 Ut penicillin, 100µg streptomycin /ml for the time period indicated. The cells then were fixed and stained with anti-LAMP-1 AF®647 (red) followed by AF®568 Phalloidin (magenta, to stain actin), and cellular and bacterial DNA stained blue (DAPI) stain. **K**= HeLa syntenin-KD cells, **C**= Control cells. 1, 2, 4, 6, 12 and 24 reveals to time points for *Salmonella* infection, while 0 depicts non infected cells.

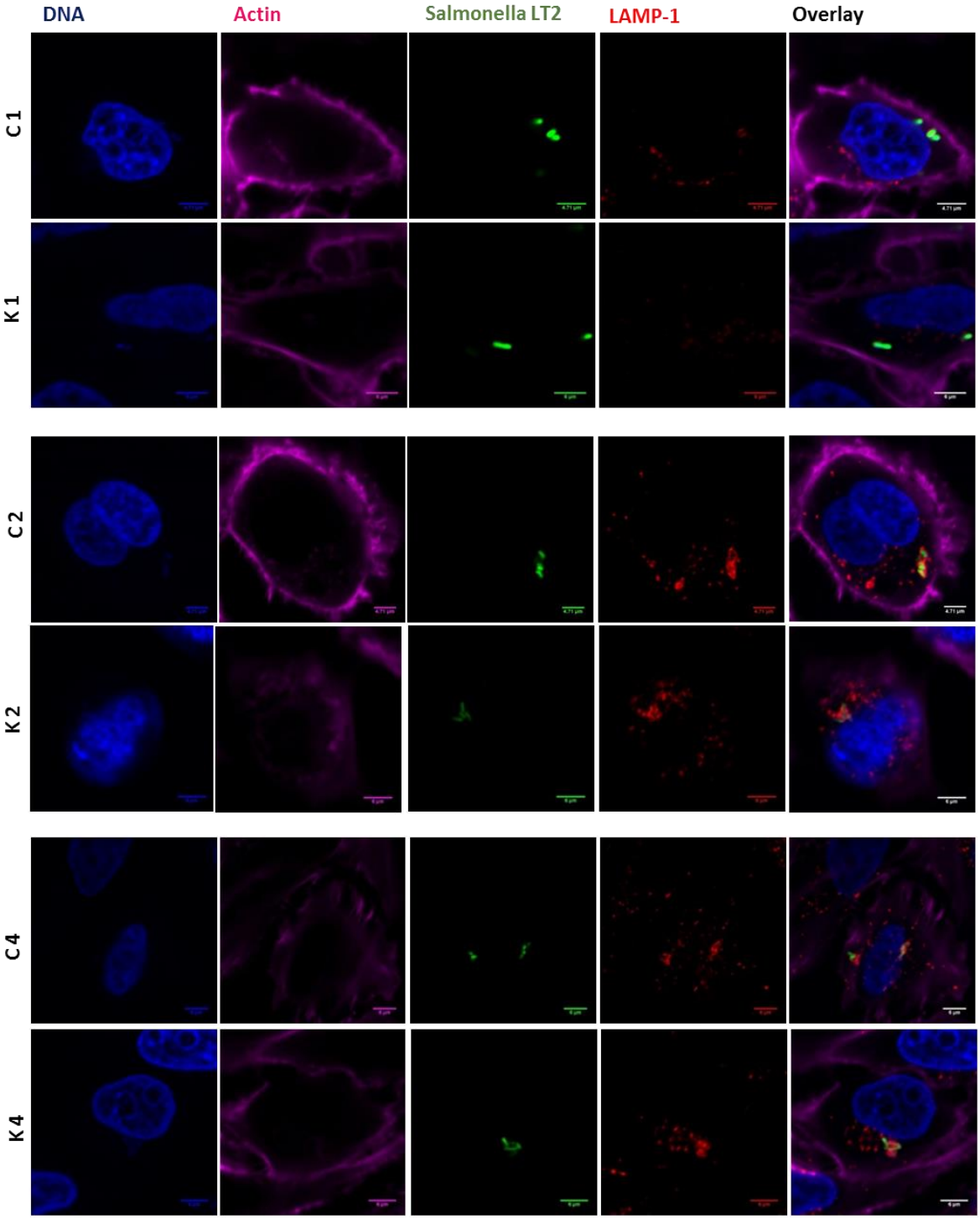
DNA
Actin
Salmonella LT2
LAMP-1
Overlay
C1
K1
C2
K2
C4
K4

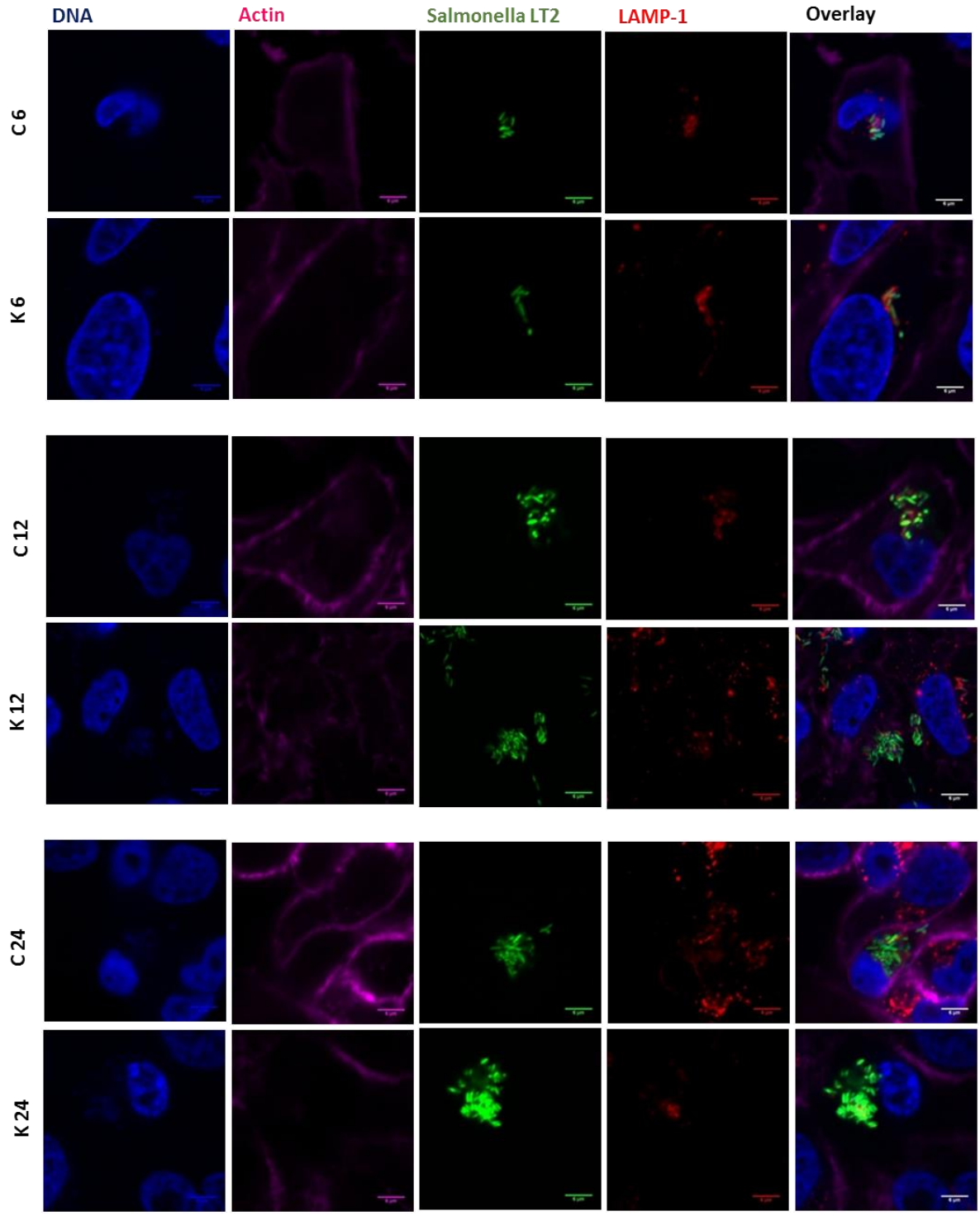

Figure 7.11: Confocal microscopy of syntenin KD or control HeLa cells infected with *Salmonella* Typhimurium LT2-GFP. HeLa cells were infected at 100 MOI for 1 hour, as described in (2.2.6), then incubated with 100 Ut penicillin, 100µg streptomycin /ml for the time period indicated. The cells then were fixed and stained with anti-LAMP-1 AF®647 (red) followed by AF®568 Phalloidin (magenta, to stain actin), and cellular and bacterial DNA stained blue (DAPI) stain. **K**= HeLa syntenin-KD cells, **C**= Control cells. 1, 2, 4, 6, 12 and 24 time points for *Salmonella* infection, while 0 mean non infected cells.

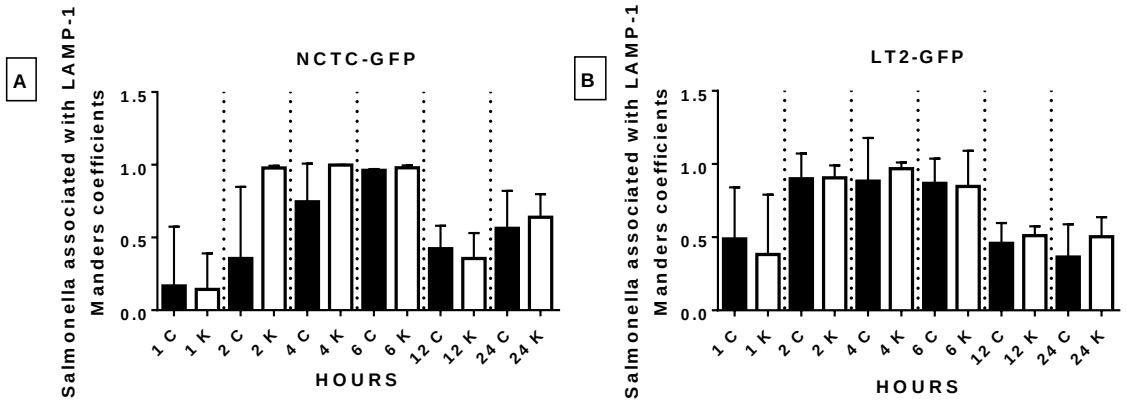

Figure 7.12: Analysis of confocal microscopy images of syntenin KD or control HeLa cells infected with *Salmonella* Typhimurium-GFP strains. HeLa cells were infected at 100 MOI for 1 hour, as described in (2.2.6), then incubated with 100 U penicillin, 100µg streptomycin /ml for the time period indicated. The cells then were fixed and stained with anti-LAMP-1 AF®647. Images were analysed using Fiji analysis software using Manders coefficients test to quantify co-localisation of *Salmonella* (GFP/green) NCTC12023 **(A**) and LT2 **(B)** and LAMP-1 (AF®647/far red). The co-localisation analysis value is between 0 (no co-localisation) to 1 (optimum co-localisation). **K**= HeLa syntenin-KD cells, **C**= Control cells. 1, 2, 4, 6, 12 and 24 reveals to time points for *Salmonella* infection.

7.4 Discussion

The 33 kd scaffolding protein, syntenin-1, is broadly expressed in different cell types and tumours and is involved in regulating membrane and cytoplasmic protein signalling pathways (Yang, 2007). It has been shown to form a direct and stable association with tetraspanin CD63 and is postulated to be a constituent of TEM (Latysheva, Muratov et al. 2006). Syntenin-1 expression regulated CD63 internalisation and overexpression of syntenin-1 reduced internalisation of CD63. In the present study, we investigated HeLa cells that had been stably knocked down for syntenin expression by transfection with a plasmid encoding shRNA specific for syntenin. Knockdown of syntenin expression was verified independently by Western blotting compared to control HeLa cells transfected with empty vector. Analysis by flow cytometry showed no significant differences in cell surface CD63 expression between syntenin-KD and control cells (Figure 7.4), but there were slight but significantly higher levels of CD63 in permeabilised KD cells indicating higher intracellular levels of this tetraspanin. Since Latysheva and co-workers showed that overexpression of syntenin-1 reduced CD63 internalisation (Latysheva, Muratov et al. 2006), knock down of syntenin-1 might increase CD63 internalisation that could, consequently, increase expression of CD63 to compensate. A slight, but significant increase in total CD81, was also observed, and this tetraspanin was shown by Latysheva and co-workers to associate with syntenin indirectly, probably through its interaction with CD63.

CD151 was the only tetraspanin investigated that showed a difference in cell surface expression, with a slight but significant decrease in the level on unfixed syntenin-1 KD cells relative to controls. A possible interaction between cell surface CD151 and syntenin-1 was not reported in the previous study (Latysheva, Muratov et al. 2006). It would be interesting to determine if CD151 and syntenin could be co-immunoprecipitated from whole cell lysates of HeLa cells. Interestingly, CD151 is known to be strongly associated with integrins including α3β1, α6β1, α6β4 and α7β1 integrins (Hemler 2014) and syntenin is reported to facilitate the assembly of β1 integrin signalling complexes on the plasma membrane (Hwangbo, Park et al. 2011). Syntenin also strongly associates with syndecan, which also has been shown to be involved with β1 integrin cell adhesion (Gama-de-Souza, Cyreno-Oliveira et al. 2008). Thus, integrins (α_1, α_6 and β_1) expression in both cell lines were also investigated, as shown in (Figure 7.6). A significant reduction of β_1 integrin in syntenin-KD cells was observed compared with control cells, however, no significant change in either α_3 or α_6 integrin surface expression was observed. This suggested, therefore, the reduction in CD151 expression in syntenin-KD cells may be linked to its integrin β_1 association. This could be affected by knock-down of syntenin or through syndecan.

As discussed previously in this thesis, *Salmonella* Typhimurium has the ability of to infect mammalian non phagocytic cells by a sequence of steps starting from bacterial adhesion to host cells, activation of *Salmonella* T3SS-1 and spreading a wave of off effector proteins to trigger the rearrangement of the host cells actin-cytoskeleton (Misselwitz, Kreibich et al. 2011). Here, both control and syntenin-1 knock down HeLa cells were infected by *S.* Typhimurium. The infection rate was relatively low, but comparable with that seen in wild type HeLa cells (Figure 4.15) and again the LT2 strain showed greater infectivity than the NCTC strain. Infection of syntenin-1 KD cells was consistently higher compared to control cells and this showed greatest significance in the increased number of NCTC bacteria internalised by the syntenin-1 KD cells (Figure 7.7 E). Analysis of images obtained of GFP-bacteria taken up by the two cell lines also suggested increased uptake by the syntenin-1 KD cells and co-localisation of NCTC bacteria and LAMP-1 occurred earlier in the syntenin-1 KD cells (Figures 7.12). However, there were no significant differences in adhesion of the bacteria to the cell lines after 1 hour (the time period used for infection) (Figure 7.8).

These studies were undertaken since previous data on human MDM indicated that surface expression of CD63 is important in adhesion of *S.* Typhimurium to these cells. Syntenin-1 has previously been shown to regulate internalisation of CD63 (Latysheva, Muratov et al. 2006), but surprisingly there was no significant change in surface levels of CD63 between control and syntenin-1 KD cells. Interestingly, however, preliminary results from stochastic

optical resolution microscopy (STORM), have shown a significant change in cell membrane CD63 distribution and clustering between the cell lines. In brief, clusters of CD63 are smaller in terms of diameter and area in syntenin KD cells compared with control HeLa cells (Megan Jones, MSc student project, 2016). This, together with the observed decrease in CD151 expression, suggests some disruption of TEM on the syntenin KD cells; however, there is no clear relationship between the increased infection in the syntenin-1 KD cells and the tetraspanins. As reported in chapter 4, antibodies to tetraspanins, including CD63, had no effect on infection of *Salmonella* Typhimurium by wild type HeLa cells. The differences in infection may therefore relate to the interactions of syntenin with other partner proteins involved in plasma membrane/cytoskeletal proteins signalling. As mentioned previously, syntenin-1 binds syndecans, a family of proteoglycans with heterogeneous heparan sulphate chains (Grootjans, Zimmermann et al. 1997). Interestingly, it has been shown that *S.* Typhimurium can utilise heparan sulphate as a means of adhering to and invading host cells. This is mediated by PagN, a bacterial outer membrane protein (Lambert and Smith 2009). It is possible that alterations in syndecan organisation or trafficking in the syntenin-1 KD cells has some effect on infection of the Hela cells by *S.* Typhimurium. Syndecan-1 and syndecan-4 have been shown to have a role in *Neisseria gonorrhoeae* adhesion and uptake; over expression of syndecan-1 and 4 in HeLa cells led to increased *Neisseria gonorrhoeae* uptake compared with WT control and it was concluded that syndecan may serve as a receptor for *Neisseria gonorrhoeae* (Freissler, Meyer auf der Heyde et al. 2000). Furthermore, Syndecan-1 KO epithelial cells show more resistance to *Staphylococcus aureus* infection (Hayashida, Amano et al. 2011).

The intracellular *Salmonella* survive through disrupting and arresting the maturation pathway of the invasion vacuole and, consequently, this provides a safe place for *Salmonella* replication (Brumell and Grinstein 2004). The SCV is found to acquire lysosomal membrane glycoprotein Lamp1, CD63 and vacuole ATPase (Martinez-Lorenzo, Meresse et al. 2001). In addition to these lysosomal markers, the host proteins Rab5, EEA1 and late Rab7 endosomal marker are also acquired during the early steps of SCV biogenesis. The involvement of early and late endosomal markers presents the potential for host/SCV interaction along with the action of T3SS effectors such as SifA (required for SCV membrane stability) to provide *Salmonella* Typhimurium an intracellular niche to replicate. Maturation of the SCV occurs by specific interactions with the endocytic pathway, in which most of the SCVs are surrounded by Golgi network membranes after invasion of epithelial cells (da Silva, Cruz et al. 2012) and as discussed in Chapter 1. The T3SS effector protein SipC is involved in acquiring LAMP-1 protein through its association with the host cell protein Syntaxin6

(Madan, Rastogi et al. 2012). Loss of SCV integrity has been shown to lead to increased cytosolic *Salmonella* replication in HeLa cells and this could arise by targeting either the SCV effectors involved or the cells endosomal system (Brumell, Tang et al. 2002). It is suggested that maintaining SCV in epithelial cells may prevent antigen presentation via MHCI and activation of proinflammatory responses. LAMP-1 has been shown to be a good SCV marker, so this protein was used for confocal microscopy. Preliminary experiments showed a noticeable reduction in LAMP-1 expression in syntenin-KD cells by flow cytometry (Figure 7.9). However, no noticeable differences in LAMP-1 association with *Salmonella* was observed in syntenin-KD compared with control cells. A highly significant association of LAMP-1 with replicating intracellular *Salmonella* was observed after 2 hours infection and this increased at 4 to 6 hour. Nonetheless, this association decreased after 12 to 24 hours post infection at the time when the internalized bacteria show a high level of replication.

In macrophages, *Salmonella* could overcome lysosomal action by containing every single bacterium in a single SCV resulting in increased SCVs and *Salmonella* replication inside the cells. This is reported to deplete the number of acidic lysosomes in infected cells as a result of increasing *Salmonella* multiplication as the cell cannot produce enough acidic lysosomes to target the rising number of SCVs (Eswarappa, Negi et al. 2010).

Chapter 8: General discussion

Tetraspanins are increasingly observed to be of importance in various cell activities and have attracted the interest of many researchers due to their role in infections (Hassuna, Monk et al. 2009, van Spriel and Figdor 2010, Green, Monk et al. 2011, Monk and Partridge 2012). Nevertheless, relatively little research has been published describing the association of tetraspanins with bacterial infection processes. Work from our group indicates that certain tetraspanins are involved in bacterial adhesion and uptake; mAb specific for CD9, CD63 and CD151, the corresponding recombinant EC2 domains and siRNA knockdown of each of these tetraspanins reduced *Neisseria meningitidis* adhesion to human epithelial cells (Green, Monk et al, 2011; Cozens, 2015, PhD thesis, University of Sheffield). In addition, tetraspanins were implicated in the adhesion of a range of other bacteria (*Neisseria lactamica*, *Streptococcus pneumonia*, *Escherichia coli*, *Staphylococcus aureus*) to epithelial cells (Green, Monk et al, 2011), suggesting a general bacterial adhesion mechanism involving TEM. More recently, reagents targeting CD9 have been shown to reduce adhesion of *Staphylococcus aureus* to human keratinocytes and a 3-D model of human skin (Ventress, PhD thesis, University of Sheffield 2016; Ventress et al., manuscript submitted). Of particular relevance to this work, anti-CD63 mAb, siRNA CD63 knockdown and recombinant tetraspanin EC2 proteins also reduced *Salmonella* Typhimurium uptake by human primary MDMs (Hassuna, 2010, PhD thesis, University of Sheffield). However, more studies are needed to understand this association.

The ability of *Salmonella* to attach to, invade and replicate in wide range of host cells and cell lines representing either phagocytic on non-phagocytic cell types (Finlay, Ruschkowski et al. 1991, Mills and Finlay 1994, Lajarin, Rubio et al. 1996, Haraga, Ohlson et al. 2008, Rosales-Reyes, Perez-Lopez et al. 2012) make this bacteria ideal as a model to investigate the involvement of tetraspanin proteins in the infection process. As previously discussed, the ability to invade non-phagocytic cells is mediated by T3SS-1 (Rosselin, Abed et al. 2011), whereas macrophage infection can also be mediated by phagocytosis (Aderem and Underhill 1999). *Salmonella* is able to survive in macrophages and these cells may play an important role in bacterial survival and spread (Lathrop, Binder et al. 2015). In the present study, different cell lines, representing mouse and human macrophages as well as human epithelial cells, were used to investigate the potential effect of tetraspanin proteins on *Salmonella* infection.

Previous studies in the laboratory investigated the role of tetraspanins in the uptake of *Salmonella enterica* serovar Typhimurium by human monocyte derived macrophages

(MDMs). Specific monoclonal antibodies (mAbs) for various tetraspanins showed different effects, enhancing (CD37) or inhibiting (CD63) *Salmonella* binding to cells. The inhibition of *Salmonella* binding to MDMs was shown by using recombinant proteins corresponding to CD63-EC2 and CD9-EC2. In addition, the siRNA-mediated knockdown of CD63 also reduced *Salmonella* Typhimurium adhesion (Hassuna, PhD thesis, University of Sheffield 2010)

Immunofluorescence microscopy showed that CD63 co-localized with *Salmonella* containing vacuoles (SCVs) at different time periods after infection. Overall from this study an important role for tetraspanin CD63 in the initial binding of *Salmonella* Typhimurium to macrophages was suggested, with the likely involvement of other tetraspanins (Hassuna, PhD thesis, University of Sheffield 2010). However, one of the drawbacks of relying on MDMs are donor variation and the difficulty of generating these cells in large amounts. Therefore, using macrophage cell lines such as J774.2 and RAW 247 could overcome this problem. However, these cell lines are of murine origin and relatively few antibodies to native murine tetraspanins are available. Thus, we also aimed to develop a human macrophage cell line model of infection using human THP-1 cells to investigate the role of tetraspanins in *Salmonella* infection. In parallel, tools were developed including *Salmonella* self-expressing fluorescent proteins and a flow cytometry assay to assess *Salmonella* infection, which could help to obtain rapid and objective results. Approaches used to investigate the function of tetraspanins included the use of specific monoclonal antibodies, recombinant EC2 proteins and a stable CD9 knock-out macrophage cell line. Furthermore, the role of the CD63 tetraspanin partner protein, syntenin, on *Salmonella* infection of HeLa cells was also studied.

Screening surface expression of the tetraspanin proteins showed a similar pattern for the mouse macrophage cell models J774, RAW (Figures 3.1 and 3.3) and WT mouse macrophages (Figure 6.3), with highest expression for CD9 followed by relatively high levels of CD81, while CD63 showed lower expression in RAW and WT mouse macrophages with no expression on J774. By contrast, macrophages derived from human THP-1 cells, showed higher expression of CD63 than CD9, with relatively high expression of CD81 compared with the mouse macrophage cell lines (Figure 3.5). Differences in expression patterns were also observed in the epithelial cell lines used, HEC-1-B and HeLa; although both cell lines showed high expression of CD9 and CD81, higher expression of CD151 was observed in HeLa cells (Figure 3.9) with only low expression of this tetraspanin on HEC-1-B (Figure 3.7).

Chapter 3 also describes attempts to generate fluorescent bacteria to try to enhance and facilitate assessing *Salmonella* infection. Different vectors carrying the GFP or RFP genes were used. The GFP protein seems to be stably expressed and detected in both *Salmonella* strains by FACS (Figure 3.12), either as *Salmonella*-GFP alone or in cells associated with *Salmonella*-GFP. A 28 kDa DsRed fluorescent protein that shows less susceptibility to pH (4.5-12), more resistance to an acidic environment than GFP and less sensitive to photo-bleaching (Baird, Zacharias et al. 2000) could offer a good *Salmonella* detector particularly with tetraspanin-GFP tagged protein. However, in contrast to GFP, generating high and stable self-expressing RFP *Salmonella* seemed to be more difficult, despite the fluorescent protein being well-expressed in *E. coli*. The percentage of positive cells and fluorescence intensity for *Salmonella* expressing DsRed were unstable and varied depending on *Salmonella* strains, time period of incubation and concentration of selective antibiotic (Chapter 3, section 3.3.3). This could be related to more time being needed to obtain dimerization and maturation (Baird, Zacharias et al. 2000). Therefore, choosing another RFP protein, mCherry was recommended. The expression of mCherry in *Salmonella* was successful, although lower expression of this florescent protein was observed after 2 hours incubation compared with overnight cultures. mCherry has the advantage of no overlapping in emission detected either by fluorescence microscopy or by FACS, in contrast to DsRed (as described in section 3.3.3). The mCherry fluorescent protein was found to be relevant for bacterial investigations combined with GFP expressing cells or FITC-labelled antibodies for fluorescence microscopy.

8.1 Development of tools to assess *Salmonella* infection

Flow cytometry analysis has the potential to offer a rapid and appropriate method to study bacteria-host invasion. Other workers have reported it to be comparable with other methods for investigating bacterial pathogenicity and bacterial: host interaction, particularly when combined with self-fluorescence expressing bacteria (Valdivia and Falkow 1998, Pils, Schmitter et al. 2006, Trouillet, Rasigade et al. 2011). Nevertheless, high levels of fluorescent protein expression or features of the plasmid construct used could interfere with *Salmonella* invasion properties (Wendland and Bumann 2002, Clark, Martinez-Argudo et al. 2009). Here, a flow cytometry assay was developed for assessing infection, and shown to be comparable with the microscopy assay with the advantage of giving more objective results. In assays where antibodies were used to stain *Salmonella* after infection, the results were very comparable with the conventional fluorescence microscopy method (Chapter 4, comparing the results shown in Figure 4.3 and 4.4 with Figure 4.10; Figure 4.9 with 4.11). Interestingly, a lower MOI was needed to reach similar infection levels in the flow cytometry assay, and

we speculate that when cells are incubated with bacteria in suspension, bacterial binding may be facilitated compared to cells adhered to coverslips.

8.2 Tetraspanins effects on *Salmonella* uptake

The overall results show a significant reduction in *Salmonella* NCTC12023 infection after treating the mouse macrophage cell model with anti-CD9 and CD81 prior to *Salmonella* infection (Figure 4.3, Figure 4.4, Figure 4.10, and Figure 6.7 B). This contrasts with previous studies on human MDM, where no inhibition with anti-CD9 mAbs was observed; however recombinant soluble CD9-EC2 proteins inhibited *Salmonella* association with human MDM suggesting that this tetraspanin is involved in this process (Hassuna, PhD thesis, University of Sheffield 2010), and it has been found that anti-CD9 antibody inhibited adhesion of bacteria to human epithelial cell lines (Green, PhD thesis, University of Sheffield 2010). Interestingly, in the present study, no effect on cell associated bacteria in human THP-1 derived macrophages was noticed (Figure 4.5) when these were pre-treated with the same anti-CD9 antibody used in the human MDM experiments, where it also showed no effect. The differences in the effects of the anti-CD9 antibodies may relate to differences between mouse and human cell CD9 or the relative levels of CD9 expression compared with other tetraspanins including CD63, (as described in chapter 3, Figure 3.1, 3.3 and 3.5) that may affect TEMs structure and organisation. There were no effects with anti-CD63 in contrast to previous studies, but this is likely to be due to the apparent absence of CD63 on the mouse macrophage cell line used. As found in the previous studies on human MDM, anti-CD63 antibodies inhibited association of *Salmonella* NCTC12023 to THP-1 derived macrophages. In contrast, anti-CD81 and anti-CD151 antibodies caused inhibition of infection of THP-1 macrophages, whereas no effect was seen with human MDM. The level of tetraspanin expression (chapter 3) may account for the differences in cell-bacteria association, since low levels of CD151 were shown to be expressed in human MDMs (Hassuna, PhD thesis, University of Sheffield 2010). Interestingly, anti-CD151 antibodies were previously found to reduce *Neisseria meningitidis* adhesion to human epithelial cells (Green, Monk et al. 2011) and found to be required for *Listeria monocytogenes* invasion of the human epithelial HeLa cell line (Tham, Gouin et al. 2010).

Different patterns of results were seen in some cases for cells infected with the *Salmonella* LT2 strain compared to NCTC12023 post anti-tetraspanin treatment (comparing Figure 4.6 with 4.7; Figure 4.14 in macrophages derived THP-1 and in undifferentiated THP-1 respectively). In macrophages derived from THP-1 by phorbol ester treatment, the inhibitory effect of anti-CD63, anti-CD81 and anti-CD151 antibody pre-treatment is more pronounced

in cells infected with *Salmonella* NCTC12023 than for the LT2 strain. Also no reduction by anti-CD81 was observed for undifferentiated THP1 cells infected with LT2, in contrast to the NCTC12023 strain. Higher rates of infection were observed for the LT2 strain compared with NCTC12023 in epithelial cell lines (Figure 4.11 E and F and G and H (HEC-1-B); Figures 7.7 and 7.8 (HeLa cells). This could perhaps relate to differences in SPI-1-T3SS expression depending on *Salmonella* strains. It has been reported that *S.* NCTC12023 has less ability to invade epithelial cell lines, which may be due to low expression of prgH that is important for needle complex formation in other *Salmonella* Typhimurium strains (Clark, Perrett et al. 2011). As expected, *Salmonella* were attached to and internalised by HEC-1-B and HeLa cells after one hour incubation (results described and discussed in chapter 4 and chapter 7). However, no significant change in cells associated with bacteria on pre-treatment with anti-tetraspanin antibodies was observed in HEC-1-B cells infected with either of the *Salmonella* strains (Figures 4.9 and 4.11). This finding appears to contrast with a previous study that showed a reduction in cells associated with attached *Salmonella* NCTC12023 in HEC-1-B cells that had been pre-treated with a combination of all three antibodies (CD9, CD63 and CD151) before infection (Green, 2010, thesis, University of Sheffield). Using a combination of all three antibodies could have a greater effect on TEMs by disrupting wider areas and affecting various tetraspanin associated proteins within the structure of TEMs. The results presented here could also indicate less involvement of tetraspanins and uptake mediated by *Salmonella* T3SS. Interestingly, infection of MDMs by *Salmonella* induced to express high levels of T3SS was less affected by anti-CD63 antibodies (Noha Hassuna, PhD thesis 2010). This also contrasts with results reported that anti-CD81 reduced *Listeria meningitidis* uptake by HeLa cells (Tham, Gouin et al. 2010). Different bacterial types, strains and mode of uptake might cause this diversity in tetraspanins responses.

8.3 Recombinant EC2 domain effects on *Salmonella* uptake

As previously discussed, recombinant tetraspanin EC2s, including CD9-EC2, have been shown to inhibit bacterial binding to human epithelial cells (Green, Monk et al 2011; Daniel Cozens, PhD thesis University of Sheffield 2015). It was suggested that the soluble EC2s were disrupting interactions of native membrane tetraspanins in TEMs that were proposed to act as "adhesion platforms" for the bacterial adhesion. This was similar to the finding that CD9-EC2 inhibited attachment of human leukocytes to endothelial cells. Here, the suggested mechanism, supported by electron microscopy and fluorescence imaging, was that this recombinant protein competed with the native membrane CD9-EC2 and interfered with its action for its heterophilic and homophilic protein associations (Barreiro, Zamai et al. 2008).

Also as previously reported soluble recombinant CD9 EC2 inhibited adhesion of *Salmonella* Typhimurium to human MDM (Noha Hassuna, PhD thesis, University of Sheffield 2010). Therefore, a recombinant version of the EC2 of tetraspanin CD9 was also used in the present study to investigate the role of this tetraspanin in *Salmonella* uptake by J774 cells as described in Chapter 5. Soluble, recombinant versions of human CD9 (hCD9) that had previously been produced in our lab were first used, since there is high homology between human and mouse CD9-EC2 (77% identity). In addition, hCD9-EC2 was functionally active in inhibiting giant cell formation induced by *Burkholderia thailandensis* in J774 cells (Atiga Elgawidi, personal communication).

No significant change in cells associated with bacteria was seen, even in cells pre-treated with high concentrations of EC2 (1000nM) prior to infection. This was surprising, since as described in chapter 4, a significant reduction in cells associated with bacteria on anti-CD9 pre-treatment of in J774 cells was demonstrated (Figure 5.1). The same preparation of EC2 had been shown to be correctly folded and detected using conformation-sensitive antibodies. It also had biologically activity in other assays, inhibiting *N. meningitidis* adhesion to human HEC-1B epithelial cells (Dan Cozens, PhD thesis, University of Sheffield 2015) and giant cell formation induced by *B. thailandensis* in J774 cells as described above. Nonetheless, species variation may be important in some functions. DNA corresponding to mouse CD9 EC2 was therefore cloned and used successfully to generate recombinant mouse CD9-EC2-GST. This was produced and purified and detected by monoclonal antibodies targeting mouse CD9 (chapter 5, Figure 5.8, 5.9 and 5.11 B) but not human CD9 (Figure 5.11 C). Pre-treatment of J774 with mCD9-EC2-GST before *Salmonella* NCTC strain infection again showed no significant effect compared with the GST control. However, this preparation of mCD9-EC2 was biologically active in another assay involving mouse macrophages, as it suppressed J774 fusion induced by *Burkholderia thailandensis* (Atiga Elgawidi, personal communication).

The differences in results between cells treated with antibodies or with recombinant EC2 domain may indicate that *Salmonella* binding to J774 cells is not dependent on TEMs and the antibodies are acting in a different way here. Alternatively, it could relate to the differences in methods used to assess bacterial infection (the flow cytometry method was carried out in the current study while Green et al (2011) used immunofluorescence microscopy, although the methods appeared very comparable when the effects of antibodies were investigated). If time had permitted, it would have been useful to investigate the effects of the CD9-EC2 proteins on bacterial adhesion to epithelial cell lines using flow cytometry. Alternatively, it could be that the recombinant EC2 lacks some feature needed for activity in this particular

instance. It may have been interesting to look at other tetraspanin EC2s, for instance CD81, since antibodies to this tetraspanin also affected *Salmonella* infection of mouse macrophages. Further investigation is also needed to gain insight into the dynamics of action of EC2 and/or antibodies in *Salmonella* infection, such as electron microscopy or super resolution microscopy and using labelled EC2 protein to investigate its binding to cells. Unlike *N. meningitidis*, little is known about "receptors" for *Salmonella*.

To further investigate the role of CD9 in infection of mouse macrophages by *Salmonella*, macrophage cell lines derived from CD9 KO and corresponding wild type mice were used, as detailed in Chapter 6. There was no difference in the infection of CD9KO or WT macrophages by the NCTC12023 strain of *Salmonella*, but surprisingly CD9KO macrophages were more susceptible to infection by the LT2 strain. However, the corresponding wild type macrophages were less susceptible to infection by the LT2 strain compared with the NCTC12023 strain. This contrasts with human epithelial cells, where as described above, the LT2 strain showed greater infectivity. This might be related to the differences in *Salmonella* Typhimurium strains T3SS effector protein expression, as mentioned previously (Clark, Perrett et al. 2011). Moreover, it has been indicated that the T3SS is also important for *Salmonella* survival after uptake by macrophages (Cirillo, Valdivia et al. 1998). The differences in *Salmonella* strains uptake could also relate to differences in the uptake mechanism, with the LT2 strain seeming to be more resistant to infection by the phagocytosis route than the *Salmonella* strain NCTC12023 in the wild type macrophage cell line.

CD9 gene knock out also affected protein expression of other tetraspanin members; a significant reduction in cell surface expression of CD81 in CD9 KO cells was found. CD9 and CD81 are known to associate with one another (Gustafson-Wagner and Stipp 2013) and this suggests a role for CD9 in correct trafficking of CD81 in these cells. In RNA microarray analysis, expression of several genes were found to be highly and significantly ($p \leq 0.05$ and 1.5, $\log^2$, fold change) affected after knocking-out CD9, either downregulated (including Xist, Cdkn2a and Smpl3a) or upregulated (including Pvrl3 and Spink5). These results present the possible role of CD9 in the expression of these proteins at mRNA level. Further study may be needed to confirm these changes using qPCR and their protein expression levels using antibodies.

8.4 Syntenin and *Salmonella* infection in HeLa cells

A direct association of syntenin-1 with tetraspanin CD63 has been shown and the protein is postulated to be a constituent of TEM and affect CD63 internalisation (Latysheva, Muratov et al. 2006). CD63 involvement in *Salmonella* uptake has shown previously using MDMs (Hassuna, PhD thesis, University of Sheffield 2010) and in the present study anti-CD63 antibodies reduced *S.* Typhimurium NCTC12023 association with THP-1 derived macrophages (Chapter 4). It was therefore of interest to investigate a direct or indirect role for syntenin-1 in *Salmonella* infection using HeLa cells stably knocked down for syntenin expression. As described in chapter 7, (Figure 7.4), there was little difference in cell surface expression of CD63 although higher cytosolic levels of CD63 were observed in syntenin KD HeLa cells; this could relate to the role of syntenin in CD63 internalisation (as discussed in 7.4). However, interestingly, preliminary STORM microscopy results have shown that surface CD63 distribution and clustering were significantly changed between the cell lines (described in chapter 7, 7.4) (Megan Jones, MSc student project, 2016). Furthermore, a reduction of CD151 expression was observed in syntenin KD cells. CD151 is directly associated with integrins including α3, α6β1, α6β4 and α7β1 integrins (Hemler 2014), and enhances their signalling complex assembly on cell membranes (Hwangbo, Park et al. 2011). The β1integrin subunit expression, but not α3 and α6 subunits, was significantly decreased on the syntenin KD cells. An association of syntenin with syndecan that is also associated with β1 integrin cell adhesion molecules has been reported (Gama-de-Souza, Cyreno-Oliveira et al. 2008). *Salmonella* infection was assessed by flow cytometry and the results supported by immunofluorescence imaging of infected cells; the *S.* LT2 strain showed a higher infection rate compared with NCTC12023 strain, and in both strains, syntenin KD cells were more susceptible to infection than control cells (chapter 7, Figure 7.7). However, no significant changes were observed in the early stages of *Salmonella* adhesion, even though, from previous studies, CD63 appeared to be important to *Salmonella* adhesion into MDMs. Also, as reported in Chapter 4, antibodies to CD63 had no effect on uptake of GFP-*Salmonella* by wild type HeLa cells. The results with the reduction of CD151 and β1 expression in syntenin KD cells, together with preliminary STORM microscopy, suggested disruption of TEM in syntenin KD cells. However, there is no clear link here between TEM and bacterial adhesion as was found previously for human macrophages. As discussed in Chapter 7, the effects of syntenin knock down may therefore relate to its interaction with other partner proteins such as syndecan. Syntenin-1 is an adaptor protein that is known to be involved receptor trafficking (Beekman and Coffer 2008) and may be involved in actin remodelling (Gordon-Alonzo et al 2012). These processes could be important in *Salmonella* entry into non-phagocytic cells by the T3SS system.

8.5 Other future directions

Using murine cell lines have many advantages as cell model; however there are limited numbers of commercial antibodies currently available to native mouse versions of the tetraspanins. Despite this, some antibodies against mouse tetraspanins are becoming commercially available, but these are often raised against peptides or recombinant proteins. Such antibodies against mouse CD37 and CD151 were tested but did not recognize native tetraspanins on the surface of mouse macrophages cell lines. It may be worth testing additional commercially available antibodies to mouse tetraspanins to investigate their roles in *Salmonella* infection. The commercially available antibodies may be useful for looking at levels of expression of different tetraspanins in Western blotting, but they cannot be used for functional studies if they do not recognise native proteins.

The CD9KO mouse macrophages cells that were generated from CD9KO mice (Le Naour, Rubinstein et al. 2000) showed no difference in *Salmonella* NCTC12023 infection; however, interestingly CD9 KO mouse macrophages was more susceptible to *S.* LT2 strain. Hence, more experiments are needed to understand the cells behavior in relation to strain variation, particularly in long term infection and whether there are any differences in tetraspanin expression related with the *Salmonella* strains and time periods of infection. Also, regarding the stable CD9-GFP expressing J774 cell line that was generated in this study, it would be worth investigating the effect of overexpression of CD9 on *Salmonella* infection. Since CD81 was downregulated in CD9 overexpressing cells, it would be worth checking the expression of other tetraspanins by western blotting. In addition, many tetraspanin KO mice (CD37, CD81 or CD151) have been generated in different studies (Gartlan, Belz et al. 2010, Makkawi, Moheimani et al. 2015, Martinez del Hoyo, Ramirez-Huesca et al. 2015), and it would be useful to try generate immortal bone marrow derived macrophages from these mice. It would also be interesting to use these tetraspanin-KO mice to investigate the immune response following systemic infection with *Salmonella.* Also, using primary renal and hepatic cells from these KO mice could offer a good tool to obtain a better understanding of the infection process in the absence of particular tetraspanins. A similar study has been published more recently that investigated the effect of knockout of CD81 in mice infected with *Listeria monocytogenes* (Martinez del Hoyo, Ramirez-Huesca et al. 2015). As mentioned previously, such CD81 -/- mice were more susceptible to infection and a role for CD81in negatively regulating the immune response was demonstrated. Also, knocking out tetraspanins in cell lines using the CRISPR-Cas9 system could offer another good way to generate tetraspanin-KO cell lines.

Studying the expression of tetraspanins at the mRNA level offers a good tool to investigate the differences in tetraspanin expression profile in a wider context. RNA microarray analysis, increasingly, has been applied in many studies (Margalit, Somech et al. 2005, Jeffery, Higgins et al. 2006). This method could be used to investigate global changes in many different proteins, including tetraspanin and partner proteins, at the mRNA level. The gene responses to bacterial infection at the mRNA level was investigated in RAW264.7 mouse macrophages infected with *Brucella abortus* bacteria using microarray analysis (Eskra, Mathison et al. 2003). It will be useful to try screening the possible changes, at the transcription level, of gene expression during the infection process and in persistent infection with *Salmonella*.

Co-immunoprecipitation trials with CD9, CD81 and other possibly associated tetraspanins or tetraspanin partner proteins, particularly integrins, was within the initial aims in this study. However, time limitation prevented this being possible. These types of experiment could help to detect possible interactions between tetraspanins and putative *Salmonella* receptors since little is known about these.

Bibliography

Ach, T., M. Ziemer, J. Dawczynski, J. Strobel, G. Sauer and H. Deissler (2010). "Differential expression of tetraspanin CD9 in basal cell and squamous cell carcinomas of the skin and actinic keratosis." Oncol Lett **1**(1): 37-40.

Aderem, A. and D. M. Underhill (1999). "Mechanisms of phagocytosis in macrophages." Annu Rev Immunol **17**: 593-623.

Agbor, T. A. and B. A. McCormick (2011). "*Salmonella* effectors: important players modulating host cell function during infection." Cell Microbiol **13**(12): 1858-1869.

Akutsu, H., T. Miura, M. Machida, J. Birumachi, A. Hamada, M. Yamada, S. Sullivan, K. Miyado and A. Umezawa (2009). "Maintenance of pluripotency and self-renewal ability of mouse embryonic stem cells in the absence of tetraspanin CD9." Differentiation **78**(2-3): 137-142.

Allison, D. B., X. Cui, G. P. Page and M. Sabripour (2006). "Microarray data analysis: from disarray to consolidation and consensus." Nature reviews. Genetics **7**(1): 55-65.

Andreu, Z. and M. Yanez-Mo (2014). "Tetraspanins in extracellular vesicle formation and function." Front Immunol **5**: 442.

Andrews, P. W., B. B. Knowles and P. N. Goodfellow (1981). "A human cell-surface antigen defined by a monoclonal antibody and controlled by a gene on chromosome 12." Somatic Cell Genet **7**(4): 435-443.

Antoine, R. and C. Locht (1992). "Isolation and molecular characterization of a novel broad-host-range plasmid from Bordetella bronchiseptica with sequence similarities to plasmids from gram-positive organisms." Mol Microbiol **6**(13): 1785-1799.

Anzai, N., Y. Lee, B. S. Youn, S. Fukuda, Y. J. Kim, C. Mantel, M. Akashi and H. E. Broxmeyer (2002). "C-kit associated with the transmembrane 4 superfamily proteins constitutes a functionally distinct subunit in human hematopoietic progenitors." Blood **99**(12): 4413-4421.

Aoude, L. G., K. A. Wadt, A. L. Pritchard and N. K. Hayward (2015). "Genetics of familial melanoma: 20 years after CDKN2A." Pigment cell & melanoma research **28**(2): 148-160.

Arnaud, M. P., A. Vallee, G. Robert, J. Bonneau, C. Leroy, N. Varin-Blank, A. G. Rio, M. B. Troadec, M. D. Galibert and V. Gandemer (2015). "CD9, a key actor in the dissemination of lymphoblastic leukemia, modulating CXCR4-mediated migration via RAC1 signaling." Blood **126**(15): 1802-1812.

Arpaia, N., J. Godec, L. Lau, K. E. Sivick, L. M. McLaughlin, M. B. Jones, T. Dracheva, S. N. Peterson, D. M. Monack and G. M. Barton (2011). "TLR signaling is required for *Salmonella* typhimurium virulence." Cell **144**(5): 675-688.

Artavanis-Tsakonas, K., P. V. Kasperkovitz, E. Papa, M. L. Cardenas, N. S. Khan, A. G. Van der Veen, H. L. Ploegh and J. M. Vyas (2011). "The Tetraspanin CD82 Is Specifically Recruited

to Fungal and Bacterial Phagosomes prior to Acidification." Infection and Immunity **79**(3): 1098-1106.

Artavanis-Tsakonas, K., P. V. Kasperkovitz, E. Papa, M. L. Cardenas, N. S. Khan, A. G. Van der Veen, H. L. Ploegh and J. M. Vyas (2011). "The tetraspanin CD82 is specifically recruited to fungal and bacterial phagosomes prior to acidification." Infect Immun **79**(3): 1098-1106.

Artavanis-Tsakonas, K., J. C. Love, H. L. Ploegh and J. M. Vyas (2006). "Recruitment of CD63 to Cryptococcus neoformans phagosomes requires acidification." Proc Natl Acad Sci U S A **103**(43): 15945-15950.

Auwerx, J. (1991). "The human leukemia cell line, THP-1: a multifacetted model for the study of monocyte-macrophage differentiation." Experientia **47**(1): 22-31.

Azorsa, D. O., J. A. Hyman and J. E. Hildreth (1991). "CD63/Pltgp40: a platelet activation antigen identical to the stage-specific, melanoma-associated antigen ME491." Blood **78**(2): 280-284.

Bakshi, C. S., V. P. Singh, M. W. Wood, P. W. Jones, T. S. Wallis and E. E. Galyov (2000). "Identification of SopE2, a *Salmonella* Secreted Protein Which Is Highly Homologous to SopE and Involved in Bacterial Invasion of Epithelial Cells." Journal of Bacteriology **182**(8): 2341-2344.

Bailey, R. L., J. M. Herbert, K. Khan, V. L. Heath, R. Bicknell and M. G. Tomlinson (2011). "The emerging role of tetraspanin microdomains on endothelial cells." Biochem Soc Trans **39**(6): 1667-1673.

Baird, G. S., D. A. Zacharias and R. Y. Tsien (2000). "Biochemistry, mutagenesis, and oligomerization of DsRed, a red fluorescent protein from coral." Proc Natl Acad Sci U S A **97**(22): 11984-11989.

Bakowski, M. A., V. Braun, G. Y. Lam, T. Yeung, W. D. Heo, T. Meyer, B. B. Finlay, S. Grinstein and J. H. Brumell (2010). "The phosphoinositide phosphatase SopB manipulates membrane surface charge and trafficking of the *Salmonella*-containing vacuole." Cell Host Microbe **7**(6): 453-462.

Baldwin, G., V. Novitskaya, R. Sadej, E. Pochec, A. Litynska, C. Hartmann, J. Williams, L. Ashman, J. A. Eble and F. Berditchevski (2008). "Tetraspanin CD151 regulates glycosylation of (alpha)3(beta)1 integrin." J Biol Chem **283**(51): 35445-35454.

Baneyx, F. (1999). "Recombinant protein expression in *Escherichia coli*." Curr Opin Biotechnol **10**(5): 411-421.

Baneyx, F. and M. Mujacic (2004). "Recombinant protein folding and misfolding in Escherichia coli." Nat Biotechnol **22**(11): 1399-1408.

Bar, E., A. Gladiator, S. Bastidas, B. Roschitzki, H. Acha-Orbea, A. Oxenius and S. LeibundGut-Landmann (2012). "A novel Th cell epitope of *Candida albicans* mediates protection from fungal infection." J Immunol **188**(11): 5636-5643.

Bari, R., Y. H. Zhang, F. Zhang, N. X. Wang, C. S. Stipp, J. J. Zheng and X. A. Zhang (2009). "Transmembrane Interactions Are Needed for KAI1/CD82-Mediated Suppression of Cancer Invasion and Metastasis." American Journal of Pathology **174**(2): 647-660.

Barreiro, O., M. Yanez-Mo, M. Sala-Valdes, M. D. Gutierrez-Lopez, S. Ovalle, A. Higginbottom, P. N. Monk, C. Cabanas and F. Sanchez-Madrid (2005). "Endothelial tetraspanin microdomains regulate leukocyte firm adhesion during extravasation." Blood **105**(7): 2852-2861.

Barreiro, O., M. Zamai, M. Yanez-Mo, E. Tejera, P. Lopez-Romero, P. N. Monk, E. Gratton, V. R. Caiolfa and F. Sanchez-Madrid (2008). "Endothelial adhesion receptors are recruited to adherent leukocytes by inclusion in preformed tetraspanin nanoplatforms." J Cell Biol **183**(3): 527-542.

Bartosch, B. and J. Dubuisson (2010). "Recent advances in hepatitis C virus cell entry." Viruses **2**(3): 692-709.

Beatty, W. L. (2008). "Late Endocytic Multivesicular Bodies Intersect the Chlamydial Inclusion in the Absence of CD63." Infection and Immunity **76**(7): 2872-2881.

Beekman, J. M., L. P. Verhagen, N. Geijsen and P. J. Coffer (2009). "Regulation of myelopoiesis through syntenin-mediated modulation of IL-5 receptor output." Blood **114**(18): 3917-3927.

Berditchevski, F. (2001). "Complexes of tetraspanins with integrins: more than meets the eye." J Cell Sci **114**(Pt 23): 4143-4151.

Berditchevski, F., G. Bazzoni and M. E. Hemler (1995). "Specific association of CD63 with the VLA-3 and VLA-6 integrins." J Biol Chem **270**(30): 17784-17790.

Berditchevski, F., E. Gilbert, M. R. Griffiths, S. Fitter, L. Ashman and S. J. Jenner (2001). "Analysis of the CD151-alpha3beta1 integrin and CD151-tetraspanin interactions by mutagenesis." J Biol Chem **276**(44): 41165-41174.

Berditchevski, F. and E. Odintsova (2007). "Tetraspanins as regulators of protein trafficking." Traffic **8**(2): 89-96.

Berditchevski, F., M. M. Zutter and M. E. Hemler (1996). "Characterization of novel complexes on the cell surface between integrins and proteins with 4 transmembrane domains (TM4 proteins)." Mol Biol Cell **7**(2): 193-207.

Bevis, B. J. and B. S. Glick (2002). "Rapidly maturing variants of the Discosoma red fluorescent protein (DsRed)." Nat Biotechnol **20**(1): 83-87.

Bhavsar, A. P., J. A. Guttman and B. B. Finlay (2007). "Manipulation of host-cell pathways by bacterial pathogens." Nature **449**(7164): 827-834.

Boesze-Battaglia, K., F. P. Stefano, C. Fitzgerald and S. Muller-Weeks (2007). "ROM-1 potentiates photoreceptor specific membrane fusion processes." Exp Eye Res **84**(1): 22-31.

Bonifacino, J. S. and L. M. Traub (2003). "Signals for sorting of transmembrane proteins to endosomes and lysosomes." Annu Rev Biochem **72**: 395-447.

Boucheix, C. and E. Rubinstein (2001). "Tetraspanins." Cell Mol Life Sci **58**(9): 1189-1205.

Boukerche, H., Z. Z. Su, L. Emdad, P. Baril, B. Balme, L. Thomas, A. Randolph, K. Valerie, D. Sarkar and P. B. Fisher (2005). "mda-9/Syntenin: a positive regulator of melanoma metastasis." Cancer Res **65**(23): 10901-10911.

Boukerche, H., Z. Z. Su, C. Prevot, D. Sarkar and P. B. Fisher (2008). "mda-9/Syntenin promotes metastasis in human melanoma cells by activating c-Src." Proc Natl Acad Sci U S A **105**(41): 15914-15919.

Brenner, F. W., R. G. Villar, F. J. Angulo, R. Tauxe and B. Swaminathan (2000). "*Salmonella* nomenclature - Guest commentary." Journal of Clinical Microbiology **38**(7): 2465-2467.

Brockdorff, N., A. Ashworth, G. F. Kay, P. Cooper, S. Smith, V. M. McCabe, D. P. Norris, G. D. Penny, D. Patel and S. Rastan (1991). "Conservation of position and exclusive expression of mouse Xist from the inactive X chromosome." Nature **351**(6324): 329-331.

Brumell, J. H. and S. Grinstein (2004). "*Salmonella* redirects phagosomal maturation." Curr Opin Microbiol **7**(1): 78-84.

Brumell, J. H., P. Tang, M. L. Zaharik and B. B. Finlay (2002). "Disruption of the *Salmonella*-containing vacuole leads to increased replication of *Salmonella* enterica serovar typhimurium in the cytosol of epithelial cells." Infection and Immunity **70**(6): 3264-3270.

Buckner, M. M. and B. B. Finlay (2011). "Host-microbe interaction: Innate immunity cues virulence." Nature **472**(7342): 179-180.

Bumann, D. (2002). "Examination of *Salmonella* gene expression in an infected mammalian host using the green fluorescent protein and two-colour flow cytometry." Mol Microbiol **43**(5): 1269-1283.

Burkinshaw, B. J., G. Prehna, L. J. Worrall and N. C. Strynadka (2012). "Structure of *Salmonella* effector protein SopB N-terminal domain in complex with host Rho GTPase Cdc42." The Journal of biological chemistry **287**(16): 13348-13355.

Cannon, K. S. and P. Cresswell (2001). "Quality control of transmembrane domain assembly in the tetraspanin CD82." EMBO J **20**(10): 2443-2453.

Capecchi, M. R. (1989). "Altering the genome by homologous recombination." Science **244**(4910): 1288-1292.

Carloni, V., A. Mazzocca, T. Mello, A. Galli and *S. Capaccioli* (2012). "Cell fusion promotes chemoresistance in metastatic colon carcinoma." Oncogene.

Carter, P. B. and F. M. Collins (1974). "The route of enteric infection in normal mice." J Exp Med **139**(5): 1189-1203.

Caughey, B. and B. Chesebro (1997). "Prion protein and the transmissible spongiform encephalopathies." Trends Cell Biol **7**(2): 56-62.

Charrin, S., S. Jouannet, C. Boucheix and E. Rubinstein (2014). "Tetraspanins at a glance." Journal of Cell Science **127**(Pt 17): 3641-3648.

Charrin, S., M. Latil, S. Soave, A. Polesskaya, F. Chretien, C. Boucheix and E. Rubinstein (2013). "Normal muscle regeneration requires tight control of muscle cell fusion by tetraspanins CD9 and CD81." Nat Commun **4**: 1674.

Charrin, S., F. Le Naour, M. Oualid, M. Billard, G. Faure, S. M. Hanash, C. Boucheix and E. Rubinstein (2001). "The major CD9 and CD81 molecular partner. Identification and characterization of the complexes." J Biol Chem **276**(17): 14329-14337.

Charrin, S., F. le Naour, O. Silvie, P.-E. Milhiet, C. Boucheix and E. Rubinstein (2009). "Lateral organization of membrane proteins: tetraspanins spin their web." The Biochemical journal **420**(2): 133-154.

Charrin, S., S. Manie, M. Oualid, M. Billard, C. Boucheix and E. Rubinstein (2002). "Differential stability of tetraspanin/tetraspanin interactions: role of palmitoylation." FEBS Lett **516**(1-3): 139-144.

Charrin, S., S. Yalaoui, B. Bartosch, L. Cocquerel, J. F. Franetich, C. Boucheix, D. Mazier, E. Rubinstein and O. Silvie (2009). "The Ig domain protein CD9P-1 down-regulates CD81 ability to support Plasmodium yoelii infection." J Biol Chem **284**(46): 31572-31578.

Chatterjee, N., J. Stegmuller, P. Schatzle, K. Karram, M. Koroll, H. B. Werner, K. A. Nave and J. Trotter (2008). "Interaction of syntenin-1 and the NG2 proteoglycan in migratory oligodendrocyte precursor cells." J Biol Chem **283**(13): 8310-8317.

Cheminay, C., D. Chakravortty and M. Hensel (2004). "Role of neutrophils in murine salmonellosis." Infect Immun **72**(1): 468-477.

Chen, F., Y. Du, Z. Zhang, G. Chen, M. Zhang, H. B. Shu, Z. Zhai and D. Chen (2008). "Syntenin negatively regulates TRAF6-mediated IL-1R/TLR4 signaling." Cell Signal **20**(4): 666-674.

Cheng, B. H., Y. Liu, X. Xuei, C. P. Liao, D. Lu, M. E. Lasbury, P. J. Durant and C. H. Lee (2010). "Microarray studies on effects of Pneumocystis carinii infection on global gene expression in alveolar macrophages." BMC Microbiol **10**: 103.

Cherukuri, A., R. H. Carter, S. Brooks, W. Bornmann, R. Finn, C. S. Dowd and S. K. Pierce (2004). "B cell signaling is regulated by induced palmitoylation of CD81." J Biol Chem **279**(30): 31973-31982.

Chessa, D., C. W. Dorsey, M. Winter and A. J. Baumler (2008). "Binding specificity of *Salmonella* plasmid-encoded fimbriae assessed by glycomics." J Biol Chem **283**(13): 8118-8124.

Cirillo, D. M., R. H. Valdivia, D. M. Monack and S. Falkow (1998). "Macrophage-dependent induction of the *Salmonella* pathogenicity island 2 type III secretion system and its role in intracellular survival." Molecular Microbiology **30**(1): 175-188.

Clark, L., I. Martinez-Argudo, T. J. Humphrey and M. A. Jepson (2009). "GFP plasmid-induced defects in *Salmonella* invasion depend on plasmid architecture, not protein expression." Microbiology **155**(Pt 2): 461-467.

Clark, L., C. A. Perrett, L. Malt, C. Harward, S. Humphrey, K. A. Jepson, I. Martinez-Argudo, L. J. Carney, R. M. La Ragione, T. J. Humphrey and M. A. Jepson (2011). "Differences in *Salmonella* enterica serovar Typhimurium strain invasiveness are associated with heterogeneity in SPI-1 gene expression." Microbiology **157**(Pt 7): 2072-2083.

Coburn, B., G. A. Grassl and B. B. Finlay (2007). "*Salmonella*, the host and disease: a brief review." Immunol Cell Biol **85**(2): 112-118.

Collinson, S. K., P. C. Doig, J. L. Doran, S. Clouthier, T. J. Trust and W. W. Kay (1993). "Thin, aggregative fimbriae mediate binding of *Salmonella* enteritidis to fibronectin." J Bacteriol **175**(1): 12-18.

Costa, S., A. Almeida, A. Castro and L. Domingues (2014). "Fusion tags for protein solubility, purification and immunogenicity in *Escherichia coli*: the novel Fh8 system." Front Microbiol **5**: 63.

Cox, G. W., B. J. Mathieson, L. Gandino, E. Blasi, D. Radzioch and L. Varesio (1989). "Heterogeneity of hematopoietic cells immortalized by v-myc/v-raf recombinant retrovirus infection of bone marrow or fetal liver." J Natl Cancer Inst **81**(19): 1492-1496.

Craft, J. C. (2008). "Challenges facing drug development for malaria." Curr Opin Microbiol **11**(5): 428-433.

da Silva, C. V., L. Cruz, S. Araujo Nda, M. B. Angeloni, B. B. Fonseca, O. Gomes Ade, R. Carvalho Fdos, A. L. Goncalves and F. Barbosa Bde (2012). "A glance at *Listeria* and *Salmonella* cell invasion: different strategies to promote host actin polymerization." Int J Med Microbiol **302**(1): 19-32.

Dadwal, S. S., B. Tegtmeier, R. Nakamura, J. Kriengkauykiat, J. Ito, S. J. Forman and V. Pullarkat (2011). "Nontyphoidal *Salmonella* infection among recipients of hematopoietic SCT." Bone Marrow Transplant **46**(6): 880-883.

Dang, Z., K. Yagi, Y. Oku, H. Kouguchi, K. Kajino, J. Matsumoto, R. Nakao, H. Wakaguri, A. Toyoda, H. Yin and C. Sugimoto (2012). "A pilot study on developing mucosal vaccine against alveolar echinococcosis (AE) using recombinant tetraspanin 3: Vaccine efficacy and immunology." PLoS Negl Trop Dis **6**(3): e1570.

Das, S. K., S. K. Bhutia, B. Azab, T. P. Kegelman, L. Peachy, P. K. Santhekadur, S. Dasgupta, R. Dash, P. Dent, S. Grant, L. Emdad, M. Pellecchia, D. Sarkar and P. B. Fisher (2013). "MDA-9/syntenin and IGFBP-2 promote angiogenesis in human melanoma." Cancer Res **73**(2): 844-854.

Das, S. K., S. K. Bhutia, T. P. Kegelman, L. Peachy, R. A. Oyesanya, S. Dasgupta, U. K. Sokhi, B. Azab, R. Dash, B. A. Quinn, K. Kim, P. M. Barral, Z. Z. Su, H. Boukerche, D. Sarkar and P. B. Fisher (2012). "MDA-9/syntenin: a positive gatekeeper of melanoma metastasis." Front Biosci (Landmark Ed) **17**: 1-15.

Das, S. K., S. K. Bhutia, U. K. Sokhi, B. Azab, Z. Z. Su, H. Boukerche, T. Anwar, E. L. Moen, D. Chatterjee, M. Pellecchia, D. Sarkar and P. B. Fisher (2012). "Raf kinase inhibitor RKIP inhibits MDA-9/syntenin-mediated metastasis in melanoma." Cancer Res **72**(23): 6217-6226.

Davis, C., H. J. Harris, K. Hu, H. E. Drummer, J. A. McKeating, J. G. Mullins and P. Balfe (2012). "In silico directed mutagenesis identifies the CD81/claudin-1 hepatitis C virus receptor interface." Cell Microbiol **14**(12): 1892-1903.

de, S. A. G. R., G. N. Fontes, D. Leao, G. M. Rocha, B. Pontes, C. Sant'Anna, W. de Souza and S. Frases (2016). "Cryptococcus neoformans capsular polysaccharides form branched and complex filamentous networks viewed by high-resolution microscopy." J Struct Biol **193**(1): 75-82.

Delaguillaumie, A., J. Harriague, S. Kohanna, G. Bismuth, E. Rubinstein, M. Seigneuret and H. Conjeaud (2004). "Tetraspanin CD82 controls the association of cholesterol-dependent

microdomains with the actin cytoskeleton in T lymphocytes: relevance to co-stimulation." J Cell Sci **117**(Pt 22): 5269-5282.

Delandre, C., T. R. Penabaz, A. L. Passarelli, S. K. Chapes and R. J. Clem (2009). "Mutation of juxtamembrane cysteines in the tetraspanin CD81 affects palmitoylation and alters interaction with other proteins at the cell surface." Exp Cell Res **315**(11): 1953-1963.

Demain, A. L. and P. Vaishnav (2009). "Production of recombinant proteins by microbes and higher organisms." Biotechnol Adv **27**(3): 297-306.

DeSalle, R., T.-T. Sun, T. Bergmann and A. Garcia-España (2013). The Evolution of Tetraspanins Through a Phylogenetic Lens. Tetraspanins. F. Berditchevski and E. Rubinstein. Dordrecht, Springer Netherlands**:** 31-45.

Dhanoa, A. and Q. K. Fatt (2009). "Non-typhoidal *Salmonella* bacteraemia: epidemiology, clinical characteristics and its' association with severe immunosuppression." Ann Clin Microbiol Antimicrob **8**: 15.

Doh-Ura, K., E. Mekada, K. Ogomori and T. Iwaki (2000). "Enhanced CD9 Expression in the Mouse and Human Brains Infected with Transmissible Spongiform Encephalopathies." Journal of Neuropathology & Experimental Neurology **59**(9): 774-785.

Dorsey, C. W., M. C. Laarakker, A. D. Humphries, E. H. Weening and A. J. Baumler (2005). "*Salmonella* enterica serotype Typhimurium MisL is an intestinal colonization factor that binds fibronectin." Mol Microbiol **57**(1): 196-211.

Drecktrah, D., L. A. Knodler, R. Ireland and O. Steele-Mortimer (2006). "The mechanism of *Salmonella* entry determines the vacuolar environment and intracellular gene expression." Traffic **7**(1): 39-51.

Duarte, J., F. Herbert, V. Guiyedi, J. F. Franetich, J. Roland, P. A. Cazenave, D. Mazier, M. Kombila, C. Fesel and S. Pied (2012). "High Levels of Immunoglobulin E Autoantibody to 14-3-3 {varepsilon} Protein Correlate With Protection Against Severe Plasmodium falciparum Malaria." J Infect Dis **206**(11): 1781-1789.

Duffield, A., E. J. Kamsteeg, A. N. Brown, P. Pagel and M. J. Caplan (2003). "The tetraspanin CD63 enhances the internalization of the H,K-ATPase beta-subunit." Proc Natl Acad Sci U S A **100**(26): 15560-15565.

Earnest, J. T., M. P. Hantak, J. E. Park and T. Gallagher (2015). "Coronavirus and influenza virus proteolytic priming takes place in tetraspanin-enriched membrane microdomains." Journal of Virology **89**(11): 6093-6104.

Edskes, H. K. and R. B. Wickner (2004). "Transmissible spongiform encephalopathies: prion proof in progress." Nature **430**(7003): 977-979.

Elliott, R. W. and K. J. Moore (1996). "Mouse chromosome 6." Mammalian Genome **8**(1): S114-S135.

Eskra, L., A. Mathison and G. Splitter (2003). "Microarray analysis of mRNA levels from RAW264.7 macrophages infected with Brucella abortus." Infect Immun **71**(3): 1125-1133.

Espenel, C., E. Margeat, P. Dosset, C. Arduise, C. Le Grimellec, C. A. Royer, C. Boucheix, E. Rubinstein and P. E. Milhiet (2008). "Single-molecule analysis of CD9 dynamics and partitioning reveals multiple modes of interaction in the tetraspanin web." J Cell Biol **182**(4): 765-776.

Estrach, S., J. Legg and F. M. Watt (2007). "Syntenin mediates Delta1-induced cohesiveness of epidermal stem cells in culture." J Cell Sci **120**(Pt 16): 2944-2952.

Eswarappa, S. M., V. D. Negi, S. Chakraborty, B. K. Chandrasekhar Sagar and D. Chakravortty (2010). "Division of the *Salmonella*-containing vacuole and depletion of acidic lysosomes in *Salmonella*-infected host cells are novel strategies of *Salmonella* enterica to avoid lysosomes." Infection and Immunity **78**(1): 68-79.

Evans, J. P. (2001). "Fertilin beta and other ADAMs as integrin ligands: insights into cell adhesion and fertilization." Bioessays **23**(7): 628-639.

Fabrega, A. and J. Vila (2013). "*Salmonella* enterica serovar Typhimurium skills to succeed in the host: virulence and regulation." Clinical microbiology reviews **26**(2): 308-341.

Fabrega, A. and J. Vila (2013). "*Salmonella* enterica Serovar Typhimurium Skills To Succeed in the Host: Virulence and Regulation." Clin Microbiol Rev **26**(2): 308-341.

Fan, J. and P. J. Brindley (1998). "Characterization of cDNAs encoding a new family of tetraspanins from schistosomes—the Sj25 family." Gene **219**(1–2): 1-8.

Fanaei, M., P. N. Monk and L. J. Partridge (2011). "The role of tetraspanins in fusion." Biochem Soc Trans **39**(2): 524-528.

Farquhar, M. J., H. J. Harris and J. A. McKeating (2011). "Hepatitis C virus entry and the tetraspanin CD81." Biochem Soc Trans **39**(2): 532-536.

Farquhar, M. J., K. Hu, H. J. Harris, C. Davis, C. L. Brimacombe, S. J. Fletcher, T. F. Baumert, J. Z. Rappoport, P. Balfe and J. A. McKeating (2012). "Hepatitis C virus induces CD81 and claudin-1 endocytosis." J Virol **86**(8): 4305-4316.

Feneant, L., S. Levy and L. Cocquerel (2014). "CD81 and hepatitis C virus (HCV) infection." Viruses **6**(2): 535-572.

Feng, J., C. Huang, J. D. Wren, D. W. Wang, J. Yan, J. Zhang, Y. Sun, X. Han and X. A. Zhang (2015). "Tetraspanin CD82: a suppressor of solid tumors and a modulator of membrane heterogeneity." Cancer metastasis reviews.

Figdor, C. G. and A. B. van Spriel (2010). "Fungal pattern-recognition receptors and tetraspanins: partners on antigen-presenting cells." Trends in Immunology **31**(3): 91-96.

Figueira, R. and D. W. Holden (2012). "Functions of the *Salmonella* pathogenicity island 2 (SPI-2) type III secretion system effectors." Microbiology **158**(Pt 5): 1147-1161.

Finlay, B. B. and P. Cossart (1997). "Exploitation of mammalian host cell functions by bacterial pathogens." Science **276**(5313): 718-725.

Finlay, B. B., S. Ruschkowski and S. Dedhar (1991). "Cytoskeletal rearrangements accompanying *Salmonella* entry into epithelial cells." Journal of cell science **99 (Pt 2)**: 283-296.

Fitter, S., T. J. Tetaz, M. C. Berndt and L. K. Ashman (1995). "Molecular cloning of cDNA encoding a novel platelet-endothelial cell tetra-span antigen, PETA-3." Blood **86**(4): 1348-1355.

Flint, M., T. von Hahn, J. Zhang, M. Farquhar, C. T. Jones, P. Balfe, C. M. Rice and J. A. McKeating (2006). "Diverse CD81 proteins support hepatitis C virus infection." J Virol **80**(22): 11331-11342.

Freissler, E., A. Meyer auf der Heyde, G. David, T. F. Meyer and C. Dehio (2000). "Syndecan-1 and syndecan-4 can mediate the invasion of OpaHSPG-expressing *Neisseria gonorrhoeae* into epithelial cells." Cellular Microbiology **2**(1): 69-82.

Friand, V., G. David and P. Zimmermann (2015). "Syntenin and syndecan in the biogenesis of exosomes." Biol Cell **107**(10): 331-341.

Friebel, A., H. Ilchmann, M. Aepfelbacher, K. Ehrbar, W. Machleidt and W. D. Hardt (2001). "SopE and SopE2 from *Salmonella* typhimurium activate different sets of RhoGTPases of the host cell." J Biol Chem **276**(36): 34035-34040.

Funakoshi, T., I. Tachibana, Y. Hoshida, H. Kimura, Y. Takeda, T. Kijima, K. Nishino, H. Goto, T. Yoneda, T. Kumagai, T. Osaki, S. Hayashi, K. Aozasa and I. Kawase (2003). "Expression of tetraspanins in human lung cancer cells: frequent downregulation of CD9 and its contribution to cell motility in small cell lung cancer." Oncogene **22**(5): 674-687.

Galan, J. E. (1996). "Molecular genetic bases of *Salmonella* entry into host cells." Molecular microbiology **20**(2): 263-271.

Gama-de-Souza, L. N., E. Cyreno-Oliveira, V. M. Freitas, E. S. Melo, V. F. Vilas-Boas, A. S. Moriscot and R. G. Jaeger (2008). "Adhesion and protease activity in cell lines from human salivary gland tumors are regulated by the laminin-derived peptide AG73, syndecan-1 and beta1 integrin." Matrix biology : journal of the International Society for Matrix Biology **27**(5): 402-419.

Garcia-España, A., R. Mares, T.-T. Sun and R. DeSalle (2009). "Intron Evolution: Testing Hypotheses of Intron Evolution Using the Phylogenomics of Tetraspanins." PLoS ONE **4**(3): e4680.

Garcia, E., M. Pion, A. Pelchen-Matthews, L. Collinson, J. F. Arrighi, G. Blot, F. Leuba, J. M. Escola, N. Demaurex, M. Marsh and V. Piguet (2005). "HIV-1 trafficking to the dendritic cell-T-cell infectious synapse uses a pathway of tetraspanin sorting to the immunological synapse." Traffic **6**(6): 488-501.

Gartlan, K. H., G. T. Belz, J. M. Tarrant, G. Minigo, M. Katsara, K. C. Sheng, M. Sofi, A. B. van Spriel, V. Apostolopoulos, M. Plebanski, L. Robb and M. D. Wright (2010). "A complementary role for the tetraspanins CD37 and Tssc6 in cellular immunity." J Immunol **185**(6): 3158-3166.

Gecchele, E., M. Merlin, A. Brozzetti, A. Falorni, M. Pezzotti and L. Avesani (2015). "A comparative analysis of recombinant protein expression in different biofactories: bacteria, insect cells and plant systems." J Vis Exp(97).

Georgiou, G. and P. Valax (1996). "Expression of correctly folded proteins in *Escherichia coli*." Curr Opin Biotechnol **7**(2): 190-197.

Gey, G., W. Coffman and M. T. Kubicek (1952). Tissue culture studies of the proliferative capacity of cervical carcinoma and normal epithelium. Cancer research, AMER ASSOC CANCER RESEARCH PO BOX 11806, BIRMINGHAM, AL 35202.

Giannella, R. A., O. Washington, P. Gemski and S. B. Formal (1973). "Invasion of HeLa cells by *Salmonella* typhimurium: a model for study of invasiveness of *Salmonella*." J Infect Dis **128**(1): 69-75.

Giannella, R. A., O. Washington, P. Gemski and S. B. Formal (1973). "Invasion of HeLa Cells by *Salmonella* typhimurium: A Model for Study of Invasiveness of *Salmonella*." Journal of Infectious Diseases **128**(1): 69-75.

Gilberthorpe, N. J., M. E. Lee, T. M. Stevanin, R. C. Read and R. K. Poole (2007). "NsrR: a key regulator circumventing *Salmonella* enterica serovar Typhimurium oxidative and nitrosative stress in vitro and in IFN-gamma-stimulated J774.2 macrophages." Microbiology **153**(Pt 6): 1756-1771.

Gilsanz, A., L. Sanchez-Martin, M. D. Gutierrez-Lopez, S. Ovalle, Y. Machado-Pineda, R. Reyes, G. W. Swart, C. G. Figdor, E. M. Lafuente and C. Cabanas (2012). "ALCAM/CD166 adhesive function is regulated by the tetraspanin CD9." Cell Mol Life Sci.

Gilsanz, A., L. Sanchez-Martin, M. D. Gutierrez-Lopez, S. Ovalle, Y. Machado-Pineda, R. Reyes, G. W. Swart, C. G. Figdor, E. M. Lafuente and C. Cabanas (2013). "ALCAM/CD166 adhesive function is regulated by the tetraspanin CD9." Cell Mol Life Sci **70**(3): 475-493.

Gimferrer, I., A. Ibanez, M. Farnos, M. R. Sarrias, R. Fenutria, S. Rosello, P. Zimmermann, G. David, J. Vives, C. Serra-Pages and F. Lozano (2005). "The lymphocyte receptor CD6 interacts with syntenin-1, a scaffolding protein containing PDZ domains." J Immunol **175**(3): 1406-1414.

Gordon-Alonso, M., V. Rocha-Perugini, S. Alvarez, O. Moreno-Gonzalo, A. Ursa, S. Lopez-Martin, N. Izquierdo-Useros, J. Martinez-Picado, M. A. Munoz-Fernandez, M. Yanez-Mo and F. Sanchez-Madrid (2012). "The PDZ-adaptor protein syntenin-1 regulates HIV-1 entry." Mol Biol Cell **23**(12): 2253-2263.

Gordon-Alonso, M., M. Yanez-Mo, O. Barreiro, S. Alvarez, M. A. Munoz-Fernandez, A. Valenzuela-Fernandez and F. Sanchez-Madrid (2006). "Tetraspanins CD9 and CD81 modulate HIV-1-induced membrane fusion." J Immunol **177**(8): 5129-5137.

Gordon, M. A. (2008). "*Salmonella* infections in immunocompromised adults." J Infect **56**(6): 413-422.

Govoni, G., F. Canonne-Hergaux, C. G. Pfeifer, S. L. Marcus, S. D. Mills, D. J. Hackam, S. Grinstein, D. Malo, B. B. Finlay and P. Gros (1999). "Functional expression of Nramp1 in vitro in the murine macrophage line RAW264.7." Infect Immun **67**(5): 2225-2232.

Green, L. R., P. N. Monk, L. J. Partridge, P. Morris, A. R. Gorringe and R. C. Read (2011). "Cooperative Role for Tetraspanins in Adhesin-Mediated Attachment of Bacterial Species to Human Epithelial Cells." Infection and Immunity **79**(6): 2241-2249.

Griffiss, J. M., C. J. Lammel, J. Wang, N. P. Dekker and G. F. Brooks (1999). "*Neisseria gonorrhoeae* coordinately uses Pili and Opa to activate HEC-1-B cell microvilli, which causes engulfment of the gonococci." Infect Immun **67**(7): 3469-3480.

Griffiths, R. E., K. J. Heesom and D. J. Anstee (2007). "Normal prion protein trafficking in cultured human erythroblasts." Blood **110**(13): 4518-4525.

Grigorov, B., V. Attuil-Audenis, F. Perugi, M. Nedelec, S. Watson, C. Pique, J. L. Darlix, H. Conjeaud and D. Muriaux (2009). "A role for CD81 on the late steps of HIV-1 replication in a chronically infected T cell line." Retrovirology **6**: 28.

Grootjans, J. J., G. Reekmans, H. Ceulemans and G. David (2000). "Syntenin-syndecan binding requires syndecan-synteny and the co-operation of both PDZ domains of syntenin." J Biol Chem **275**(26): 19933-19941.

Grootjans, J. J., P. Zimmermann, G. Reekmans, A. Smets, G. Degeest, J. Durr and G. David (1997). "Syntenin, a PDZ protein that binds syndecan cytoplasmic domains." Proc Natl Acad Sci U S A **94**(25): 13683-13688.

Gu, L., S. Zhou, L. Zhu, C. Liang and X. Chen (2015). "Small-Molecule Inhibitors of the Type III Secretion System." Molecules **20**(9): 17659-17674.

Guan, K. L. and J. E. Dixon (1991). "Eukaryotic proteins expressed in *Escherichia coli*: an improved thrombin cleavage and purification procedure of fusion proteins with glutathione S-transferase." Anal Biochem **192**(2): 262-267.

Gui, L., B. Wang, F. H. Li, Y. M. Sun, Z. Luo and J. H. Xiang (2012). "Blocking the large extracellular loop (LEL) domain of FcTetraspanin-3 could inhibit the infection of white spot syndrome virus (WSSV) in Chinese shrimp, Fenneropenaeus chinensis." Fish Shellfish Immunol **32**(6): 1008-1015.

Gulan, G., Z. Jotanovic, H. Jurdana, B. Sestan, J. Ravlic-Gulan and N. Brncic (2010). "*Salmonella* typhimurium osteomyelitis of the femur in patient with Crohn's disease." Wien Klin Wochenschr **122**(13-14): 437-440.

Guo, M., T. Huang, Y. Cui, B. Pan, A. Shen, Y. Sun, Y. Yi, Y. Wang, G. Xiao and G. Sun (2008). "PrPC interacts with tetraspanin-7 through bovine PrP154-182 containing alpha-helix 1." Biochem Biophys Res Commun **365**(1): 154-157.

Gustafson-Wagner, E. and C. S. Stipp (2013). "The CD9/CD81 tetraspanin complex and tetraspanin CD151 regulate alpha3beta1 integrin-dependent tumor cell behaviors by overlapping but distinct mechanisms." PLoS One **8**(4): e61834.

Gutierrez-Lopez, M. D., A. Gilsanz, M. Yanez-Mo, S. Ovalle, E. M. Lafuente, C. Dominguez, P. N. Monk, I. Gonzalez-Alvaro, F. Sanchez-Madrid and C. Cabanas (2011). "The sheddase activity of ADAM17/TACE is regulated by the tetraspanin CD9." Cell Mol Life Sci **68**(19): 3275-3292.

Ha, C. T., R. Waterhouse, J. Wessells, J. A. Wu and G. S. Dveksler (2005). "Binding of pregnancy-specific glycoprotein 17 to CD9 on macrophages induces secretion of IL-10, IL-6, PGE2, and TGF-beta1." Journal of leukocyte biology **77**(6): 948-957.

Haase, A. T. (1999). "Population biology of HIV-1 infection: viral and CD4+ T cell demographics and dynamics in lymphatic tissues." Annu Rev Immunol **17**: 625-656.

Haidinger, W., M. P. Szostak, W. Beisker and W. Lubitz (2001). "Green fluorescent protein (GFP)-dependent separation of bacterial ghosts from intact cells by FACS." Cytometry **44**(2): 106-112.

Halova, I., L. Draberova, M. Bambouskova, M. Machyna, L. Stegurova, D. Smrz and P. Draber (2013). "Cross-talk between tetraspanin CD9 and transmembrane adaptor protein non-T cell activation linker (NTAL) in mast cell activation and chemotaxis." J Biol Chem **288**(14): 9801-9814.

Hammond, C., L. K. Denzin, M. Pan, J. M. Griffith, H. J. Geuze and P. Cresswell (1998). "The tetraspan protein CD82 is a resident of MHC class II compartments where it associates with HLA-DR, -DM, and -DO molecules." J Immunol **161**(7): 3282-3291.

Hansen-Wester, I. and M. Hensel (2001). "*Salmonella* pathogenicity islands encoding type III secretion systems." Microbes Infect **3**(7): 549-559.

Haraga, A., M. B. Ohlson and S. I. Miller (2008). "*Salmonella*e interplay with host cells." Nat Rev Microbiol **6**(1): 53-66.

Harris, H. J., C. Davis, J. G. Mullins, K. Hu, M. Goodall, M. J. Farquhar, C. J. Mee, K. McCaffrey, S. Young, H. Drummer, P. Balfe and J. A. McKeating (2010). "Claudin association with CD81 defines hepatitis C virus entry." J Biol Chem **285**(27): 21092-21102.

Hartshorn, C., J. E. Rice and L. J. Wangh (2002). "Developmentally-regulated changes of Xist RNA levels in single preimplantation mouse embryos, as revealed by quantitative real-time PCR." Molecular reproduction and development **61**(4): 425-436.

Hassuna, N., P. N. Monk, G. W. Moseley and L. J. Partridge (2009). "Strategies for Targeting Tetraspanin Proteins: Potential Therapeutic Applications in Microbial Infections." BioDrugs **23**(6): 341-359.

Hautefort, I., M. J. Proenca and J. C. Hinton (2003). "Single-copy green fluorescent protein gene fusions allow accurate measurement of *Salmonella* gene expression in vitro and during infection of mammalian cells." Appl Environ Microbiol **69**(12): 7480-7491.

Hayashida, A., S. Amano and P. W. Park (2011). "Syndecan-1 promotes *Staphylococcus aureus* corneal infection by counteracting neutrophil-mediated host defense." The Journal of biological chemistry **286**(5): 3288-3297.

Helmke, B. M., M. Polychronidis, A. Benner, M. Thome, J. Arribas and M. Deichmann (2004). "Melanoma metastasis is associated with enhanced expression of the syntenin gene." Oncol Rep **12**(2): 221-228.

Hemler, M. E. (2001). "Specific tetraspanin functions." J Cell Biol **155**(7): 1103-1107.

Hemler, M. E. (2003). "Tetraspanin proteins mediate cellular penetration, invasion, and fusion events and define a novel type of membrane microdomain." Annu Rev Cell Dev Biol **19**: 397-422.

Hemler, M. E. (2005). "Tetraspanin functions and associated microdomains." Nat Rev Mol Cell Biol **6**(10): 801-811.

Hemler, M. E. (2008). "Targeting of tetraspanin proteins--potential benefits and strategies." Nat Rev Drug Discov **7**(9): 747-758.

Hemler, M. E. (2014). "Tetraspanin proteins promote multiple cancer stages." Nature reviews. Cancer **14**(1): 49-60.

Hensel, M., T. Nikolaus and C. Egelseer (1999). "Molecular and functional analysis indicates a mosaic structure of *Salmonella* pathogenicity island 2." Mol Microbiol **31**(2): 489-498.

Hercend, T., L. M. Nadler, J. M. Pesando, E. L. Reinherz, S. F. Schlossman and J. Ritz (1981). "Expression of a 26,000-dalton glycoprotein on activated human T cells." Cellular immunology **64**(1): 192-199.

Herr, M. J., S. E. Mabry and L. K. Jennings (2014). "Tetraspanin CD9 regulates cell contraction and actin arrangement via RhoA in human vascular smooth muscle cells." PLoS One **9**(9): e106999.

Herzog, C. R., S. Noh, L. E. Lantry, K. L. Guan and M. You (1999). "Cdkn2a encodes functional variation of p16INK4a but not p19ARF, which confers selection in mouse lung tumorigenesis." Molecular carcinogenesis **25**(2): 92-98.

Higginbottom, A., Y. Takahashi, L. Bolling, S. A. Coonrod, J. M. White, L. J. Partridge and P. N. Monk (2003). "Structural requirements for the inhibitory action of the CD9 large extracellular domain in sperm/oocyte binding and fusion." Biochem Biophys Res Commun **311**(1): 208-214.

Hirano, T., T. Higuchi, M. Ueda, T. Inoue, N. Kataoka, M. Maeda, H. Fujiwara and S. Fujii (1999). "CD9 is expressed in extravillous trophoblasts in association with integrin alpha3 and integrin alpha5." Mol Hum Reprod **5**(2): 162-167.

Hirbec, H., S. Martin and J. M. Henley (2005). "Syntenin is involved in the developmental regulation of neuronal membrane architecture." Mol Cell Neurosci **28**(4): 737-746.

Ho, S. H., F. Martin, A. Higginbottom, L. J. Partridge, V. Parthasarathy, G. W. Moseley, P. Lopez, C. Cheng-Mayer and P. N. Monk (2006). "Recombinant extracellular domains of tetraspanin proteins are potent inhibitors of the infection of macrophages by human immunodeficiency virus type 1." Journal of Virology **80**(13): 6487-6496.

Hohmann, E. L. (2001). "Nontyphoidal salmonellosis." Clin Infect Dis **32**(2): 263-269.

Hoiseth, S. K. and B. A. Stocker (1981). "Aromatic-dependent *Salmonella* typhimurium are non-virulent and effective as live vaccines." Nature **291**(5812): 238-239.

Hong, I. K., D. I. Jeoung, K. S. Ha, Y. M. Kim and H. Lee (2012). "Tetraspanin CD151 stimulates adhesion-dependent activation of Ras, Rac, and Cdc42 by facilitating molecular association between beta1 integrins and small GTPases." J Biol Chem **287**(38): 32027-32039.

Horsley, V. and G. K. Pavlath (2004). "Forming a Multinucleated Cell: Molecules That Regulate Myoblast Fusion." Cells Tissues Organs **176**(1-3): 67-78.

Huang, C., T. Taki, M. Adachi, M. Yagita, S. Sawada, A. Takabayashi, H. Inufusa, O. Yoshie and M. Miyake (1997). "MRP-1/CD9 and KAI1/CD82 expression in normal and various cancer tissues." International journal of oncology **11**(5): 1045-1051.

Huang da, W., B. T. Sherman and R. A. Lempicki (2009). "Systematic and integrative analysis of large gene lists using DAVID bioinformatics resources." Nature protocols **4**(1): 44-57.

Huang, W., M. Febbraio and R. L. Silverstein (2011). "CD9 tetraspanin interacts with CD36 on the surface of macrophages: a possible regulatory influence on uptake of oxidized low density lipoprotein." PLoS One **6**(12): e29092.

Hudson, D. L., A. N. Layton, T. R. Field, A. J. Bowen, H. Wolf-Watz, M. Elofsson, M. P. Stevens and E. E. Galyov (2007). "Inhibition of type III secretion in *Salmonella* enterica serovar Typhimurium by small-molecule inhibitors." Antimicrob Agents Chemother **51**(7): 2631-2635.

Hulme, R. S., A. Higginbottom, J. Palmer, L. J. Partridge and P. N. Monk (2014). "Distinct regions of the large extracellular domain of tetraspanin CD9 are involved in the control of human multinucleated giant cell formation." PLoS One **9**(12): e116289.

Hwangbo, C., J. Park and J. H. Lee (2011). "mda-9/Syntenin protein positively regulates the activation of Akt protein by facilitating integrin-linked kinase adaptor function during adhesion to type I collagen." J Biol Chem **286**(38): 33601-33612.

Hwangbo, C., N. Tae, S. Lee, O. Kim, O. K. Park, J. Kim, S. H. Kwon and J. H. Lee (2015). "Syntenin regulates TGF-beta1-induced Smad activation and the epithelial-to-mesenchymal transition by inhibiting caveolin-mediated TGF-beta type I receptor internalization." Oncogene.

Indig, F. E., F. Diaz-Gonzalez and M. H. Ginsberg (1997). "Analysis of the tetraspanin CD9-integrin alphaIIbbeta3 (GPIIb-IIIa) complex in platelet membranes and transfected cells." Biochem J **327 (Pt 1)**: 291-298.

Ipinza, F., B. Collao, D. Monsalva, V. H. Bustamante, R. Luraschi, M. Alegria-Arcos, D. E. Almonacid, D. Aguayo, I. L. Calderon, F. Gil, C. A. Santiviago, E. H. Morales, E. Calva and C. P. Saavedra (2014). "Participation of the *Salmonella* OmpD porin in the infection of RAW264.7 macrophages and BALB/c mice." PLoS One **9**(10): e111062.

Israels, S. J. and E. M. McMillan-Ward (2007). "Platelet tetraspanin complexes and their association with lipid rafts." Thromb Haemost **98**(5): 1081-1087.

Israels, S. J. and E. M. McMillan-Ward (2010). "Palmitoylation supports the association of tetraspanin CD63 with CD9 and integrin alphaIIbbeta3 in activated platelets." Thromb Res **125**(2): 152-158.

Issenhuth-Jeanjean, S., P. Roggentin, M. Mikoleit, M. Guibourdenche, E. de Pinna, S. Nair, P. I. Fields and F. X. Weill (2014). "Supplement 2008-2010 (no. 48) to the White-Kauffmann-Le Minor scheme." Research in Microbiology **165**(7): 526-530.

Iwai, K., M. Ishii, S. Ohshima, K. Miyatake and Y. Saeki (2007). "Expression and function of transmembrane-4 superfamily (tetraspanin) proteins in osteoclasts: reciprocal roles of Tspan-5 and NET-6 during osteoclastogenesis." Allergol Int **56**(4): 457-463.

Iwasaki, T., Y. Takeda, K. Maruyama, Y. Yokosaki, K. Tsujino, S. Tetsumoto, H. Kuhara, K. Nakanishi, Y. Otani, Y. Jin, S. Kohmo, H. Hirata, R. Takahashi, M. Suzuki, K. Inoue, I. Nagatomo, S. Goya, T. Kijima, T. Kumagai, I. Tachibana, I. Kawase and A. Kumanogoh (2013). "Deletion of tetraspanin CD9 diminishes lymphangiogenesis in vivo and in vitro." J Biol Chem **288**(4): 2118-2131.

Jaffe, S. R., B. Strutton, Z. Levarski, J. Pandhal and P. C. Wright (2014). "*Escherichia coli* as a glycoprotein production host: recent developments and challenges." Curr Opin Biotechnol **30**: 205-210.

Jahan, S., S. Khaliq, B. Samreen, B. Ijaz, M. Khan, W. Ahmad, U. A. Ashfaq and S. Hassan (2011). "Effect of combined siRNA of HCV E2 gene and HCV receptors against HCV." Virol J **8**: 295.

Jahan, S., B. Samreen, S. Khaliq, B. Ijaz, M. Khan, M. H. Siddique, W. Ahmad and S. Hassan (2011). "HCV entry receptors as potential targets for siRNA-based inhibition of HCV." Genet Vaccines Ther **9**: 15.

Jannatipour, M., P. Dion, S. Khan, H. Jindal, X. Fan, J. Laganiere, A. H. Chishti and G. A. Rouleau (2001). "Schwannomin isoform-1 interacts with syntenin via PDZ domains." The Journal of biological chemistry **276**(35): 33093-33100.

Jeffery, I. B., D. G. Higgins and A. C. Culhane (2006). "Comparison and evaluation of methods for generating differentially expressed gene lists from microarray data." BMC bioinformatics **7**: 359.

Jennings, L. K., J. T. Crossno, Jr., C. F. Fox, M. M. White and C. A. Green (1994). "Platelet p24/CD9, a member of the tetraspanin family of proteins." Ann N Y Acad Sci **714**: 175-184.

Johansson, C., M. Ingman and M. Jo Wick (2006). "Elevated neutrophil, macrophage and dendritic cell numbers characterize immune cell populations in mice chronically infected with *Salmonella*." Microb Pathog **41**(2-3): 49-58.

Jolly, C. and Q. J. Sattentau (2007). "Human immunodeficiency virus type 1 assembly, budding, and cell-cell spread in T cells take place in tetraspanin-enriched plasma membrane domains." J Virol **81**(15): 7873-7884.

Jones, B. D., N. Ghori and S. Falkow (1994). "*Salmonella* typhimurium initiates murine infection by penetrating and destroying the specialized epithelial M cells of the Peyer's patches." J Exp Med **180**(1): 15-23.

Jones, G. W., L. A. Richardson and D. Uhlman (1981). "The invasion of HeLa cells by *Salmonella* typhimurium: reversible and irreversible bacterial attachment and the role of bacterial motility." J Gen Microbiol **127**(2): 351-360.

Jones, N. H., M. J. Borowitz and R. S. Metzgar (1982). "Characterization and distribution of a 24,000-molecular weight antigen defined by a monoclonal antibody (DU-ALL-1) elicited to common acute lymphoblastic leukemia (cALL) cells." Leukemia research **6**(4): 449-464.

Kang, B. S., D. R. Cooper, F. Jelen, Y. Devedjiev, U. Derewenda, Z. Dauter, J. Otlewski and Z. S. Derewenda (2003). "PDZ tandem of human syntenin: crystal structure and functional properties." Structure **11**(4): 459-468.

Karlsson, G., E. Rorby, C. Pina, S. Soneji, K. Reckzeh, K. Miharada, C. Karlsson, Y. Guo, C. Fugazza, R. Gupta, J. H. Martens, H. G. Stunnenberg, S. Karlsson and T. Enver (2013). "The tetraspanin CD9 affords high-purity capture of all murine hematopoietic stem cells." Cell Rep **4**(4): 642-648.

Kashef, J., T. Diana, M. Oelgeschlager and I. Nazarenko (2012). "Expression of the tetraspanin family members Tspan3, Tspan4, Tspan5 and Tspan7 during Xenopus laevis embryonic development." Gene Expr Patterns.

Katnik-Prastowska, I., J. Lis and A. Matejuk (2014). "Glycosylation of uroplakins. Implications for bladder physiopathology." Glycoconj J **31**(9): 623-636.

Kazarov, A. R., X. Yang, C. S. Stipp, B. Sehgal and M. E. Hemler (2002). "An extracellular site on tetraspanin CD151 determines alpha 3 and alpha 6 integrin-dependent cellular morphology." J Cell Biol **158**(7): 1299-1309.

Kegelman, T. P., S. K. Das, L. Emdad, B. Hu, M. E. Menezes, P. Bhoopathi, X. Y. Wang, M. Pellecchia, D. Sarkar and P. B. Fisher (2015). "Targeting tumor invasion: the roles of MDA-9/Syntenin." Expert Opin Ther Targets **19**(1): 97-112.

Kelley, L. A., S. Mezulis, C. M. Yates, M. N. Wass and M. J. E. Sternberg (2015). "The Phyre2 web portal for protein modeling, prediction and analysis." Nat. Protocols **10**(6): 845-858.

Kennedy, M. B. (1995). "Origin of PDZ (DHR, GLGF) domains." Trends in biochemical sciences **20**(9): 350.

Khan, S., V. A. Kumar, N. Sidharthan, A. Mehta, B. Backer and K. R. Dinesh (2015). "*Salmonella* Typhimurium pneumonia in a patient with multiple myeloma." Trop Doct **45**(2): 135-136.

Kim, J. Y., Y. G. Kim and G. M. Lee (2012). "CHO cells in biotechnology for production of recombinant proteins: current state and further potential." Appl Microbiol Biotechnol **93**(3): 917-930.

Kitadokoro, K., D. Bordo, G. Galli, R. Petracca, F. Falugi, S. Abrignani, G. Grandi and M. Bolognesi (2001). "CD81 extracellular domain 3D structure: insight into the tetraspanin superfamily structural motifs." EMBO J **20**(1-2): 12-18.

Knodler, L. A., B. B. Finlay and O. Steele-Mortimer (2005). "The *Salmonella* effector protein SopB protects epithelial cells from apoptosis by sustained activation of Akt." J Biol Chem **280**(10): 9058-9064.

Kohler, G. and C. Milstein (1975). "Continuous Cultures of Fused Cells Secreting Antibody of Predefined Specificity." Nature **256**(5517): 495-497.

Kohmo, S., T. Kijima, Y. Otani, M. Mori, T. Minami, R. Takahashi, I. Nagatomo, Y. Takeda, H. Kida, S. Goya, M. Yoshida, T. Kumagai, I. Tachibana, S. Yokota and I. Kawase (2010). "Cell surface tetraspanin CD9 mediates chemoresistance in small cell lung cancer." Cancer Res **70**(20): 8025-8035.

Komorowski, S., B. Baranowska and M. Maleszewski (2006). "CD9 protein appears on growing mouse oocytes at the time when they develop the ability to fuse with spermatozoa." Zygote **14**(2): 119-123.

Kovalenko, O. V., X. H. Yang and M. E. Hemler (2007). "A novel cysteine cross-linking method reveals a direct association between claudin-1 and tetraspanin CD9." Molecular & cellular proteomics : MCP **6**(11): 1855-1867.

Krachler, A. M. and K. Orth (2013). "Targeting the bacteria-host interface: strategies in anti-adhesion therapy." Virulence **4**(4): 284-294.

Kubori, T., Y. Matsushima, D. Nakamura, J. Uralil, M. Lara-Tejero, A. Sukhan, J. E. Galan and S. I. Aizawa (1998). "Supramolecular structure of the *Salmonella* typhimurium type III protein secretion system." Science **280**(5363): 602-605.

Kukkonen, M., T. Raunio, R. Virkola, K. Lahteenmaki, P. H. Makela, P. Klemm, S. Clegg and T. K. Korhonen (1993). "Basement membrane carbohydrate as a target for bacterial adhesion: binding of type I fimbriae of *Salmonella* enterica and *Escherichia coli* to laminin." Mol Microbiol **7**(2): 229-237.

Kuramoto, H., S. Tamura and Y. Notake (1972). "Establishment of a Cell Line of Human Endometrial Adenocarcinoma in-Vitro." American Journal of Obstetrics and Gynecology **114**(8): 1012-1019.

Kuramoto, H., S. Tamura and Y. Notake (1972). "Establishment of a cell line of human endometrial adenocarcinoma in vitro." Am J Obstet Gynecol **114**(8): 1012-1019.

Kurzeder, C., B. Koppold, G. Sauer, S. Pabst, R. Kreienberg and H. Deissler (2007). "CD9 promotes adeno-associated virus type 2 infection of mammary carcinoma cells with low cell surface expression of heparan sulphate proteoglycans." Int J Mol Med **19**(2): 325-333.

Lachke, S. A., A. W. Higgins, M. Inagaki, I. Saadi, Q. Xi, M. Long, B. J. Quade, M. E. Talkowski, J. F. Gusella, A. Fujimoto, M. L. Robinson, Y. Yang, Q. T. Duong, I. Shapira, B. Motro, J. Miyoshi, Y. Takai, C. C. Morton and R. L. Maas (2012). "The cell adhesion gene PVRL3 is associated with congenital ocular defects." Human genetics **131**(2): 235-250.

Lagaudriere-Gesbert, C., S. Lebel-Binay, C. Hubeau, D. Fradelizi and H. Conjeaud (1998). "Signaling through the tetraspanin CD82 triggers its association with the cytoskeleton leading to sustained morphological changes and T cell activation." Eur J Immunol **28**(12): 4332-4344.

Lagendijk, E. L., S. Validov, G. E. Lamers, S. de Weert and G. V. Bloemberg (2010). "Genetic tools for tagging Gram-negative bacteria with mCherry for visualization in vitro and in natural habitats, biofilm and pathogenicity studies." FEMS Microbiol Lett **305**(1): 81-90.

Lahiri, A., P. Das and D. Chakravortty (2008). "Arginase modulates *Salmonella* induced nitric oxide production in RAW264.7 macrophages and is required for *Salmonella* pathogenesis in mice model of infection." Microbes Infect **10**(10-11): 1166-1174.

Lai, X. H., J. G. Xu, S. Melgar and B. E. Uhlin (1999). "An apoptotic response by J774 macrophage cells is common upon infection with diarrheagenic *Escherichia coli*." FEMS microbiology letters **172**(1): 29-34.

Lajarin, F., G. Rubio, J. Galvez and P. Garcia-Penarrubia (1996). "Adhesion, invasion and intracellular replication of *Salmonella* typhimurium in a murine hepatocyte cell line.

Effect of cytokines and LPS on antibacterial activity of hepatocytes." Microb Pathog **21**(5): 319-329.

Lakew, W., A. Girma and E. Triche (2013). "*Salmonella* enterica Serotype Arizonae Meningitis in a Neonate." Case Rep Pediatr **2013**: 813495.

Lambele, M., H. Koppensteiner, M. Symeonides, N. H. Roy, J. Chan, M. Schindler and M. Thali (2015). "Vpu is the main determinant for tetraspanin downregulation in HIV-1-infected cells." Journal of Virology **89**(6): 3247-3255.

Lambert, M. A. and S. G. J. Smith (2009). "The PagN protein mediates invasion via interaction with proteoglycan." Fems Microbiology Letters **297**(2): 209-216.

Lambou, K., D. Tharreau, A. Kohler, C. Sirven, M. Marguerettaz, C. Barbisan, A. C. Sexton, E. M. Kellner, F. Martin, B. J. Howlett, M. J. Orbach and M. H. Lebrun (2008). "Fungi have three tetraspanin families with distinct functions." BMC Genomics **9**: 63.

Landry, J. J. M., P. T. Pyl, T. Rausch, T. Zichner, M. M. Tekkedil, A. M. Stütz, A. Jauch, R. S. Aiyar, G. Pau, N. Delhomme, J. Gagneur, J. O. Korbel, W. Huber and L. M. Steinmetz (2013). "The Genomic and Transcriptomic Landscape of a HeLa Cell Line." G3: Genes|Genomes|Genetics **3**(8): 1213-1224.

Lantos, P. L. (1992). "From slow virus to prion: a review of transmissible spongiform encephalopathies." Histopathology **20**(1): 1-11.

Lapalombella, R., Y. Y. Yeh, L. Wang, A. Ramanunni, S. Rafiq, S. Jha, J. Staubli, D. M. Lucas, R. Mani, S. E. Herman, A. J. Johnson, A. Lozanski, L. Andritsos, J. Jones, J. M. Flynn, B. Lannutti, P. Thompson, P. Algate, S. Stromatt, D. Jarjoura, X. Mo, D. Wang, C. S. Chen, G. Lozanski, N. A. Heerema, S. Tridandapani, M. A. Freitas, N. Muthusamy and J. C. Byrd (2012). "Tetraspanin CD37 directly mediates transduction of survival and apoptotic signals." Cancer Cell **21**(5): 694-708.

LaRock, D. L., A. Chaudhary and S. I. Miller (2015). "*Salmonella*e interactions with host processes." Nature reviews. Microbiology **13**(4): 191-205.

Larsson, L. I., B. Bjerregaard and J. F. Talts (2008). "Cell fusions in mammals." Histochem Cell Biol **129**(5): 551-561.

Lathrop, S. K., K. A. Binder, T. Starr, K. G. Cooper, A. Chong, A. B. Carmody and O. Steele-Mortimer (2015). "Replication of *Salmonella* enterica Serovar Typhimurium in Human Monocyte-Derived Macrophages." Infect Immun **83**(7): 2661-2671.

Latysheva, N., G. Muratov, S. Rajesh, M. Padgett, N. A. Hotchin, M. Overduin and F. Berditchevski (2006). "Syntenin-1 is a new component of tetraspanin-enriched microdomains: mechanisms and consequences of the interaction of syntenin-1 with CD63." Mol Cell Biol **26**(20): 7707-7718.

Layton, A. N., D. L. Hudson, A. Thompson, J. C. Hinton, J. M. Stevens, E. E. Galyov and M. P. Stevens (2010). "Salicylidene acylhydrazide-mediated inhibition of type III secretion system-1 in *Salmonella* enterica serovar Typhimurium is associated with iron restriction and can be reversed by free iron." FEMS Microbiol Lett **302**(2): 114-122.

Le Minor, L., M. Veron and M. Popoff (1982). "[A proposal for *Salmonella* nomenclature]." Ann Microbiol (Paris) **133**(2): 245-254.

Le Naour, F., E. Rubinstein, C. Jasmin, M. Prenant and C. Boucheix (2000). "Severely reduced female fertility in CD9-deficient mice." Science **287**(5451): 319-321.

Lee, G. (2011). "Uroplakins in the lower urinary tract." Int Neurourol J **15**(1): 4-12.

Lee, H., Y. Kim, Y. Choi, S. Choi, E. Hong and E. S. Oh (2011). "Syndecan-2 cytoplasmic domain regulates colon cancer cell migration via interaction with syntenin-1." Biochem Biophys Res Commun **409**(1): 148-153.

Lee, J. G., J. H. Ahn, T. Jin Kim, J. Ho Lee and J. H. Choi (2015). "Mutant p53 promotes ovarian cancer cell adhesion to mesothelial cells via integrin beta4 and Akt signals." Scientific reports **5**: 12642.

Lee, M., M. Hadi, G. Hallden and G. W. Aponte (2005). "Peptide YY and neuropeptide Y induce villin expression, reduce adhesion, and enhance migration in small intestinal cells through the regulation of CD63, matrix metalloproteinase-3, and Cdc42 activity." J Biol Chem **280**(1): 125-136.

Lee, W. S., S. D. Puthucheary and A. Omar (1999). "*Salmonella* meningitis and its complications in infants." J Paediatr Child Health **35**(4): 379-382.

Levy, S. (2014). "Function of the tetraspanin molecule CD81 in B and T cells." Immunologic research **58**(2-3): 179-185.

Levy, S. and T. Shoham (2005). "Protein-protein interactions in the tetraspanin web." Physiology (Bethesda) **20**: 218-224.

Li, G., N. Dziuba, B. Friedrich, J. L. Murray and M. R. Ferguson (2011). "A post-entry role for CD63 in early HIV-1 replication." Virology **412**(2): 315-324.

Li, G., M. A. Endsley, A. Somasunderam, S. L. Gbota, M. I. Mbaka, J. L. Murray and M. R. Ferguson (2014). "The dual role of tetraspanin CD63 in HIV-1 replication." Virology journal **11**: 23.

Li, H., N. Liu, W. T. Wang, J. Y. Wang and W. Y. Gao (2015). "Cloning and characterization of GST fusion tag stabilized large subunit of *Escherichia coli* acetohydroxyacid synthase I." J Biosci Bioeng.

Liss, V. and M. Hensel (2015). "Take the tube: remodelling of the endosomal system by intracellular *Salmonella* enterica." Cell Microbiol **17**(5): 639-647.

Liu, W. M. and X. A. Zhang (2006). "KAI1/CD82, a tumor metastasis suppressor." Cancer Letters **240**(2): 183-194.

Liu, Z., H. Shi, L. C. Szymczak, T. Aydin, S. Yun, K. Constas, A. Schaeffer, S. Ranjan, S. Kubba, E. Alam, D. E. McMahon, J. He, N. Shwartz, C. Tian, Y. Plavskin, A. Lindy, N. A. Dad, S. Sheth, N. M. Amin, S. Zimmerman, D. Liu, E. M. Schwarz, H. Smith, M. W. Krause and J. Liu (2015). "Promotion of bone morphogenetic protein signaling by tetraspanins and glycosphingolipids." PLoS genetics **11**(5): e1005221.

Longhurst, C. M., J. D. Jacobs, M. M. White, J. T. Crossno, Jr., D. A. Fitzgerald, J. Bao, T. J. Fitzgerald, R. Raghow and L. K. Jennings (2002). "Chinese hamster ovary cell motility to

fibronectin is modulated by the second extracellular loop of CD9. Identification of a putative fibronectin binding site." J Biol Chem **277**(36): 32445-32452.

Lovelace, M. D., M. L. Yap, J. Yip, W. Muller, O. Wijburg and D. E. Jackson (2013). "Absence of platelet endothelial cell adhesion molecule 1, PECAM-1/CD31, in vivo increases resistance to *Salmonella* enterica serovar Typhimurium in mice." Infect Immun **81**(6): 1952-1963.

Lozahic, S., D. Christiansen, S. Manie, D. Gerlier, M. Billard, C. Boucheix and E. Rubinstein (2000). "CD46 (membrane cofactor protein) associates with multiple beta1 integrins and tetraspans." Eur J Immunol **30**(3): 900-907.

Luyten, A., E. Mortier, C. Van Campenhout, V. Taelman, G. Degeest, G. Wuytens, K. Lambaerts, G. David, E. J. Bellefroid and P. Zimmermann (2008). "The postsynaptic density 95/disc-large/zona occludens protein syntenin directly interacts with frizzled 7 and supports noncanonical Wnt signaling." Mol Biol Cell **19**(4): 1594-1604.

Ma, L., G. Zhang and M. P. Doyle (2011). "Green fluorescent protein labeling of *Listeria*, *Salmonella*, and *Escherichia coli* O157:H7 for safety-related studies." PLoS One **6**(4): e18083.

Madan, R., R. Rastogi, S. Parashuraman and A. Mukhopadhyay (2012). "*Salmonella* acquires lysosome-associated membrane protein 1 (LAMP1) on phagosomes from Golgi via SipC protein-mediated recruitment of host Syntaxin6." The Journal of biological chemistry **287**(8): 5574-5587.

Maecker, H. T., S. C. Todd and S. Levy (1997). "The tetraspanin superfamily: molecular facilitators." FASEB journal : official publication of the Federation of American Societies for Experimental Biology **11**(6): 428-442.

Maess, M. B., B. Wittig, A. Cignarella and S. Lorkowski (2014). "Reduced PMA enhances the responsiveness of transfected THP-1 macrophages to polarizing stimuli." J Immunol Methods **402**(1-2): 76-81.

Makkawi, M., F. Moheimani, R. Alserihi, D. Howells, M. Wright, L. Ashman and D. E. Jackson (2015). "A complementary role for tetraspanin superfamily member CD151 and ADP purinergic P2Y12 receptor in platelets." Thromb Haemost **114**(5): 1004-1019.

Makrides, S. C. (1996). "Strategies for achieving high-level expression of genes in *Escherichia coli*." Microbiol Rev **60**(3): 512-538.

Mandomando, I., E. Macete, B. Sigauque, L. Morais, L. Quinto, J. Sacarlal, M. Espasa, X. Valles, Q. Bassat, P. Aide, T. Nhampossa, S. Machevo, J. Ruiz, A. Nhacolo, C. Menendez, K. L. Kotloff, A. Roca, M. M. Levine and P. L. Alonso (2009). "Invasive non-typhoidal *Salmonella* in Mozambican children." Trop Med Int Health **14**(12): 1467-1474.

Mannion, B. A., F. Berditchevski, S. K. Kraeft, L. B. Chen and M. E. Hemler (1996). "Transmembrane-4 superfamily proteins CD81 (TAPA-1), CD82, CD63, and CD53 specifically associated with integrin alpha 4 beta 1 (CD49d/CD29)." J Immunol **157**(5): 2039-2047.

Marcus, S. L., J. H. Brumell, C. G. Pfeifer and B. B. Finlay (2000). "*Salmonella* pathogenicity islands: big virulence in small packages." Microbes Infect **2**(2): 145-156.

Margalit, O., R. Somech, N. Amariglio and G. Rechavi (2005). "Microarray-based gene expression profiling of hematologic malignancies: basic concepts and clinical applications." Blood reviews **19**(4): 223-234.

Marks, M. S., H. Ohno, T. Kirchnausen and J. S. Bonracino (1997). "Protein sorting by tyrosine-based signals: adapting to the Ys and wherefores." Trends Cell Biol **7**(3): 124-128.

Martin, F., D. M. Roth, D. A. Jans, C. W. Pouton, L. J. Partridge, P. N. Monk and G. W. Moseley (2005). "Tetraspanins in viral infections: a fundamental role in viral biology?" Journal of Virology **79**(17): 10839-10851.

Martin, F., D. M. Roth, D. A. Jans, C. W. Pouton, L. J. Partridge, P. N. Monk and G. W. Moseley (2005). "Tetraspanins in Viral Infections: a Fundamental Role in Viral Biology?" Journal of virology **79**(17): 10839-10851.

Martin, F., D. M. Roth, D. A. Jans, C. W. Pouton, L. J. Partridge, P. N. Monk and G. W. Moseley (2005). "Tetraspanins in viral infections: a fundamental role in viral biology?" J Virol **79**(17): 10839-10851.

Martinez-Lorenzo, M. J., S. Meresse, C. de Chastellier and J. P. Gorvel (2001). "Unusual intracellular trafficking of *Salmonella* typhimurium in human melanoma cells." Cell Microbiol **3**(6): 407-416.

Martinez del Hoyo, G., M. Ramirez-Huesca, S. Levy, C. Boucheix, E. Rubinstein, M. Minguito de la Escalera, L. Gonzalez-Cintado, C. Ardavin, E. Veiga, M. Yanez-Mo and F. Sanchez-Madrid (2015). "CD81 controls immunity to *Listeria* infection through rac-dependent inhibition of proinflammatory mediator release and activation of cytotoxic T cells." Journal of immunology (Baltimore, Md : 1950) **194**(12): 6090-6101.

Masciopinto, F., S. Campagnoli, S. Abrignani, Y. Uematsu and P. Pileri (2001). "The small extracellular loop of CD81 is necessary for optimal surface expression of the large loop, a putative HCV receptor." Virus Res **80**(1-2): 1-10.

Mazurov, D., L. Barbashova and A. Filatov (2013). "Tetraspanin protein CD9 interacts with metalloprotease CD10 and enhances its release via exosomes." FEBS J **280**(5): 1200-1213.

Mazurov, D., L. Barbashova and A. Filatov (2013). "Tetraspanin protein CD9 interacts with metalloprotease CD10 and enhances its release via exosomes." FEBS J.

Mazurov, D., G. Heidecker and D. Derse (2006). "HTLV-1 Gag protein associates with CD82 tetraspanin microdomains at the plasma membrane." Virology **346**(1): 194-204.

Mazurov, D., G. Heidecker and D. Derse (2007). "The inner loop of tetraspanins CD82 and CD81 mediates interactions with human T cell lymphotrophic virus type 1 Gag protein." J Biol Chem **282**(6): 3896-3903.

Mazzocca, A., V. Carloni, S. Sciammetta, C. Cordella, P. Pantaleo, A. Caldini, P. Gentilini and M. Pinzani (2002). "Expression of transmembrane 4 superfamily (TM4SF) proteins and their role in hepatic stellate cell motility and wound healing migration." J Hepatol **37**(3): 322-330.

McCarrey, J. R. and D. D. Dilworth (1992). "Expression of Xist in mouse germ cells correlates with X-chromosome inactivation." Nature genetics **2**(3): 200-203.

Meerschaert, K., E. Bruyneel, O. De Wever, B. Vanloo, C. Boucherie, M. Bracke, J. Vandekerckhove and J. Gettemans (2007). "The tandem PDZ domains of syntenin promote cell invasion." Exp Cell Res **313**(9): 1790-1804.

Meerschaert, K., E. Remue, A. De Ganck, A. Staes, C. Boucherie, K. Gevaert, J. Vandekerckhove, L. Kleiman and J. Gettemans (2008). "The tandem PDZ protein Syntenin interacts with the aminoacyl tRNA synthetase complex in a lysyl-tRNA synthetase-dependent manner." J Proteome Res **7**(11): 4962-4973.

Meuleman, P., J. Hesselgesser, M. Paulson, T. Vanwolleghem, I. Desombere, H. Reiser and G. Leroux-Roels (2008). "Anti-CD81 antibodies can prevent a hepatitis C virus infection in vivo." Hepatology **48**(6): 1761-1768.

Miao, W. M., E. Vasile, W. S. Lane and J. Lawler (2001). "CD36 associates with CD9 and integrins on human blood platelets." Blood **97**(6): 1689-1696.

Miller, B. J., E. Georges-Labouesse, P. Primakoff and D. G. Myles (2000). "Normal fertilization occurs with eggs lacking the integrin alpha6beta1 and is CD9-dependent." J Cell Biol **149**(6): 1289-1296.

Mills, S. D. and B. B. Finlay (1994). "Comparison of *Salmonella* typhi and *Salmonella* typhimurium invasion, intracellular growth and localization in cultured human epithelial cells." Microb Pathog **17**(6): 409-423.

Min, G., M. Stolz, G. Zhou, F. Liang, P. Sebbel, D. Stoffler, R. Glockshuber, T.-T. Sun, U. Aebi and X.-P. Kong (2002). "Localization of uroplakin Ia, the urothelial receptor for bacterial adhesin FimH, on the six inner domains of the 16 nm urothelial plaque particle." Journal of Molecular Biology **317**(5): 697-706.

Misselwitz, B., S. K. Kreibich, S. Rout, B. Stecher, B. Periaswamy and W. D. Hardt (2011). "*Salmonella* enterica serovar Typhimurium binds to HeLa cells via Fim-mediated reversible adhesion and irreversible type three secretion system 1-mediated docking." Infection and Immunity **79**(1): 330-341.

Monack, D. M. (2012). "*Salmonella* persistence and transmission strategies." Current Opinion in Microbiology **15**(1): 100-107.

Monk, P. N. and L. J. Partridge (2012). "Tetraspanins: gateways for infection." Infect Disord Drug Targets **12**(1): 4-17.

Montpellier, C., B. A. Tews, J. Poitrimole, V. Rocha-Perugini, V. D'Arienzo, J. Potel, X. A. Zhang, E. Rubinstein, J. Dubuisson and L. Cocquerel (2011). "Interacting regions of CD81 and two of its partners, EWI-2 and EWI-2wint, and their effect on hepatitis C virus infection." J Biol Chem **286**(16): 13954-13965.

Moore, K., S. A. Cooper and D. B. Jones (1987). "Use of the monoclonal antibody WR17, identifying the CD37 gp40-45 Kd antigen complex, in the diagnosis of B-lymphoid malignancy." J Pathol **152**(1): 13-21.

Muranova, T. A., S. N. Ruzheinikov, A. Higginbottom, J. A. Clipson, G. M. Blackburn, P. Wentworth, A. Datta, D. W. Rice and L. J. Partridge (2004). "Crystallization of a carbamatase catalytic antibody Fab fragment and its complex with a transition-state analogue." Acta Crystallogr D Biol Crystallogr **60**(Pt 1): 172-174.

Muroi, Y., T. Sakurai, A. Hanashi, K. Kubota, K. Nagaoka and K. Imakawa (2009). "CD9 regulates transcription factor GCM1 and ERVWE1 expression through the cAMP/protein kinase A signaling pathway." Reproduction **138**(6): 945-951.

Norris, F. A., M. P. Wilson, T. S. Wallis, E. E. Galyov and P. W. Majerus (1998). "SopB, a protein required for virulence of *Salmonella* dublin, is an inositol phosphate phosphatase." Proc Natl Acad Sci U S A **95**(24): 14057-14059.

O'Donnell, E. A., D. N. Ernst and R. Hingorani (2013). "Multiparameter flow cytometry: advances in high resolution analysis." Immune Netw **13**(2): 43-54.

Ochman, H., F. C. Soncini, F. Solomon and E. A. Groisman (1996). "Identification of a pathogenicity island required for *Salmonella* survival in host cells." Proceedings of the National Academy of Sciences of the United States of America **93**(15): 7800-7804.

Oh, Y. K., C. Alpuche-Aranda, E. Berthiaume, T. Jinks, S. I. Miller and J. A. Swanson (1996). "Rapid and complete fusion of macrophage lysosomes with phagosomes containing *Salmonella* typhimurium." Infect Immun **64**(9): 3877-3883.

Ohno, K., M. Koroll, O. El Far, P. Scholze, J. Gomeza and H. Betz (2004). "The neuronal glycine transporter 2 interacts with the PDZ domain protein syntenin-1." Mol Cell Neurosci **26**(4): 518-529.

Ono, M., K. Handa, D. A. Withers and S. Hakomori (2000). "Glycosylation effect on membrane domain (GEM) involved in cell adhesion and motility: a preliminary note on functional alpha3, alpha5-CD82 glycosylation complex in ldlD 14 cells." Biochem Biophys Res Commun **279**(3): 744-750.

Ortiz, D., E. M. Siegal, C. Kramer, B. K. Khandheria and E. Brauer (2014). "Nontyphoidal cardiac salmonellosis: two case reports and a review of the literature." Tex Heart Inst J **41**(4): 401-406.

Pan, Y., C. Brown, X. Wang and E. E. Geisert (2007). "The developmental regulation of CD81 in the rat retina." Mol Vis **13**: 181-189.

Park, K. R., T. Inoue, M. Ueda, T. Hirano, T. Higuchi, M. Maeda, I. Konishi, H. Fujiwara and S. Fujii (2000). "CD9 is expressed on human endometrial epithelial cells in association with integrins alpha(6), alpha(3) and beta(1)." Mol Hum Reprod **6**(3): 252-257.

Parker, P., L. Sando, R. Pearson, K. Kongsuwan, R. L. Tellam and S. Smith (2010). "Bovine Muc1 inhibits binding of enteric bacteria to Caco-2 cells." Glycoconj J **27**(1): 89-97.

Parthasarathy, V., F. Martin, A. Higginbottom, H. Murray, G. W. Moseley, R. C. Read, G. Mal, R. Hulme, P. N. Monk and L. J. Partridge (2009). "Distinct roles for tetraspanins CD9, CD63 and CD81 in the formation of multinucleated giant cells." Immunology **127**(2): 237-248.

Peng, Y. F., K. Mandai, H. Nakanishi, W. Ikeda, M. Asada, Y. Momose, S. Shibamoto, K. Yanagihara, H. Shiozaki, M. Monden, M. Takeichi and Y. Takai (2002). "Restoration of E-

cadherin-based cell-cell adhesion by overexpression of nectin in HSC-39 cells, a human signet ring cell gastric cancer cell line." Oncogene **21**(26): 4108-4119.

Perwitasari, O., X. Yan, S. Johnson, C. White, P. Brooks, S. M. Tompkins and R. A. Tripp (2013). "Targeting organic anion transporter 3 with probenecid as a novel anti-influenza a virus strategy." Antimicrobial agents and chemotherapy **57**(1): 475-483.

Petrovic, D., Z. Stamataki, E. Dempsey, L. Golden-Mason, M. Freeley, D. Doherty, D. Prichard, C. Keogh, J. Conroy, S. Mitchell, Y. Volkov, J. A. McKeating, C. O'Farrelly, D. Kelleher and A. Long (2011). "Hepatitis C virus targets the T cell secretory machinery as a mechanism of immune evasion." Hepatology **53**(6): 1846-1853.

Pileri, P., Y. Uematsu, S. Campagnoli, G. Galli, F. Falugi, R. Petracca, A. J. Weiner, M. Houghton, D. Rosa, G. Grandi and S. Abrignani (1998). "Binding of hepatitis C virus to CD81." Science **282**(5390): 938-941.

Pils, S., T. Schmitter, F. Neske and C. R. Hauck (2006). "Quantification of bacterial invasion into adherent cells by flow cytometry." J Microbiol Methods **65**(2): 301-310.

Pinder, A. C. and R. G. McClelland (1994). "Rapid assay for pathogenic *Salmonella* organisms by immunofluorescence flow cytometry." J Microsc **176**(Pt 1): 17-22.

Pique, C., C. Lagaudriere-Gesbert, L. Delamarre, A. R. Rosenberg, H. Conjeaud and M. C. Dokhelar (2000). "Interaction of CD82 tetraspanin proteins with HTLV-1 envelope glycoproteins inhibits cell-to-cell fusion and virus transmission." Virology **276**(2): 455-465.

Piratae, S., S. Tesana, M. K. Jones, P. J. Brindley, A. Loukas, E. Lovas, V. Eursitthichai, B. Sripa, S. Thanasuwan and T. Laha (2012). "Molecular Characterization of a Tetraspanin from the Human Liver Fluke, Opisthorchis viverrini." PLoS Negl Trop Dis **6**(12): e1939.

Podolska, A., B. Kaczkowski, T. Litman, M. Fredholm and S. Cirera (2011). "How the RNA isolation method can affect microRNA microarray results." Acta biochimica Polonica **58**(4): 535-540.

Pols, M. S. and J. Klumperman (2009). "Trafficking and function of the tetraspanin CD63." Exp Cell Res **315**(9): 1584-1592.

Ponting, C. P. (1997). "Evidence for PDZ domains in bacteria, yeast, and plants." Protein science : a publication of the Protein Society **6**(2): 464-468.

Powner, D., P. M. Kopp, S. J. Monkley, D. R. Critchley and F. Berditchevski (2011). "Tetraspanin CD9 in cell migration." Biochem Soc Trans **39**(2): 563-567.

Que, F., S. Wu and R. Huang (2013). "*Salmonella* pathogenicity island 1(SPI-1) at work." Curr Microbiol **66**(6): 582-587.

Radford, K. J., R. F. Thorne and P. Hersey (1996). "CD63 associates with transmembrane 4 superfamily members, CD9 and CD81, and with beta 1 integrins in human melanoma." Biochem Biophys Res Commun **222**(1): 13-18.

Rajashekar, R., D. Liebl, D. Chikkaballi, V. Liss and M. Hensel (2014). "Live cell imaging reveals novel functions of *Salmonella* enterica SPI2-T3SS effector proteins in remodeling of the host cell endosomal system." PLoS ONE **9**(12): e115423.

Rajesh, S., P. Sridhar, B. A. Tews, L. Feneant, L. Cocquerel, D. G. Ward, F. Berditchevski and M. Overduin (2012). "Structural basis of ligand interactions of the large extracellular domain of tetraspanin CD81." J Virol **86**(18): 9606-9616.

Ralph, P. and I. Nakoinz (1975). "Phagocytosis and cytolysis by a macrophage tumour and its cloned cell line." Nature **257**(5525): 393-394.

Ralph, P. and I. Nakoinz (1977). "Antibody-dependent killing of erythrocyte and tumor targets by macrophage-related cell lines: enhancement by PPD and LPS." J Immunol **119**(3): 950-954.

Rana, S. and M. Zoller (2011). "Exosome target cell selection and the importance of exosomal tetraspanins: a hypothesis." Biochem Soc Trans **39**(2): 559-562.

Ranjan, A., S. M. Bane and R. D. Kalraiya (2014). "Glycosylation of the laminin receptor (alpha3beta1) regulates its association with tetraspanin CD151: Impact on cell spreading, motility, degradation and invasion of basement membrane by tumor cells." Exp Cell Res **322**(2): 249-264.

Rescigno, M., M. Urbano, B. Valzasina, M. Francolini, G. Rotta, R. Bonasio, F. Granucci, J. P. Kraehenbuhl and P. Ricciardi-Castagnoli (2001). "Dendritic cells express tight junction proteins and penetrate gut epithelial monolayers to sample bacteria." Nat Immunol **2**(4): 361-367.

Reyes, R., A. Monjas, M. Yanez-Mo, B. Cardenes, G. Morlino, A. Gilsanz, Y. Machado-Pineda, E. Lafuente, P. Monk, F. Sanchez-Madrid and C. Cabanas (2015). "Different states of integrin LFA-1 aggregation are controlled through its association with tetraspanin CD9." Biochim Biophys Acta **1853**(10 Pt A): 2464-2480.

Ringner, M. (2008). "What is principal component analysis?" Nature Biotechnology **26**(3): 303-304.

Risinger, J. I., M. Custer, L. Feigenbaum, R. M. Simpson, S. B. Hoover, J. D. Webster, G. V. Chandramouli, L. Tessarollo and J. C. Barrett (2014). "Normal viability of Kai1/Cd82 deficient mice." Mol Carcinog **53**(8): 610-624.

Rittenour, W. R. and S. D. Harris (2008). "Characterization of Fusarium graminearum Mes1 reveals roles in cell-surface organization and virulence." Fungal Genet Biol **45**(6): 933-946.

Robijns, S. C., S. Roberfroid, S. Van Puyvelde, B. De Pauw, E. Uceda Santamaria, A. De Weerdt, D. De Coster, K. Hermans, S. C. De Keersmaecker, J. Vanderleyden and H. P. Steenackers (2014). "A GFP promoter fusion library for the study of *Salmonella* biofilm formation and the mode of action of biofilm inhibitors." Biofouling **30**(5): 605-625.

Rollenhagen, C. and D. Bumann (2006). "Salmonella enterica highly expressed genes are disease specific." Infect Immun **74**(3): 1649-1660.

Rosales-Reyes, R., A. Perez-Lopez, C. Sanchez-Gomez, R. R. Hernandez-Mote, D. Castro-Eguiluz, V. Ortiz-Navarrete and C. M. Alpuche-Aranda (2012). "*Salmonella* infects B cells by macropinocytosis and formation of spacious phagosomes but does not induce pyroptosis in favor of its survival." Microb Pathog **52**(6): 367-374.

Rosselin, M., N. Abed, I. Virlogeux-Payant, E. Bottreau, P.-Y. Sizaret, P. Velge and A. Wiedemann (2011). "Heterogeneity of type III secretion system (T3SS)-1-independent entry mechanisms used by *Salmonella* Enteritidis to invade different cell types." Microbiology **157**(3): 839-847.

Roucourt, B., S. Meeussen, J. Bao, P. Zimmermann and G. David (2015). "Heparanase activates the syndecan-syntenin-ALIX exosome pathway." Cell Res **25**(4): 412-428.

Rous, B. A., B. J. Reaves, G. Ihrke, J. A. Briggs, S. R. Gray, D. J. Stephens, G. Banting and J. P. Luzio (2002). "Role of adaptor complex AP-3 in targeting wild-type and mutated CD63 to lysosomes." Mol Biol Cell **13**(3): 1071-1082.

Rubinstein, E., A. Ziyyat, M. Prenant, E. Wrobel, J. P. Wolf, S. Levy, F. Le Naour and C. Boucheix (2006). "Reduced fertility of female mice lacking CD81." Dev Biol **290**(2): 351-358.

Rubinstein, E., A. Ziyyat, J. P. Wolf, F. Le Naour and C. Boucheix (2006). "The molecular players of sperm-egg fusion in mammals." Seminars in cell & developmental biology **17**(2): 254-263.

Ruiz-Mateos, E., A. Pelchen-Matthews, M. Deneka and M. Marsh (2008). "CD63 is not required for production of infectious human immunodeficiency virus type 1 in human macrophages." J Virol **82**(10): 4751-4761.

Runge, K., J. Evans, Z. He, S. Gupta, K. McDonald , H. Stahlberg, P. Primakoff and D. Myles (2007). "Oocyte CD9 is enriched on the microvillar membrane and required for normal microvillar shape and distribution." Dev Biol **304**(1): 317-325.

Sala-Valdes, M., N. Ailane, C. Greco, E. Rubinstein and C. Boucheix (2012). "Targeting tetraspanins in cancer." Expert opinion on therapeutic targets **16**(10): 985-997.

Sala-Valdes, M., A. Ursa, S. Charrin, E. Rubinstein, M. E. Hemler, F. Sanchez-Madrid and M. Yanez-Mo (2006). "EWI-2 and EWI-F link the tetraspanin web to the actin cytoskeleton through their direct association with ezrin-radixin-moesin proteins." J Biol Chem **281**(28): 19665-19675.

Salcedo, S. P., M. Noursadeghi, J. Cohen and D. W. Holden (2001). "Intracellular replication of *Salmonella* typhimurium strains in specific subsets of splenic macrophages in vivo." Cell Microbiol **3**(9): 587-597.

Sánchez-Vargas, F. M., M. A. Abu-El-Haija and O. G. Gómez-Duarte (2011). "*Salmonella* infections: An update on epidemiology, management, and prevention." Travel Medicine and Infectious Disease **9**(6): 263-277.

Santhi, L. P., S. Sunkoji, S. Siddiram and S. S. Sanghai (2012). "Patent research in salmonellosis prevention." Food Research International **45**(2): 809-818.

Sarkar, D., H. Boukerche, Z. Z. Su and P. B. Fisher (2004). "mda-9/syntenin: recent insights into a novel cell signaling and metastasis-associated gene." Pharmacol Ther **104**(2): 101-115.

Satoh-Horikawa, K., H. Nakanishi, K. Takahashi, M. Miyahara, M. Nishimura, K. Tachibana, A. Mizoguchi and Y. Takai (2000). "Nectin-3, a new member of immunoglobulin-like cell adhesion molecules that shows homophilic and heterophilic cell-cell adhesion activities." The Journal of biological chemistry **275**(14): 10291-10299.

Scheffer, K. D., F. Berditchevski and L. Florin (2014). "The tetraspanin CD151 in papillomavirus infection." Viruses **6**(2): 893-908.

Scherer, W. F., J. T. Syverton and G. O. Gey (1953). "Studies on the propagation in vitro of poliomyelitis viruses. IV. Viral multiplication in a stable strain of human malignant epithelial cells (strain HeLa) derived from an epidermoid carcinoma of the cervix." J Exp Med **97**(5): 695-710.

Schlieker, C., B. Bukau and A. Mogk (2002). "Prevention and reversion of protein aggregation by molecular chaperones in the *E. coli* cytosol: implications for their applicability in biotechnology." J Biotechnol **96**(1): 13-21.

Schlumberger, M. C. and W. D. Hardt (2006). "*Salmonella* type III secretion effectors: pulling the host cell's strings." Curr Opin Microbiol **9**(1): 46-54.

Scholz, C. J., G. Sauer and H. Deissler (2009). "Glycosylation of tetraspanin Tspan-1 at four distinct sites promotes its transition through the endoplasmic reticulum." Protein Pept Lett **16**(10): 1244-1248.

Schroeder, A., O. Mueller, S. Stocker, R. Salowsky, M. Leiber, M. Gassmann, S. Lightfoot, W. Menzel, M. Granzow and T. Ragg (2006). "The RIN: an RNA integrity number for assigning integrity values to RNA measurements." BMC Mol Biol **7**: 3.

Schwende, H., E. Fitzke, P. Ambs and P. Dieter (1996). "Differences in the state of differentiation of THP-1 cells induced by phorbol ester and 1,25-dihydroxyvitamin D-3." Journal of Leukocyte Biology **59**(4): 555-561.

Seigneuret, M. (2006). "Complete Predicted Three-Dimensional Structure of the FacilitatorTransmembrane Protein and Hepatitis C Virus Receptor CD81: Conserved and Variable Structural Domains in the Tetraspanin Superfamily." Biophysical Journal **90**: 212–227.

Seigneuret, M., A. Delaguillaumie, C. Lagaudriere-Gesbert and H. Conjeaud (2001). "Structure of the tetraspanin main extracellular domain. A partially conserved fold with a structurally variable domain insertion." J Biol Chem **276**(43): 40055-40064.

Shanmukhappa, K., J. K. Kim and S. Kapil (2007). "Role of CD151, A tetraspanin, in porcine reproductive and respiratory syndrome virus infection." Virol J **4**: 62.

Sharma, C., X. H. Yang and M. E. Hemler (2008). "DHHC2 affects palmitoylation, stability, and functions of tetraspanins CD9 and CD151." Mol Biol Cell **19**(8): 3415-3425.

Shea, J. E., M. Hensel, C. Gleeson and D. W. Holden (1996). "Identification of a virulence locus encoding a second type III secretion system in *Salmonella* typhimurium." Proc Natl Acad Sci U S A **93**(6): 2593-2597.

Shi, G. M., A. W. Ke, J. Zhou, X. Y. Wang, Y. Xu, Z. B. Ding, R. P. Devbhandari, X. Y. Huang, S. J. Qiu, Y. H. Shi, Z. Dai, X. R. Yang, G. H. Yang and J. Fan (2010). "CD151 modulates expression of matrix metalloproteinase 9 and promotes neoangiogenesis and progression of hepatocellular carcinoma." Hepatology **52**(1): 183-196.

Shigeta, M., N. Sanzen, M. Ozawa, J. Gu, H. Hasegawa and K. Sekiguchi (2003). "CD151 regulates epithelial cell-cell adhesion through PKC- and Cdc42-dependent actin cytoskeletal reorganization." J Cell Biol **163**(1): 165-176.

Silvie, O., J. F. Franetich, C. Boucheix, E. Rubinstein and D. Mazier (2007). "Alternative invasion pathways for Plasmodium berghei sporozoites." Int J Parasitol **37**(2): 173-182.

Silvie, O., E. Rubinstein, J. F. Franetich, M. Prenant, E. Belnoue, L. Renia, L. Hannoun, W. Eling, S. Levy, C. Boucheix and D. Mazier (2003). "Hepatocyte CD81 is required for Plasmodium falciparum and Plasmodium yoelii sporozoite infectivity." Nat Med **9**(1): 93-96.

Singethan, K., N. Muller, S. Schubert, D. Luttge, D. N. Krementsov, S. R. Khurana, G. Krohne, S. Schneider-Schaulies, M. Thali and J. Schneider-Schaulies (2008). "CD9 clustering and formation of microvilli zippers between contacting cells regulates virus-induced cell fusion." Traffic **9**(6): 924-935.

Sirerol-Piquer, M. S., A. Cebrian-Silla, C. Alfaro-Cervello, U. Gomez-Pinedo, M. Soriano-Navarro and J. M. Verdugo (2012). "GFP immunogold staining, from light to electron microscopy, in mammalian cells." Micron **43**(5): 589-599.

Skaar, K., H. J. Korza, M. Tarry, P. Sekyrova and M. Hogbom (2015). "Expression and Subcellular Distribution of GFP-Tagged Human Tetraspanin Proteins in Saccharomyces cerevisiae." PLoS One **10**(7): e0134041.

Sly, L. M., D. G. Guiney and N. E. Reiner (2002). "*Salmonella* enterica serovar Typhimurium periplasmic superoxide dismutases SodCI and SodCII are required for protection against the phagocyte oxidative burst." Infect Immun **70**(9): 5312-5315.

Sorensen, H. P. and K. K. Mortensen (2005). "Advanced genetic strategies for recombinant protein expression in *Escherichia coli*." J Biotechnol **115**(2): 113-128.

Sorensen, M., C. Lippuner, T. Kaiser, A. Misslitz, T. Aebischer and D. Bumann (2003). "Rapidly maturing red fluorescent protein variants with strongly enhanced brightness in bacteria." FEBS Lett **552**(2-3): 110-114.

Spector, M. P. and W. J. Kenyon (2012). "Resistance and survival strategies of *Salmonella* enterica to environmental stresses." Food Research International **45**(2): 455-481.

Srichaisupakit, A., T. Ohashi, R. Misaki and K. Fujiyama (2015). "Production of initial-stage eukaryotic N-glycan and its protein glycosylation in *Escherichia coli*." J Biosci Bioeng **119**(4): 399-405.

Steele-Mortimer, O. (2008). "The *Salmonella*-containing vacuole: moving with the times." Curr Opin Microbiol **11**(1): 38-45.

Stevens, J. M., R. L. Ulrich, L. A. Taylor, M. W. Wood, D. Deshazer, M. P. Stevens and E. E. Galyov (2005). "Actin-binding proteins from Burkholderia mallei and Burkholderia thailandensis can functionally compensate for the actin-based motility defect of a Burkholderia pseudomallei bimA mutant." J Bacteriol **187**(22): 7857-7862.

Stevenson, M., A. J. Baillie and R. M. E. Richards (1984). "An Invitro Model of Intracellular Bacterial-Infection Using the Murie Macrophage Cell Line-J774-2." Journal of Pharmacy and Pharmacology **36**(2): 90-94.

Stier, S., G. Totzke, E. Grunewald, T. Neuhaus, S. Fronhoffs, A. Sachinidis, H. Vetter, K. Schulze-Osthoff and Y. Ko (2000). "Identification of syntenin and other TNF-inducible genes in human umbilical arterial endothelial cells by suppression subtractive hybridization." FEBS Lett **467**(2-3): 299-304.

Stipp, C. S., T. V. Kolesnikova and M. E. Hemler (2001). "EWI-2 is a major CD9 and CD81 partner and member of a novel Ig protein subfamily." J Biol Chem **276**(44): 40545-40554.

Stipp, C. S., T. V. Kolesnikova and M. E. Hemler (2003). "Functional domains in tetraspanin proteins." Trends Biochem Sci **28**(2): 106-112.

Stipp, C. S., D. Orlicky and M. E. Hemler (2001). "FPRP, a major, highly stoichiometric, highly specific CD81- and CD9-associated protein." J Biol Chem **276**(7): 4853-4862.

Sutovsky, P. (2009). "Sperm-egg adhesion and fusion in mammals." Expert Rev Mol Med **11**: e11.

Symeonides, M., M. Lambele, N. H. Roy and M. Thali (2014). "Evidence showing that tetraspanins inhibit HIV-1-induced cell-cell fusion at a post-hemifusion stage." Viruses **6**(3): 1078-1090.

Szpirer, C. Y., M. Faelen and M. Couturier (2001). "Mobilization function of the pBHR1 plasmid, a derivative of the broad-host-range plasmid pBBR1." J Bacteriol **183**(6): 2101-2110.

Tachibana, I., J. Bodorova, F. Berditchevski, M. M. Zutter and M. E. Hemler (1997). "NAG-2, a novel transmembrane-4 superfamily (TM4SF) protein that complexes with integrins and other TM4SF proteins." J Biol Chem **272**(46): 29181-29189.

Tachibana, I. and M. E. Hemler (1999). "Role of transmembrane 4 superfamily (TM4SF) proteins CD9 and CD81 in muscle cell fusion and myotube maintenance." J Cell Biol **146**(4): 893-904.

Takahashi, Y., D. Bigler, Y. Ito and J. M. White (2001). "Sequence-specific interaction between the disintegrin domain of mouse ADAM 3 and murine eggs: role of beta1 integrin-associated proteins CD9, CD81, and CD98." Mol Biol Cell **12**(4): 809-820.

Takeda, Y., A. R. Kazarov, C. E. Butterfield, B. D. Hopkins, L. E. Benjamin, A. Kaipainen and M. E. Hemler (2007). "Deletion of tetraspanin Cd151 results in decreased pathologic angiogenesis in vivo and in vitro." Blood **109**(4): 1524-1532.

Takeda, Y., I. Tachibana, K. Miyado, M. Kobayashi, T. Miyazaki, T. Funakoshi, H. Kimura, H. Yamane, Y. Saito, H. Goto, T. Yoneda, M. Yoshida, T. Kumagai, T. Osaki, S. Hayashi, I. Kawase and E. Mekada (2003). "Tetraspanins CD9 and CD81 function to prevent the fusion of mononuclear phagocytes." J Cell Biol **161**(5): 945-956.

Tamura, K., M. Ikutani, T. Yoshida, A. Tanaka-Hayashi, T. Yanagibashi, R. Inoue, Y. Nagai, Y. Adachi, T. Miyawaki, K. Takatsu and H. Mori (2015). "Increased production of intestinal immunoglobulins in Syntenin-1-deficient mice." Immunobiology **220**(5): 597-604.

Tang, Y., J. R. Guest, P. J. Artymiuk, R. C. Read and J. Green (2004). "Post-transcriptional regulation of bacterial motility by aconitase proteins." Mol Microbiol **51**(6): 1817-1826.

Tanigawa, M., K. Miyamoto, S. Kobayashi, M. Sato, H. Akutsu, M. Okabe, E. Mekada, K. Sakakibara, M. Miyado, A. Umezawa and K. Miyado (2008). "Possible involvement of CD81 in acrosome reaction of sperm in mice." Mol Reprod Dev **75**(1): 150-155.

Tarrant, J. M., L. Robb, A. B. van Spriel and M. D. Wright (2003). "Tetraspanins: molecular organisers of the leukocyte surface." Trends Immunol **24**(11): 610-617.

Taylor, M. V. (2000). "Muscle development: molecules of myoblast fusion." Curr Biol **10**(17): R646-648.

Terpe, K. (2003). "Overview of tag protein fusions: from molecular and biochemical fundamentals to commercial systems." Appl Microbiol Biotechnol **60**(5): 523-533.

Thali, M. (2011). "Tetraspanin functions during HIV-1 and influenza virus replication." Biochem Soc Trans **39**(2): 529-531.

Tham, T. N., E. Gouin, E. Rubinstein, C. Boucheix, P. Cossart and J. Pizarro-Cerda (2010). "Tetraspanin CD81 is required for *Listeria* monocytogenes invasion." Infection and Immunity **78**(1): 204-209.

Tham, T. N., E. Gouin, E. Rubinstein, C. Boucheix, P. Cossart and J. Pizarro-Cerda (2010). "Tetraspanin CD81 is required for *Listeria* monocytogenes invasion." Infect Immun **78**(1): 204-209.

Thone, F., B. Schwanhausser, D. Becker, M. Ballmaier and D. Bumann (2007). "FACS-isolation of *Salmonella*-infected cells with defined bacterial load from mouse spleen." J Microbiol Methods **71**(3): 220-224.

Tippett, E., P. U. Cameron, M. Marsh and S. M. Crowe (2013). "Characterization of tetraspanins CD9, CD53, CD63, and CD81 in monocytes and macrophages in HIV-1 infection." J Leukoc Biol.

Tippett, E., P. U. Cameron, M. Marsh and S. M. Crowe (2013). "Characterization of tetraspanins CD9, CD53, CD63, and CD81 in monocytes and macrophages in HIV-1 infection." J Leukoc Biol **93**(6): 913-920.

Todres, E., J. B. Nardi and H. M. Robertson (2000). "The tetraspanin superfamily in insects." Insect Mol Biol **9**(6): 581-590.

Tominaga, N., K. Hagiwara, N. Kosaka, K. Honma, H. Nakagama and T. Ochiya (2014). "RPN2-mediated glycosylation of tetraspanin CD63 regulates breast cancer cell malignancy." Molecular cancer **13**: 134.

Toyo-oka, K., Y. Yashiro-Ohtani, C. S. Park, X. G. Tai, K. Miyake, T. Hamaoka and H. Fujiwara (1999). "Association of a tetraspanin CD9 with CD5 on the T cell surface: role of particular transmembrane domains in the association." Int Immunol **11**(12): 2043-2052.

Traini, M., C. M. Quinn, C. Sandoval, E. Johansson, K. Schroder, M. Kockx, P. J. Meikle, W. Jessup and L. Kritharides (2014). "Sphingomyelin phosphodiesterase acid-like 3A (SMPDL3A) is a novel nucleotide phosphodiesterase regulated by cholesterol in human macrophages." The Journal of biological chemistry **289**(47): 32895-32913.

Traore, K., M. A. Trush, M. George, Jr., E. W. Spannhake, W. Anderson and A. Asseffa (2005). "Signal transduction of phorbol 12-myristate 13-acetate (PMA)-induced growth inhibition of human monocytic leukemia THP-1 cells is reactive oxygen dependent." Leuk Res **29**(8): 863-879.

Trouillet, S., J. P. Rasigade, Y. Lhoste, T. Ferry, F. Vandenesch, J. Etienne and F. Laurent (2011). "A novel flow cytometry-based assay for the quantification of *Staphylococcus aureus* adhesion to and invasion of eukaryotic cells." J Microbiol Methods **86**(2): 145-149.

Tsai, Y. C. and A. M. Weissman (2010). "The Unfolded Protein Response, Degradation from Endoplasmic Reticulum and Cancer." Genes Cancer **1**(7): 764-778.

Tsuchiya, S., Y. Kobayashi, Y. Goto, H. Okumura, S. Nakae, T. Konno and K. Tada (1982). "Induction of Maturation in Cultured Human Monocytic Leukemia-Cells by a Phorbol Diester." Cancer Research **42**(4): 1530-1536.

Tsuchiya, S., M. Yamabe, Y. Yamaguchi, Y. Kobayashi, T. Konno and K. Tada (1980). "Establishment and characterization of a human acute monocytic leukemia cell line (THP-1)." International journal of cancer Journal international du cancer **26**(2): 171-176.

Tsukamoto, S., M. Takeuchi, T. Kawaguchi, E. Togasaki, A. Yamazaki, Y. Sugita, T. Muto, S. Sakai, Y. Takeda, C. Ohwada, E. Sakaida, N. Shimizu, K. Nishii, M. Jiang, K. Yokote, H. Bujo and C. Nakaseko (2014). "Tetraspanin CD9 modulates ADAM17-mediated shedding of LR11 in leukocytes." Exp Mol Med **46**: e89.

Tu, L., X. P. Kong, T. T. Sun and G. Kreibich (2006). "Integrity of all four transmembrane domains of the tetraspanin uroplakin Ib is required for its exit from the ER." J Cell Sci **119**(Pt 24): 5077-5086.

Uygur, E., K. Reddy, F. U. Ozkan, S. Soylemez, O. Aydin and S. Senol (2013). "*Salmonella* enteridis Septic Arthritis: A Report of Two Cases." Case Rep Infect Dis **2013**: 642805.

Valdivia, R. H. (2008). "Chlamydia effector proteins and new insights into chlamydial cellular microbiology." Current opinion in microbiology **11**(1): 53-59.

Valdivia, R. H. and S. Falkow (1998). "Flow cytometry and bacterial pathogenesis." Curr Opin Microbiol **1**(3): 359-363.

Valdivia, R. H., A. E. Hromockyj, D. Monack, L. Ramakrishnan and S. Falkow (1996). "Applications for green fluorescent protein (GFP) in the study of host-pathogen interactions." Gene **173**(1 Spec No): 47-52.

Van Dilla, M. A., T. T. Trujillo, P. F. Mullaney and J. R. Coulter (1969). "Cell microfluorometry: a method for rapid fluorescence measurement." Science **163**(3872): 1213-1214.

van Spriel, A. B. and C. G. Figdor (2010). "The role of tetraspanins in the pathogenesis of infectious diseases." Microbes Infect **12**(2): 106-112.

van Spriel, A. B., M. Sofi, K. H. Gartlan, A. van der Schaaf, I. Verschueren, R. Torensma, R. A. Raymakers, B. E. Loveland, M. G. Netea, G. J. Adema, M. D. Wright and C. G. Figdor (2009). "The tetraspanin protein CD37 regulates IgA responses and anti-fungal immunity." PLoS Pathog **5**(3): e1000338.

Vergunst, A. C., A. H. Meijer, S. A. Renshaw and D. O'Callaghan (2010). "Burkholderia cenocepacia creates an intramacrophage replication niche in zebrafish embryos, followed by bacterial dissemination and establishment of systemic infection." Infect Immun **78**(4): 1495-1508

Virtaneva, K. I., P. Angelisova, T. Baumruker, V. Horejsi, H. Nevanlinna and J. Schroder (1993). "The genes for CD37, CD53, and R2, all members of a novel gene family, are located on different chromosomes." Immunogenetics **37**(6): 461-465.

Wacker, M., D. Linton, P. G. Hitchen, M. Nita-Lazar, S. M. Haslam, S. J. North, M. Panico, H. R. Morris, A. Dell, B. W. Wren and M. Aebi (2002). "N-linked glycosylation in Campylobacter jejuni and its functional transfer into *E. coli*." Science **298**(5599): 1790-1793.

Wang, F., K. Vandepoele and M. Van Lijsebettens (2012). "Tetraspanin genes in plants." Plant Sci **190**: 9-15.

Wang, H., G. Min, R. Glockshuber, T.-T. Sun and X.-P. Kong (2009). "Uropathogenic *E. coli* Adhesin-Induced Host Cell Receptor Conformational Changes: Implications in Transmembrane Signaling Transduction." Journal of Molecular Biology **392**(2): 352-361.

Wang, H. X., T. V. Kolesnikova, C. Denison, S. P. Gygi and M. E. Hemler (2011). "The C-terminal tail of tetraspanin protein CD9 contributes to its function and molecular organization." J Cell Sci **124**(Pt 16): 2702-2710.

Wang, H. X., Q. Li, C. Sharma, K. Knoblich and M. E. Hemler (2011). "Tetraspanin protein contributions to cancer." Biochem Soc Trans **39**(2): 547-552.

Wendland, M. and D. Bumann (2002). "Optimization of GFP levels for analyzing *Salmonella* gene expression during an infection." FEBS Lett **521**(1-3): 105-108.

Weng, J., D. N. Krementsov, S. Khurana, N. H. Roy and M. Thali (2009). "Formation of syncytia is repressed by tetraspanins in human immunodeficiency virus type 1-producing cells." J Virol **83**(15): 7467-7474.

Wilken, L. R. and Z. L. Nikolov (2012). "Recovery and purification of plant-made recombinant proteins." Biotechnol Adv **30**(2): 419-433.

Winter, S. E., P. Thiennimitr, M. G. Winter, B. P. Butler, D. L. Huseby, R. W. Crawford, J. M. Russell, C. L. Bevins, L. G. Adams, R. M. Tsolis, J. R. Roth and A. J. Baumler (2010). "Gut inflammation provides a respiratory electron acceptor for *Salmonella*." Nature **467**(7314): 426-429.

Wong, G. E., X. Zhu, C. E. Prater, E. Oh and J. P. Evans (2001). "Analysis of fertilin alpha (ADAM1)-mediated sperm-egg cell adhesion during fertilization and identification of an adhesion-mediating sequence in the disintegrin-like domain." J Biol Chem **276**(27): 24937-24945.

Wood, M. W., R. Rosqvist, P. B. Mullan, M. H. Edwards and E. E. Galyov (1996). "SopE, a secreted protein of *Salmonella dublin,* is translocated into the target eukaryotic cell via a sip-dependent mechanism and promotes bacterial entry." Mol Microbiol **22**(2): 327-338.

Wu, X. R., T. T. Sun and J. J. Medina (1996). "In vitro binding of type 1-fimbriated *Escherichia coli* to uroplakins Ia and Ib: relation to urinary tract infections." Proc Natl Acad Sci U S A **93**(18): 9630-9635.

Xu, C., Y. H. Zhang, M. Thangavel, M. M. Richardson, L. Liu, B. Zhou, Y. Zheng, R. S. Ostrom and X. A. Zhang (2009). "CD82 endocytosis and cholesterol-dependent reorganization of tetraspanin webs and lipid rafts." FASEB J **23**(10): 3273-3288.

Yalaoui, S., T. Huby, J. F. Franetich, A. Gego, A. Rametti, M. Moreau, X. Collet, A. Siau, G. J. van Gemert, R. W. Sauerwein, A. J. Luty, J. C. Vaillant, L. Hannoun, J. Chapman, D. Mazier and P. Froissard (2008). "Scavenger receptor BI boosts hepatocyte permissiveness to Plasmodium infection." Cell Host Microbe **4**(3): 283-292.

Yanez-Mo, M., O. Barreiro, M. Gordon-Alonso, M. Sala-Valdes and F. Sanchez-Madrid (2009). "Tetraspanin-enriched microdomains: a functional unit in cell plasma membranes." Trends Cell Biol **19**(9): 434-446.

Yanez-Mo, M., M. Mittelbrunn and F. Sanchez-Madrid (2001). "Tetraspanins and intercellular interactions." Microcirculation **8**(3): 153-168.

Yanez-Mo, M., F. Sanchez-Madrid and C. Cabanas (2011). "Membrane proteases and tetraspanins." Biochem Soc Trans **39**(2): 541-546.

Yang, X., C. Claas, S. K. Kraeft, L. B. Chen, Z. Wang, J. A. Kreidberg and M. E. Hemler (2002). "Palmitoylation of tetraspanin proteins: modulation of CD151 lateral interactions, subcellular distribution, and integrin-dependent cell morphology." Mol Biol Cell **13**(3): 767-781.

Yang, X., O. V. Kovalenko, W. Tang, C. Claas, C. S. Stipp and M. E. Hemler (2004). "Palmitoylation supports assembly and function of integrin-tetraspanin complexes." J Cell Biol **167**(6): 1231-1240.

Yin, J., G. Li, X. Ren and G. Herrler (2007). "Select what you need: a comparative evaluation of the advantages and limitations of frequently used expression systems for foreign genes." J Biotechnol **127**(3): 335-347.

Yoshida, T., H. Ebina and Y. Koyanagi (2009). "N-linked glycan-dependent interaction of CD63 with CXCR4 at the Golgi apparatus induces downregulation of CXCR4." Microbiol Immunol **53**(11): 629-635.

Yunta, M. and P. A. Lazo (2003). "Tetraspanin proteins as organisers of membrane microdomains and signalling complexes." Cell Signal **15**(6): 559-564.

Zaidi, E., R. Bachur and M. Harper (1999). "Non-typhi *Salmonella* bacteremia in children." Pediatr Infect Dis J **18**(12): 1073-1077.

Zeiner, S. A., B. E. Dwyer and S. Clegg (2012). "FimA, FimF, and FimH are necessary for assembly of type 1 fimbriae on *Salmonella* enterica serovar Typhimurium." Infect Immun **80**(9): 3289-3296.

Zhang, F., J. Kotha, L. K. Jennings and X. A. Zhang (2009). "Tetraspanins and vascular functions." Cardiovasc Res **83**(1): 7-15.

Zhang, F., H. Liu, G. M. Jiang, H. S. Wang, X. F. Wang, H. Wang, R. Fang, S. H. Cai and J. Du (2015). "Changes in the proteomic profile during the differential polarization status of the human monocyte-derived macrophage THP-1 cell line." Proteomics **15**(4): 773-786.

Zhang, X. A., A. L. Bontrager and M. E. Hemler (2001). "Transmembrane-4 superfamily proteins associate with activated protein kinase C (PKC) and link PKC to specific beta(1) integrins." J Biol Chem **276**(27): 25005-25013.

Zhang, X. A. and C. Huang (2012). "Tetraspanins and cell membrane tubular structures." Cell Mol Life Sci **69**(17): 2843-2852.

Zhao, Y. Y., M. Takahashi, J. G. Gu, E. Miyoshi, A. Matsumoto, S. Kitazume and N. Taniguchi (2008). "Functional roles of N-glycans in cell signaling and cell adhesion in cancer." Cancer Sci **99**(7): 1304-1310.

Zhong, D., J. H. Ran, W. Y. Tang, X. D. Zhang, Y. Tan, G. J. Chen, X. S. Li and Y. Yan (2012). "Mda-9/syntenin promotes human brain glioma migration through focal adhesion kinase (FAK)-JNK and FAK-AKT signaling." Asian Pac J Cancer Prev **13**(6): 2897-2901.

Zhou, B., L. Liu, M. Reddivari and X. A. Zhang (2004). "The palmitoylation of metastasis suppressor KAI1/CD82 is important for its motility- and invasiveness-inhibitory activity." Cancer Res **64**(20): 7455-7463.

Zhu, G. Z., B. J. Miller, C. Boucheix, E. Rubinstein, C. C. Liu, R. O. Hynes, D. G. Myles and P. Primakoff (2002). "Residues SFQ (173-175) in the large extracellular loop of CD9 are required for gamete fusion." Development **129**(8): 1995-2002.

Zhu, Y. Z., Y. Luo, M. M. Cao, Y. Liu, X. Q. Liu, W. Wang, D. G. Wu, M. Guan, Q. Q. Xu, H. Ren, P. Zhao and Z. T. Qi (2012). "Significance of palmitoylation of CD81 on its association with tetraspanin-enriched microdomains and mediating hepatitis C virus cell entry." Virology **429**(2): 112-123.

Ziegler, S., B. Kronenberger, B. A. Albrecht, A. Kaul, A. L. Gamer, C. D. Klein and R. W. Hartmann (2009). "Development and evaluation of a FACS-based medium-throughput assay for HCV entry inhibitors." J Biomol Screen **14**(6): 620-626.

Zimmermann, P., K. Meerschaert, G. Reekmans, I. Leenaerts, J. V. Small, J. Vandekerckhove, G. David and J. Gettemans (2002). "PIP(2)-PDZ domain binding controls the association of syntenin with the plasma membrane." Mol Cell **9**(6): 1215-1225.

Zimmermann, P., D. Tomatis, M. Rosas, J. Grootjans, I. Leenaerts, G. Degeest, G. Reekmans, C. Coomans and G. David (2001). "Characterization of syntenin, a syndecan-binding PDZ protein, as a component of cell adhesion sites and microfilaments." Mol Biol Cell **12**(2): 339-350.

Zimmermann, P., Z. Zhang, G. Degeest, E. Mortier, I. Leenaerts, C. Coomans, J. Schulz, F. N'Kuli, P. J. Courtoy and G. David (2005). "Syndecan recycling [corrected] is controlled by syntenin-PIP2 interaction and Arf6." Dev Cell **9**(3): 377-388.

Ziyyat, A., E. Rubinstein, F. Monier-Gavelle, V. Barraud, O. Kulski, M. Prenant, C. Boucheix, M. Bomsel and J. P. Wolf (2006). "CD9 controls the formation of clusters that contain tetraspanins and the integrin alpha 6 beta 1, which are involved in human and mouse gamete fusion." J Cell Sci **119**(Pt 3): 416-424.

Zuidscherwoude, M., F. Gottfert, V. M. Dunlock, C. G. Figdor, G. van den Bogaart and A. B. van Spriel (2015). "The tetraspanin web revisited by super-resolution microscopy." Scientific reports **5**: 12201.